



Pacific Northwest
NATIONAL LABORATORY

Proudly Operated by Battelle Since 1965

Enhanced Hanford Low-Activity Waste Glass Property Data Development: Phase 1

November 2017

RL Russell
T Jin
BP McCarthy
LP Darnell
DE Rinehart
CC Bonham

V Gervasio
JM Mayer
CL Arendt
JB Lang
MJ Schweiger
JD Vienna

DISCLAIMER

This report was prepared as an account of work sponsored by an agency of the United States Government. Neither the United States Government nor any agency thereof, nor Battelle Memorial Institute, nor any of their employees, makes **any warranty, express or implied, or assumes any legal liability or responsibility for the accuracy, completeness, or usefulness of any information, apparatus, product, or process disclosed, or represents that its use would not infringe privately owned rights.** Reference herein to any specific commercial product, process, or service by trade name, trademark, manufacturer, or otherwise does not necessarily constitute or imply its endorsement, recommendation, or favoring by the United States Government or any agency thereof, or Battelle Memorial Institute. The views and opinions of authors expressed herein do not necessarily state or reflect those of the United States Government or any agency thereof.

PACIFIC NORTHWEST NATIONAL LABORATORY
operated by
BATTELLE
for the
UNITED STATES DEPARTMENT OF ENERGY
under Contract DE-AC05-76RL01830

Printed in the United States of America

Available to DOE and DOE contractors from the
Office of Scientific and Technical Information,
P.O. Box 62, Oak Ridge, TN 37831-0062;
ph: (865) 576-8401
fax: (865) 576-5728
email: reports@adonis.osti.gov

Available to the public from the National Technical Information Service
5301 Shawnee Rd., Alexandria, VA 22312
ph: (800) 553-NTIS (6847)
email: orders@ntis.gov <<http://www.ntis.gov/about/form.aspx>>
Online ordering: <http://www.ntis.gov>



This document was printed on recycled paper.

(8/2010)

Enhanced Hanford Low-Activity Waste Glass Property Data Development: Phase 1

November 2017

RL Russell
T Jin
BP McCarthy
LP Darnell
DE Rinehart
CC Bonham

V Gervasio
JM Mayer
CL Arendt
JB Lang
MJ Schweiger
JD Vienna

Prepared for
the U.S. Department of Energy
under Contract DE-AC05-76RL01830

Pacific Northwest National Laboratory
Richland, Washington 99352

Executive Summary

This report summarizes and analyzes data collected on a first test matrix of 36 low-activity waste (LAW) glass compositions intended to expand the LAW glass composition region over which glass property models are valid. The 36 LAW glass compositions were selected using statistical layered experimental design to explore a new glass composition region that overlaps and expands beyond the previously explored LAW glass composition region. The layered design of 36 LAW glasses consisted of 18 outer-layer glasses, 13 inner-layer glasses, a center glass (two replicates), and a glass previously tested at another laboratory (three replicates). The outer-layer glass compositions include extrema of the glass compositions that extend across and slightly beyond the compositions that are expected to be targeted for production. The analyses performed on these glasses include chemical composition (for target compositional verification), density, viscosity, electrical conductivity, crystal fraction, Canister Centerline Cooling with crystal identification, Product Consistency Test response, sulfur solubility, iron redox, and Vapor Hydration Test response. This report documents and discusses the results obtained from this testing.

Acronyms and Abbreviations

BNI	Bechtel National, Inc.
CCC	Canister Centerline Cooling
DIW	deionized water
DOE	U.S. Department of Energy
EC	electrical conductivity
EGCR	experimental glass composition region
EWG	Enhanced Waste Glass
HDI	“How Do I...?” (web-based standards system at PNNL)
IC	ion chromatography
IL	inner layer
ICP-AES	inductively coupled plasma–atomic emission spectroscopy
KH	potassium hydroxide (digestion)
LAW	low-activity waste
LM	lithium metaborate/tetraborate (fusion)
MCC	multiple-component constraints
NR	normalized release
OL	outer layer
ORP	Office of River Protection
PCT	Product Consistency Test
PF	peroxide fusion
PNNL	Pacific Northwest National Laboratory
QA	quality assurance
R&D	research and development
SCC	single-component constraints
SEM	scanning electron microscope
SRNL	Savannah River National Laboratory
VFT	Vogel- Fulcher-Tamman
VHT	Vapor Hydration Test
VSL	Vitreous State Laboratory
WTP	Waste Treatment and Immobilization Plant
XRD	x-ray diffraction
XRF	x-ray fluorescence

Contents

Executive Summary	iii
Acronyms and Abbreviations	v
1.0 Introduction	1.1
1.1 Status of LAW Experimental Glass Composition Regions and Waste Loading Constraints....	1.1
1.2 Phase 1 Enhanced LAW Experimental Glass Composition Region and Test Matrix.....	1.3
1.3 Quality Assurance	1.6
1.3.1 PNNL Quality Assurance Program	1.6
1.3.2 EWG Quality Assurance Program	1.6
2.0 Test Methods	2.1
2.1 Glass Fabrication.....	2.1
2.2 Chemical Analysis of Glass Composition.....	2.1
2.3 Glass Density	2.3
2.4 Viscosity.....	2.3
2.5 Electrical Conductivity.....	2.4
2.6 Equilibrium Crystal Fraction.....	2.4
2.7 Canister Centerline Cooling and Crystal Identification	2.5
2.8 Product Consistency Test.....	2.6
2.9 Vapor Hydration Test.....	2.6
2.10 Sulfur Solubility	2.8
2.11 Iron Redox.....	2.8
3.0 Results and Discussion	3.1
3.1 Chemical Analysis of Glass Composition.....	3.1
3.2 Density	3.2
3.3 Viscosity (η).....	3.3
3.4 Electrical Conductivity.....	3.11
3.5 Crystal Fraction of Heat-Treated Glasses	3.14
3.6 Crystal Identification in Canister Centerline Cooling Glasses.....	3.17
3.7 Product Consistency Test.....	3.20
3.8 Vapor Hydration Test.....	3.25
3.9 Sulfur Solubility Results	3.27
3.10 Iron Redox Measurement	3.5
3.11 Matrix Glasses Needing Composition Modification.....	3.6
3.11.1 Glass New-OL-8788	3.7
3.11.2 New-OL-45748	3.11
3.11.3 New-OL-54017	3.14
3.11.4 New-OL-62909	3.16

3.11.5 New-OL-65959	3.20
3.11.6 New-OL-108249	3.23
3.11.7 New-OL-116208	3.27
3.11.8 New-OL-127708	3.30
3.12 Matrix Glasses with Salt Segregation	3.33
3.12.1 New-OL-108249	3.33
3.12.2 New-OL-116208	3.35
4.0 Summary.....	4.1
5.0 References	5.1
Appendix A – Analyzed Glass Compositions	A.1
Appendix B – Viscosity Data	B.1
Appendix C – Electrical Conductivity Data	C.1
Appendix D – Canister Centerline Cooling Glass Photographs	D.1
Appendix E – X-Ray Diffraction Spectra of Canister Centerline Cooling Treated Glasses	E.1
Appendix F – Vapor Hydration Test Results.....	F.1
Appendix G – Analyses for Baseline and Sulfur Saturated Glasses.....	G.1

Figures

Figure 1.1. Plot of Glass Waste Loading Constraints for the Current WTP and Advanced ORP LAW Glasses as Projected on the Basis of $\text{Na}_2\text{O} + 0.66\text{K}_2\text{O}$ versus SO_3 Concentrations in Glass (based on Muller et al. 2004, 2010)	1.2
Figure 2.1. Plot of Temperature Schedule during CCC Treatment of Hanford LAW Glasses	2.6
Figure 2.2. Apparatus for Conducting VHTs	2.7
Figure 3.1. Predicted versus Measured Density for Phase 1 Enhanced LAW Glasses	3.3
Figure 3.2. Predicted Versus Measured Viscosity Data for Phase 1 Enhanced LAW Glasses	3.11
Figure 3.3. Predicted versus Measured Electrical Conductivity for LAW Phase 1 Enhanced Glasses	3.14
Figure 3.4. Optical Micrograph of Cassiterite Crystals in Glass New-IL-94020 Held at 952°C for 24 h	3.16
Figure 3.5. Optical Micrograph of Baddeleyite Crystals in Glass New-OL-8788(Mod) Held at 1043°C for 24 h	3.16
Figure 3.6. Photograph of Glass LAW-ORP-LD1(1) Cooled in a Pt Crucible with Crystals Along Edge	3.19
Figure 3.7. Photograph of Glass LAW-ORP-LD1(1) Cooled in a Quartz Crucible without Crystals along Edge	3.20
Figure 3.8. Comparison of Natural Logarithm PCT Normalized Release (g/m^2) of B and Li with Na for Quenched Samples of LAW Phase 1 Enhanced Glasses	3.23
Figure 3.9. Comparison of Natural Logarithm PCT Normalized Release (g/m^2) of B and Li with Na for CCC Samples of LAW Phase 1 Enhanced Glasses	3.23
Figure 3.10. Comparison of Natural Logarithm of PCT Normalized Release (g/m^2) of B, Li, and Na for Quenched and CCC-Treated Samples of LAW Phase 1 Enhanced Glasses	3.24
Figure 3.11. Comparison of Natural Logarithm of PCT Normalized Release (g/m^2) of B, Li, and Na for Quenched and CCC-Treated Samples that Contain Nepheline of LAW Phase 1 Enhanced Glasses	3.24
Figure 3.12. VHT Response Compared to the Total Normalized Alkali Mass Fraction [$\text{Nalk} = \text{Na}_2\text{O} + 0.66(\text{K}_2\text{O}) + 2(\text{Li}_2\text{O})$] Content of the Glass	3.26
Figure 3.13. Photograph of Glass New-OL-65959(Mod) Before (Right) and After (Left) VHT	3.27
Figure 3.14. Analyzed Sulfur Concentration in the Baseline and the Sulfur-Saturated Glasses	3.3
Figure 3.15. Predicted versus Measured SO_3 Solubility for LAW Phase 1 Enhanced Glasses	3.5
Figure 3.16. Photograph of First Melt of New-OL-8788 Glass with Increased Melt Temperature to 1325°C for 90 min	3.8
Figure 3.17. Photograph of First Compositional Modification of New-OL-8788 Glass Melted at 1350°C for 90 min (plastic disk is 12 cm diameter)	3.8
Figure 3.18. Photograph of Second Compositional Modification of New-OL-8788 Glass Melted at 1325°C for 60 min (plastic disk is 12 cm diameter)	3.9
Figure 3.19. Photograph of Third Modification of New-OL-8788 Glass Melted at 1300°C for 60 min (plastic disk is 12 cm diameter)	3.10
Figure 3.20. Photograph of Fourth Modification of New-OL-8788 Glass Melted at 1300°C for 60 min (plastic disk is 12 cm diameter)	3.10

Figure 3.21. Photograph of Final Compositional Modification of New-OL-8788 Glass Melted at 1300°C for 60 min (plastic disk is 12 cm diameter)	3.11
Figure 3.22. Photograph of New-OL-45748 Glass from Bottom of Crucible after First Modification Melted at 1300°C for 90 min.....	3.12
Figure 3.23. Photographs of Glass New-OL-45748 Color Comparison with Oxidizing Conditions (top) and Reducing Conditions (bottom) (plastic disk is 12 cm diameter).....	3.13
Figure 3.24. Photograph of Melt of New-OL-45748 with Tin Oxalate Substituted for SnO ₂ in Original Composition Melted at 1300°C for 60 min.....	3.14
Figure 3.25. Photograph of Glass New-OL-54017 Original Composition Melted at 1200°C for 85 min	3.15
Figure 3.26. XRD Pattern of Original New-OL-54017 Composition.....	3.15
Figure 3.27. Photograph of Glass New-OL-54017 Final Composition with Tin Oxalate Melted at 1250°C for 90 min (plastic disk is 12 cm diameter)	3.16
Figure 3.28. Photograph of Glass New-OL-62909 Original Composition Melted at 1300°C for 60 min	3.17
Figure 3.29. XRD Pattern of Original New-OL-62909 Composition.....	3.17
Figure 3.30. Optical Micrograph of Undissolved Particles in the New-OL-62909 Initial Melt	3.18
Figure 3.31. Photograph of First Modification of Glass New-OL-62909 Melted at 1300°C for 60 min (plastic disk is 12 cm diameter)	3.18
Figure 3.32. Photograph of Second Modification of Glass New-OL-62909 Melted at 1300°C for 90 min (plastic disk is 12 cm diameter).....	3.19
Figure 3.33. Photograph of Final Modification of Glass New-OL-62909 Melted at 1300°C for 60 min (plastic disk is 12 cm diameter).....	3.19
Figure 3.34. Photograph of Glass New-OL-65959 Original Composition with Large Ceramic Pieces Melted at 1275°C for 75 min	3.21
Figure 3.35. XRD Pattern of Original New-OL-65959 Composition.....	3.21
Figure 3.36. Photograph of Glass New-OL-65959 First Modification Melted at 1250°C for 60 min (plastic disk is 12 cm diameter)	3.22
Figure 3.37. Photograph of Glass New-OL-65959 Second Modification Melted at 1250°C for 60 min (plastic disk is 12 cm diameter)	3.22
Figure 3.38. Photograph of Glass New-OL-65959 Final Modification Melted at 1250°C for 60 min (plastic disk is 12 cm diameter)	3.23
Figure 3.39. Photograph of Glass New-OL-108249 Original Composition Melted at 1200°C for 65 min	3.23
Figure 3.40. Photograph of Glass New-OL-108249 4 th Modification Melted at 1150°C for 60 min	3.25
Figure 3.41. Photograph of Glass New-OL-108249 5 th Modification Melted at 1200°C for 60 min (plastic disk is 12 cm diameter)	3.26
Figure 3.42. Photographs of Glass New-OL-108249 6 th Modification Melted at 1250°C for 60 min	3.27
Figure 3.43. Photograph of Glass New-OL-116208 1 st Modification Melted at 1200°C for 60 min	3.28
Figure 3.44. Photograph of Glass New-OL-116208 2 nd Modification Melted at 1200°C for 60 min (plastic disk is 12 cm diameter)	3.29

Figure 3.45. Photograph of Glass New-OL-116208 Original Composition Melted at 1200°C for 65 min (plastic disk is 12 cm diameter).....	3.29
Figure 3.46. Photograph of Glass New-OL-116208 3 rd Modification Melted at 1200°C for 65 min.....	3.30
Figure 3.47. Photograph of Glass New-OL-127708 Original Composition Melted at 1350°C for 60 min (plastic disk is 12 cm diameter).....	3.31
Figure 3.48. XRD Pattern of Original New-OL-127708 Composition.....	3.31
Figure 3.49. Photograph of Glass New-OL-127708 after 1 st Modification Melted at 1300°C for 90 min (plastic disk is 12 cm diameter).....	3.32
Figure 3.50. Photograph of Glass New-OL-127708 after 3 rd Modification Melted at 1300°C for 60 min (plastic disk is 12 cm diameter).....	3.32
Figure 3.51. Photograph of Glass New-OL-127708 Final Composition Melted at 1300°C for 60 min (plastic disk is 12 cm diameter)	3.33
Figure 3.52. Photograph of Glass New-OL-108249 1 st Melt after 1 st Sulfur Washing Melted at 1150°C for 60 min.....	3.34
Figure 3.53. Photograph of Glass New-OL-108249 2 nd Melt (1300°C for 60 min) after 2 nd Sulfur Washing (plastic disk is 12 cm diameter)	3.34
Figure 3.54. Photograph of Glass New-OL-108249 Final Modified Composition Melted at 1300°C for 60 min (plastic disk is 12 cm diameter)	3.34
Figure 3.55. Photograph of Glass New-OL-116208 Melt after 1 st Sulfate Washing Melted at 1200°C for 60 min.....	3.35
Figure 3.56. Photograph of Glass New-OL-116208 Final Composition after Final Pour Melted at 1300°C for 60 min (plastic disk is 12 cm diameter)	3.36

Tables

Table 1.1. Lower and Upper Bounds of Single-Component Constraints(a) for the Outer and Inner Layers of the 15-Component Enhanced Low-Activity Waste Experimental Glass Composition Region.....	1.4
Table 1.2. Lower and Upper Bounds of Multiple-Component Constraints for the Outer and Inner Layers of a 15-Component Enhanced Low-Activity Waste Experimental Glass Composition Region.....	1.5
Table 1.3. Targeted Compositions for the Phase 1 Enhanced LAW Glasses (mass fractions) (Page 1 of 4).....	1.2
Table 2.1. Melting Temperatures and Times Used in Fabricating the Phase 1 Enhanced LAW Waste Glasses	2.2
Table 2.2. Preparation and Measurement Methods Used in Reporting the Measured Concentrations of Each of the Analytes of the Study Glasses	2.3
Table 2.3. Temperature Schedule during Canister Centerline Cooling Treatment of Hanford LAW Glasses	2.5
Table 3.1. Measured Densities of Phase 1 Enhanced LAW Glasses	3.2
Table 3.2. Measured η (Pa·s) Values Versus Target Temperature (a) (in the sequence of measurement) for the Phase 1 Enhanced LAW Glasses Tested.....	3.7
Table 3.2. Measured η (Pa·s) Values Versus Target Temperature (a) (in the sequence of measurement) for the Phase 1 Enhanced LAW Glasses Tested (cont.)	3.8
Table 3.3. Fitted Coefficients of Arrhenius and VFT Models for Viscosity of LAW Phase 1 Enhanced Glasses.....	3.9
Table 3.4. Measured Electrical Conductivity (S/m) Values Versus Temperatures for the LAW Phase 1 Enhanced Glasses	3.12
Table 3.4. Measured Electrical Conductivity (S/m) Values Versus Temperatures for the LAW Phase 1 Enhanced Glasses (cont.).....	3.13
Table 3.5. Weight Percent Crystallinity and Identification of Crystals by XRD in Heat-Treated Glasses	3.15
Table 3.6. Weight Percent Crystallinity and Identification of Crystals by XRD in CCC-Treated Glasses	3.17
Table 3.7. PCT Normalized Concentration Release Results Taken from Fox et al. (2015a,b).....	3.20
Table 3.8. VHT Results from the LAW Phase 1 Enhanced Glasses.....	3.25
Table 3.9. Target and Measured Values of SO ₃ (mass fraction).....	3.1
Table 3.10. List of SO ₃ Solubility Model Components and Coefficients (Vienna et al 2014)	3.5
Table 3.11. Iron Redox Results of LAW Glass	3.6
Table 3.12. Composition and Melt Temperature Modifications Made to LAW Phase 1 Enhanced Glass New-OL-8788.....	3.7
Table 3.13. Composition Modifications Made to Glass New-OL-45748	3.12
Table 3.14. Composition Modifications Made to Glass New-OL-54017	3.14
Table 3.15. Composition Modifications Made to Glass New-OL-62909	3.16
Table 3.16. Composition and Melt Temperature Modifications Made to Glass New-OL-65959	3.20

Table 3.17. Composition Modifications Made to Glass New-OL-108249	3.24
Table 3.18. Composition Modifications Made to Glass New-OL-116208	3.28
Table 3.19. Composition Modifications Made to Glass New-OL-127708	3.30
Table 3.20. Glass New-OL-108249 Sulfate Washing.....	3.35
Table 3.21. Glass New-OL-116208 Sulfate Washing.....	3.36

1.0 Introduction

The U.S. Department of Energy's (DOE) Office of River Protection (ORP) asked Pacific Northwest National Laboratory (PNNL) to provide expert evaluation and experimental work in support of the River Protection Project vitrification technology development (DOE 2012). This work was performed under the PNNL project titled "ORP Glass Support Work." One task of this project—Enhanced Hanford Waste Glass Models—is the subject of this report. The long-term objective of this work is to expand the Hanford Site low-activity waste (LAW) glass database and property-composition models to cover the balance of the Hanford Site tank waste treatment and immobilization mission.

This report presents the glass compositions and glass property data developed in Phase 1 of the enhanced Hanford LAW glass property data development effort. When the data development effort for enhanced Hanford LAW glasses is complete, enhanced LAW glass property models will be developed. Section 1.1 summarizes the status of the LAW glass composition regions and waste loading constraints prior to the data development effort documented in this report. Section 1.2 summarizes the LAW Phase 1 glass composition region and test matrix, previously discussed by Piepel et al. (2015, 2016). Section 1.3 documents the Quality Assurance program used in performing the work discussed in this report.

1.1 Status of LAW Experimental Glass Composition Regions and Waste Loading Constraints

In this document, the term *experimental glass composition region* (EGCR) is used to refer to a composition region of glasses that has been (or will be) experimentally explored through fabricating glasses and testing their properties. Ideally, an EGCR should include all glass compositions that will satisfy processing and product-quality related constraints, as well as glass compositions that fail one or more constraints. Experimental data collected on glass compositions covering the EGCR then provide information for developing property-composition models that can 1) discriminate between glass compositions that satisfy and fail the requirements, and 2) adequately predict glass properties of compositions that satisfy all requirements. The term *qualified glass composition region* then refers to the subset of the EGCR for which all processing and product-quality constraints are satisfied with sufficient confidence, after accounting for applicable uncertainties.

The Hanford Tank Waste Treatment and Immobilization Plant (WTP) project has developed glass property-composition models to formulate compositions and qualify LAW glasses for disposal (Piepel et al. 2007). These models are based on data from crucible-scale tests with simulants, crucible-scale tests with actual waste, and scaled-melter tests with simulants collected under the Bechtel National, Inc. (BNI) contract to design, construct, and commission the WTP (DOE 2000). Because the scope of the BNI contract is limited to operating the plant for only 20 days with a limited amount of waste, the data and resulting glass property-composition models only cover a fraction of the LAW glass compositions needed for the entire Hanford Site mission. In addition, the data and models developed by BNI are targeted at glasses that only modestly exceed contract minimum waste loadings rather than maximum achievable waste loadings.

Current processing and product-quality "constraints" are dominated by model validity regions and stand-in constraints for properties that are not easily measured or predicted. The model validity constraints reflect only the region of qualified data available for models to predict the properties of interest (i.e., boundaries of the EGCR). The stand-in constraints are employed in lieu of constraints on the properties to be controlled. For example, the weight percent (wt%) of SO₃ targeted in glass is currently limited because the salt accumulation in the melter was not modeled for WTP glasses, and the

equilibrium fraction of crystals at 950°C is limited to 1 volume percent (vol%) because crystal blockages of the melter pour-spout were not modeled. To determine the ultimate waste loading of glass, these constraints based on limited data availability must be replaced with constraints based on true operating and product performance property limits. To this end, we seek to develop 1) glass property data across broader glass composition regions and 2) methods to measure (directly or indirectly) and model the properties that fundamentally limit the melter operating limits or the performance property limits of the glass.

The LAW feed is dominated by sodium salts. The ratio of sulfur to sodium in the waste is a key determinant of waste loading and glass formulation. At high alkali concentrations, the waste loading is limited primarily by the durability of the resulting glass. At high-sulfur (represented as SO₃) concentrations, the waste loading is limited primarily by salt accumulation in the melter.

The LAW glasses currently formulated for WTP (Kim and Vienna 2012) have relatively conservative alkali and sulfur loading limits, as shown by the red constraint in Figure 1.1. The waste loading is currently determined by the ratio of normalized alkali (Na₂O + 0.66K₂O) to sulfur (as SO₃) in the waste. Where the alkali/sulfur ratio for a particular waste intersects the red line will determine the loading of that waste in glass using the current WTP LAW glass constraints. Additional loading constraints were added for halides, chromate, and phosphates as well.

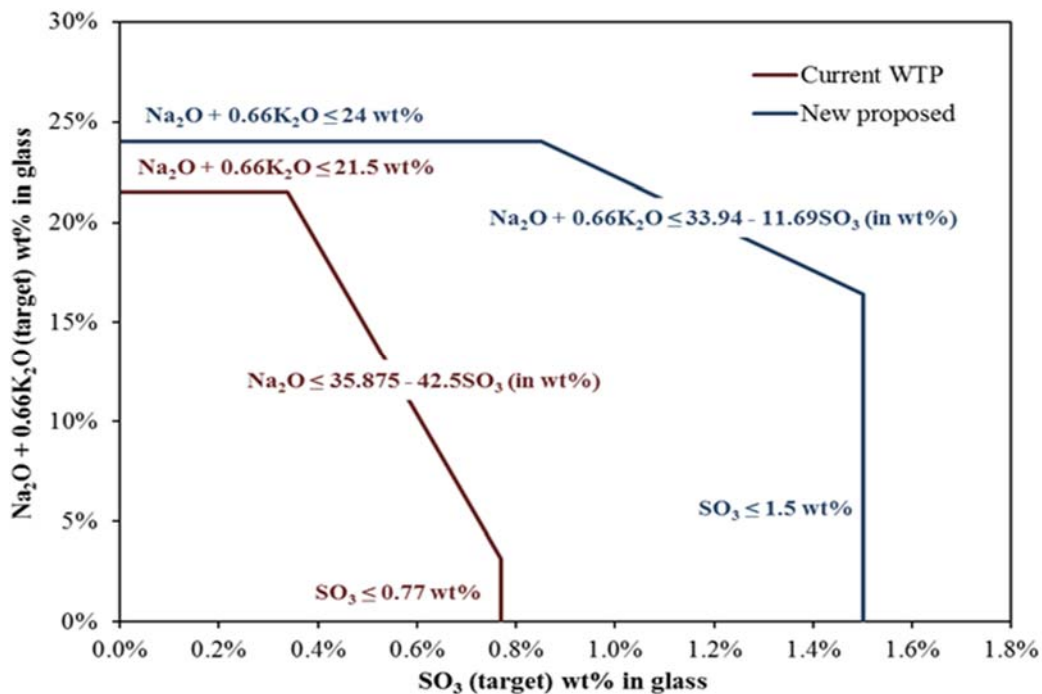


Figure 1.1. Plot of Glass Waste Loading Constraints for the Current WTP and Advanced ORP LAW Glasses as Projected on the Basis of Na₂O + 0.66K₂O versus SO₃ Concentrations in Glass (based on Muller et al. 2004, 2010)

More recently, new high-waste-loading formulations have been developed by The Catholic University of America and PNNL in support of ORP (Matlack et al. 2005a, 2005b, 2006a, 2006b, 2007, 2009; Vienna et al. 2002, 2003a, 2003b, 2004a, 2004b; Aloy et al. 2006; and Kim et al. 2003). The resulting data are summarized in Muller et al. (2012) and Vienna et al. (2003a, 2003b, 2013), with some newer data not yet reported. The basic conclusions of these studies are that loadings for specific wastes in glass can be

increased significantly over what would be allowed by current WTP constraints. Examples of the gains made in recent studies include the following:

- LAW sulfur loadings of 1.5 wt% (as SO₃) were successfully processed, which is roughly double the 0.77 wt% allowed by the current WTP LAW EGCR.
- LAW normalized alkali loadings of 24 wt% have been achieved compared to the 21 wt% maximum in the current WTP LAW EGCR.

These advances (upper blue line) are compared with the WTP baseline waste loading constraints (lower red line) in Figure 1.1 (based on Muller et al. 2010). In this figure, the SO₃ limits (SO₃ = 0.77 or 1.5 wt%) are used to reduce the risk of salt accumulation in the melter. If salt does accumulate in the melter, the useful life of components that are adjacent to or pass through the melt line may be significantly reduced. The horizontal lines represent alkali limits in glass (Na₂O+0.66K₂O = 21.5 or 24 wt%) above which there is high risk of exceeding the current WTP contract specifications for Product Consistency Test (PCT) and Vapor Hydration Test (VHT) responses for glass durability (DOE 2000). The sloped lines in between these two end constraints represent the limits of the formulations tested to-date in balancing the full range of glass properties in a single glass. That is to say, glasses can be formulated for high SO₃ loading or for high alkali loadings; but, compromises must be made to achieve high concentrations of both. The sloped lines therefore represent the current state of formulations tested to achieve this balance. Future testing and modeling efforts should be made to describe each of the fundamental properties (salt formation, PCT and VHT responses, viscosity, electrical conductivity, refractory corrosion, etc.) as functions of target glass compositions. Although most of these models exist for the current WTP baseline glasses, they need to be updated for the expanded glass composition region in order to optimize glass compositions for each waste while simultaneously meeting all the processing and product constraints.

The matrix of current LAW glass compositions with available property data, shows two somewhat distinct composition sub-regions (the current WTP and the advanced ORP glasses). The question is raised whether 1) we need to develop a single, combined, EGCR or if 2) it would be more effective to focus on the advanced LAW EGCR without ties to the lower loaded region. For this study, PNNL explored only the advanced LAW EGCR corresponding to the sub-region with the higher waste loading. Data for the region with the lower waste loading will be used if warranted based on evaluation of the combined database. The current Catholic University of America testing program is attempting to bridge the gap between the two sub-regions (Muller et al. 2013a, 2013b).

1.2 Phase 1 Enhanced LAW Experimental Glass Composition Region and Test Matrix

The objective of the task was to generate data on different LAW glass compositions to ultimately support the development, validation, and implementation of glass property models that are capable of achieving high waste loading for the full region of Hanford LAW compositions. To extend the models beyond our current knowledge space, a new enhanced LAW EGCR was developed. Table 1.1 lists the 15 LAW glass components selected for variation in the experimental work, including an “Others” component mix discussed subsequently. Certain components were chosen for variation in the experimental work for specific reasons. The components SnO₂ and ZrO₂ were included because they can decrease the VHT response. The components V₂O₅ and Li₂O were included because they can increase the SO₃ retention in the glass. Finally, the components ZnO and Cr₂O₃ were included because they can decrease refractory corrosion. The upper bound for K₂O was limited to 1.5% as that is expected to cover 99% of the LAW feed (other testing will expand the K₂O concentration range to cover the full anticipated EGCR).

Table 1.1. Lower and Upper Bounds of Single-Component Constraints(a) for the Outer and Inner Layers of the 15-Component Enhanced Low-Activity Waste Experimental Glass Composition Region

Component	Outer Layer		Inner Layer		Center Point
	Lower Bound	Upper Bound	Lower Bound	Upper Bound	
Al ₂ O ₃	0.035	0.1385	0.0625	0.1150	0.09
B ₂ O ₃	0.06	0.1375	0.08	0.1175	0.10
CaO	0	0.1224	0.0275	0.09	0.055
Fe ₂ O ₃	0	0.015	0.0050	0.0125	0.01
K ₂ O	0	0.015	0.002	0.01	0.004
Li ₂ O	0	0.05	0.01	0.035	0.02
MgO	0	0.035	0.005	0.025	0.015
Na ₂ O	0.10	0.26	0.15	0.23	0.19
SiO ₂	0.34	0.47	0.3675	0.4325	0.3955
SO ₃	0.001	0.02	0.004	0.013	0.007
SnO ₂	0	0.05	0.01	0.035	0.02
V ₂ O ₅	0	0.04	0.005	0.03	0.02
ZnO	0.01	0.05	0.02	0.04	0.03
ZrO ₂	0	0.065	0.015	0.0475	0.03
Others ^(b)	0.004	0.03	0.075	0.02	0.0135

(a) The lower and upper bounds of the single-component constraints are in terms of mass fractions of the components, such that the mass fractions of all 15 components must sum to 1.0000.

(b) The Others component was composed of the following mixture of four minor components (expressed as mass fractions): Cl = 0.156, Cr₂O₃ = 0.104, F = 0.236, and P₂O₅ = 0.504.

The enhanced LAW EGCR was specified by the single-component constraints (SCC) listed in Table 1.1 and the multiple-component constraints (MCC) listed in Table 1.2. Table 1.1 and Table 1.2 list SCCs and MCCs separately for the outer and inner layers of the enhanced LAW EGCR. The outer-layer SCCs and MCCs were chosen to 1) overlap and expand beyond the previously explored EGCR, and 2) include more extreme LAW glass compositions based on current projections of the waste feed and associated glass formulations. The lower and upper bounds for the inner-layer SCCs are roughly half way between the lower and upper bounds for the outer-layer SCCs and the center-point values. For more discussion of how the components, SCCs, and MCCs were chosen, see Appendix A of Piepel et al. (2016).

Table 1.2. Lower and Upper Bounds of Multiple-Component Constraints for the Outer and Inner Layers of a 15-Component Enhanced Low-Activity Waste Experimental Glass Composition Region

Expression (units)^(a)	Outer Layer		Inner Layer	
	Lower Bound	Upper Bound	Lower Bound	Upper Bound
Nalk (mf) ^(b)	0.15	0.265	0.195	0.2515
ZrO ₂ +SnO ₂ (mf)	0.03	0.11	0.04	0.08
η_{1150} (Pa·s) ^(c)	1	10	3	7
SO ₃ Solubility (wt%)	–	Solubility Limit ^(d)	–	Solubility Limit ^(d)

(a) mf = mass fraction, wt% = weight percent.

(b) $Nalk = Na_2O + 0.66(K_2O) + 2(Li_2O)$

(c) η_{1150} = viscosity at 1150°C, expressed as a linear mixture model, as discussed by Piepel et al. (2015, 2016).

(d) The SO₃ solubility limit is expressed as a partial quadratic mixture model, as discussed by Piepel et al. (2015, 2016).

The 36 Phase 1 enhanced LAW glass compositions that were tested comprise a statistical layered design (Piepel et al. 1993, Cooley et al. 2003, Piepel et al. 2005) consisting of 18 glasses on the outer layer (OL) of the EGCR, 13 glasses on the inner layer (IL) of the EGCR, a glass in the center of the EGCR (two replicates), and a glass of interest tested at the Vitreous State Laboratory (VSL) at The Catholic University of America (three replicates). For more discussion of how the layered design glass compositions were selected, see Piepel et al. (2015, 2016). The 36 as-designed LAW glass target compositions are listed in

Table 1.3.

Four of the glasses in this study required some modifications to their compositions for them to melt and form single-phase glasses. Another two glasses had sulfate precipitate out of the melt and, therefore, had to have the sulfate decreased in the final glass composition. Two other glasses needed to have the tin added as tin oxalate instead of tin oxide in order for the tin to dissolve into the glass. This topic is discussed in more detail in Section 3.11. These modified target glass compositions are listed in

Table 1.3 beside the as-designed compositions with the extension “Mod” added to the glass identification. Note that glass property data were generated only for the “Mod” glasses, not their original “as-designed” counterparts.

This report summarizes the experimental methods to fabricate, heat treat, and test the 36-glass test matrix consisting of the following (all prepared at PNNL):

- 18 outer-layer glass compositions,
- 13 inner-layer glass compositions,
- Centroid glass, enhanced waste glass (EWG)-LAW-Centroid (two replicates), and
- VSL tested glass designated as LAW-ORP-LD1 (three replicates).

The centroid and the VSL tested glasses were prepared and measured in duplicate and triplicate, respectively, resulting in a total of 36 glasses prepared and properties measured with 33 distinct target compositions. Measured properties relating to glass performance and processing are described in this report and provided in appendices.

Table 1.3. Targeted Compositions for the Phase 1 Enhanced LAW Glasses (mass fractions) (Page 1 of 4)

Component	Glass ID												
	New-IL-456	New-IL-1721	New-IL-5253	New-IL-5255	New-IL-42295	New-IL-70316	New-IL-87749	New-IL-93907	New-IL-94020	New-IL-103151	New-IL-151542	New-IL-166697	New-IL-166731
Al ₂ O ₃	0.0625	0.0625	0.0625	0.0625	0.0625	0.0625	0.1150	0.1150	0.1150	0.0625	0.0625	0.1125	0.1150
B ₂ O ₃	0.0800	0.1175	0.1175	0.1175	0.1175	0.0800	0.0800	0.1175	0.0800	0.0800	0.0974	0.1022	0.0931
CaO	0.0900	0.0275	0.0275	0.0275	0.0275	0.0900	0.0900	0.0275	0.0353	0.0275	0.0900	0.0275	0.0275
Cl	0.0012	0.0031	0.0012	0.0012	0.0012	0.0012	0.0012	0.0012	0.0012	0.0012	0.0031	0.0031	0.0031
Cr ₂ O ₃	0.0008	0.0021	0.0008	0.0008	0.0008	0.0008	0.0008	0.0008	0.0008	0.0008	0.0021	0.0021	0.0021
Cs ₂ O	0.0000	0.0000	0.0000	0.0000	0.0000	0.0000	0.0000	0.0000	0.0000	0.0000	0.0000	0.0000	0.0000
F	0.0018	0.0047	0.0018	0.0018	0.0018	0.0018	0.0018	0.0018	0.0018	0.0018	0.0047	0.0047	0.0047
Fe ₂ O ₃	0.0125	0.0125	0.0125	0.0125	0.0125	0.0125	0.0125	0.0125	0.0125	0.0125	0.0125	0.0125	0.0050
K ₂ O	0.0020	0.0100	0.0020	0.0020	0.0020	0.0100	0.0100	0.0100	0.0020	0.0100	0.0020	0.0100	0.0020
Li ₂ O	0.0350	0.0350	0.0350	0.0350	0.0350	0.0100	0.0350	0.0350	0.0350	0.0100	0.0100	0.0350	0.0350
MgO	0.0250	0.0050	0.0250	0.0250	0.0250	0.0250	0.0050	0.0050	0.0250	0.0250	0.0250	0.0050	0.0250
Na ₂ O	0.1500	0.1645	0.1500	0.1800	0.1748	0.2023	0.1749	0.1512	0.1500	0.2249	0.1737	0.1749	0.1802
NiO	0.0000	0.0000	0.0000	0.0000	0.0000	0.0000	0.0000	0.0000	0.0000	0.0000	0.0000	0.0000	0.0000
P ₂ O ₅	0.0038	0.0101	0.0038	0.0038	0.0038	0.0038	0.0038	0.0038	0.0038	0.0038	0.0101	0.0101	0.0101
PbO	0.0000	0.0000	0.0000	0.0000	0.0000	0.0000	0.0000	0.0000	0.0000	0.0000	0.0000	0.0000	0.0000
SiO ₂	0.4315	0.4325	0.3975	0.3675	0.4242	0.3872	0.3741	0.4325	0.4325	0.4184	0.3939	0.3675	0.3675
SO ₃	0.0040	0.0130	0.0130	0.0130	0.0040	0.0130	0.0040	0.0113	0.0102	0.0117	0.0130	0.0129	0.0127
SnO ₂	0.0350	0.0350	0.0350	0.0350	0.0100	0.0350	0.0270	0.0350	0.0350	0.0250	0.0350	0.0350	0.0320
V ₂ O ₅	0.0300	0.0300	0.0300	0.0300	0.0300	0.0300	0.0300	0.0050	0.0050	0.0300	0.0300	0.0300	0.0300
ZnO	0.0200	0.0200	0.0400	0.0400	0.0200	0.0200	0.0200	0.0200	0.0400	0.0400	0.0200	0.0400	0.0400
ZrO ₂	0.0150	0.0150	0.0450	0.0450	0.0475	0.0150	0.0150	0.0150	0.0150	0.0150	0.0150	0.0150	0.0150
Total^(a)	1.0001	1.0000	1.0001	1.0001	1.0001	1.0001	1.0001	1.0001	1.0001	1.0001	1.0000	1.0000	1.0000

(a) The mass fractions of the glass compositions were originally calculated to more than four decimal places, so rounding to four decimal places caused the totals to differ from 1.0000 by ± 0.0001 .

Table 1.4. Targeted Compositions for the Phase 1 Enhanced LAW Glasses (mass fractions) (Page 2 of 4)

Component	Glass ID											
	New-OL-8445	New-OL-8788	New-OL-8788(Mod)	New-OL-14844	New-OL-15493	New-OL-17130	New-OL-45748	New-OL-45748 (Sn Mod)	New-OL-54017	New-OL-54017 (Sn Mod)	New-OL-57284	New-OL-62380
Al ₂ O ₃	0.1241	0.1385	0.1235	0.0350	0.0350	0.0350	0.1385	0.1385	0.0350	0.0350	0.0350	0.0350
B ₂ O ₃	0.1375	0.0600	0.0600	0.0615	0.0600	0.1375	0.0600	0.0600	0.0600	0.0600	0.1375	0.1375
CaO	0.1224	0.0005	0.0005	0.1224	0.1224	0.0165	0.1224	0.1224	0.1117	0.1117	0.0298	0.1224
Cl	0.0047	0.0047	0.0047	0.0047	0.0006	0.0047	0.0047	0.0047	0.0006	0.0006	0.0047	0.0011
Cr ₂ O ₃	0.0031	0.0031	0.0031	0.0031	0.0004	0.0031	0.0031	0.0031	0.0004	0.0004	0.0031	0.0008
Cs ₂ O	0.0000	0.0000	0.0000	0.0000	0.0000	0.0000	0.0000	0.0000	0.0000	0.0000	0.0000	0.0000
F	0.0071	0.0071	0.0071	0.0071	0.0009	0.0071	0.0071	0.0071	0.0009	0.0009	0.0071	0.0017
Fe ₂ O ₃	0.0000	0.0150	0.0150	0.0000	0.0000	0.0150	0.0150	0.0150	0.0150	0.0150	0.0000	0.0150
K ₂ O	0.0150	0.0150	0.0150	0.0150	0.0150	0.0000	0.0000	0.0000	0.0000	0.0000	0.0150	0.0150
Li ₂ O	0.0201	0.0201	0.0250	0.0500	0.0000	0.0500	0.0500	0.0500	0.0000	0.0000	0.0000	0.0000
MgO	0.0350	0.0350	0.0350	0.0350	0.0350	0.0000	0.0000	0.0000	0.0350	0.0350	0.0000	0.0000
Na ₂ O	0.1000	0.1000	0.1300	0.1551	0.2551	0.1650	0.1140	0.1140	0.1500	0.1500	0.1401	0.1401
NiO	0.0000	0.0000	0.0000	0.0000	0.0000	0.0000	0.0000	0.0000	0.0000	0.0000	0.0000	0.0000
P ₂ O ₅	0.0151	0.0151	0.0151	0.0151	0.0020	0.0151	0.0151	0.0151	0.0020	0.0020	0.0151	0.0037
PbO	0.0000	0.0000	0.0000	0.0000	0.0000	0.0000	0.0000	0.0000	0.0000	0.0000	0.0000	0.0000
SiO ₂	0.3400	0.4700	0.4600	0.3400	0.3925	0.4700	0.3400	0.3400	0.4700	0.4700	0.4700	0.3400
SO ₃	0.0010	0.0010	0.0010	0.0010	0.0010	0.0010	0.0010	0.0010	0.0010	0.0010	0.0010	0.0010
SnO ₂	0.0000	0.0000	0.0000	0.0000	0.0300	0.0300	0.0500	0.0500 ^(b)	0.0500	0.0500 ^(b)	0.0000	0.0450
V ₂ O ₅	0.0000	0.0000	0.0000	0.0400	0.0400	0.0400	0.0291	0.0291	0.0185	0.0185	0.0400	0.0266
ZnO	0.0100	0.0500	0.0500	0.0500	0.0100	0.0100	0.0500	0.0500	0.0500	0.0500	0.0500	0.0500
ZrO ₂	0.0650	0.0650	0.0550	0.0650	0.0000	0.0000	0.0000	0.0000	0.0000	0.0000	0.0516	0.0650
Total^(a)	1.0001	1.0001	1.0000	1.0000	0.9999	1.0000	1.0000	1.0000	1.0001	1.0001	1.0000	0.9999

(a) The mass fractions of the glass compositions were originally calculated to more than four decimal places, so rounding to four decimal places caused the totals to differ from 1.0000 by ±0.0001.

(b) This was added as tin oxalate and not SnO₂.

Table 1.5. Targeted Compositions for the Phase 1 Enhanced LAW Glasses (mass fractions) (Page 3 of 4)

Component	Glass ID											
	New-OL-62909	New-OL-62909(Mod)	New-OL-65959	New-OL-65959(Mod)	New-OL-80309	New-OL-90780	New-OL-100210	New-OL-108249	New-OL-108249 (SO ₃ Mod)	New-OL-116208	New-OL-116208 (SO ₃ Mod)	New-OL-122817
Al ₂ O ₃	0.1385	0.1235	0.1385	0.1385	0.0350	0.1385	0.0350	0.1195	0.1203	0.0350	0.0353	0.0350
B ₂ O ₃	0.0890	0.0890	0.1305	0.1305	0.1375	0.1375	0.0600	0.0600	0.0604	0.0600	0.0605	0.0600
CaO	0.1224	0.1224	0.0000	0.0000	0.0000	0.0000	0.0189	0.1000	0.1007	0.1224	0.1235	0.1224
Cl	0.0047	0.0047	0.0006	0.0006	0.0006	0.0047	0.0047	0.0047	0.0047	0.0047	0.0047	0.0047
Cr ₂ O ₃	0.0031	0.0031	0.0004	0.0004	0.0004	0.0031	0.0031	0.0031	0.0031	0.0031	0.0031	0.0031
Cs ₂ O	0.0000	0.0000	0.0000	0.0000	0.0000	0.0000	0.0000	0.0000	0.0000	0.0000	0.0000	0.0000
F	0.0071	0.0071	0.0009	0.0009	0.0009	0.0071	0.0071	0.0071	0.0071	0.0071	0.0072	0.0071
Fe ₂ O ₃	0.0000	0.0000	0.0000	0.0000	0.0150	0.0000	0.0000	0.0150	0.0151	0.0150	0.0151	0.0150
K ₂ O	0.0000	0.0000	0.0000	0.0000	0.0150	0.0150	0.0000	0.0150	0.0151	0.0000	0.0000	0.0150
Li ₂ O	0.0250	0.0250	0.0500	0.0500	0.0500	0.0500	0.0000	0.0500	0.0503	0.0500	0.0505	0.0000
MgO	0.0350	0.0350	0.0350	0.0350	0.0350	0.0350	0.0350	0.0000	0.0000	0.0350	0.0353	0.0000
Na ₂ O	0.1000	0.1300	0.1650	0.1650	0.1510	0.1551	0.2600	0.1551	0.1561	0.1619	0.1634	0.1860
NiO	0.0000	0.0000	0.0000	0.0000	0.0000	0.0000	0.0000	0.0000	0.0000	0.0000	0.0000	0.0000
P ₂ O ₅	0.0151	0.0151	0.0020	0.0020	0.0020	0.0151	0.0151	0.0151	0.0152	0.0151	0.0152	0.0151
PbO	0.0000	0.0000	0.0000	0.0000	0.0000	0.0000	0.0000	0.0000	0.0000	0.0000	0.0000	0.0000
SiO ₂	0.3400	0.3350	0.3400	0.3450	0.3400	0.3425	0.4700	0.3400	0.3423	0.3400	0.3431	0.4417
SO ₃	0.0010	0.0010	0.0010	0.0010	0.0175	0.0164	0.0091	0.0154	0.0089	0.0182	0.0093	0.0149
SnO ₂	0.0441	0.0441 ^(b)	0.0500	0.0450 ^(b)	0.0450	0.0300	0.0320	0.0500	0.0503	0.0450	0.0454	0.0300
V ₂ O ₅	0.0000	0.0000	0.0360	0.0360	0.0400	0.0400	0.0000	0.0000	0.0000	0.0125	0.0126	0.0400
ZnO	0.0100	0.0100	0.0500	0.0500	0.0500	0.0100	0.0500	0.0500	0.0503	0.0100	0.0101	0.0100
ZrO ₂	0.0650	0.0550	0.0000	0.0000	0.0650	0.0000	0.0000	0.0000	0.0000	0.0650	0.0656	0.0000
Total^(a)	1.0000	1.0000	0.9999	0.9999	0.9999	1.0000	1.0000	1.0000	0.9999	1.0000	0.9999	1.0000

(a) The mass fractions of the glass compositions were originally calculated to more than four decimal places, so rounding to four decimal places caused the totals to differ from 1.0000 by ±0.0001.

(b) This was added as tin oxalate and not SnO₂.

Table 1.6. Targeted Compositions for the Phase 1 Enhanced LAW Glasses (mass fractions) (Page 4 of 4)

Component	Glass ID						
	New-OL-127708	New-OL-127708(Mod)	EWG-LAW-Centroid-1	EWG-LAW-Centroid-2	LAW-ORP-LD1(1)	LAW-ORP-LD1(2)	LAW-ORP-LD1(3)
Al ₂ O ₃	0.1344	0.1094	0.0900	0.0900	0.1015	0.1015	0.1015
B ₂ O ₃	0.1375	0.1375	0.1000	0.1000	0.1204	0.1204	0.1204
CaO	0.0030	0.0030	0.0550	0.0550	0.0801	0.0801	0.0801
Cl	0.0006	0.0006	0.0021	0.0021	0.0033	0.0033	0.0033
Cr ₂ O ₃	0.0004	0.0004	0.0014	0.0014	0.0050	0.0050	0.0050
Cs ₂ O	0.0000	0.0000	0.0000	0.0000	0.0013	0.0013	0.0013
F	0.0009	0.0009	0.0032	0.0032	0.0017	0.0017	0.0017
Fe ₂ O ₃	0.0150	0.0150	0.0100	0.0100	0.0100	0.0100	0.0100
K ₂ O	0.0150	0.0150	0.0040	0.0040	0.0016	0.0016	0.0016
Li ₂ O	0.0201	0.0201	0.0200	0.0200	0.0000	0.0000	0.0000
MgO	0.0350	0.0350	0.0150	0.0150	0.0100	0.0100	0.0100
Na ₂ O	0.1000	0.1250	0.1900	0.1900	0.2098	0.2098	0.2098
NiO	0.0000	0.0000	0.0000	0.0000	0.0004	0.0004	0.0004
P ₂ O ₅	0.0020	0.0020	0.0068	0.0068	0.0029	0.0029	0.0029
PbO	0.0000	0.0000	0.0000	0.0000	0.0001	0.0001	0.0001
SiO ₂	0.4700	0.4700	0.3955	0.3955	0.3714	0.3714	0.3714
SO ₃	0.0061	0.0061	0.0070	0.0070	0.0106	0.0106	0.0106
SnO ₂	0.0500	0.0500 ^(b)	0.0200	0.0200	0.0000	0.0000	0.0000
V ₂ O ₅	0.0000	0.0000	0.0200	0.0200	0.0100	0.0100	0.0100
ZnO	0.0100	0.0100	0.0300	0.0300	0.0300	0.0300	0.0300
ZrO ₂	0.0000	0.0000	0.0300	0.0300	0.0300	0.0300	0.0300
Total^(a)	1.0000	1.0000	1.0000	1.0000	1.0001	1.0001	1.0001

(a) The mass fractions of the glass compositions were originally calculated to more than four decimal places, so rounding to four decimal places caused the totals to differ from 1.0000 by ± 0.0001 .

(b) This was added as tin oxalate and not SnO₂.

1.3 Quality Assurance

1.3.1 PNNL Quality Assurance Program

The PNNL Quality Assurance (QA) Program is based upon the requirements as defined in DOE Order 414.1D, *Quality Assurance*, and 10 CFR 830, *Energy/Nuclear Safety Management*, Subpart A, *Quality Assurance Requirements* (a.k.a., the Quality Rule). PNNL has chosen to implement the following consensus standards in a graded approach:

- ASME NQA-1-2000, *Quality Assurance Requirements for Nuclear Facility Applications*, Part I, “Requirements for Quality Assurance Programs for Nuclear Facilities”
- ASME NQA-1-2000, Part II, Subpart 2.7, “Quality Assurance Requirements for Computer Software for Nuclear Facility Applications,” including problem reporting and corrective action
- ASME NQA-1-2000, Part IV, Subpart 4.2, “Guidance on Graded Application of Quality Assurance (QA) for Nuclear-Related Research and Development.”

The PNNL *Quality Assurance Program Description / Quality Management M&O Program Description* describes the Laboratory-level QA program that applies to all work performed by PNNL. Laboratory-level procedures for implementing the QA requirements described in the standards identified above are deployed through PNNL’s web-based “How Do I...?” (HDI) system, which is a standards-based system for managing and deploying requirements and procedures to PNNL staff. The HDI procedures (called Workflows and Work Controls) provide detailed guidance for performing some types of tasks, such as protecting classified information and procuring items and services, as well as general guidelines for performing research-related tasks, such as preparing and reviewing calculations and calibrating and controlling measuring and test equipment.

1.3.2 EWG Quality Assurance Program

Until May 31, 2016, the Enhanced Waste Glass Project used the Washington River Protection Solutions Waste Form Testing Program (WWFTP) QA program as the basis for performing work. The WWFTP QA program implements the requirements of NQA-1-2008, *Quality Assurance Requirements for Nuclear Facility Applications*, and NQA-1a-2009, Addenda to ASME NQA-1-2008, *Quality Assurance Requirements for Nuclear Facility Applications*, graded on the approach presented in NQA-1-2008, Part IV, Subpart 4.2. On June 1, 2016, the Enhanced Waste Glass Project transferred to the PNNL nuclear quality assurance program; this program establishes an ASME NQA-1-2012, 10 CFR 830, Subpart A DOE Order (O) 414.1D compliant QA program for use by research and development (R&D) projects and programs that are compatible with the editions of ASME NQA-1 2000 through 2012.

All of the work reported in this document was performed to the QA level of Applied Research:

Applied research work activities (or deliverables) apply to nuclear and non-nuclear R&D (work activities or deliverables) that are processes initiated-with-the-intent of solving a specific problem or meeting a practical need. For applied research activities, grading is minimal and largely contingent upon the complexity of the research and the ability to duplicate the research if data were lost. The elements of QA grading, including the level of documentation, were applied to the program-, project-, and task- levels.

Analytical results from test instruction TI-EWG-0015⁽¹⁾ were qualified as acceptable through the “Qualifying Existing Data” process documented in EWG-DQP-0003⁽²⁾ and EWG-DQR-0003.⁽³⁾

¹ Lang, JB. 2014. EWG-Low Activity Waste (LAW) Glass Studies. TI-EWG-0015, Rev. 0, Pacific Northwest National Laboratory, Richland, WA.

² Meier, KM. 2016. Data Qualification Plan for Test Instruction EWG-015. EWG-DQP-0003, Rev. 0, Pacific Northwest National Laboratory, Richland, WA.

³ Meier, KM. 2016. Data Qualification Report for Test Instruction EWG-015. EWG-DQR-0003, Rev. 0, Pacific Northwest National Laboratory, Richland, WA.

2.0 Test Methods

This section describes how the data was obtained for these glasses; including the glass fabrication, chemical composition analysis, density, viscosity, electrical conductivity, crystal fraction, secondary phase identification, PCT, VHT, iron redox, and sulfate solubility measurements for the test glasses.

2.1 Glass Fabrication

Glass fabrication was performed according to the PNNL procedure GDL-GBM-1.⁽¹⁾ Single metal oxides, single metal carbonates, and sodium salts were mixed in the appropriate masses to form the target glass composition. Each glass was melted in a Pt-alloy crucible using a two-step melt process. The first melt was of raw materials after mechanically mixing in an agate milling chamber for 2 min and V-blending for 30 min. Melting was performed at temperatures ranging from 1150°C to 1300°C for 1 h to 1.5 h. A second melt of the glass was accomplished after the quenched glass was ground to a fine powder in a tungsten carbide vibratory mill. Generally, the second melt was at the same temperature or 25°C to 50°C higher than the initial melt and 1 h to 1.5 h in duration. See Table 2.1 for specific melt times and temperatures for each glass. A few of the matrix glasses required temperatures up to 1300°C and more than two iterations of grinding and melting to fully dissolve all the starting materials.

2.2 Chemical Analysis of Glass Composition

To confirm that the “as-fabricated” glasses corresponded to the specified target compositions, a representative sample of each glass was chemically analyzed at the Savannah River National Laboratory (SRNL) Process Science Analytical Laboratory. Three preparation techniques, including sodium peroxide fusion (PF), lithium metaborate/tetraborate fusion (LM), and potassium hydroxide digestion (KH) were used to prepare the glass samples, in duplicate, for analysis.

Each sample was analyzed, twice for each element of interest, by inductively coupled plasma–atomic emission spectroscopy (ICP-AES) and ion chromatography (IC) for a total of four measurements per element. Glass composition standards were also intermittently measured to assess the performance of the ICP-AES and IC instruments over the course of these analyses. Specifically, several samples of the low-level reference material were included as part of the analytical plan. The preparation and measurement methods used for each of the reported glass analytes are listed in Table 2.2.

A detailed analysis of the chemical composition measurements is published elsewhere (Fox et al. 2015a and 2015b). A short summary of these analyses is included in Section 3.1.

¹ Schweiger, MJ. 2014. *Glass Development Lab Procedure: Glass Batching and Melting*. GDL-GBM-1, Pacific Northwest National Laboratory, Richland, WA.

Table 2.1. Melting Temperatures and Times Used in Fabricating the Phase 1 Enhanced LAW Waste Glasses

Glass ID	First Melt			Second and More Melts		
	Date	Temp. (°C)	Time (h)	Date	Temp. (°C)	Time (h)
New-IL-456	6/20/14	1150	1	6/23/14, 6/23/14, 6/23/14	1150, 1175, 1200	1, 1, 1
New-IL-1721	9/10/14	1150	1	9/11/14	1150	1
New-IL-5253	10/7/14	1200	1	10/8/14	1150	1
New-IL-5255	9/25/14	1175	1	9/29/14	1175	1
New-IL-42295	6/24/14	1150	1	6/27/14	1150	1
New-IL-70316	9/23/14	1200	1	9/24/14	1200	1
New-IL-87749	7/2/14	1200	1.5	7/3/14	1225	1
New-IL-93907	9/30/14	1150	1	9/30/14	1150	1
New-IL-94020	7/15/14	1200	1	7/15/14, 7/16/14, 7/17/14	1275, 1275, 1275	1, 1.5, 1
New-IL-103151	7/18/14	1200	1.25	7/21/14	1225	1.5
New-IL-151542	9/11/14	1200	1	9/16/14	1200	1
New-IL-166697	10/2/14	1200	1	10/3/14	1250	1
New-IL-166731	9/3/14	1200	1	9/4/14	1200	1.5
New-OL-8445	7/21/14	1200	1	7/23/14, 7/23/14	1225, 1225	1.5, 1
New-OL-8788(Mod)	10/21/14	1300	1	10/22/14	1300	1
New-OL-14844	6/12/14	1150	1	6/16/14, 8/13/14	1150, 1250	1.5, 1.5
New-OL-15493	8/19/14	1200	1	8/21/14	1200	1
New-OL-17130	6/10/14	1150	1.25	6/11/14	1150	1
New-OL-45748(Sn Mod)	10/9/14	1300	1	10/10/14	1300	1
New-OL-54017(Sn Mod)	10/23/14	1250	1.5	10/28/14	1250	1
New-OL-57284	7/29/14	1225	1	7/30/14	1225	1
New-OL-62380	8/13/14	1300	1	8/18/14	1275	1
New-OL-62909(Mod)	11/11/14	1300	1	11/12/14	1300	1
New-OL-65959(Mod)	10/29/14	1250	1	10/30/14	1225	1
New-OL-80309	9/8/14	1200	1	9/9/14	1300	1.5
New-OL-90780	8/25/14	1150	1	8/26/14	1175	1.5
New-OL-100210	7/6/14	1225	1	7/7/14	1225	1
New-OL-108249(SO ₃ Mod)	12/18/14	1100	1	12/30/14	1300	1
New-OL-116208(SO ₃ Mod)	2/24/15	1300	1	2/25/15	1300	1
New-OL-122817	8/21/14	1200	1	8/25/14	1200	1
New-OL-127708(Mod)	11/4/14	1300	1	11/5/14	1300	1
EWG-LAW-Centroid-1	8/12/14	1150	1	8/12/14	1150	1
EWG-LAW-Centroid-2	8/21/14	1150	1	8/25/14	1150	1
LAW-ORP-LD1(1)	8/6/14	1200	1	8/6/14	1300	1
LAW-ORP-LD1(2)	10/15/14	1125	1	10/16/14	1300	1
LAW-ORP-LD1(3)	2/6/15	1250	1	2/12/15, 2/13/15	1250, 1300	1, 1

Table 2.2. Preparation and Measurement Methods Used in Reporting the Measured Concentrations of Each of the Analytes of the Study Glasses

Analyte	Preparation Method	Measurement Method
Al	PF	ICP-AES
B	PF	ICP-AES
Ca	LM	ICP-AES
Cl	KH	IC
Cr	LM	ICP-AES
F	KH	IC
Fe	PF	ICP-AES
K	LM	ICP-AES
Li	PF	ICP-AES
Mg	LM	ICP-AES
Na	LM	ICP-AES
P	LM	ICP-AES
Si	PF	ICP-AES
Sn	LM	ICP-AES
S	LM	ICP-AES
V	LM	ICP-AES
Zn	LM	ICP-AES
Zr	LM	ICP-AES

PF = peroxide fusion
LM = lithium metaborate/tetraborate fusion
KH = potassium hydroxide digestion
ICP-AES = inductively coupled plasma-atomic emission spectrometry
IC = ion chromatography

2.3 Glass Density

The room temperature density of each glass was measured according to OP-WTPSP-008⁽¹⁾ using a MicroMeritics AccuPyc II 1340 gas pycnometer (MicroMeritics, Norcross, Georgia) with approximately 0.1 mg of glass pieces. The glass was loaded into a vial and placed within the instrument. The instrument then determined the density by the difference in amount of helium gas needed to fill the vial. After five runs for each glass, the average glass densities were calculated. The pycnometer was calibrated before and after measurements for that day using a National Institute of Standards and Technology traceable standard tungsten carbide ball.

2.4 Viscosity

The viscosity of each glass was measured as a function of temperature following GDL-Visc-Test-01, Rev. 0⁽²⁾ using a Brookfield rotating spindle digital viscometer (DV-III) (Brookfield, Middleboro, Massachusetts) staged above a high-temperature Deltech® furnace (Deltech, Denver, Colorado) and equipped with a Pt/Rh spindle which fit through a hole in the top of the furnace. A 50-mL glass sample, determined by weight and glass density, was added into a Pt/Rh alloy crucible and placed into the furnace set at 1150°C. The spindle was immersed in the molten glass in the center of the crucible with the lower end of the rod at 5.1 mm above the bottom of the crucible. A thermocouple was located directly under the bottom, center of the crucible. The furnace was set to the required ramp/soak schedule and spindle torque and temperature was recorded. The temperature sequence was 1150°C, 1050°C, 950°C, 1150°C, 1250°C,

¹ Rinehart DE. 2011. *Density Using a Gas Pycnometer*. OP-WTPSP-008, Rev. 1, Pacific Northwest National Laboratory, Richland, Washington.

² Crum JV. 2013. *PNWD Procedure: High Temperature Viscosity Measurement*. GDL-Visc-Test-01, Rev. 0.

and then 1150°C. The soak time was 30 min at each temperature. The hysteresis approach allowed for the potential impacts of crystallization (at lower temperatures) and volatility (at high temperatures) to be assessed (via reproducibility) at the repeated nominal temperature. The viscometer was calibrated with a standard glass (Defense Waste Processing Facility startup frit) both before and after the measurements (Crum et al. 2012).

2.5 Electrical Conductivity

The electrical conductivities (EC) of the molten glasses were calculated as a function of temperature using a probe with two platinum-10% rhodium blades according to procedure GDL-Elec-Test-01, Rev. 1.⁽¹⁾ About 50-mL of post-viscosity measured glass was added to a Pt/Rh alloy crucible and placed into the furnace at 1100°C. The probe was then lowered through a hole in the top of the furnace into the melt, making sure that the probe was in the center of the crucible. The EC was calculated using the automated Solartron Analytical 1455 Cell Test System (Solartron Analytical, Oak Ridge, Tennessee) connected to the probe. Data was recorded at 1200, 1100, 1000, and 900°C after roughly 45-min soaks at each temperature, allowing the program to collect impedance data at frequencies of 10,000 Hz, 1000 Hz, 100 Hz and 63 Hz 5 min apart at the end of each temperature setting when the sample was at thermal equilibrium. Only the 1000 Hz frequency data were used in the EC calculation because these were the closest values to predicted impedance in the melter.

The EC system was checked at specified intervals in 0.1 M and 1 M KCl solutions at room temperature to determine a cell constant. Two measurements were taken at intervals of ~ 5 min for each solution. The cell constant was then used to calculate the conductivity of each glass melt.

2.6 Equilibrium Crystal Fraction

Equilibrium crystal fraction as a function of temperature (C_T) was measured in Pt-alloy crucibles and boats with tight fitting lids (to minimize volatility) according to the standard ASTM International procedure *Standard Test Method for Determining Liquidus Temperature of Immobilized Waste Glasses and Simulated Waste Glasses* (ASTM C1720). The heat treatment times and temperatures were 24 ± 2 h at 950°C to 1150°C to ensure equilibrium was achieved without excessive volatility. The samples were then quenched and analyzed by x-ray diffraction (XRD).

The C_T s of each crystalline phase formed during heat treatment was analyzed by XRD according to Section 12.4.4 of the standard ASTM International procedure *Standard Test Method for Determining Liquidus Temperature of Immobilized Waste Glasses and Simulated Waste Glasses* (ASTM C1720). Powdered glass samples were prepared using roughly 5 wt% CaF₂ as an internal standard phase with between 1.5 g and 2.5 g of glass powder. Glass and CaF₂ were milled together for 2 min in a 10 cm³ tungsten carbide disc mill. The powdered samples were loaded into plastic holders and analyzed using a Bruker D8 Advance XRD (Bruker AXS Inc., Madison, Wisconsin) with Cu K α emission. Samples were scanned at a 0.04° 2 θ step size, 4-sec dwell time, from 10° to 70° 2 θ scan range. XRD spectra were analyzed with Jade[®] 6.0 Software (MDI, Inc., Livermore, California) for phase identification. Full-pattern Rietveld refinement using RIQAS[®] 4 (MDI, Inc., Livermore, California) was performed to quantify the fraction of each crystal phase in some samples with high crystalline content. Optical microscopy-image analysis (OM-IA) and a JEOL 5900 scanning electron microscope (SEM) were also used to examine the crystalline phases found in some glass samples.

¹ Crum JV. 2014. *PNWD Procedure: High-Temperature Electrical Conductivity*. GDL-Elec-Test-01, Rev. 1.

2.7 Canister Centerline Cooling and Crystal Identification

A portion (~100 g) of each test glass was subjected to a simulated Canister Centerline Cooling (CCC) heat treatment according to the simulated CCC temperature profile shown in Table 2.3 and Figure 2.1. This profile is the temperature schedule of CCC treatment for Hanford LAW glasses planned for use at WTP⁽¹⁾ and modified by PNNL to include a 30-min soak at the glass melt temperature before the cooling began. Pieces of quenched glass, <1cm in diameter, were placed in a Pt-alloy crucible and covered with a Pt-alloy lid. The glass samples in simulated CCC were brought to a target temperature of the glass melting temperature and held for 30 min. Then they were quickly cooled to 1114°C. The cooling profile was then started from 1114°C to room temperature based on nine cooling segments shown in Table 2.3.

Table 2.3. Temperature Schedule during Canister Centerline Cooling Treatment of Hanford LAW Glasses

Canister Centerline Cooling Treatment Schedule			
Segment	Time (min)	Start Temperature (°C)	Rate (°C/min)
1	-30	Melt temp	0
2	0	1114	-7.125
3	0-16	1000	-1.754
4	16-73	900	-0.615
5	73-195	825	-0.312
6	195-355	775	-0.175
7	355-640	725	-0.130
8	640-1600	600	-0.095
9	1600-3710	Room temp	NA

Several of the glasses formed a crystalline layer around the edge of the Pt-alloy crucible during the CCC treatment. Therefore, different methods and types of crucibles were used to try to eliminate this feature. It was found that when molten glass was cooled in a quartz crucible this phenomenon did not occur, as discussed further in Section 3.6.

The amount and type of crystalline phases that formed during CCC treatment were analyzed by XRD according to Section 12.4.4 of the standard ASTM International procedure *Standard Test Method for Determining Liquidus Temperature of Immobilized Waste Glasses and Simulated Waste Glasses* (ASTM C1720). Powdered glass samples were prepared using roughly 5 wt% CaF₂ as an internal standard phase with between 1.5 g and 2.5 g of powdered glass. Glass and CaF₂ were milled together for 2 min in a 10 cm³ tungsten carbide disc mill. The powdered glass samples were loaded into XRD sample holders and scanned at a 0.04° 2θ step size, 4-sec dwell time, from 10° to 70° 2θ scan range. XRD spectra were analyzed with Jade[®] 6.0 Software (MDI, Inc., Livermore, California) for phase identification. Full-pattern Rietveld refinement using RIQAS[®] 4 (MDI, Inc., Livermore, California) was performed to quantify the amounts of crystal phases on some samples with high crystalline content. OM-IA and SEM were also used to examine the crystalline phases found in some CCC glass samples.

¹ Memorandum, Canister Centerline Cooling Data, Revision 1, CCN: 074851, RPP-WTP, October 29, 2003.

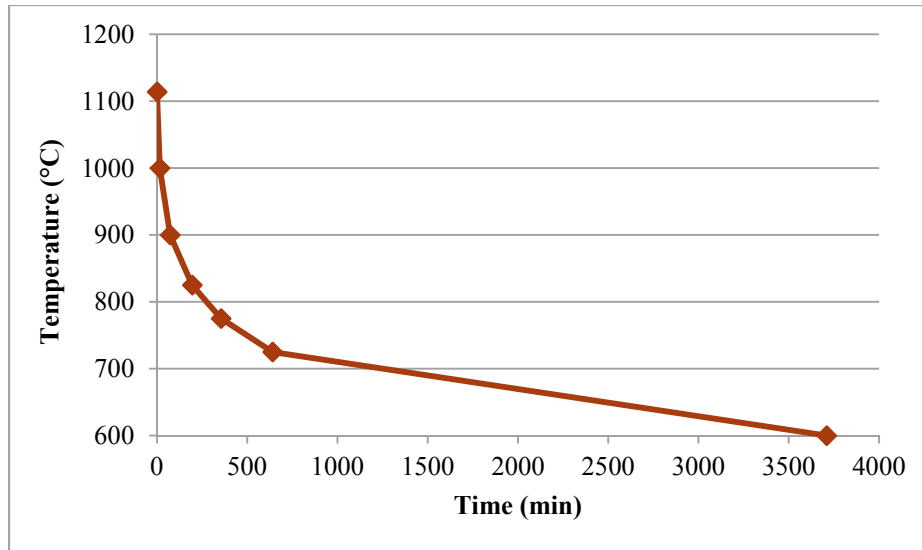


Figure 2.1. Plot of Temperature Schedule during CCC Treatment of Hanford LAW Glasses

2.8 Product Consistency Test

PCT responses were measured in triplicate at SRNL for quenched and CCC samples of each glass using Method A of the standard ASTM International procedure *Standard Test Methods for Determining Chemical Durability of Nuclear, Hazardous, and Mixed Waste Glasses and Multiphase Glass Ceramics: The Product Consistency Test (PCT)* (ASTM C1285). Also included in the PCT experimental test matrix and tested in triplicate were the Environmental Assessment (Jantzen et al. 1993) glass, the Approved Reference Material (Mellinger and Daniel 1984) glass, and blanks. Glass samples were ground, sieved to -100 +200 mesh, washed, and prepared according to the standard ASTM International procedure. The prepared glass was added to water in a 1 g to 10 mL ratio, resulting in a glass surface area-to-solution volume ratio of approximately 2000 m⁻¹. The vessels used were desensitized Type 304L stainless steel. The vessels were closed, sealed, and placed into an oven at 90 ±2°C for 7 days ±3 h.

After the 7-day PCT, the vessels were removed from the oven and allowed to cool to room temperature. The final mass of the vessel and the solution pH were recorded on a data sheet. Each test solution was then filtered through a 0.45-µm-size filter and acidified with concentrated, high-purity HNO₃ to 1 vol% to assure that the cations remained in solution. The resulting solutions were analyzed by the Process Science Analytical Laboratory at SRNL for Si, Na, B, and Li. Samples of a multi-element, standard solution were also analyzed as a check on the accuracy of the ICP-AES. Normalized release rates were calculated based on target, measured, and bias-corrected compositions using the average of the logarithms of the leachate concentrations. Results from the PCT work are published elsewhere (Fox et al. 2015a, 2015b), and a short summary of these results is included in Section 3.7.

2.9 Vapor Hydration Test

In the VHT, monolithic glass samples were exposed to water vapor at 200°C in sealed stainless steel vessels for 1, 7 and 24 days according to the standard ASTM International procedure *Standard Test Method for Measuring Waste Glass or Glass Ceramic Durability by Vapor Hydration Test* (ASTM C1663). Roughly 1-mm by 10-mm by 10-mm samples were cut from annealed or CCC-treated LAW glass bars using a diamond-impregnated saw. All sides of the cut sample were polished to 600-grit surface finishes with silicon carbide paper.

Polished samples were hung from stainless steel supports on Pt wire within a stainless steel container as shown in Figure 2.2. Deionized water (DIW) was added to the bottom of the vessel so that enough water was present to react with the specimen without sufficient water to reflux during testing (~0.20 g). The samples were heated and held at 200°C in a convection oven for the specified time period. The LAW glasses were tested for 24 days initially. Then, the glasses that completely corroded after that test duration were tested for 7 days. Finally, the glasses that completely corroded after 7 days were tested for 1 day.

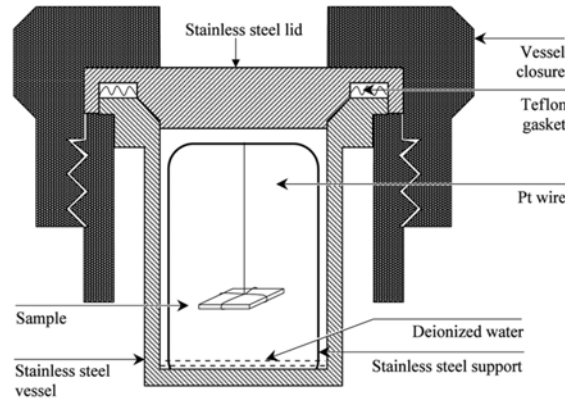


Figure 2.2. Apparatus for Conducting VHTs

After removal from the oven, vessels were weighed and then quenched in cold water. The specimens were removed from the vessels and cross-sectioned with or without epoxy (depending on the stability of each sample) for analysis by OM-IA and/or SEM to determine the amount of glass altered during the test.

The remaining glass thickness of the VHT specimen was determined by performing at least 10 measurements distributed (roughly equally) across the crack-free cross section of the sample. Then, the average and standard deviation of the 10 thickness measurements of the remaining glass were calculated. The amount of glass altered per unit surface area of specimen was determined from the average thickness of unaltered glass according to

$$m = \frac{1}{2} \rho (d_i - d_r) = \frac{m_i}{2w_i l_i} \left(1 - \frac{d_r}{d_i} \right), \quad (2.1)$$

where,

- w_i, d_i, l_i = initial specimen width, thickness, and length, respectively
- d_r = average thickness of remaining glass layer
- m_i = initial specimen mass
- m = mass of glass converted to alteration products per unit surface area
- ρ = glass density.

The average rate of corrosion was calculated as $r_a = m/t$, where t is the corrosion time. Vienna et al. (2001) showed that, if the average rate of corrosion at 200°C is

$$r_a = m/t < 50 \text{ g}/(\text{m}^2 \cdot \text{d}) \quad (2.2)$$

then the final rate of corrosion, $r_\infty < 50 \text{ g}/(\text{m}^2 \cdot \text{d})$, meets the current ORP requirement for LAW glass performance as long as the test is run for at least 7 d.

2.10 Sulfur Solubility

Sulfur solubility in the LAW Phase 1 Matrix glasses was measured using the procedure found in EWG-TI-026.⁽¹⁾ The procedure is briefly described in this section.

There are three primary phases of testing with each glass:

1. Saturation with sodium sulfate
2. DIW Wash Test
3. Analysis.

Saturation with sodium sulfate was performed by taking 100 g of each LAW matrix glass (except one sample of LAW-ORP-LD1(3), of which 80 g was used). The starting glass was ground and sieved through a #120 sieve (125 μm). Then, 7.64 g of Na_2SO_4 was mixed with the 100 g of sized glass powder to maintain a 4 mol% SO_3 in the glass/salt system. The mixture of glass and Na_2SO_4 was melted at 1150°C for 1 h in a Pt/Rh alloy crucible with a tight fitting lid. After melting, the mixture was poured onto a steel plate and quenched. The mixture was again crushed and sieved through a #120 sieve (125 μm), and placed back into the Pt/Rh alloy crucible to melt at 1150°C for 1 h the second time. After the second melting, the mixture was quenched by pouring on a steel plate, crushed, sieved, and melted under the same conditions for the third time. The glass, after three-times re-melting and re-mixing, was crushed and sieved through the #120 sieve (125 μm) sieve.

Each of the ground and sieved samples was washed with DIW to remove excess salts prior to further analysis. Four grams of each glass/salt mixture was measured and added to a beaker after three-times re-melting and re-mixing of each sample. Then 50 g of DIW were added to the beaker. The beaker was placed in an ultrasonic bath for 3 min to wash the glass powder. After washing, the water and glass from the beaker were vacuum filtered through a 0.2 μm polyvinylidene difluoride membrane disc filter installed on a 47 mm magnetic filter funnel. An additional 50 g DIW was used to rinse the beaker and the sample in the funnel, which was also filtered and collected in the same flask. A total of 100 g DIW was used for washing one sample.

The washed glasses and the wash solutions were analyzed by ICP-AES and IC at SRNL. A total of 18 elements were analyzed. The following 16 elements were analyzed by ICP-AES: Al, B, Ca, Cr, Fe, K, Li, Mg, Na, P, Si, S, Sn, V, Zn, and Zr. Cl, SO_4 , and F were analyzed by IC.

2.11 Iron Redox

For the tin to be soluble in the glasses, a few glasses were prepared using tin(II) oxalate (SnC_2O_4) instead of SnO_2 . Because tin(II) is a reducing agent, an effort was made to determine how much of the iron in these glasses was affected. The Fe^{2+} concentration in the samples was determined using the Stucki method (Stucki 1981). The samples were digested with $\text{HF-H}_2\text{SO}_4$ in the presence of 1,10-phenanthroline. The Fe^{2+} forms a colored complex with the 1,10-phenanthroline which is measured spectrophotometrically against a calibration curve that is also taken through the digestion procedure. The total iron in the digestates was determined by ICP-AES. The Fe^{3+} was determined by the difference. Using the Fe^{2+} and the calculated Fe^{3+} , the $\text{Fe}^{2+}/\text{Fe}^{3+}$ was also calculated.

¹ Jin, T. 2016. *Test Instruction for Sulfate Solubility for LAW Phase 1 Matrix Glasses*. EWG-TI-026.

3.0 Results and Discussion

This section describes the test results for the chemical composition, density, viscosity, EC, crystal fraction, secondary phase identification, PCT, VHT, sulfate solubility, iron redox, and glass composition modifications for these LAW glasses studied.

3.1 Chemical Analysis of Glass Composition

The targeted and average measured component concentrations (wt%) in the quenched glasses are presented in Appendix A. The composition analyses of the glass samples were performed as described in Section 2.2.

Plots of the measured oxide values and measured versus targeted compositions are presented in Exhibit A-2 and Exhibit A-4 of Fox et al. (2015a, 2015b). Some observations of the analysis can be made.

- There appear to be some differences among the calibration blocks for the Na₂O measurements.
- There appears to be scatter among the SiO₂ values for some of the study glasses.
- There appears to be scatter among the B₂O₃ and Na₂O values for the study glasses.
- The measured Cl, SO₃, and F values appear to be biased somewhat low.
- Glass New-OL-108249 (SO₃ Mod) contained a small but measureable amount of MgO, while the targeted MgO concentration for this glass was zero. This measurement was confirmed via an additional preparation and measurement.
- All of the measured sums of oxides for the first set of study glasses fell within the interval of 96 wt% to 101 wt%, indicating recovery of all components. The second set of measured sums of oxides for the study glasses fell within the interval of 97.9 wt% to 100.7 wt%, indicating recovery of all components. Comparisons of the targeted and measured chemical compositions showed that the measured values for the glasses were within 10% (relative) of the targeted concentrations for those components present at more than 5 wt%.

The Al₂O₃ concentration of glass EWG-LAW-ORP-LD1(3) was about 45% higher than the targeted value with B₂O₃, CaO, Na₂O, SiO₂, ZnO, and ZrO₂ below their targeted values. Upon further inspection we determined that the incorrect aluminum source had been batched into the glass giving it a different composition than intended. Therefore, based on the compositional analysis of these glasses, we concluded that the targeted compositions are adequate for use in future work to develop property-composition models except for the EWG-LAW-ORP-LD1(3). This glass composition was modified from the target composition to the composition that actually was used.

The plots of measured oxide concentrations and measured versus targeted oxide concentrations in Exhibit A-1 and Exhibit A-4 of the Fox et al. (2015a,b) reports were considered to assess whether any components volatilized. In these plots, the data points associated with the measured Cl, F, and SO₃ concentrations were observed to be somewhat scattered. Some Cl, F, and SO₃ volatilization is likely, but the scatter in the measured values makes it difficult to quantify. Other than this observation, there was no indication of significant volatilization.

3.2 Density

This section presents and discusses the results of the glass density measurements obtained using the methods discussed in Section 2.3. The results of the glass density measurements are shown in Table 3.1. The densities ranged from approximately 2.5 g/cm³ to 2.9 g/cm³. The WTP Contract Specification 2 (DOE 2000) for package dimension, weight, and void fraction limits the glass density to 3.7 g/cm³, which all of these glasses met. Figure 3.1 compares these measured density results to predicted density results obtained from the density model

$$\rho = \frac{\sum_{i=1}^N M_i x_i}{V}, \quad (3.1)$$

where M_i is the molecular mass of the i^{th} component, x_i is the mole fraction of the i^{th} component, and V is molar volume (Vienna et al. 2003b). The predicted density from the model was higher than the measured density for all but two of the glass compositions. This difference indicates that the density model should to be re-fit to account for data in the enhanced LAW glass composition region. It is recommended that more data be obtained in this composition region and then a new model be developed to predict the glass density before the WTP vitrification facility begins operation.

Table 3.1. Measured Densities of Phase 1 Enhanced LAW Glasses

Glass ID	Measured Density (g/cm³)	Glass ID	Measured Density (g/cm³)
New-IL-456	2.70	New-OL-45748 (Sn Mod)	2.78
New-IL-1721	2.63	New-OL-54017 (Sn Mod)	2.79
New-IL-5253	2.70	New-OL-57284	2.63
New-IL-5255	2.72	New-OL-62380	2.87
New-IL-42295	2.64	New-OL-62909 (Mod)	2.79
New-IL-70316	2.70	New-OL-65959 (Mod)	2.66
New-IL-87749	2.70	New-OL-80309	2.76
New-IL-93907	2.61	New-OL-90780	2.53
New-IL-94020	2.67	New-OL-100210	2.65
New-IL-103151	2.68	New-OL-108249 (SO ₃ Mod)	2.74
New-IL-151542	2.70	New-OL-116208 (SO ₃ Mod)	2.82
New-IL-166697	2.66	New-OL-122817	2.69
New-IL-166731	2.66	New-OL-127708 (Mod)	2.58
New-OL-8445	2.69	EWG-LAW-Centroid-1	2.67
New-OL-8788 (Mod)	2.64	EWG-LAW-Centroid-2	2.68
New-OL-14844	2.79	LAW-ORP-LD1(1)	2.66
New-OL-15493	2.70	LAW-ORP-LD1(2)	2.67
New-OL-17130	2.59	LAW-ORP-LD1(3)	2.63

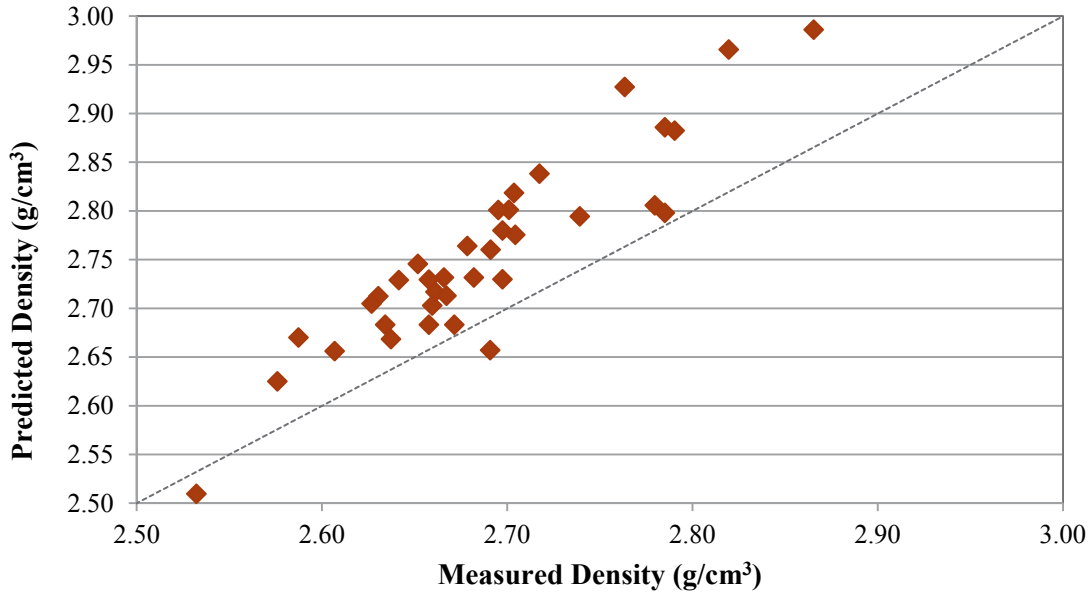


Figure 3.1. Predicted versus Measured Density for Phase 1 Enhanced LAW Glasses

3.3 Viscosity (η)

This section presents and discusses the viscosity results obtained using the methods discussed in Section 2.4. The results of the viscosity measurements are listed in Appendix B and summarized in Table 3.2. The temperature sequence used was 1150°C, 1050°C, 950°C, 1150°C, 1250°C, and then 1150°C. The soak time was 30 min at each temperature. The hysteresis approach allowed for the potential impacts of crystallization (at lower temperatures) and volatility (at higher temperatures) to be assessed (via reproducibility) with repeated measurements at roughly 1150°C. Viscosities at low temperatures (950 and sometimes 1050°C) were not measured for several glasses (New-IL-93907, New-IL-94020, New-IL-166731, New-OL-8788(Mod), New-OL-54017 (Sn Mod), New-OL-57284, New-OL-62909(Mod), New-OL-122817, New-OL-127708(Mod), and LAW-ORP-LD1(3)) because the viscosity had increased beyond the ~50 Pa·s upper limit for the viscometer.

Two model forms are widely used to fit viscosity-temperature data for each waste glass. The first model form is the Arrhenius equation

$$\ln(\eta) = A + \frac{B}{T_K} \quad (3.2)$$

where A and B are independent of temperature and temperature (T_K) is in K ($T(^{\circ}\text{C}) + 273.15$). The values for the A and B coefficients are shown in

Table 3.3. Measured η (Pa·s) Values Versus Target Temperature (a) (in the sequence of measurement) for the Phase 1 Enhanced LAW Glasses Tested (cont.)

Glass ID	1150		1250		1150	
	Measured T (°C)	Measured η (Pa·s)	Measured T (°C)	Measured η (Pa·s)	Measured T (°C)	Measured η (Pa·s)
New-IL-456	1135	2.545	1234	1.240	1140	2.649
New-IL-1721	1135	2.808	1234	1.473	1140	2.983
New-IL-5253	1135	2.558	1234	1.296	1140	2.696
New-IL-5255	1135	1.497	1235	0.755	1140	1.557
New-IL-42295	1133	2.442	1233	1.261	1140	2.463
New-IL-70316	1134	2.273	1234	1.155	1142	2.395
New-IL-87749	1134	2.259	1234	1.126	1140	2.339
New-IL-93907	1153	4.896	1243	2.762	1138	5.300
New-IL-94020	1150	5.593	1249	2.901	1159	5.263
New-IL-103151	1135	3.282	1235	1.646	1140	3.530
New-IL-151542	1134	2.698	1234	1.363	1140	2.897
New-IL-166697	1135	2.876	1234	1.384	1140	2.869
New-IL-166731	1156	2.449	1250	1.302	1140	2.961
New-OL-8445	1134	3.190	1234	1.473	1140	3.406
New-OL-8788 (Mod)	1153	24.841	1251	8.515	1151	26.956
New-OL-14844	1134	0.556	1234	0.253	1140	0.487
New-OL-15493	1134	1.312	1234	0.607	1140	1.298
New-OL-17130	1133	1.692	1233	0.882	1140	1.726
New-OL-45748 (Sn Mod)	1133	3.104	1233	1.475	1141	3.546
New-OL-54017 (Sn Mod)	1151	5.200	1251	2.595	1148	5.526
New-OL-57284	1152	7.259	1245	4.301	1143	8.336
New-OL-62380	1134	2.019	1234	0.813	1140	2.049
New-OL-62909 (Mod)	1151	4.074	1246	1.395	1149	5.021
New-OL-65959 (Mod)	1121	1.534	1224	0.873	1139	1.773
New-OL-80309	1134	0.826	1234	0.398	1141	0.879
New-OL-90780	1134	2.322	1234	1.263	1140	2.322
New-OL-100210	1134	4.802	1233	2.281	1140	4.858
New-OL-108249 (SO ₃ Mod)	1123	2.049	1226	0.724	-- ^(b)	-- ^(b)
New-OL-116208 (SO ₃ Mod)	1130	0.807	1231	0.333	1138	0.878
New-OL-122817	1154	3.435	1235	1.867	1140	4.192
New-OL-127708 (Mod)	1155	7.491	1252	4.603	-- ^(b)	-- ^(b)
EWG-LAW-Centroid-1	1134	3.161	1234	1.626	1140	3.413
EWG-LAW-Centroid-2	1133	3.113	1233	1.563	1139	3.305
LAW-ORP-LD1(1)	1134	3.366	1234	1.619	1141	3.497
LAW-ORP-LD1(2)	1135	3.348	1235	1.604	1141	3.399
LAW-ORP-LD1(3)	1130	5.335	1226	2.810	1135	5.381

(a) A “-” denotes that the glass viscosity was too high to measure at the target temperature.

(b) These values were inaccurate for these glasses.

Table 3.4 for each glass. The second model is the Vogel- Fulcher-Tamman- (VFT) model

$$\ln(\eta) = E + \frac{F}{T_k - T_0} \quad (3.3)$$

where E, F, and T_0 are temperature independent and composition dependent coefficients and T_K is the temperature in K ($T(^{\circ}\text{C}) + 273.15$). This model can be used to estimate the effect of temperature on viscosity over a wide range of temperatures for silicate-based glasses. Therefore, this model was also applied to the data for each glass and the E, F, and T_0 coefficients for each glass are also shown in

Table 3.3. Measured η (Pa·s) Values Versus Target Temperature (a) (in the sequence of measurement) for the Phase 1 Enhanced LAW Glasses Tested (cont.)

Target T , $^{\circ}\text{C}$	1150		1250		1150	
	Measured T ($^{\circ}\text{C}$)	Measured η (Pa·s)	Measured T ($^{\circ}\text{C}$)	Measured η (Pa·s)	Measured T ($^{\circ}\text{C}$)	Measured η (Pa·s)
New-IL-456	1135	2.545	1234	1.240	1140	2.649
New-IL-1721	1135	2.808	1234	1.473	1140	2.983
New-IL-5253	1135	2.558	1234	1.296	1140	2.696
New-IL-5255	1135	1.497	1235	0.755	1140	1.557
New-IL-42295	1133	2.442	1233	1.261	1140	2.463
New-IL-70316	1134	2.273	1234	1.155	1142	2.395
New-IL-87749	1134	2.259	1234	1.126	1140	2.339
New-IL-93907	1153	4.896	1243	2.762	1138	5.300
New-IL-94020	1150	5.593	1249	2.901	1159	5.263
New-IL-103151	1135	3.282	1235	1.646	1140	3.530
New-IL-151542	1134	2.698	1234	1.363	1140	2.897
New-IL-166697	1135	2.876	1234	1.384	1140	2.869
New-IL-166731	1156	2.449	1250	1.302	1140	2.961
New-OL-8445	1134	3.190	1234	1.473	1140	3.406
New-OL-8788 (Mod)	1153	24.841	1251	8.515	1151	26.956
New-OL-14844	1134	0.556	1234	0.253	1140	0.487
New-OL-15493	1134	1.312	1234	0.607	1140	1.298
New-OL-17130	1133	1.692	1233	0.882	1140	1.726
New-OL-45748 (Sn Mod)	1133	3.104	1233	1.475	1141	3.546
New-OL-54017 (Sn Mod)	1151	5.200	1251	2.595	1148	5.526
New-OL-57284	1152	7.259	1245	4.301	1143	8.336
New-OL-62380	1134	2.019	1234	0.813	1140	2.049
New-OL-62909 (Mod)	1151	4.074	1246	1.395	1149	5.021
New-OL-65959 (Mod)	1121	1.534	1224	0.873	1139	1.773
New-OL-80309	1134	0.826	1234	0.398	1141	0.879
New-OL-90780	1134	2.322	1234	1.263	1140	2.322
New-OL-100210	1134	4.802	1233	2.281	1140	4.858
New-OL-108249 (SO ₃ Mod)	1123	2.049	1226	0.724	-- ^(b)	-- ^(b)
New-OL-116208 (SO ₃ Mod)	1130	0.807	1231	0.333	1138	0.878
New-OL-122817	1154	3.435	1235	1.867	1140	4.192
New-OL-127708 (Mod)	1155	7.491	1252	4.603	-- ^(b)	-- ^(b)
EWG-LAW-Centroid-1	1134	3.161	1234	1.626	1140	3.413
EWG-LAW-Centroid-2	1133	3.113	1233	1.563	1139	3.305
LAW-ORP-LD1(1)	1134	3.366	1234	1.619	1141	3.497
LAW-ORP-LD1(2)	1135	3.348	1235	1.604	1141	3.399
LAW-ORP-LD1(3)	1130	5.335	1226	2.810	1135	5.381

(c) A "--" denotes that the glass viscosity was too high to measure at the target temperature.

(d) These values were inaccurate for these glasses.

Table 3.4. Furthermore,

Table 3.3. Measured η (Pa·s) Values Versus Target Temperature (a) (in the sequence of measurement) for the Phase 1 Enhanced LAW Glasses Tested (cont.)

Target T , °C	1150		1250		1150	
	Measured T (°C)	Measured η (Pa·s)	Measured T (°C)	Measured η (Pa·s)	Measured T (°C)	Measured η (Pa·s)
New-IL-456	1135	2.545	1234	1.240	1140	2.649
New-IL-1721	1135	2.808	1234	1.473	1140	2.983
New-IL-5253	1135	2.558	1234	1.296	1140	2.696
New-IL-5255	1135	1.497	1235	0.755	1140	1.557
New-IL-42295	1133	2.442	1233	1.261	1140	2.463
New-IL-70316	1134	2.273	1234	1.155	1142	2.395
New-IL-87749	1134	2.259	1234	1.126	1140	2.339
New-IL-93907	1153	4.896	1243	2.762	1138	5.300
New-IL-94020	1150	5.593	1249	2.901	1159	5.263
New-IL-103151	1135	3.282	1235	1.646	1140	3.530
New-IL-151542	1134	2.698	1234	1.363	1140	2.897
New-IL-166697	1135	2.876	1234	1.384	1140	2.869
New-IL-166731	1156	2.449	1250	1.302	1140	2.961
New-OL-8445	1134	3.190	1234	1.473	1140	3.406
New-OL-8788 (Mod)	1153	24.841	1251	8.515	1151	26.956
New-OL-14844	1134	0.556	1234	0.253	1140	0.487
New-OL-15493	1134	1.312	1234	0.607	1140	1.298
New-OL-17130	1133	1.692	1233	0.882	1140	1.726
New-OL-45748 (Sn Mod)	1133	3.104	1233	1.475	1141	3.546
New-OL-54017 (Sn Mod)	1151	5.200	1251	2.595	1148	5.526
New-OL-57284	1152	7.259	1245	4.301	1143	8.336
New-OL-62380	1134	2.019	1234	0.813	1140	2.049
New-OL-62909 (Mod)	1151	4.074	1246	1.395	1149	5.021
New-OL-65959 (Mod)	1121	1.534	1224	0.873	1139	1.773
New-OL-80309	1134	0.826	1234	0.398	1141	0.879
New-OL-90780	1134	2.322	1234	1.263	1140	2.322
New-OL-100210	1134	4.802	1233	2.281	1140	4.858
New-OL-108249 (SO ₃ Mod)	1123	2.049	1226	0.724	-- ^(b)	-- ^(b)
New-OL-116208 (SO ₃ Mod)	1130	0.807	1231	0.333	1138	0.878
New-OL-122817	1154	3.435	1235	1.867	1140	4.192
New-OL-127708 (Mod)	1155	7.491	1252	4.603	-- ^(b)	-- ^(b)
EWG-LAW-Centroid-1	1134	3.161	1234	1.626	1140	3.413
EWG-LAW-Centroid-2	1133	3.113	1233	1.563	1139	3.305
LAW-ORP-LD1(1)	1134	3.366	1234	1.619	1141	3.497
LAW-ORP-LD1(2)	1135	3.348	1235	1.604	1141	3.399
LAW-ORP-LD1(3)	1130	5.335	1226	2.810	1135	5.381

Target T , °C	1150		1250		1150	
Glass ID	Measured T (°C)	Measured η (Pa·s)	Measured T (°C)	Measured η (Pa·s)	Measured T (°C)	Measured η (Pa·s)

(e) A “-” denotes that the glass viscosity was too high to measure at the target temperature.
(f) These values were inaccurate for these glasses.

Table 3.4 summarizes the viscosity results at 1150°C (η_{1150}) calculated using equation (3.2 or 3.3) fit to each glasses measured data. As noted in Table 3.2, the measured temperatures were often slightly different from the target temperatures and the calculation was based on the more accurate measured temperature-viscosity data (the original viscosity-temperature data set shown in Appendix B). The η_{1150} was calculated by the VFT equation (Equation 3.3) for most of the glasses except two (New-OL-8788(Mod) and New-OL-122817) with odd viscosity-temperature pairs and unfeasible VFT fitting, on which Arrhenius fitting was applied instead.

Table 3.2. Measured η (Pa·s) Values Versus Target Temperature (a) (in the sequence of measurement) for the Phase 1 Enhanced LAW Glasses Tested

Target T , °C	1150		1050		950	
Glass ID	Measured T (°C)	Measured η (Pa·s)	Measured T (°C)	Measured η (Pa·s)	Measured T (°C)	Measured η (Pa·s)
New-IL-456	1138	2.528	1041	5.420	943	19.540
New-IL-1721	1138	2.808	1041	5.615	943	18.770
New-IL-5253	1138	2.552	1041	5.516	943	20.724
New-IL-5255	1137	1.473	1041	3.764	943	9.402
New-IL-42295	1136	2.410	1040	5.044	943	14.687
New-IL-70316	1137	2.265	1041	5.133	943	18.847
New-IL-87749	1137	2.214	1040	4.944	943	14.808
New-IL-93907	1137	5.163	1041	12.906	-- (a)	-- (a)
New-IL-94020	1137	8.486	1068	44.076	-- (a)	-- (a)
New-IL-103151	1138	3.278	1041	6.677	944	25.357
New-IL-151542	1137	2.697	1041	6.027	944	26.439
New-IL-166697	1137	2.686	1041	5.719	943	21.721
New-IL-166731	1137	2.924	1041	12.350	-- (a)	-- (a)
New-OL-8445	1138	3.245	1041	7.482	944	36.983
New-OL-8788 (Mod)	1138	28.911	-- (a)	-- (a)	-- (a)	-- (a)
New-OL-14844	1138	0.489	1041	1.370	943	3.775
New-OL-15493	1137	1.207	1041	3.070	943	7.710
New-OL-17130	1137	1.598	1041	3.674	942	8.045
New-OL-45748 (Sn Mod)	1137	3.057	1042	7.248	945	32.956
New-OL-54017 (Sn Mod)	1138	5.761	1042	21.226	-- (a)	-- (a)
New-OL-57284	1138	8.361	1041	31.233	-- (a)	-- (a)
New-OL-62380	1137	1.889	1041	5.345	943	31.276
New-OL-62909 (Mod)	1137	4.905	1042	23.766	-- (a)	-- (a)
New-OL-65959 (Mod)	1127	1.595	1033	4.672	938	13.984
New-OL-80309	1138	0.889	1042	2.780	944	6.414
New-OL-90780	1137	2.376	1041	5.689	943	20.895
New-OL-100210	1138	4.869	1041	10.881	943	48.452

Target T , °C	1150		1050		950	
	Measured T (°C)	Measured η (Pa·s)	Measured T (°C)	Measured η (Pa·s)	Measured T (°C)	Measured η (Pa·s)
New-OL-108249 (SO ₃ Mod)	1130	2.437	1037	5.770	941	25.191
New-OL-116208 (SO ₃ Mod)	1134	0.816	1038	2.203	942	10.334
New-OL-122817	1138	3.839	1041	8.621	-- (a)	-- (a)
New-OL-127708 (Mod)	1137	8.692	1041	28.694	-- (a)	-- (a)
EWG-LAW-Centroid-1	1137	3.089	1041	6.396	943	24.556
EWG-LAW-Centroid-2	1136	3.124	1040	6.345	943	24.256
LAW-ORP-LD1(1)	1137	3.292	1041	6.977	943	29.978
LAW-ORP-LD1(2)	1138	3.388	1042	7.052	944	30.888
LAW-ORP-LD1(3)	1130	5.310	1037	14.468	-- (a)	-- (a)

(g) A "--" denotes that the glass viscosity was too high to measure at the target temperature.
(h) These values were inaccurate for these glasses.

Table 3.3. Measured η (Pa·s) Values Versus Target Temperature (a) (in the sequence of measurement) for the Phase 1 Enhanced LAW Glasses Tested (cont.)

Target T , °C	1150		1250		1150	
	Measured T (°C)	Measured η (Pa·s)	Measured T (°C)	Measured η (Pa·s)	Measured T (°C)	Measured η (Pa·s)
New-IL-456	1135	2.545	1234	1.240	1140	2.649
New-IL-1721	1135	2.808	1234	1.473	1140	2.983
New-IL-5253	1135	2.558	1234	1.296	1140	2.696
New-IL-5255	1135	1.497	1235	0.755	1140	1.557
New-IL-42295	1133	2.442	1233	1.261	1140	2.463
New-IL-70316	1134	2.273	1234	1.155	1142	2.395
New-IL-87749	1134	2.259	1234	1.126	1140	2.339
New-IL-93907	1153	4.896	1243	2.762	1138	5.300
New-IL-94020	1150	5.593	1249	2.901	1159	5.263
New-IL-103151	1135	3.282	1235	1.646	1140	3.530
New-IL-151542	1134	2.698	1234	1.363	1140	2.897
New-IL-166697	1135	2.876	1234	1.384	1140	2.869
New-IL-166731	1156	2.449	1250	1.302	1140	2.961
New-OL-8445	1134	3.190	1234	1.473	1140	3.406
New-OL-8788 (Mod)	1153	24.841	1251	8.515	1151	26.956
New-OL-14844	1134	0.556	1234	0.253	1140	0.487
New-OL-15493	1134	1.312	1234	0.607	1140	1.298
New-OL-17130	1133	1.692	1233	0.882	1140	1.726
New-OL-45748 (Sn Mod)	1133	3.104	1233	1.475	1141	3.546
New-OL-54017 (Sn Mod)	1151	5.200	1251	2.595	1148	5.526
New-OL-57284	1152	7.259	1245	4.301	1143	8.336
New-OL-62380	1134	2.019	1234	0.813	1140	2.049
New-OL-62909 (Mod)	1151	4.074	1246	1.395	1149	5.021
New-OL-65959 (Mod)	1121	1.534	1224	0.873	1139	1.773
New-OL-80309	1134	0.826	1234	0.398	1141	0.879
New-OL-90780	1134	2.322	1234	1.263	1140	2.322
New-OL-100210	1134	4.802	1233	2.281	1140	4.858
New-OL-108249 (SO ₃ Mod)	1123	2.049	1226	0.724	-- (b)	-- (b)
New-OL-116208 (SO ₃ Mod)	1130	0.807	1231	0.333	1138	0.878
New-OL-122817	1154	3.435	1235	1.867	1140	4.192
New-OL-127708 (Mod)	1155	7.491	1252	4.603	-- (b)	-- (b)

Target T , °C	1150		1250		1150	
	Measured T (°C)	Measured η (Pa·s)	Measured T (°C)	Measured η (Pa·s)	Measured T (°C)	Measured η (Pa·s)
EWG-LAW-Centroid-1	1134	3.161	1234	1.626	1140	3.413
EWG-LAW-Centroid-2	1133	3.113	1233	1.563	1139	3.305
LAW-ORP-LD1(1)	1134	3.366	1234	1.619	1141	3.497
LAW-ORP-LD1(2)	1135	3.348	1235	1.604	1141	3.399
LAW-ORP-LD1(3)	1130	5.335	1226	2.810	1135	5.381

(i) A “-” denotes that the glass viscosity was too high to measure at the target temperature.
(j) These values were inaccurate for these glasses.

Table 3.4. Fitted Coefficients of Arrhenius and VFT Models for Viscosity of LAW Phase 1 Enhanced Glasses

Glass ID	Arrhenius Coefficients			VFT Coefficients		η_{1150} (Pa·s) ^(b)
	A, ln[Pa·s]	B, ln[Pa·s]-K	E, ln[Pa·s]	F, ln[Pa·s]-K	T_0 , K	
New-IL-456	-11.198	17127	-4.586	3948	692.6	2.266
New-IL-1721	-10.142	15791	-3.643	3136	738.0	2.545
New-IL-5253	-11.292	17292	-3.783	2978	778.1	2.304
New-IL-5255	-10.974	16089	-10.807	15644	18.6	1.393
New-IL-42295	-10.040	15414	-5.127	5023	572.5	2.178
New-IL-70316	-11.559	17512	-4.179	3273	755.5	2.061
New-IL-87749	-10.622	16139	-6.064	6198	507.8	2.029
New-IL-93907	-9.095	15241	-2.097	1906	904.5	4.847
New-IL-94020	-19.358	30508	-0.320	368	1251.7	6.198
New-IL-103151	-10.787	16923	-3.236	2688	800.3	2.943
New-IL-151542	-12.158	18607	-3.070	2172	874.2	2.423
New-IL-166697	-11.080	17086	-3.602	2878	784.1	2.464
New-IL-166731	-14.206	21749	-1.919	898	1111.6	2.619
New-OL-8445	-13.059	20107	-3.545	2638	847.4	2.821
New-OL-8788 (Mod) ^(a)	-13.499	23846	-- ^(a)	-- ^(a)	-- ^(a)	25.969
New-OL-14844	-12.966	17387	-10.457	11286	259.9	0.470
New-OL-15493	-11.173	16100	-14.704	27007	-395.7	1.155
New-OL-17130	-9.429	14026	-14.171	29679	-609.3	1.540
New-OL-45748 (Sn Mod)	-12.670	19530	-3.734	2869	820.2	2.788
New-OL-54017 (Sn Mod)	-12.515	20304	-1.541	1142	1066.6	5.272
New-OL-57284	-11.697	19687	-0.266	656	1137.1	7.604
New-OL-62380	-15.495	22847	-5.081	3404	816.1	1.691
New-OL-62909 (Mod)	-18.020	27796	-8.576	7547	672.4	4.378
New-OL-65959 (Mod)	-12.337	18081	-5.545	4459	667.7	1.430
New-OL-80309	-12.978	18159	-26.512	72885	-1347.5	0.814
New-OL-90780	-11.832	17959	-3.621	2648	818.8	2.139
New-OL-100210	-11.956	19103	-3.230	2829	817.4	4.220
New-OL-108249 (SO ₃ Mod)	-15.154	22274	-13.209	17353	156.8	1.639
New-OL-116208 (SO ₃ Mod)	-15.461	21505	-7.445	5348	667.3	0.691
New-OL-122817 ^(a)	-9.679	15584	-- ^(a)	-- ^(a)	-- ^(a)	3.568
New-OL-127708 (Mod)	-10.146	17566	0.102	534	1150.2	7.825
EWG-LAW-Centroid-1	-10.774	16848	-2.937	2348	832.5	2.825

Glass ID	Arrhenius Coefficients			VFT Coefficients		η_{1150} (Pa·s) ^(b)
	A, ln[Pa·s]	B, ln[Pa·s]-K	E, ln[Pa·s]	F, ln[Pa·s]-K	T ₀ , K	
EWG-LAW-Centroid-2	-10.919	17015	-3.252	2631	806.4	2.755
LAW-ORP-LD1(1)	-11.588	18065	-3.125	2458	838.3	2.937
LAW-ORP-LD1(2)	-11.792	18362	-3.183	2485	840.2	2.946
LAW-ORP-LD1(3)	-10.459	17114	-1.944	1588	966.2	4.618

(a) VFT fitting not applicable.

(b) VFT model was used to calculate η_{1150} ; only when VFT not applicable, Arrhenius model was used.

Figure 3.2 displays a plot of the ln(predicted viscosity) values against the ln(measured viscosity) values based on the latest LAW model from Piepel et al. (2016) and shown in Equation (3.4). Although the viscosity produced a reasonably straight line, the model was under-predicting what the values were measured to be, especially at lower viscosities. Therefore, it would be useful to re-fit the model to account for this data.

$$\begin{aligned}
\ln(\eta_{1150}) = & 15.0259(g_{Al_2O_3}) - 5.8836(g_{B_2O_3}) - 5.3224(g_{CaO}) - 0.0395(g_{Fe_2O_3}) \\
& - 0.9015(g_{K_2O}) - 31.5781(g_{Li_2O}) - 3.2548(g_{MgO}) - 7.3212(g_{Na_2O}) \\
& + 11.3813(g_{SiO_2}) + 3.7336(g_{SO_3}) + 5.1123(g_{SnO_2}) - 4.8736(g_{V_2O_5}) \\
& - 2.0498(g_{ZnO}) + 11.5939(g_{ZrO_2}) + 0.4703(g_{Others1})
\end{aligned} \tag{3.4}$$

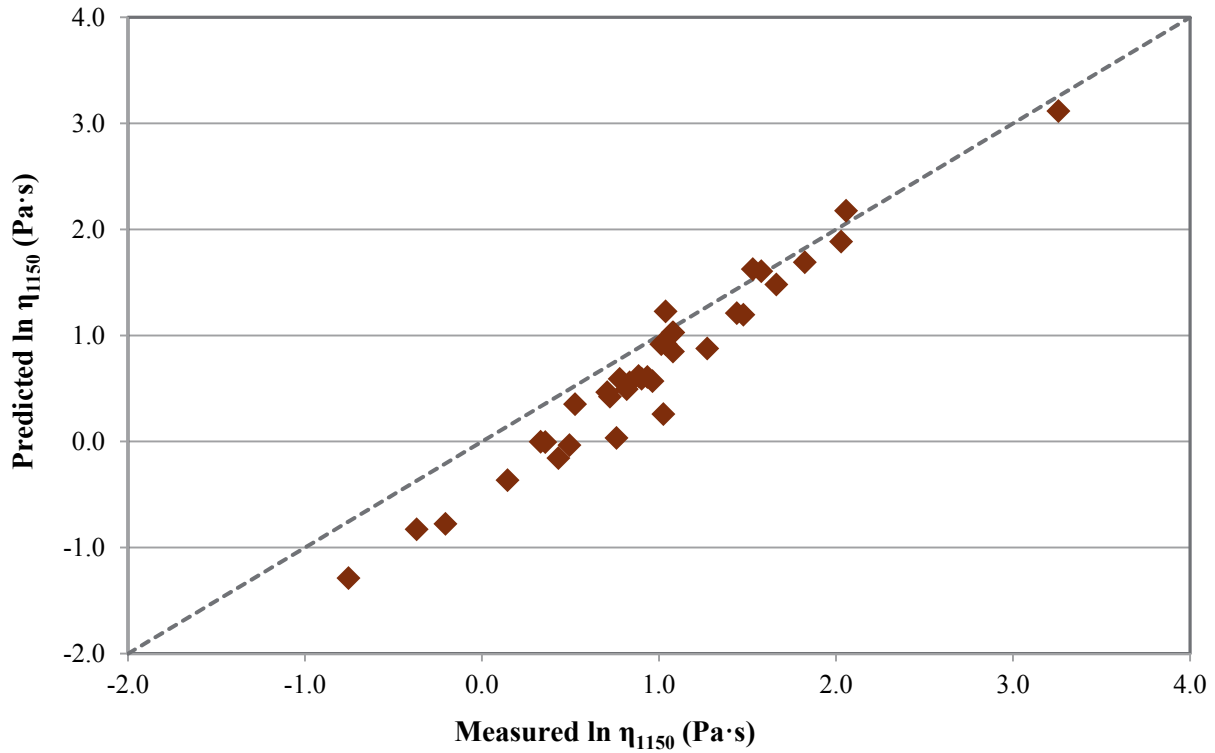


Figure 3.2. Predicted Versus Measured Viscosity Data for Phase 1 Enhanced LAW Glasses

3.4 Electrical Conductivity

This section presents and discusses the EC results obtained using the methods discussed in Section 2.5.

Table 3.5 lists the EC versus temperature data for each of the glasses, and Appendix C shows the plots for the EC versus temperature data obtained from the EC experiments.

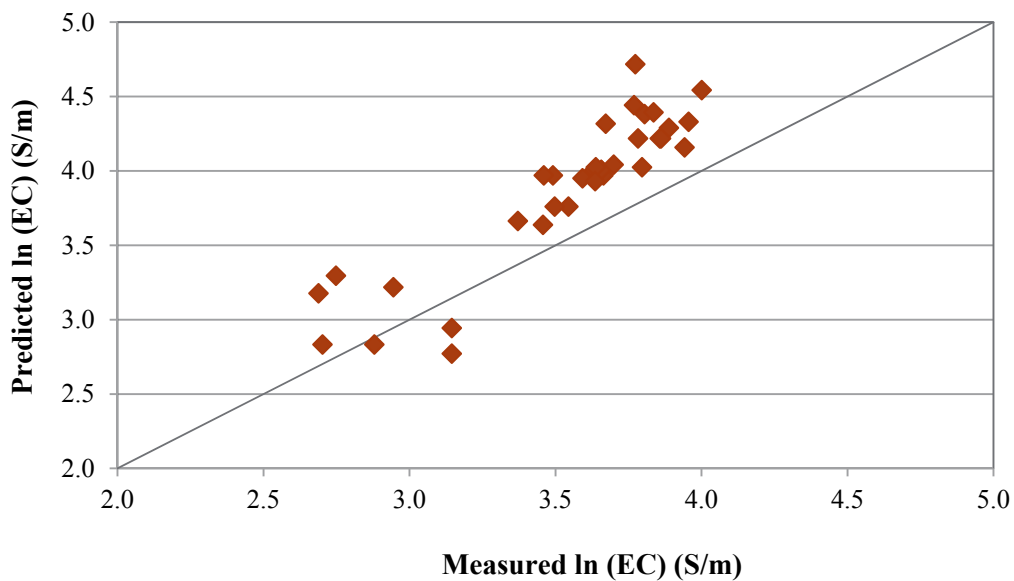


Figure 3.3 shows the ln(EC) plot for predicted versus measured EC, where the predicted values were produced by the modified Arrhenius equation parameters expanded as linear matrix models plus three alkali and alkaline earth cross-product terms (Model 3 [25 term] from Piepel et al. 2007) shown below:

$$\ln(\text{EC}) = \sum_{i=1}^q a_i x_i + a_{\text{CaOLi2O}} x_{\text{CaO}} x_{\text{Li2O}} + a_{\text{CaONa2O}} x_{\text{CaO}} x_{\text{Na2O}} + a_{\text{Li2ONa2O}} x_{\text{Li2O}} x_{\text{Na2O}} + E_G + \sum_{i=1}^q b_i \frac{x_i}{T} + E_T \quad (3.3)$$

The measured value at 1 kHz is plotted because this is the frequency used in the model and is closest to the real impedance. This model didn't predict this data well as it over-predicted the EC in all but three instances. This could be because of the different glass composition region that the LAW Phase 1 study explored versus the composition region explored for the models in Piepel et al. (2007). Therefore, a new model exploring a wider composition region would be useful to account for this data. It is recommended that more data be obtained in this wider composition region and then a new model be developed to predict the electrical conductivity before the WTP vitrification facility begins operation.

Table 3.5. Measured Electrical Conductivity (S/m) Values Versus Temperatures for the LAW Phase 1 Enhanced Glasses

Target T, °C	1250		1150		1150	
	Measured T (°C)	EC (S/m)	Measured T (°C)	EC (S/m)	Measured T (°C)	EC (S/m)
New-IL-456	1237	46.16	1139	34.65	1139	34.63
New-IL-1721	1237	49.39	1139	38.72	1139	38.69
New-IL-5253	1236	46.03	1139	36.29	NM	NM
New-IL-5255	1236	60.42	1140	48.77	NM	NM
New-IL-42295	1237	55.75	1140	44.51	1140	44.49
New-IL-70316	1239	48.81	1141	38.00	NM	NM
New-IL-87749	1237	51.15	1140	40.40	1140	40.42
New-IL-93907	1236	42.94	1138	33.05	1138	32.99
New-IL-94020	1236	9.76	NM	NM	NM	NM
New-IL-103151	1237	55.42	1139	44.88	NM	NM
New-IL-151542	1237	38.90	1140	29.08	NM	NM
New-IL-166697	1236	58.72	1139	47.32	NM	NM
New-IL-166731	1235	54.81	1138	43.91	1138	43.95
New-OL-8445	1237	22.62	1139	14.85	NM	NM
New-OL-8788 (Mod)	1237	24.15	1139	17.82	1139	17.81
New-OL-14844	1236	66.22	1140	52.18	NM	NM
New-OL-15493	1239	67.28	1142	54.57	NM	NM
New-OL-17130	1236	59.02	1139	47.45	NM	NM
New-OL-45748 (Sn Mod)	1230	42.43	1134	37.85	NM	NM
New-OL-54017 (Sn Mod)	1236	27.68	1139	19.01	1139	19.04
New-OL-57284	1239	20.03	1141	14.68	NM	NM
New-OL-62380	1238	18.76	1141	15.60	1141	15.56
New-OL-62909 (Mod)	1233	33.65	1136	23.23	1136	23.22
New-OL-65959 (Mod)	1239	54.78	1142	46.27	1142	46.31
New-OL-80309	1236	48.92	1139	43.26	NM	NM
New-OL-90780	1232	63.07	1136	51.51	1136	51.58
New-OL-100210	1237	50.99	1139	43.48	1139	43.53
New-OL-108249 (SO ₃ Mod)	1236	48.85	1140	39.33	NM	NM
New-OL-116208 (SO ₃ Mod)	1236	64.86	NM	NM	NM	NM

Target T, °C	1250		1150		1150	
	Measured T (°C)	EC (S/m)	Measured T (°C)	EC (S/m)	Measured T (°C)	EC (S/m)
New-OL-122817	1235	41.87	1139	31.70	NM	NM
New-OL-127708 (Mod)	1236	31.14	1139	23.15	NM	NM
EWG-LAW-Centroid-1	1238	48.32	1141	37.80	NM	NM
EWG-LAW-Centroid-2	1235	49.44	1134	38.72	1134	38.67
LAW-ORP-LD1(1)	1233	41.59	1137	32.79	NM	NM
LAW-ORP-LD1(2)	1230	49.49	1134	38.97	1134	38.98
LAW-ORP-LD1(3)	1233	41.04	1137	31.76	NM	NM

NM = not measured

Table 3.6. Measured Electrical Conductivity (S/m) Values Versus Temperatures for the LAW Phase 1 Enhanced Glasses (cont.)

Target T, °C	1050		950		950	
	Measured T (°C)	EC (S/m)	Measured T (°C)	EC (S/m)	Measured T (°C)	EC (S/m)
New-IL-456	1040	23.61	940	14.05	NM	NM
New-IL-1721	1040	27.90	941	18.21	941	18.19
New-IL-5253	1041	26.08	941	16.55	941	16.56
New-IL-5255	1040	36.50	941	24.52	941	24.53
New-IL-42295	1041	33.02	942	21.96	942	21.96
New-IL-70316	1042	27.08	943	17.26	943	17.26
New-IL-87749	1041	28.97	942	18.48	NM	NM
New-IL-93907	1040	23.24	940	14.52	940	14.49
New-IL-94020	1040	5.19	941	7.14	NM	NM
New-IL-103151	1041	34.08	941	23.58	941	23.60
New-IL-151542	1041	19.79	942	11.87	942	11.86
New-IL-166697	1040	35.33	942	23.97	941	23.96
New-IL-166731	1038	32.43	932	21.56	932	21.57
New-OL-8445	1040	8.48	941	4.10	941	4.10
New-OL-8788 (Mod)	1041	12.33	942	7.59	942	7.57
New-OL-14844	1042	40.82	942	28.04	942	28.02
New-OL-15493	1043	41.47	940	22.32	940	22.26
New-OL-17130	1040	35.82	940	24.59	940	24.60
New-OL-45748 (Sn Mod)	1036	27.20	938	17.05	937	17.06
New-OL-54017 (Sn Mod)	1041	11.65	942	6.12	942	6.11
New-OL-57284	1043	9.79	944	5.69	944	5.70
New-OL-62380	1042	10.31	943	5.49	943	5.50
New-OL-62909 (Mod)	1038	14.18	939	7.39	939	7.40
New-OL-65959 (Mod)	1044	36.68	945	24.52	944	24.38
New-OL-80309	1041	33.76	942	23.67	942	23.67
New-OL-90780	1038	38.96	939	26.97	939	26.92
New-OL-100210	1041	35.52	942	26.79	942	26.79
New-OL-108249 (SO ₃ Mod)	1041	29.25	942	19.39	942	19.39

Target T , °C	1050		950		950	
	Measured T (°C)	EC (S/m)	Measured T (°C)	EC (S/m)	Measured T (°C)	EC (S/m)
New-OL-116208 (SO ₃ Mod)	1044	43.04	954	29.76	944	29.60
New-OL-122817	1040	21.92	941	13.47	941	13.48
New-OL-127708 (Mod)	1040	15.77	942	9.36	NM	NM
EWG-LAW-Centroid-1	1042	27.34	943	17.65	943	17.65
EWG-LAW-Centroid-2	1027	27.86	919	17.71	919	17.69
LAW-ORP-LD1(1)	1039	23.97	940	15.78	940	15.75
LAW-ORP-LD1(2)	1036	28.19	938	18.25	938	18.22
LAW-ORP-LD1(3)	1038	22.59	940	14.36	940	14.37

NM = not measured

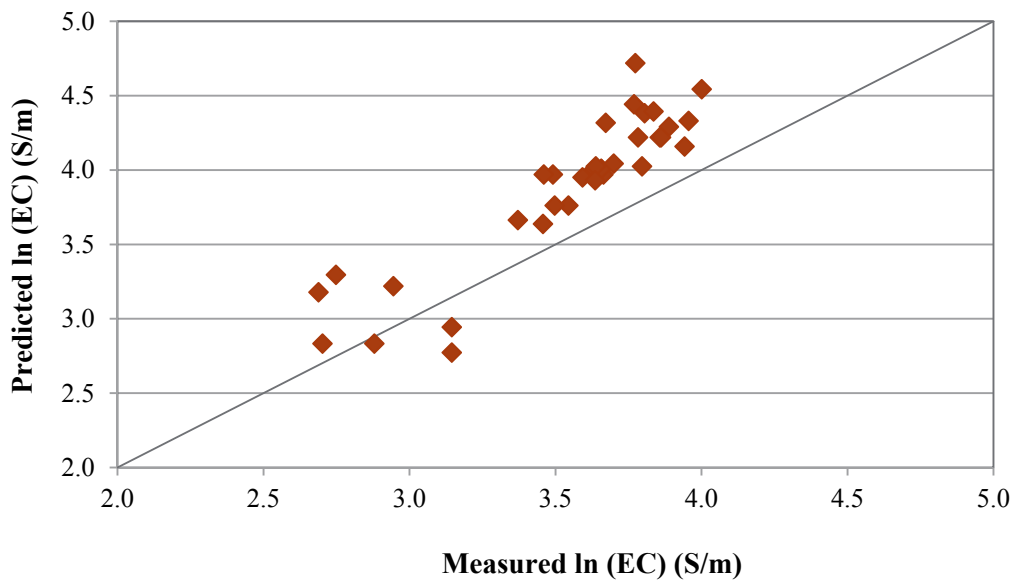


Figure 3.3. Predicted versus Measured Electrical Conductivity for LAW Phase 1 Enhanced Glasses

3.5 Crystal Fraction of Heat-Treated Glasses

This section presents and discusses the crystal fraction (C_T) results obtained using the methods discussed in Section 2.6. For each glass composition, specimens were prepared and heat treated at 950°C. For the glasses that were highly crystalline, samples were also heat treated at 1050°C and 1150°C.

At least seven glasses had insufficient crystals to perform XRD analysis when treated at 950°C. Fifteen glasses contained cassiterite (SnO₂) and four glasses contained baddeleyite (ZrO₂) when heat treated at one of the temperatures listed above. In three glasses, when they were tested at 1150°C, the cassiterite was still present, indicating the difficulty in getting it to dissolve once it forms in the melt. These results are summarized in Table 3.7. Figure 3.4 shows an example glass with significant cassiterite crystals, while Figure 3.7 shows an example glass with significant baddeleyite crystals. With over half of the glasses forming some fraction of crystal at 950°C, it is likely that crystal constraints will be required to control composition in this EGCR.

Table 3.7. Weight Percent Crystallinity and Identification of Crystals by XRD in Heat-Treated Glasses

Glass ID	Temp (°C)	Wt% Crystallinity	Crystal Phase Identification
New-IL-456	950	~0	Insufficient crystals for XRD
New-IL-1721	950	0	NA
New-IL-5253	950	0.7	Cassiterite
New-IL-5255	950	0.5	Cassiterite
New-IL-42295	950	0	NA
New-IL-70316	950	~0	Insufficient crystals for XRD
New-IL-87749	950	~0	Insufficient crystals for XRD
New-IL-93907	950	~0	Insufficient crystals for XRD
New-IL-94020	950	1.4	Cassiterite
New-IL-103151	950	0	NA
New-IL-151542	950	~0	Insufficient crystals for XRD
New-IL-166697	950	1.1	Cassiterite
New-IL-166731	950	1.3	Cassiterite
New-OL-8445	950	2.0	Baddeleyite
New-OL-8788 (Mod)	950	1.5	Fluorapatite
		2.2	Baddeleyite
New-OL-8788 (Mod)	1050	1.0	Iron Oxide
		1.5	Baddeleyite
		0.8	Chromite
New-OL-14844	950	2.4	Baddeleyite
New-OL-14844	1050	1.6	Baddeleyite
New-OL-15493	950	19.4	Combeite High
New-OL-15493	1050	0	NA
New-OL-17130	950	0	NA
New-OL-45748 (Sn Mod)	950	3.3	Cassiterite
New-OL-54017 (Sn Mod)	950	0.8	Cassiterite
New-OL-57284	950	1.6	Fluorapatite
New-OL-62380	950	0.4	Cassiterite
New-OL-62909 (Mod)	950	2.9	Cassiterite
		1.4	Baddeleyite
		1.7	SiO ₂ and Wadalite
New-OL-62909 (Mod)	1050	2.9	Cassiterite
		1.2	Baddeleyite
New-OL-62909 (Mod)	1150	1.7	Cassiterite
		0.2	Gehlenite
		2.6	Cassiterite
New-OL-65959 (Mod)	950	2.6	Cassiterite
New-OL-65959 (Mod)	1050	2.0	Cassiterite
New-OL-65959 (Mod)	1150	1.3	Cassiterite
New-OL-80309	950	1.7	Cassiterite
New-OL-90780	950	1.1	Cassiterite
New-OL-100210	950	0	NA
New-OL-108249 (SO ₃ Mod)	950	3.1	Cassiterite
		4.6	Nosean and Hauyne
		2.8	Cassiterite
New-OL-116208 (SO ₃ Mod)	950	6.8	Nasicon
		0	NA
New-OL-122817	950	0	NA
New-OL-127708 (Mod)	950	1.9	Cassiterite
New-OL-127708 (Mod)	1050	1.6	Cassiterite
New-OL-127708 (Mod)	1150	1.0	Cassiterite
EWG-LAW-Centroid-1	950	0	NA
EWG-LAW-Centroid-2	950	0	NA
LAW-ORP-LD1(1)	950	~0	Insufficient crystals for XRD
LAW-ORP-LD1(2)	950	~0	Insufficient crystals for XRD
LAW-ORP-LD1(3)	950	8.1	Hauyne, Nosean, FeNi ₂ O ₄

NA = not applicable

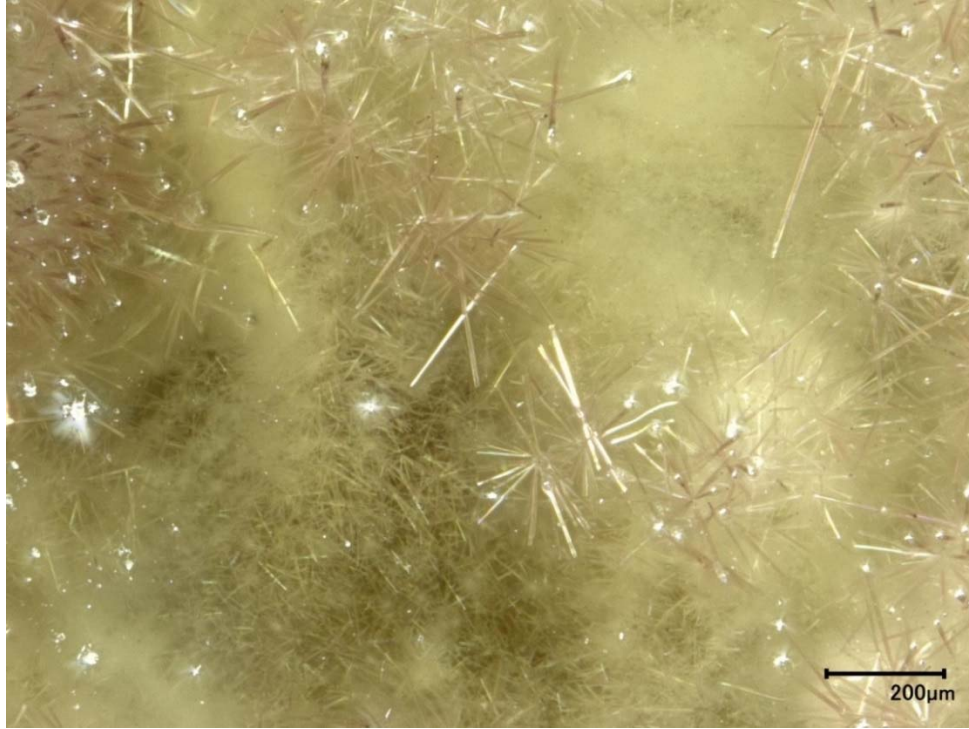


Figure 3.4. Optical Micrograph of Cassiterite Crystals in Glass New-IL-94020 Held at 952°C for 24 h

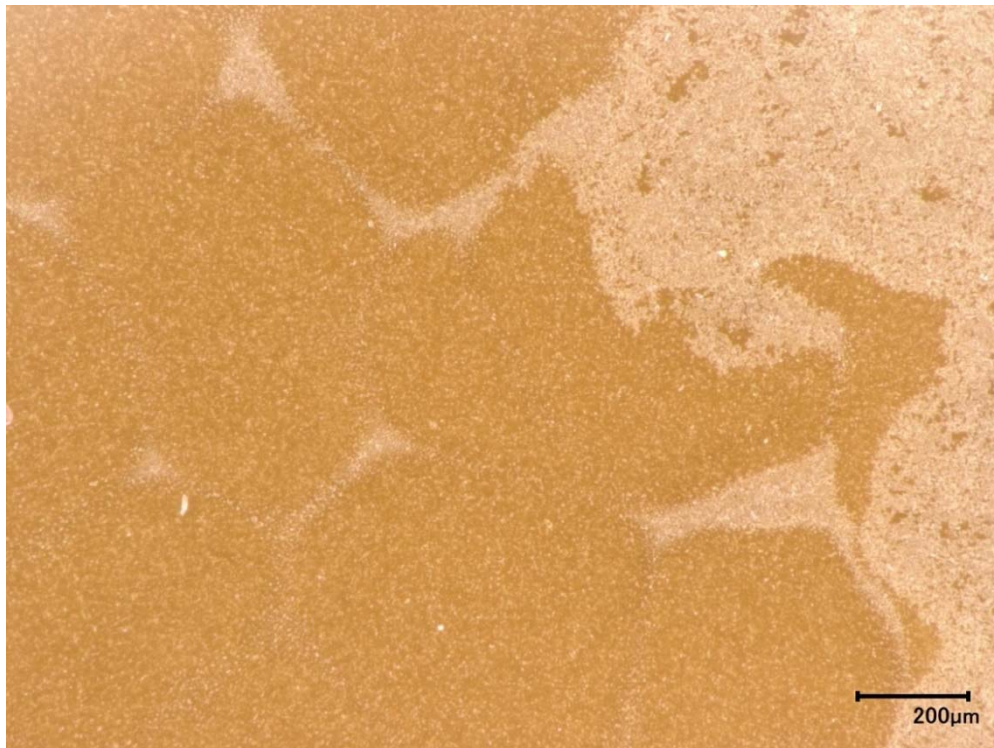


Figure 3.5. Optical Micrograph of Baddeleyite Crystals in Glass New-OL-8788(Mod) Held at 1043°C for 24 h

3.6 Crystal Identification in Canister Centerline Cooling Glasses

This section presents and discusses the crystal fraction results from CCC glasses obtained using the methods discussed in Section 2.7. XRD scans of CCC glass samples identified a variation of crystal types. The crystal types and wt% crystallinity results are summarized in Table 3.8. Table 3.8 shows the CCC results from the Pt crucibles except when surface crystallization occurred in which case the results from the quartz crucible are shown. Twenty-six glasses had crystal content of less than 5 mass% while eight glasses had crystal content greater than 10 mass% crystals. Only one glass (LAW-ORP-LD1(2)) had a crystal content between 5 and 10 mass%. Sixteen samples were not analyzed by XRD because there were either no crystals or very few crystals (not enough for XRD to detect) observed by optical microscope. See Appendix D for photos of CCC-treated glasses and Appendix E for XRD spectra obtained from them.

It was found that during cooling, several of the glasses seemed to form a heavy layer of crystals around the crucible walls, as seen in Figure 3.6. Several different methods were attempted to avoid this problem, including crucibles of different size and different materials of construction. When a quartz crucible was used, it was found that the glass could be cooled without a layer of crystals forming, with an example shown in Figure 3.7. Therefore, all melts with a layer of crystals forming around the crucible walls were retested in a quartz crucible.

Table 3.8. Weight Percent Crystallinity and Identification of Crystals by XRD in CCC-Treated Glasses

Glass ID	Starting CCC Temp (°C)	Wt% Crystallinity	Crystal Phase Identification
New-IL-456	1200	~0	Insufficient crystals for XRD
New-IL-1721	1150	~0	Insufficient crystals for XRD
New-IL-5253	1150	~0	Insufficient crystals for XRD
New-IL-5255	1200	0	No crystals found.
New-IL-42295	1150	~0	Insufficient crystals for XRD
New-IL-70316	1150	0.4	Baddeleyite, vanadian
New-IL-87749	1225	NA (qualitative only—no standard added)	Nepheline Sylvite, sodian Hauyne ² Gehlenite, magnesian Lithium Vanadium Oxide
New-IL-93907	1150	~0	Insufficient crystals for XRD
New-IL-94020	1150	1.3	Cassiterite
New-IL-103151	1250	~0	Insufficient crystals for XRD
New-IL-151542	1225	~0	Insufficient crystals for XRD
New-IL-166697	1150	2.6 9.1 0.9 0.8	Hauyne ² Nosean ¹ Cassiterite Magnesium Sulfate
New-IL-166731	1225	1.2 1.8 1.0	Hauyne ² Nosean ¹ Silicon Oxide
New-OL-8445	1150	0	No crystals found.
New-OL-8788 (Mod)	1300	0.4 0.8	Baddeleyite Iron Lithium Oxide

Glass ID	Starting CCC Temp (°C)	Wt% Crystallinity	Crystal Phase Identification		
New-OL-14844	1150	2.4	Baddeleyite, vanadian		
		0.9	Magnesium Vanadium Oxide		
		0.2	Berndtite		
		0.2	Lithium Zirconium Oxide		
		0.6	Lithium Magnesium Aluminum Sulfate		
		12.8	Akermanite, magnesian		
		0.8	Calcium Aluminum Oxide Sulfide		
		0.8	Sodium Silicate		
		13.7	Lithium Magnesium Silicate		
		1.3	Silicon Oxide		
		13.5	Combeite, High		
		0.3	Zinc Sulfide		
		New-OL-15493	1200	24.9	Nepheline
				0.9	Sodium Calcium Silicate
				1.0	Silicon Oxide
9.9	Combeite, Low				
40.3	Combeite, High				
New-OL-17130	1150	~0	Insufficient crystals for XRD		
New-OL-45748 (Sn Mod)	1300	36.7	Nepheline		
		0.3	Eucryptite		
		2.5	Cassiterite		
		0.7	Calcium Iron Oxide		
		0.9	Hercynite		
		1.1	Andradite		
		2.6	Calcium Aluminum Oxide		
		1.4	Sodium Calcium Silicate		
		0.7	Silicon Oxide		
		0.9	Cristobalite		
		1.4	Aluminum Phosphate		
New-OL-54017 (Sn Mod)	1250	NA (qualitative only—no standard added)	Cassiterite		
New-OL-57284	1225	2.8	Fluorapatite		
New-OL-62380	1300	~0	Insufficient crystals for XRD		
New-OL-62909 (Mod)	1150	34.0	Nepheline		
		2.1	Cassiterite		
New-OL-65959 (Mod)	1225	31.6	Nepheline		
		2.0	Cassiterite		
		11.2	Lithium Magnesium Silicate		
New-OL-80309	1250	0.2	Chromite		
		0.8	Sodium Sulfate		
New-OL-90780	1150	15.0	Nosean ¹		
		1.3	Sodalite		
		0.1	Quartz		
New-OL-100210	1250	~0	Insufficient crystals for XRD		
New-OL-108249 (SO ₃ Mod)	1300	24.9 ^(c)	Combeite high		
		2.3	Cassiterite		
		2.8	Sanidine (Li-exchanged)		
		5.3	Li ₃ AlO ₄		
		7.0	Imandrite		
		11.2	Nosean		
		0.1	Sn(SnF ₆)		
		1.0	Quartz low		
		1.2	Sodalite		
		0.3	K ₂ Sn ₂ O ₃		
		2.9	Fe ₂ O ₃		
		0.1	K ₂ Al ₂ (BO ₃) ₂ O		
		1.2	Elpasolite		
		3.1	SiO ₂		
		9.8	Na _{1.75} Al _{1.75} Si _{0.25} O ₄		
		24.8	Nepheline		
		8.0	Na _{1.55} Al _{1.55} Si _{0.45} O ₄		
1.6	Al ₂ (SiO ₄)O				

Glass ID	Starting CCC Temp (°C)	Wt% Crystallinity	Crystal Phase Identification
New-OL-116208 (SO ₃ Mod)	1300	5.3	Zirconsalite
		15.5 ^(c)	Combeite high
		1.1	Nepheline, sodian
		4.1	Ca ₂ (Al ₂ O ₅)
		4.6	Nosean
		2.4	Na _{1.75} Al _{1.75} Si _{0.25} O ₄
		2.3	Na _{1.55} Al _{1.55} Si _{0.45} O ₄
		0.5	Nepheline (Si-rich)
		0.02	Cristobalite
		0.9	Al(PO ₄)
		4.8	SiO ₂
		1.6	(MgO) _{0.593} (FeO) _{0.407}
		2.1	Quartz low
		0.6	Hematite
4.8	Na ₈ SnSi ₆ O ₁₈		
New-OL-122817	1200	~0	Insufficient crystals for XRD
New-OL-127708 (Mod)	1300	~0	Insufficient crystals for XRD
EWG-LAW-Centroid-1	1150	~0	Insufficient crystals for XRD
EWG-LAW-Centroid-2	1150	~0	Insufficient crystals for XRD
LAW-ORP-LD1(1)	1300	2.5	Hauyne ^(b)
		11.2	Nosean ^(a)
		1.2	Silicon Oxide
LAW-ORP-LD1(2)	1300	1.3	Hauyne ^(b)
LAW-ORP-LD1(3)	1300	6.5	Nosean ^(a)
		~0	Insufficient crystals for XRD

(a) Nosean is very similar to nepheline except it also contains sulfate.

(b) Hauyne is also similar to nepheline but contains Ca and sulfate.

(c) Not all XRD peaks fit. Quantitative values are not correct.



Figure 3.6. Photograph of Glass LAW-ORP-LD1(1) Cooled in a Pt Crucible with Crystals Along Edge



Figure 3.7. Photograph of Glass LAW-ORP-LD1(1) Cooled in a Quartz Crucible without Crystals along Edge

3.7 Product Consistency Test

This section presents and discusses the PCT results obtained using the methods discussed in Section 2.8. The PCT results are published elsewhere (Fox et al. 2015a, 2015b), but are summarized here in Table 3.9. A review of the PCT data shows that seven of the study glasses (New-IL-42295, New-OL-17130, New-IL-5255, New-OL-14844, New-OL-80309, New-OL-116208(SO₃ Mod) and New-OL-90780) had normalized release (NR) values for boron (NR [B]) and sodium (NR [Na]) that are higher than the WTP contract limit of 2 g/m² for both quenched and CCC-treated glasses. It was hoped that some of the matrix glasses would be above contract limits to supply data necessary to predict glass responses at the limit. Another four glasses are higher than the WTP PCT contract limit only for the CCC heat treatment (New-IL-166731, New-OL-15493, New-OL-65959(Mod), and New-OL-108249(SO₃ Mod)). Glass New-IL-42295 had higher PCT values for the quenched glass than for the CCC glass.

Table 3.9. PCT Normalized Concentration Release Results Taken from Fox et al. (2015a,b)

Glass ID	Type	NR[B] (g/m ²)	NR[Li] (g/m ²)	NR[Na] (g/m ²)	NR[Si] (g/m ²)
New-IL-456	Quenched	0.250	0.401	0.451	0.134
	CCC	0.254	0.370	0.382	0.124
New-IL-1721	Quenched	1.276	1.145	1.091	0.335
	CCC	0.800	0.685	0.701	0.248
New-IL-5253	Quenched	0.800	0.742	0.725	0.212
	CCC	1.105	1.002	0.904	0.256

Glass ID	Type	NR[B] (g/m²)	NR[Li] (g/m²)	NR[Na] (g/m²)	NR[Si] (g/m²)
New-IL-5255	Quenched	6.597	5.434	5.120	0.768
	CCC	6.286	5.181	4.504	0.775
New-IL-42295	Quenched	9.727	7.345	6.598	1.166
	CCC	8.150	6.525	5.815	1.111
New-IL-70316	Quenched	0.313	0.457	0.674	0.172
	CCC	0.301	0.404	0.633	0.158
New-IL-87749	Quenched	0.229	0.357	0.492	0.119
	CCC	0.156	0.337	0.434	0.107
New-IL-93907	Quenched	0.214	0.227	0.260	0.127
	CCC	0.223	0.228	0.233	0.124
New-IL-94020	Quenched	0.249	0.282	0.334	0.138
	CCC	0.204	0.256	0.282	0.123
New-IL-103151	Quenched	1.055	0.648	1.013	0.394
	CCC	0.844	0.530	0.944	0.333
New-IL-151542	Quenched	0.317	0.396	0.475	0.143
	CCC	0.336	0.397	0.469	0.145
New-IL-166697	Quenched	0.400	0.304	0.448	0.180
	CCC	0.377	0.330	0.430	0.172
New-IL-166731	Quenched	0.406	0.331	0.502	0.182
	CCC	2.351	2.050	1.457	0.356
New-OL-8445	Quenched	0.265	0.328	0.319	0.047
	CCC	0.208	0.234	0.248	0.040
New-OL-8788 (Mod)	Quenched	0.156	0.238	0.202	0.110
	CCC	0.261	0.253	0.211	0.124
New-OL-14844	Quenched	3.805	3.872	3.687	0.624
	CCC	3.499	3.479	3.394	0.566
New-OL-15493	Quenched	0.476	-- ^(a)	1.617	0.305
	CCC	44.793	-- ^(a)	20.679	1.057
New-OL-17130	Quenched	11.385	9.279	8.464	2.430
	CCC	10.719	9.234	8.170	2.487
New-OL-45748	Quenched	0.113	0.201	0.201	0.058
	CCC	0.481	0.764	0.184	0.154
New-OL-54017	Quenched	0.181	-- ^(a)	0.258	0.092
	CCC	0.101	-- ^(a)	0.226	0.086
New-OL-57284	Quenched	0.854	-- ^(a)	0.778	0.210
	CCC	1.113	-- ^(a)	0.904	0.222
New-OL-62380	Quenched	0.165	-- ^(a)	0.251	0.060
	CCC	0.126	-- ^(a)	0.227	0.053
New-OL-62909 (Mod)	Quenched	0.211	0.279	0.305	0.059
	CCC	0.132	0.216	0.224	0.073
New-OL-65959 (Mod)	Quenched	1.670	1.355	1.218	0.340
	CCC	23.234	9.006	9.191	0.257
New-OL-80309	Quenched	11.520	8.502	7.563	0.516

Glass ID	Type	NR[B] (g/m ²)	NR[Li] (g/m ²)	NR[Na] (g/m ²)	NR[Si] (g/m ²)
	CCC	5.587	4.340	3.562	0.612
New-OL-90780	Quenched	2.419	2.075	1.465	0.282
	CCC	14.070	9.675	5.992	0.296
New-OL-100210	Quenched	1.033	-- (a)	1.410	0.635
	CCC	0.98	-- (a)	1.232	0.594
New-OL-108249 (SO ₃ Mod)	Quenched	0.164	0.302	0.420	0.093
	CCC	8.055	2.457	2.279	0.066
New-OL-116208 (SO ₃ Mod)	Quenched	4.303	3.760	3.935	0.639
	CCC	9.033	3.722	5.722	0.530
New-OL-122817	Quenched	0.147	-- (a)	0.538	0.117
	CCC	0.220	-- (a)	0.466	0.107
New-OL-127708 (Mod)	Quenched	0.276	0.338	0.269	0.131
	CCC	0.260	0.343	0.219	0.136
EWG-LAW-Centroid-1	Quenched	0.402	0.346	0.524	0.160
	CCC	0.444	0.391	0.521	0.160
EWG-LAW-Centroid-2	Quenched	0.398	0.337	0.527	0.158
	CCC	0.446	0.376	0.526	0.160
LAW-ORP-LD1(1)	Quenched	0.467	-- (a)	0.596	0.137
	CCC	0.285	-- (a)	0.368	0.150
LAW-ORP-LD1(2)	Quenched	0.424	-- (a)	0.517	0.121
	CCC	0.322	-- (a)	0.414	0.136
LAW-ORP-LD1(3)	Quenched	0.303	-- (a)	0.354	0.089
	CCC	0.231	-- (a)	0.299	0.076

(a) No Li in the glass composition.

Figure 3.8 compares the PCT normalized releases of B and Li with the normalized release of Na for the quenched glass samples. This shows that \ln [NR-B] and \ln [NR-Li] values tend to be lower than \ln [NR-Na] values below about $0.72 \ln$ (g/m²). \ln [NR-Li] values are not as much lower than the \ln [NR-Na] values below $\sim 0.72 \ln$ (g.m²) as \ln [NR-B] values. Figure 3.9 compares the PCT normalized releases of B and Li with the normalized release of Na for the CCC glass samples. This figure shows that B release is higher than Na release at the higher end of the scale. The release rates form a fairly straight line but with a different slope. This may be due to crystallization in the samples during the CCC process.

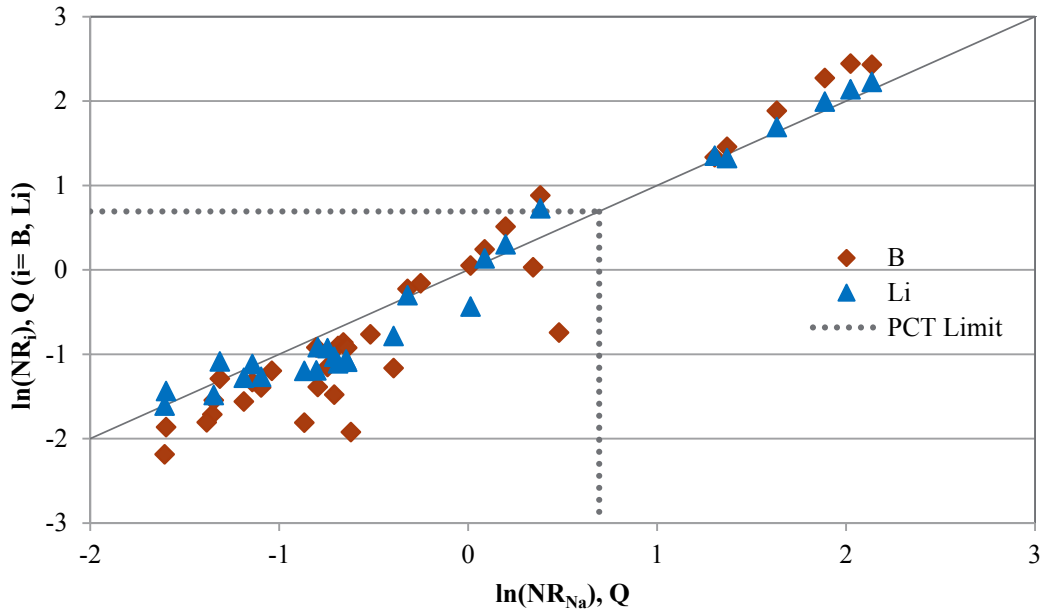


Figure 3.8. Comparison of Natural Logarithm PCT Normalized Release (g/m^2) of B and Li with Na for Quenched Samples of LAW Phase 1 Enhanced Glasses

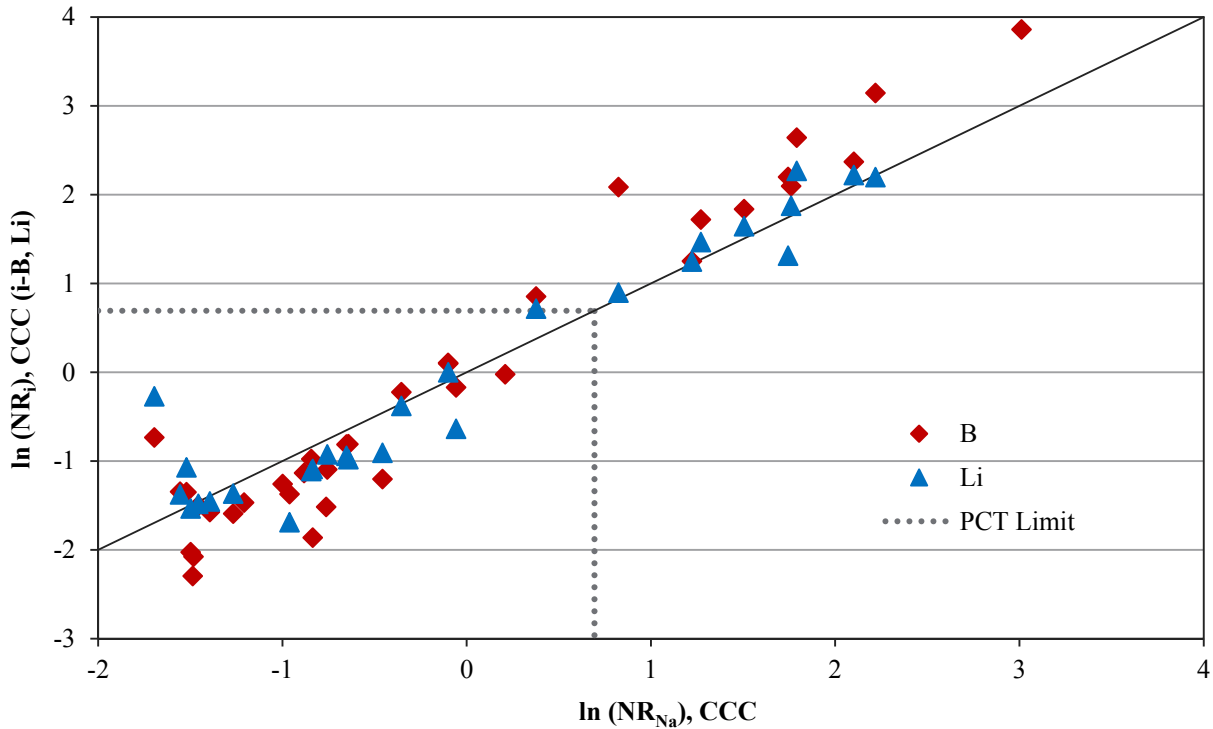


Figure 3.9. Comparison of Natural Logarithm PCT Normalized Release (g/m^2) of B and Li with Na for CCC Samples of LAW Phase 1 Enhanced Glasses

Figure 3.10 compares the logarithm normalized releases of the quenched and CCC glasses. When significant crystals containing Al and Si (>5 wt%) are present in the glass, CCC-treated samples can have

notably higher releases than quenched samples as shown in Figure 3.11. This may be because the crystals remove the glass formers (Si and Al) from the bulk glass structure and composition making the glass less durable.

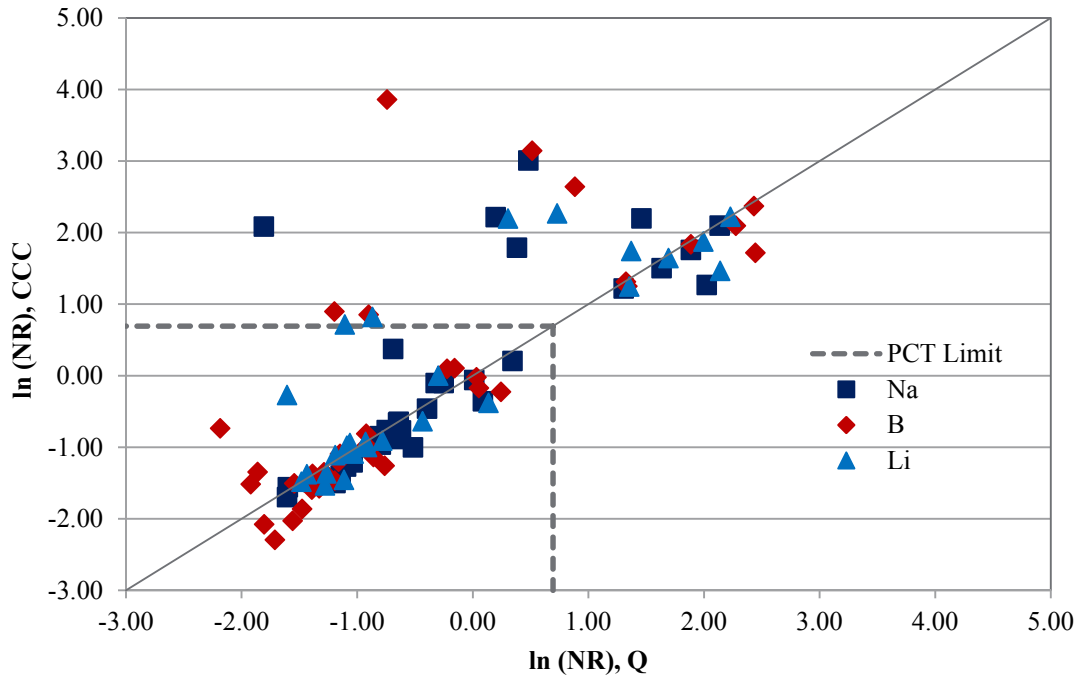


Figure 3.10. Comparison of Natural Logarithm of PCT Normalized Release (g/m²) of B, Li, and Na for Quenched and CCC-Treated Samples of LAW Phase 1 Enhanced Glasses

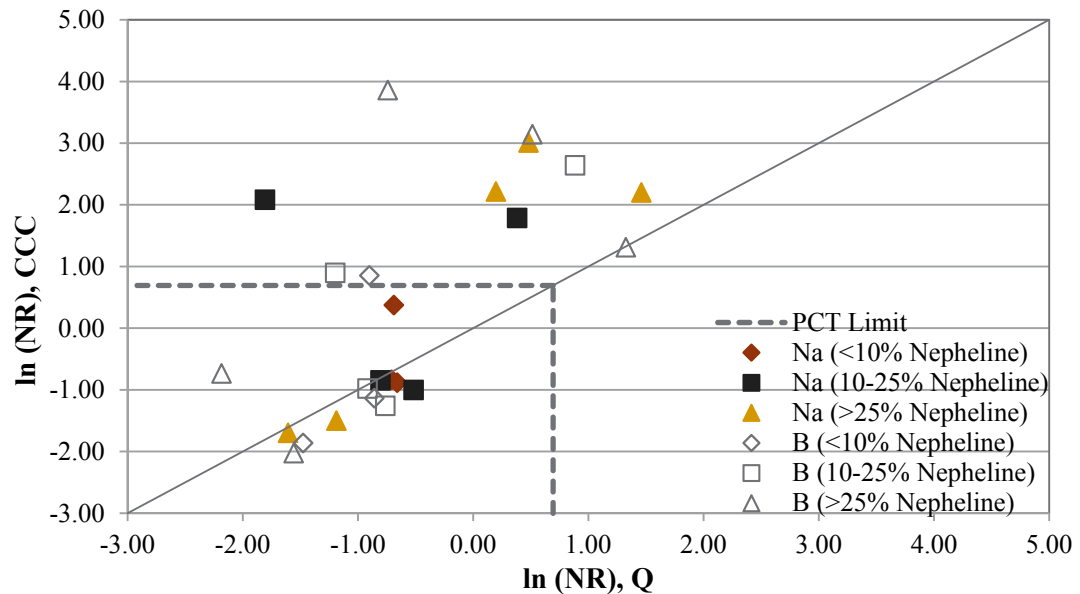


Figure 3.11. Comparison of Natural Logarithm of PCT Normalized Release (g/m²) of B, Li, and Na for Quenched and CCC-Treated Samples that Contain Nepheline of LAW Phase 1 Enhanced Glasses

3.8 Vapor Hydration Test

This section presents and discusses the VHT results obtained using the methods discussed in Section 2.9. Table 3.10 shows the corrosion rate of each glass based on the VHT. See Appendix F for the photos of the glass samples after the VHT. Fourteen of the 36 glasses were above the VHT limit with a corrosion rate of $>50 \text{ g/m}^2/\text{d}$.

Table 3.10. VHT Results from the LAW Phase 1 Enhanced Glasses

Glass ID	Density (g/cm ³)	Temp (°C)	Days	Alteration Depth (μm)	Rate (g/m ² /d)	Comparison to Limit of 50 g/m ² /d
New-IL-456	2.6974	200	24	347	19.4	39%
New-IL-1721	2.6304	200	7	505	97.4	195%
New-IL-5253	2.7036	200	24	187	10.55	21%
New-IL-5255	2.7174	200	7	503	98.17	196%
New-IL-42295	2.6415	200	7	317	59.56	119%
New-IL-70316	2.7009	200	7	352	69.8	140%
New-IL-87749	2.6974	200	7	101	19.3	39%
New-IL-93907	2.6068	200	24	687	37.7	75%
New-IL-94020	2.6672	200	24	300	16.8	34%
New-IL-103151	2.6784	200	7	1520	>320	640%
New-IL-151542	2.7043	200	24	145	8.24	16%
New-IL-166697	2.6577	200	7	427	81.2	162%
New-IL-166731	2.6612	200	7	874	165	330%
New-OL-8445	2.6908	200	24	37	2.06	4%
New-OL-8788 (Mod)	2.6372	200	24	25	1.41	3%
New-OL-14844	2.7851	200	24	53	3.11	6%
New-OL-15493	2.6952	200	1	126	>1679	3357%
New-OL-17130	2.5873	200	7	1387	255	510%
New-OL-45748 (Sn Mod)	2.7796	200	24	134	7.86	16%
New-OL-54017 (Sn Mod)	2.7903	200	24	6.3	0.364	0.7%
New-OL-57284	2.6268	200	7	1500	>279	558%
New-OL-62380	2.8654	200	24	1.4	0.084	0.2%
New-OL-62909 (Mod)	2.7851	200	24	71	4.16	8%
New-OL-65959 (Mod)	2.6595	200	7	1385	>263	525%
New-OL-80309	2.7634	200	7	1520	298.9	598%
New-OL-90780	2.5322	200	7	933	176.3	353%
New-OL-100210	2.6517	200	1	1154	1551	310%
New-OL-108249 (SO ₃ Mod)	2.7391	200	24	132	7.56	15%
New-OL-116208 (SO ₃ Mod)	2.8195	200	24	12	0.714	1%
New-OL-122817	2.6910	200	24	629	35.4	71%
New-OL-127708 (Mod)	2.5759	200	24	52	26.5	53%
EWG-LAW-Centroid-1	2.6658	200	24	291	16.3	33%
EWG-LAW-Centroid-2	2.6820	200	24	496	28.0	56%
LAW-ORP-LD1(1)	2.6577	200	24	113	6.26	13%
LAW-ORP-LD1(2)	2.6714	200	24	486	26.6	53%
LAW-ORP-LD1(3)	2.6341	200	24	46	2.5	5%

The glasses tested performed either extremely well or extremely poor with only four glasses near the corrosion rate limit. Data above and below the contract limit is necessary to develop models capable of predicting glass responses at the limit.

Figure 3.12 shows the VHT results plotted against the mass fractions of total normalized alkali [Nalk = Na₂O + 0.66(K₂O) + 2(Li₂O)] in the glasses. Basically all of the glasses up to 22 wt% alkali passed the VHT. Above 22 wt% alkali, the glasses both pass and fail the limit, presumably determined by the overall glass composition. The one data point at 15 wt% alkali that didn't pass was determined to be from a phase-separated glass that changed colors during the test from dark green to light blue (shown in Figure 3.13) and did not meet the Taylor Rule (Peeler and Hrma 1994). The Taylor Rule requires that the equation be greater than 0.2:

$$P = \frac{(g_{Na2O} + 2(g_{Li2O}))}{(g_{Na2O} + 2(g_{Li2O}) + g_{B2O3} + g_{SiO2})}$$

where g_i represents the i^{th} oxide mass fraction in glass. Glasses with <20 wt% normalized alkali are prone to immiscible phase separation which can decrease durability of the glass (Peeler and Hrma 1994).

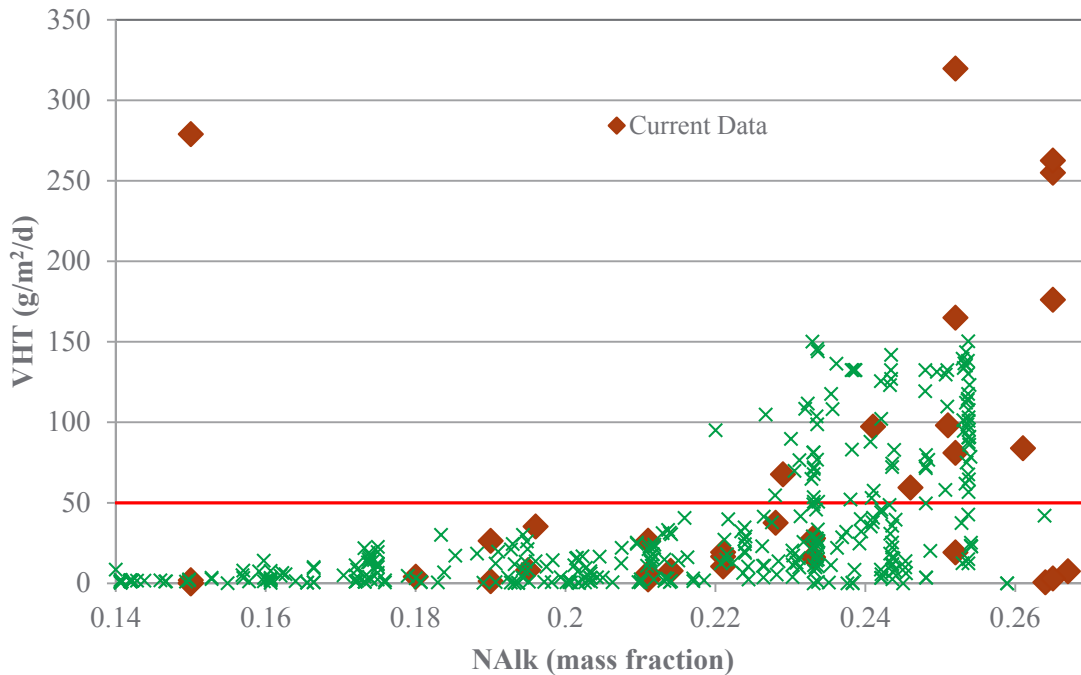


Figure 3.12. VHT Response Compared to the Total Normalized Alkali Mass Fraction [Nalk = Na₂O + 0.66(K₂O) + 2(Li₂O)] Content of the Glass



Figure 3.13. Photograph of Glass New-OL-65959(Mod) Before (Right) and After (Left) VHT

3.9 Sulfur Solubility Results

This section presents and discusses the chemical analysis results of the sulfur-saturated glasses obtained using the methods discussed in Section 2.10. For each glass, the initial glass sample and the “sulfur-saturated” sample were analyzed by ICP-AES and IC. The chemical analysis results of the baseline glasses have been presented and discussed in Section 3.1. More detailed chemical analysis results have been reported by Fox et al (2017).

Note that 38 glass samples were prepared based on 35 glass compositions (out of the 36 listed in

Table 1.3) with three duplicates which were prepared based on one sample initial glass but saturated with sulfate by PNNL and SRNL using the same experimental procedure. There were three duplicated compositions (six sulfate-saturated samples), prepared by both PNNL and SRNL to compare results.

Table 3.11 and Figure 3.14 summarize the analyzed sulfur concentration in the baseline and the sulfur-saturated glasses. The SO₃ concentrations in the initial glasses are mostly below 1 wt% (including several glasses with low SO₃ < 0.1 wt%). After sulfur saturation, there is significant increase of SO₃ mass fraction which is considered the experimentally determined SO₃ solubility of the glass. In most glasses, the SO₃ solubility (i.e., the saturated SO₃ concentrations) is around 1.5 wt%. There is only one exception, New-OL-80309, with the highest SO₃ (1.75 wt% initial and 1.67 wt% measured) in the initial glass, the SO₃ concentration decreased slightly to 1.66 wt% after sulfur saturation, SO₃ may have been super saturated in the initial glass or the differences may have been caused by technique uncertainty (which can be inferred from replicates in Table 3.11 to be of similar magnitude).

Table 3.11. Target and Measured Values of SO₃ (mass fraction)

Sample ID	Preparation Lab	Measuring Lab	SO ₃ Mass Fraction		
			Target Initial	Measured Initial	Sulfate-saturated
New-IL-456	SRNL	SRNL	0.0040	0.0038	0.0201
New-IL-1721	SRNL	SRNL	0.0130	0.0112	0.0171
New-IL-1721	PNNL	SRNL	0.0130	0.0112	0.0177
New-IL-5253	SRNL	SRNL	0.0130	0.0098	0.0150
New-IL-5255	SRNL	SRNL	0.0130	0.0120	0.0165
New-IL-42295	SRNL	SRNL	0.0040	0.0040	0.0174
New-IL-70316	SRNL	SRNL	0.0130	0.0126	0.0169
New-IL-87749	SRNL	SRNL	0.0040	0.0041	0.0172
New-IL-93907	SRNL	SRNL	0.0113	0.0095	0.0118
New-IL-94020	PNNL	SRNL	0.0102	0.0082	0.0108
New-IL-103151	SRNL	SRNL	0.0117	0.0125	0.0154
New-IL-151542	SRNL	SRNL	0.0130	0.0108	0.0174
New-IL-166697	PNNL	SRNL	0.0129	0.0111	0.0151
New-IL-166731	PNNL	SRNL	0.0127	0.0102	0.0148
New-OL-8445	SRNL	SRNL	0.0010	< 0.001	0.0139
New-OL-8788(Mod)	SRNL	SRNL	0.0010	< 0.001	0.0057
New-OL-14844	SRNL	SRNL	0.0010	< 0.001	0.0138
New-OL-15493	SRNL	SRNL	0.0010	< 0.001	0.0218
New-OL-17130	SRNL	SRNL	0.0010	< 0.001	0.0235
New-OL-45748(Sn Mod)	SRNL	SRNL	0.0010	< 0.001	0.0155
New-OL-54017(Sn Mod)	SRNL	SRNL	0.0010	< 0.001	0.0129
New-OL-57284	SRNL	SRNL	0.0010	< 0.001	0.0090
New-OL-62380	SRNL	SRNL	0.0010	< 0.001	0.0150
New-OL-62909(Mod)	PNNL	SRNL	0.0010	< 0.001	0.0129
New-OL-65959(Mod)	PNNL	SRNL	0.0010	< 0.001	0.0169
New-OL-80309	SRNL	SRNL	0.0175	0.0167	0.0159
New-OL-90780	SRNL	SRNL	0.0164	0.0131	0.0156
New-OL-100210	SRNL	SRNL	0.0091	0.0095	0.0157
New-OL-108249(SO ₃ Mod)	SRNL	SRNL	0.0089	0.0085	0.0132
New-OL-108249(SO ₃ Mod)	PNNL	SRNL	0.0089	0.0085	0.0130
New-OL-116208(SO ₃ Mod)	SRNL	SRNL	0.0093	0.0092	0.0134
New-OL-116208(SO ₃ Mod)	PNNL	SRNL	0.0093	0.0092	0.0149
New-OL-122817	SRNL	SRNL	0.0149	0.0130	0.0205
New-OL-127708(Mod)	SRNL	SRNL	0.0061	< 0.001	0.0087

Sample ID	Preparation Lab	Measuring Lab	SO₃ Mass Fraction		
			Target Initial	Measured Initial	Sulfate-saturated
EWG-LAW-Centroid-2	SRNL	SRNL	0.0070	0.0071	0.0149
LAW-ORP-LD1(1)	SRNL	SRNL	0.0106	0.0102	0.0133
LAW-ORP-LD1(2)	PNNL	SRNL	0.0106	0.0087	0.0133
LAW-ORP-LD1(3)	PNNL	SRNL	0.0101	0.0086	0.0104

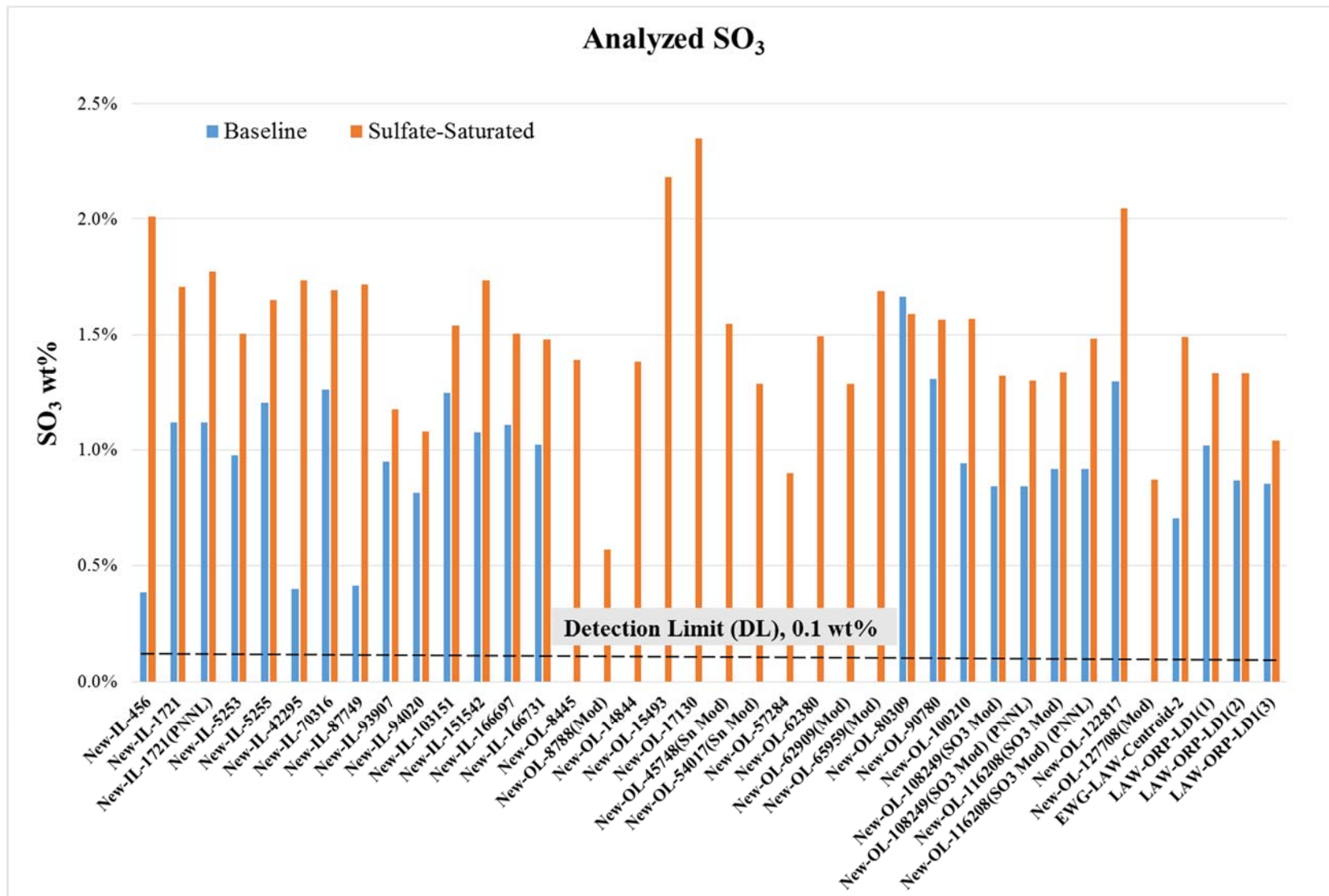


Figure 3.14. Analyzed Sulfur Concentration in the Baseline and the Sulfur-Saturated Glasses

Appendix G shows the overall analyzed glass compositions after normalization of the baseline and sulfur-saturated glass samples. Comparisons of the compositions showed that after the sulfur saturation, other major glass components only have negligible changes except when the SO₃ reaches a high level near sulfur-saturation concentration with is over 0.8 wt% SO₃ for most glasses. For the minor components, K₂O decreases which may be due to partitioning to the salt and the losses of the Cl, F, and P₂O₅ may be due to volatilization during multiple times of melting or due to partitioning in the salt.

The chemical analyses data of the sulfur-saturated glasses have been used to evaluate our preliminary SO₃ solubility model (Vienna et al. 2014). The empirical model produces the predicted SO₃ solubility using the following equation:

$$w_{\text{SO}_3}^{\text{Pred}} = \sum_{i=1}^q s_i n_i + \text{selected} \left\{ \sum_{i=1}^q s_{ii} n_i^2 + \sum_{j=1}^{q-1} \sum_{k=j+1}^q s_{jk} n_j n_k \right\} \quad (3.4)$$

where,

- $w_{\text{SO}_3}^{\text{Pred}}$ = the predicted SO₃ solubility (in wt%)
- q = the number of components in the waste glass except for SO₃
- n_i = normalized (after removing SO₃) mass fraction of the ith component
- s_i = coefficient of the ith component
- s_{ii} = coefficient for the ith component squared
- s_{jk} = coefficient for the jth and kth components cross product

The s_i coefficient is listed in Table 3.12. In this preliminary model, only Li₂O has a squared term (s_{ii}) and there are no cross-product terms (s_{jk}).

The comparison between the predicted and measured SO₃ solubility is presented in Figure 3.15. More data points are below the equal line indicating they are under-predicted by the model. This is reasonable because a large portion of data used to develop the preliminary model were not actually saturated with SO₃. The previous samples were prepared by one-time mixing and melting of the baseline glasses with Na₂SO₄, which likely did not fully saturate the glasses and achieve the true SO₃ solubility. On the other hand, the three times mixing and melting sulfur saturation method developed in this work (see Section 2.10) was shown to fully saturate test glasses with SO₃ during procedure development.⁽¹⁰⁾ The preliminary model also over-predicted the SO₃ solubility of several compositions (points above the equal line in Figure 3.15), suggesting some errors in the model fitting. Future work is required to improve SO₃ solubility prediction.

(10) Jin T, DS Kim, LP Darnell, BL Weese, NL Canfield, M Bliss, JR Davies, CC Bonham, MJ Schweiger, and AA Kruger. 2016. "Experimental Study of Sulfur Solubility in Low-Activity Waste Glass," *American Ceramic Society Glass & Optical Materials Division Annual Meeting, May 22-26, 2016*. Madison, Wisconsin.

Table 3.12. List of SO₃ Solubility Model Components and Coefficients (Vienna et al 2014)

Model Term	<i>s_i</i> Coefficient
Al ₂ O ₃	-2.091901
B ₂ O ₃	3.0440748
CaO	4.4422886
Cl	-22.65353
Cr ₂ O ₃	-13.14139
K ₂ O	0.615785
Li ₂ O	2.4739255
Na ₂ O	2.8972089
P ₂ O ₅	4.606083
SiO ₂	0.2407285
SnO ₂	-1.775325
V ₂ O ₅	7.5345478
ZrO ₂	-1.871916
Others *	-0.280272
Li ₂ O × Li ₂ O	260.20302

* Others is the sum of all components not specifically listed as model terms (i.e. those not anticipated to have a significant effect).

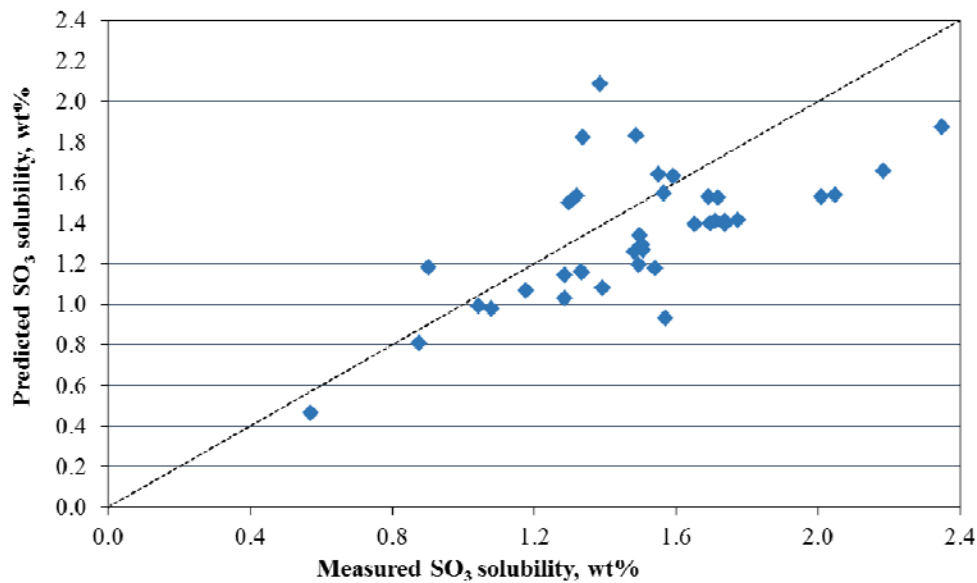


Figure 3.15. Predicted versus Measured SO₃ Solubility for LAW Phase 1 Enhanced Glasses

3.10 Iron Redox Measurement

For the tin to be soluble, some glasses were prepared using tin oxalate instead of tin oxide. Because oxalate is a reducing agent, an effort was made to determine how much of the iron in these glasses was affected. The results are shown in Table 3.13. A variety of glasses were analyzed including ones with tin oxalate and with tin oxide, along with ones with and without iron. The glass (New-IL-456) using tin oxide was not reduced as expected. Two of the three glasses with iron and tin oxalate were reduced. It is unclear at this time why the other glass (New-OL-45748) with tin oxalate and iron was not reduced. This does show that using tin oxalate most likely will result in obtaining a reduced glass.

Table 3.13. Iron Redox Results of LAW Glass

Component	Glass ID						
	LAW-ORP- LD1(2)	New-IL- 456	New-OL- 127708 (Mod)	New-OL- 45748 (Sn Mod)	New-OL- 54017 (Sn Mod)	New-OL- 62909 (Mod)	New-OL- 65959 (Mod)
Al ₂ O ₃	10.15	6.25	10.94	13.85	3.50	12.35	13.85
B ₂ O ₃	12.04	8.00	13.75	6.00	6.00	8.90	13.05
CaO	8.01	9.00	0.30	12.24	11.17	12.24	--
Cl	0.33	0.12	0.06	0.47	0.06	0.47	0.06
Cr ₂ O ₃	0.50	0.08	0.04	0.31	0.04	0.31	0.04
Cs ₂ O	0.13	-- ^(a)	--	--	--	--	--
F	0.17	0.18	0.09	0.71	0.09	0.71	0.09
Fe ₂ O ₃	1.00	1.25	1.50	1.50	1.50	--	--
K ₂ O	0.16	0.20	1.50	--	--	--	--
Li ₂ O	--	3.50	2.50	5.00	--	2.50	5.00
MgO	1.00	2.50	3.50	--	3.50	3.50	3.50
Na ₂ O	20.98	15.00	13.00	11.40	15.00	13.00	16.50
NiO	0.04	--	--	--	--	--	--
P ₂ O ₅	0.29	0.38	0.20	1.51	0.20	1.51	0.20
PbO	0.01	--	--	--	--	--	--
SiO ₂	37.14	43.15	46.51	34.00	47.00	33.50	34.50
SO ₃	1.06	0.40	0.61	0.10	0.10	0.10	0.10
SnO ₂	--	3.50	4.50 ^(b)	5.00 ^(b)	5.00 ^(b)	4.41 ^(b)	4.50 ^(b)
V ₂ O ₅	1.00	3.00	--	2.91	1.85	--	3.60
ZnO	3.00	2.00	1.00	5.00	5.00	1.00	5.00
ZrO ₂	3.00	1.50	--	--	--	5.50	--
Fe ²⁺ (mg/kg)	<49.1	<46.3	8890	<47.5	6030	49.3	<46.2
Total Fe (mg/kg)	6850	8770	11000	10500	11500	904	281
Fe ³⁺ (mg/kg)	6850	8770	2110	10500	5470	855	281
Fe ²⁺ /Fe ³⁺	<0.00717	<0.00676	4.21	<0.00452	1.10	0.0577	<0.164

(a) A dash indicates the target glass composition did not contain the component. In the case of Fe, impurities were sufficient to obtain redox data.

(b) Tin oxalate was used in the melt.

3.11 Matrix Glasses Needing Composition Modification

There were four of the OL matrix glasses that needed some modification to their composition and/or melt temperature to form homogeneous glasses. Two additional OL matrix glasses needed to have tin oxalate added instead of tin oxide and two others needed to have their SO₃ decreased to form homogenous glasses. Modifications to all of these glasses are discussed below. The modified glasses initially were prepared in either 150 g or 200 g batches. The smaller batch size was used for efficiency to determine if the composition produced a homogenous glass. The composition designated as “final” for each glass requiring modification was used to make a large, 900 g slab of glass for property measurements.

3.11.1 Glass New-OL-8788

The iterations of composition and/or melt temperature modifications made to this glass are shown in Table 3.14 with the changes for each modification in bold. Determined from previous experience, it was not attempted to melt this original composition at 1150°C based on such low Na₂O and high ZrO₂ content. However, a smaller batch of the original composition was prepared and melted at 1325°C to see if it would be successful. Therefore, the first melt increased the melt temperature from 1150°C to 1325°C without changing the chemical composition.

This melt of New-OL-8788 glass resulted in an opaque, tan glass as shown in Figure 3.16. The melt was very thick with bubbles that formed on the bottom of the melt and adhered to the crucible. There was no visual sign of excessive volatilization, but undissolved particles were observed throughout the glass after the pour.

Table 3.14. Composition and Melt Temperature Modifications Made to LAW Phase 1 Enhanced Glass New-OL-8788

Component	Glass Oxide (mass fraction)					
	Original with higher melt T	1 st Mod	2 nd Mod	3 rd Mod	4 th Mod	5 th and Final
SiO ₂	0.4700	0.4700	0.4700	0.4600	0.4550	0.4600
Al ₂ O ₃	0.1385	0.1385	0.1285	0.1285	0.1235	0.1235
B ₂ O ₃	0.0600	0.0600	0.0600	0.0600	0.0600	0.0600
Na ₂ O	0.1000	0.1150	0.1250	0.1300	0.1300	0.1300
Fe ₂ O ₃	0.0150	0.0150	0.0150	0.0150	0.0150	0.0150
CaO	0.0005	0.0005	0.0005	0.0005	0.0005	0.0005
Li ₂ O	0.0201	0.0201	0.0201	0.0250	0.0250	0.0250
SnO ₂	0.0000	0.0000	0.0000	0.0000	0.0000	0.0000
ZnO	0.0500	0.0500	0.0500	0.0500	0.0500	0.0500
ZrO ₂	0.0650	0.0500	0.0500	0.0500	0.0600	0.0550
V ₂ O ₅	0.0000	0.0000	0.0000	0.0000	0.0000	0.0000
Cl	0.0047	0.0047	0.0047	0.0047	0.0047	0.0047
Cr ₂ O ₃	0.0031	0.0031	0.0031	0.0031	0.0031	0.0031
K ₂ O	0.0150	0.0150	0.0150	0.0150	0.0150	0.0150
MgO	0.0350	0.0350	0.0350	0.0350	0.0350	0.0350
P ₂ O ₅	0.0151	0.0151	0.0151	0.0151	0.0151	0.0151
F	0.0071	0.0071	0.0071	0.0071	0.0071	0.0071
SO ₃	0.0010	0.0010	0.0010	0.0010	0.0010	0.0010
First/Second Melt Temp (°C)	1325/1325	1325/1350	1300/1325	1300	1300	1300/1300
First/Second Melt Time (min)	60/90	60/90	60/~60	60	60	60/60



Figure 3.16. Photograph of First Melt of New-OL-8788 Glass with Increased Melt Temperature to 1325°C for 90 min

For the 1st compositional modification of the New-OL-8788 glass, the Na₂O mass fraction was increased to 0.1150, the ZrO₂ mass fraction was decreased to 0.0500, and the melt temperature was increased from 1325°C to 1350°C. This modification still had inclusions present in the glass after melting for 90 min as seen in Figure 3.17, and the melt was still fairly thick on pouring.



Figure 3.17. Photograph of First Compositional Modification of New-OL-8788 Glass Melted at 1350°C for 90 min (plastic disk is 12 cm diameter)

For the 2nd compositional modification of the New-OL-8788 glass, it was decided that the Na₂O mass fraction should be increased by 0.01 and the Al₂O₃ mass fraction decreased by 0.01 compared to the 1st modification, while maintaining the ZrO₂ mass fraction at 0.05 and melting at 1300°C. The 2nd modification was still thick upon pouring, even after the second melt was at 1325°C. The glass was cloudy with undissolved particles as shown in Figure 3.18. When looking through the optical microscope, many really small particles were seen throughout the melt.



Figure 3.18. Photograph of Second Compositional Modification of New-OL-8788 Glass Melted at 1325°C for 60 min (plastic disk is 12 cm diameter)

For the 3rd compositional modification, the Na₂O and Li₂O mass fractions were each increased by another 0.005 and the SiO₂ mass fraction was reduced by 0.01, while maintaining the ZrO₂ mass fraction at 0.05 and melting at 1300°C. The 3rd compositional modification produced a nice glass without inclusions (Figure 3.19) but was very thick and difficult to pour.

In an attempt to maximize the amount of zirconium in the glass to keep the composition as close to the original as possible, we decided to maintain the Na₂O mass fraction at 0.13 and increase the ZrO₂ mass fraction to 0.06 because the initial ZrO₂ mass fraction was 0.065. This required decreasing the SiO₂ and Al₂O₃ mass fractions by 0.005 each. This 4th modification was melted at 1300°C and was very thick and difficult to pour. It formed a glass-ceramic material with lots of undissolved particles present (Figure 3.20). It looked very similar to the initial compositional melt (Figure 3.16).

Therefore, the ZrO₂ mass fraction was decreased to 0.055, the SiO₂ was increased by 0.005, and the batch was melted at 1300°C for 60 min. This 5th and final modification produced a smooth clear glass (Figure 3.21), although it was slightly thick to pour. It was decided that this would be the final modified composition for the New-OL-8788 glass to proceed with as part of the test matrix.



Figure 3.19. Photograph of Third Modification of New-OL-8788 Glass Melted at 1300°C for 60 min (plastic disk is 12 cm diameter)



Figure 3.20. Photograph of Fourth Modification of New-OL-8788 Glass Melted at 1300°C for 60 min (plastic disk is 12 cm diameter)



Figure 3.21. Photograph of Final Compositional Modification of New-OL-8788 Glass Melted at 1300°C for 60 min (plastic disk is 12 cm diameter)

3.11.2 New-OL-45748

The iterations of composition modifications made to glass New-OL-45748 are shown in Table 3.15 with the chemical changes bolded.

The original composition of the New-OL-45748 glass was melted at 1200°C for 80 min and produced a glass-ceramic material with streaks of pea-soup green and brown colors throughout the glass along with yellow-salt segregated streaks on top. After grinding the material to a fine powder, it was re-melted at 1250°C. We observed a settled ceramic-like layer on the crucible bottom that could have been SnO₂ or ZrO₂. The glass was powdered again in the grinding mill and re-melted at 1275°C for 90 min, which produced plating on the crucible bottom that looked like SnO₂ with many undissolved particles present (phase identification was based only on similar appearance to other samples containing undissolved SnO₂ and has not been confirmed experimentally).

Therefore, the Na₂O mass fraction was increased from 0.1140 to 0.1350 and the Al₂O₃ mass fraction was decreased from 0.1385 to 0.1175. After melting this first modification at 1250°C for 65 min, it still had undissolved particles on the bottom of the crucible and layers throughout. The glass was ground to a fine powder and re-melted at 1300°C for 90 min, after which a residual layer was still observed at the bottom of the crucible. It was determined by XRD that SnO₂ was precipitating out of the melt as shown in Figure 3.22.

Table 3.15. Composition Modifications Made to Glass New-OL-45748

Component	Glass Oxide Fraction			
	Original	1 st Mod	2 nd Mod	Final
SiO ₂	0.3400	0.3400	0.3400	0.3400
Al ₂ O ₃	0.1385	0.1175	0.1175	0.1385
B ₂ O ₃	0.0600	0.0600	0.0600	0.0600
Na ₂ O	0.1140	0.1350	0.1350	0.1140
Fe ₂ O ₃	0.0150	0.0150	0.0150	0.0150
CaO	0.1224	0.1224	0.1224	0.1224
Li ₂ O	0.0500	0.0500	0.0500	0.0500
SnO ₂	0.0500	0.0500	0.0500⁽¹⁾	0.0500⁽¹⁾
ZnO	0.0500	0.0500	0.0500	0.0500
ZrO ₂	0.0000	0.0000	0.0000	0.0000
V ₂ O ₅	0.0291	0.0291	0.0291	0.0291
Cl	0.0047	0.0047	0.0047	0.0047
Cr ₂ O ₃	0.0031	0.0031	0.0031	0.0031
K ₂ O	0.0000	0.0000	0.0000	0.0000
MgO	0.0000	0.0000	0.0000	0.0000
P ₂ O ₅	0.0151	0.0151	0.0151	0.0151
F	0.0071	0.0071	0.0071	0.0071
SO ₃	0.0010	0.0010	0.0010	0.0010
First/Second Melt Temp (°C)	1200/1250/1275	1250/1300	1300/1300	1300/1300
First/Second Melt Time (min)	80/NR/90	65/90	60/90	60/NR

(1) The tin was added as tin oxalate instead of SnO₂.

NR = Not recorded



Figure 3.22. Photograph of New-OL-45748 Glass from Bottom of Crucible after First Modification Melted at 1300°C for 90 min

For the next modification, tin oxalate was used instead of tin oxide in the batch and the melt temperature was increased to 1300°C. With the tin oxalate, the tin went into solution but the glass was in a reduced state as shown by the color change of the glass in Figure 3.23. Note that without the reducing conditions of the tin oxalate, the glass would be bright green and transparent similar to that seen in Figure 3.21. Glass could be produced at the original test matrix composition using tin oxalate instead of tin oxide, so the final modification includes the tin oxalate and a melt temperature of 1300°C (see Figure 3.24).



Figure 3.23. Photographs of Glass New-OL-45748 Color Comparison with Oxidizing Conditions (top) and Reducing Conditions (bottom) (plastic disk is 12 cm diameter)



Figure 3.24. Photograph of Melt of New-OL-45748 with Tin Oxalate Substituted for Tin Oxide in Original Composition Melted at 1300°C for 60 min

3.11.3 New-OL-54017

The iterations of composition modifications made to glass New-OL-54017 are shown in Table 3.16 with the changes bolded.

Table 3.16. Composition Modifications Made to Glass New-OL-54017

Component	Glass Oxide Fraction	
	Original	Final
SiO ₂	0.4700	0.4700
Al ₂ O ₃	0.0350	0.0350
B ₂ O ₃	0.0600	0.0600
Na ₂ O	0.1500	0.1500
Fe ₂ O ₃	0.0150	0.0150
CaO	0.1117	0.1117
Li ₂ O	0.0000	0.0000
SnO ₂	0.0500	0.0500⁽¹⁾
ZnO	0.0500	0.0500
ZrO ₂	0.0000	0.0000
V ₂ O ₅	0.0183	0.0183
Cl	0.0006	0.0006
Cr ₂ O ₃	0.0004	0.0004
K ₂ O	0.0000	0.0000
MgO	0.0350	0.0350
P ₂ O ₅	0.0020	0.0020
F	0.0009	0.0009
SO ₃	0.001	0.001
First/Second Melt Temp (°C)	1200/1200	1250/1250
First/Second Melt Time (min)	60/85	60/90

(1) The tin was added as tin oxalate instead of tin oxide.

It was determined that the tin oxide was not dissolving in the melt of this glass after melting twice at 1200°C up to 85 min as shown in Figure 3.25. The white inclusions found in the glass product were found to be cassiterite in the XRD pattern (shown in Figure 3.26). The final glass composition substituted tin oxalate for the tin oxide mass fraction. The tin went into solution but the glass was highly reduced as shown by the dark color change of the glass in Figure 3.27.



Figure 3.25. Photograph of Glass New-OL-54017 Original Composition Melted at 1200°C for 85 min

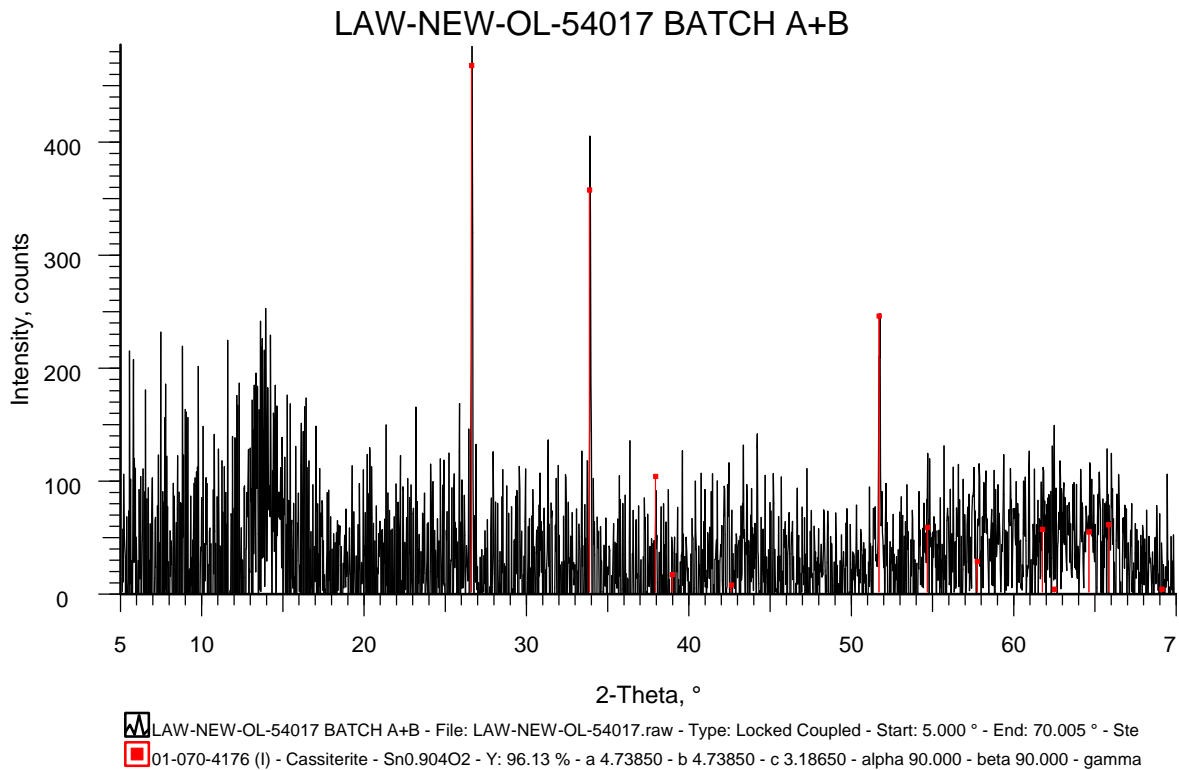


Figure 3.26. XRD Pattern of Original New-OL-54017 Glass Composition

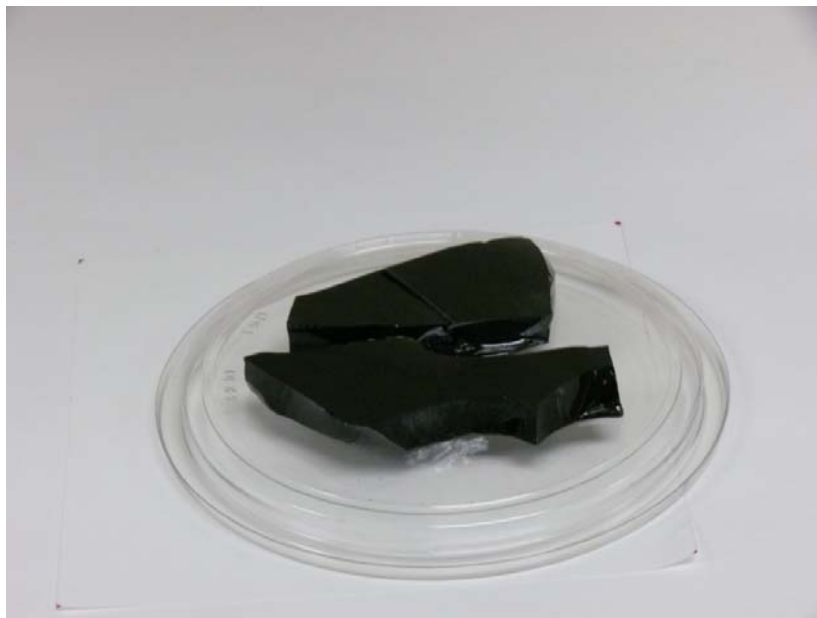


Figure 3.27. Photograph of Glass New-OL-54017 Final Composition with Tin Oxalate Melted at 1250°C for 90 min (plastic disk is 12 cm diameter)

3.11.4 New-OL-62909

The iterations of composition modifications made to the New-OL-62909 glass are shown in Table 3.17 with compositions changes bolded.

Table 3.17. Composition Modifications Made to Glass New-OL-62909

Component	Glass Oxide Fraction			
	Original	1 st Mod	2 nd Mod	Final
SiO ₂	0.3400	0.3400	0.3350	0.3350
Al ₂ O ₃	0.1385	0.1235	0.1235	0.1235
B ₂ O ₃	0.0890	0.0890	0.0890	0.0890
Na ₂ O	0.1000	0.1300	0.1300	0.1300
Fe ₂ O ₃	0.0000	0.0000	0.0000	0.0000
CaO	0.1224	0.1224	0.1224	0.1224
Li ₂ O	0.0250	0.0250	0.0250	0.0250
SnO ₂	0.0441	0.0441	0.0441	0.0441⁽¹⁾
ZnO	0.0100	0.0100	0.0100	0.0100
ZrO ₂	0.0650	0.0500	0.0550	0.0550
V ₂ O ₅	0.0000	0.0000	0.0000	0.0000
Cl	0.0047	0.0047	0.0047	0.0047
Cr ₂ O ₃	0.0031	0.0031	0.0031	0.0031
K ₂ O	0.0000	0.0000	0.0000	0.0000
MgO	0.0350	0.0350	0.0350	0.0350
P ₂ O ₅	0.0151	0.0151	0.0151	0.0151
F	0.0071	0.0071	0.0071	0.0071
SO ₃	0.0010	0.0010	0.0010	0.0010
First/Second Melt Temp (°C)	1300	1300/1300	1300/1300	1300
First/Second Melt Time (min)	~60	60/60	57/93	60

(1) The tin was added as tin oxalate instead of tin oxide.

When melted at 1300°C for 60 min, the original composition of this glass formed an opaque, glass-ceramic shown in Figure 3.28. XRD analysis found crystalline inclusions, mainly tin oxide and some baddeleyite (ZrO_2), as shown in Figure 3.29. Figure 3.30 shows what the undissolved particles looked like under magnification.



Figure 3.28. Photograph of Glass New-OL-62909 Original Composition Melted at 1300°C for 60 min

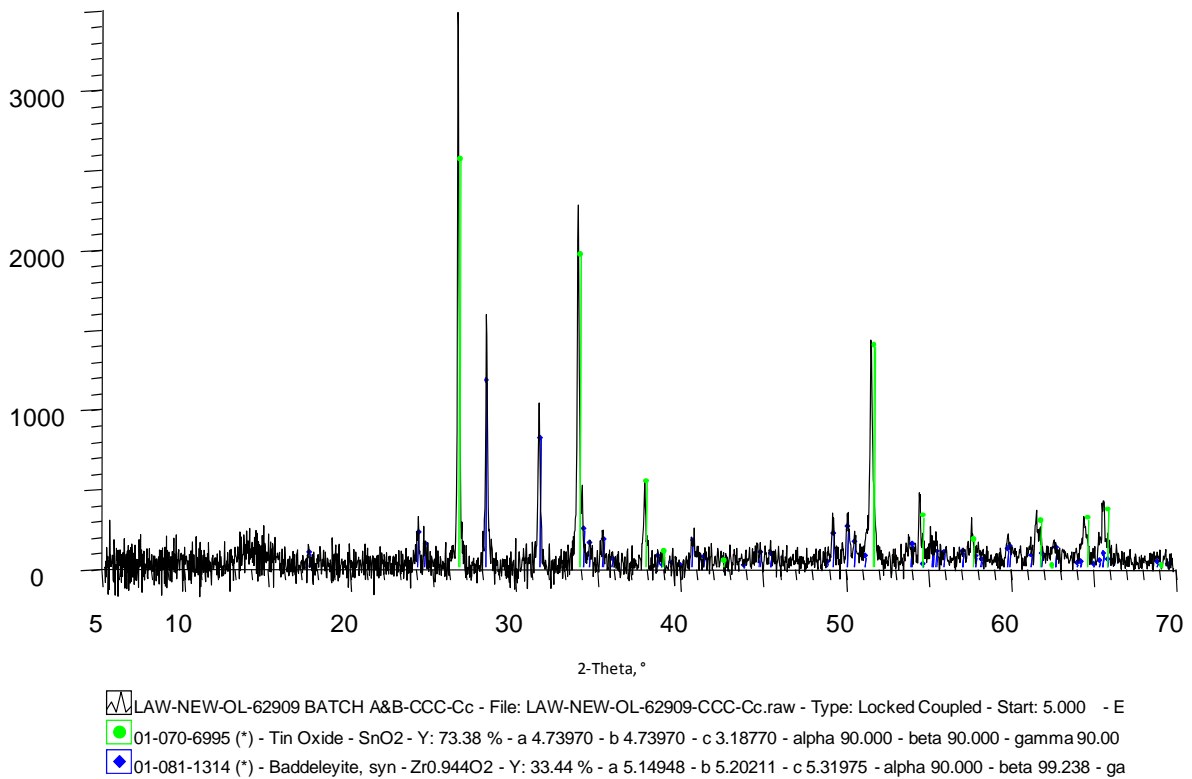


Figure 3.29. XRD Pattern of Original New-OL-62909 Glass Composition

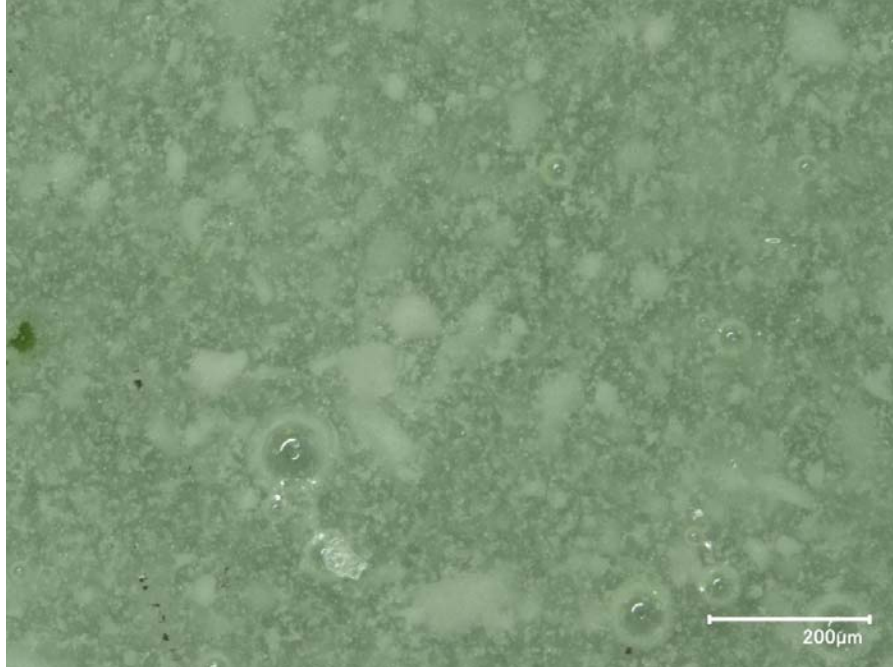


Figure 3.30. Optical Micrograph of Undissolved Particles in the New-OL-62909 Glass Initial Melt

For the first modification of the New-OL-62909 glass, the Na_2O mass fraction was increased by 0.030, ZrO_2 and Al_2O_3 mass fractions were decreased by 0.015 each, and the melt temperature was maintained at 1300°C for 60 min. This melt produced a very deep green glass as shown in Figure 3.31 with a honey-like thickness when poured.



Figure 3.31. Photograph of First Modification of Glass New-OL-62909 Melted at 1300°C for 60 min (plastic disk is 12 cm diameter)

Because these levels of ZrO_2 , SnO_2 and Al_2O_3 went into the glass, we decided to increase the ZrO_2 mass fraction to 0.01 less than original (0.055) at the expense of the SiO_2 and maintain the other components the same as the first modification. This second modification melted into a smooth and thick dark green glass with a layer of undissolved material on the crucible bottom similar to what is observed in Figure 3.32. There was also some undissolved material that was determined to be SnO_2 similar to Figure 3.4. This glass is shown in Figure 3.32 but the undissolved material cannot be seen without a microscope.

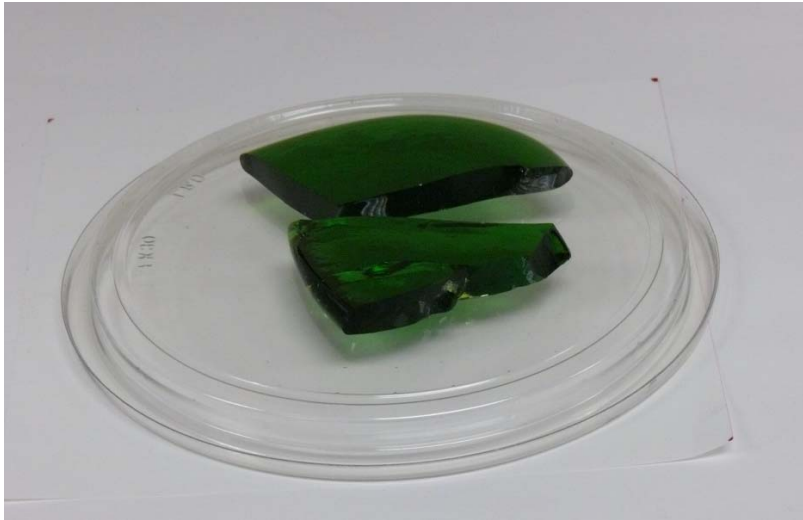


Figure 3.32. Photograph of Second Modification of Glass New-OL-62909 Melted at $1300^{\circ}C$ for 90 min (plastic disk is 12 cm diameter)

Therefore, tin oxalate replaced tin oxide in the third (and final) modification of the New-OL-62909 glass to produce a homogenous glass. This final glass composition melted very well at $1300^{\circ}C$ for 60 min and created a sea green glass with no undissolved particles present, as shown in Figure 3.33.

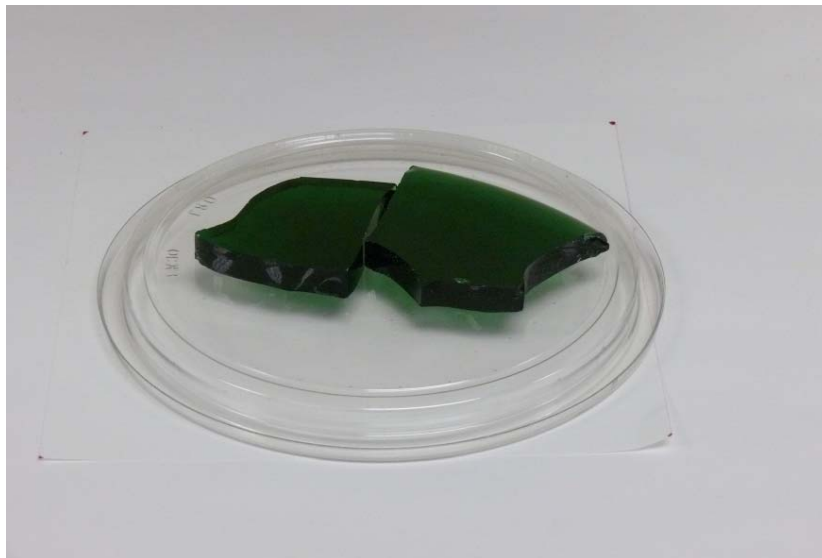


Figure 3.33. Photograph of Final Modification of Glass New-OL-62909 Melted at $1300^{\circ}C$ for 60 min (plastic disk is 12 cm diameter)

3.11.5 New-OL-65959

The iterations of composition modifications made to the New-OL-65959 glass are shown in Table 3.18 with the changes bolded.

Table 3.18. Composition and Melt Temperature Modifications Made to Glass New-OL-65959

Component	Glass Oxide Fraction			
	Original ⁽²⁾	1 st Mod	2 nd Mod	Final
SiO ₂	0.3400	0.3600	0.3400	0.3450
Al ₂ O ₃	0.1385	0.1385	0.1385	0.1385
B ₂ O ₃	0.1305	0.1305	0.1305	0.1305
Na ₂ O	0.1650	0.1650	0.1650	0.1650
Fe ₂ O ₃	0.0000	0.0000	0.0000	0.0000
CaO	0.0000	0.0000	0.0000	0.0000
Li ₂ O	0.0500	0.0500	0.0500	0.0500
SnO ₂	0.0500	0.0300	0.0500⁽¹⁾	0.0450⁽¹⁾
ZnO	0.0500	0.0500	0.0500	0.0500
ZrO ₂	0.0000	0.0000	0.0000	0.0000
V ₂ O ₅	0.0360	0.0360	0.0360	0.0360
Cl	0.0006	0.0006	0.0006	0.0006
Cr ₂ O ₃	0.0004	0.0004	0.0004	0.0004
K ₂ O	0.0000	0.0000	0.0000	0.0000
MgO	0.0350	0.0350	0.0350	0.0350
P ₂ O ₅	0.0020	0.0020	0.0020	0.0020
F	0.0009	0.0009	0.0009	0.0009
SO ₃	0.0010	0.0010	0.0010	0.0010
First/Second Melt Temp (°C)	1225/1275	1250	1300/1250	1250
First/Second Melt Time (min)	65/75	63	47/59	60

(1) The tin was added as tin oxalate instead of tin oxide.
(2) Estimated ~60 to 70g spilled during foaming.

When melted at 1275°C for 75 min, the original composition formed a green glass with swirls throughout and a ceramic-type layer on the bottom of the crucible, as shown in Figure 3.34. XRD analysis determined the non-glass material to be tin oxide as shown in Figure 3.35.

For the first modification, the tin oxide mass fraction was decreased to 0.03, and the SiO₂ mass fraction was increased to 0.36. The batch was melted at 1250°C for 60 min. This melt produced a light green glass seen in Figure 3.36, with very small undissolved particles only seen with the microscope.

For the second modification, the original composition with tin oxalate replacing the tin oxide was melted at 1300°C. This produced a reduced black glass (Figure 3.37) with hair-like crystals on the crucible bottom.

Because of the crystals on the crucible bottom, the tin oxide mass fraction was decreased to 0.045 using tin oxalate once again and the original SiO₂ mass fraction was increased by 0.005 from the original amount. The batch was melted at 1250°C for 60 min. This third and final modification produced a smooth greenish-black glass without any observed undissolved particles present, as shown in Figure 3.38.



Figure 3.34. Photograph of Glass New-OL-65959 Original Composition with Large Ceramic Pieces Melted at 1275°C for 75 min

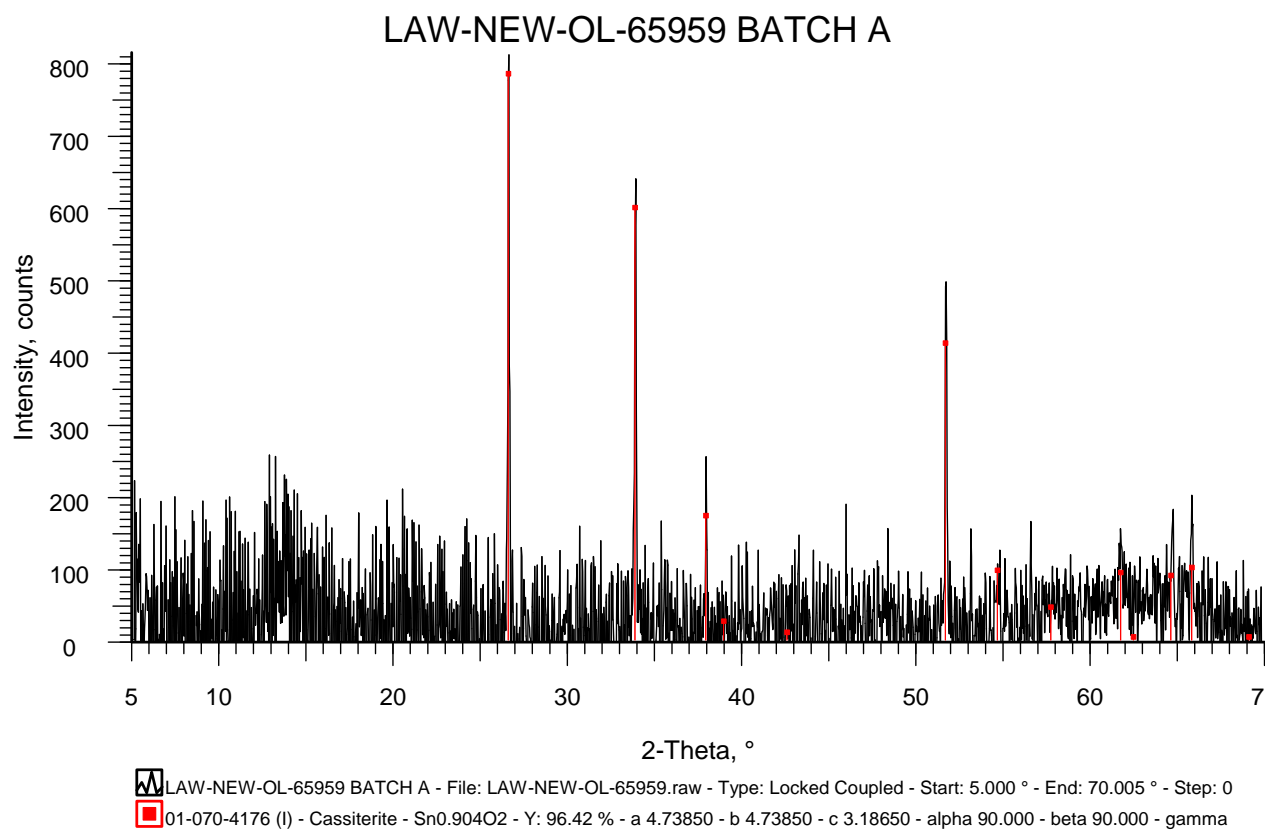


Figure 3.35. XRD Pattern of Original Glass New-OL-65959 Composition



Figure 3.36. Photograph of Glass New-OL-65959 First Modification Melted at 1250°C for 60 min (plastic disk is 12 cm diameter)



Figure 3.37. Photograph of Glass New-OL-65959 Second Modification Melted at 1250°C for 60 min (plastic disk is 12 cm diameter)



Figure 3.38. Photograph of Glass New-OL-65959 Final Modification Melted at 1250°C for 60 min (plastic disk is 12 cm diameter)

3.11.6 New-OL-108249

The original composition of the New-OL-108249 glass had salt segregation on the glass surface and extensive phase separation by color differences throughout, shown in Figure 3.39, following the second melt at 1200°C for 65 min. There was a twofold purpose with the New-OL-108249 glass modifications: 1) to find a composition near the original composition that would incorporate the original targeted SO_3 mass fraction (0.0154) into the glass and 2) to determine the SO_3 solubility level in the original composition. Modifications 1 through 8 were used to determine a composition capable of retaining the original SO_3 mass fraction. The final composition was used to validate the solubility level of SO_3 as described in Section 3.12. Iterations of composition modifications made to this glass are shown in Table 3.19 with the changes bolded.



Figure 3.39. Photograph of Glass New-OL-108249 Original Composition Melted at 1200°C for 65 min

The first modification of the New-OL-108249 glass increased SiO_2 mass fraction by 0.02 to 0.36 and the Al_2O_3 mass fraction was decreased by 0.02 to 0.0995. The modified composition was melted at 1150°C for 60 min. This formed a glass-ceramic with salt segregation in the crucible.

Table 3.19. Composition Modifications Made to Glass New-OL-108249

Component	Glass Oxide Fraction									
	Original	1 st Mod	2 nd Mod	3 rd Mod	4 th Mod	5 th Mod	6 th Mod	7 th Mod	8 th Mod	Final
SiO ₂	0.3400	0.3600	0.3650	0.3550	0.3700	0.3700	0.3332	0.3400	0.3400	0.3423
Al ₂ O ₃	0.1195	0.0995	0.1195	0.1195	0.1245	0.1195	0.1171	0.1195	0.1195	0.1203
B ₂ O ₃	0.0600	0.0600	0.0600	0.0600	0.0650	0.0600	0.0882	0.0900	0.0800	0.0604
Na ₂ O	0.1551	0.1551	0.1551	0.1551	0.1651	0.1601	0.1324	0.1351	0.1451	0.1561
Fe ₂ O ₃	0.0150	0.0150	0.0150	0.0150	0.0150	0.0150	0.0147	0.0150	0.0150	0.0151
CaO	0.1000	0.1000	0.0750	0.1000	0.0500	0.0650	0.0980	0.1000	0.1000	0.1007
Li ₂ O	0.0500	0.0500	0.0500	0.0500	0.0500	0.0500	0.0392	0.0400	0.0400	0.0503
SnO ₂	0.0500	0.0500	0.0500⁽¹⁾	0.0350⁽¹⁾	0.0500	0.0500	0.0490	0.0500	0.0500	0.0503
ZnO	0.0500	0.0500	0.0500	0.0500	0.0500	0.0500	0.0490	0.0500	0.0500	0.0503
ZrO ₂	0.0000	0.0000	0.0000	0.0000	0.0000	0.0000	0.0000	0.0000	0.0000	0.0000
V ₂ O ₅	0.0000	0.0000	0.0000	0.0000	0.0000	0.0000	0.0200	0.0000	0.0000	0.0000
Cl	0.0047	0.0047	0.0047	0.0047	0.0047	0.0047	0.0046	0.0047	0.0047	0.0047
Cr ₂ O ₃	0.0031	0.0031	0.0031	0.0031	0.0031	0.0031	0.0030	0.0031	0.0031	0.0031
K ₂ O	0.0150	0.0150	0.0150	0.0150	0.0150	0.0150	0.0147	0.0150	0.0150	0.0151
MgO	0.0000	0.0000	0.0000	0.0000	0.0000	0.0000	0.0000	0.0000	0.0000	0.0000
P ₂ O ₅	0.0151	0.0151	0.0151	0.0151	0.0151	0.0151	0.0148	0.0151	0.0151	0.0152
F	0.0071	0.0071	0.0071	0.0071	0.0071	0.0071	0.0070	0.0071	0.0071	0.0071
SO ₃	0.0154	0.0154	0.0154	0.0154	0.0154	0.0154	0.0151	0.0154	0.0154	0.0089
First/Second Melt Temp (°C)	1150/1200	1150/1150	1150	1150	1150/1150	1200/1200	1250	1200/1200	1200/ 1250	1250/1200/1300
First/Second Melt Time (min)	65/65	61/62	61	65	61/61	NR/60	60	60/NR	NR/60	60/90/60

(1) The tin was added as tin oxalate instead of tin oxide.
(2) NR = Not recorded

The second modification involved substituting tin oxalate for the tin oxide, decreasing the CaO mass fraction to 0.075, returning the Al₂O₃ to the original concentration, and increasing the SiO₂ mass fraction an additional 0.005 while still melting at 1150°C for 60 min. This formed a smooth glass-ceramic with sulfur salt inclusions throughout.

The third modification decreased the SnO₂ mass fraction (added as tin oxalate) to 0.035 and increased the SiO₂ mass fraction by 0.015 from the original while melting at 1150°C for 65 min. This melt produced a glass-ceramic with sulfur salts and phase separation with colorful streaks throughout the glass.

Therefore, reducing the CaO mass fraction to 0.05 and distributing the increase across the other main constituents (SiO₂, Al₂O₃, B₂O₃, and Na₂O) was tried in the fourth modification. This melt had undissolved particles that looked visually like cassiterite throughout the melt along with yellow sulfur segregation in the crucible as seen in Figure 3.40.



Figure 3.40. Photograph of Glass New-OL-108249 4th Modification Melted at 1150°C for 60 min

So a fifth modification decreased the CaO mass fraction by 0.035 from the original to 0.065, with corresponding increases from the original concentrations for SiO₂ and Na₂O. This modified composition was melted at 1200°C for 60 min. This produced a green glass as seen in Figure 3.41. However, there was residue at the bottom of the crucible that was yellowish in color and indicated undissolved sulfur salts.

The 6th modification involved decreasing the Na₂O mass fraction by 0.02 and Li₂O mass fraction by 0.01 while increasing the B₂O₃ mass fraction by 0.03 and V₂O₅ mass fraction by 0.02 and melting at 1250°C for 60 min. This produced a brownish glass with sulfur seen mainly in the crucible as shown in Figure 3.42. The next modification was similar to the previous one, except that it eliminated the V₂O₅ distributing the increase across the other constituents and was melted at 1200°C for 60 min. Visually it appeared that SnO₂ formed as a thin layer on the crucible bottom and sulfur formed around the edges in the crucible.

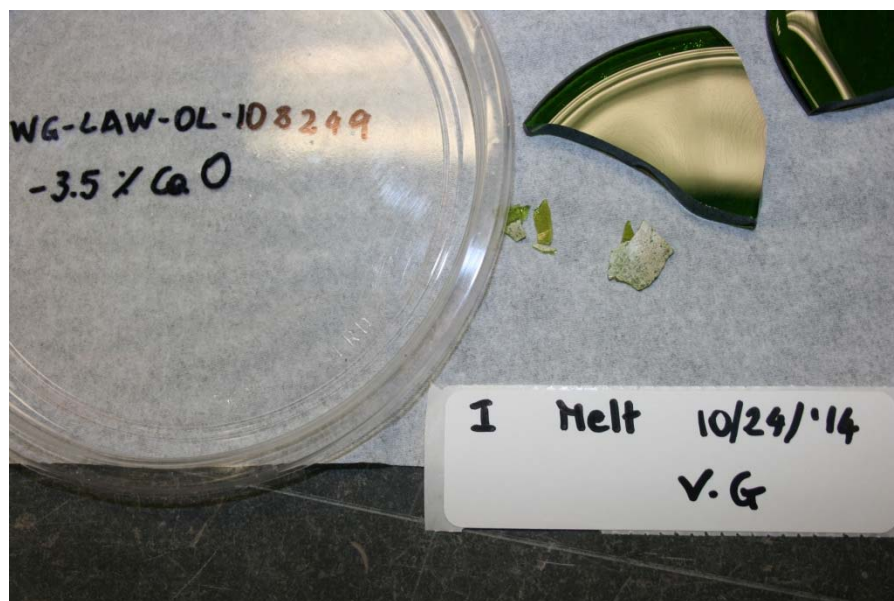


Figure 3.41. Photograph of Glass New-OL-108249 5th Modification Melted at 1200°C for 60 min (plastic disk is 12 cm diameter)

The last modification reduced the Na₂O and Li₂O mass fractions each by 0.01, increased the B₂O₃ mass fraction by 0.02, and used a melt temperature of 1200°C for 60 min. Sulfur formed on top of the glass and around the edges in the crucible after the first melt. After the second melt, a tan layer of what visually appeared to be SnO₂ formed on the bottom of the crucible with a green opaque glass.

The eight attempts to modify the New-OL-108249 glass composition did not have the desired success in retaining sulfur in the glass. As discussed in Section 3.12.1, a final modified composition was selected based on determining the sulfur solubility in the glass. The SO₃ mass fraction in the glass was substituted for the target SO₃ value, and the mass fractions of the remaining components were normalized so the mass fractions of all components (including SO₃) summed to unity. The modified glass composition was then re-batched and melted and used as the final composition, as shown in Table 3.19.



Figure 3.42. Photographs of Glass New-OL-108249 6th Modification Melted at 1250°C for 60 min

3.11.7 New-OL-116208

The original composition of the New-OL-116208 glass had salt segregation on the glass surface following the second melt at 1200°C for 65 min as shown in Figure 3.45. The same twofold method used in Section 3.11.6 with the New-OL-108249 glass was used here: 1) to find a composition near the original composition that would incorporate the original targeted content of 1.82 wt% SO₃ into the glass and 2) to determine the solubility level SO₃ level in the original composition. Modifications 1 through 3 were used to determine a composition capable of retaining the original SO₃ mass fraction. The final composition was used to validate the solubility level of SO₃ in the glass after the final melt accomplished without salt segregation (described in Section 3.12.2).

The iterations of composition modifications made to this glass are shown in Table 3.20 with the changes bolded.

Table 3.20. Composition Modifications Made to Glass New-OL-116208

Component	Glass Oxide Fraction				
	Original	1 st Mod	2 nd Mod	3 rd Mod	Final
SiO ₂	0.3400	0.3400	0.3400	0.3340	0.3431
Al ₂ O ₃	0.0350	0.0350	0.0350	0.0344	0.0353
B ₂ O ₃	0.0600	0.0850	0.0900	0.0589	0.0605
Na ₂ O	0.1619	0.1619	0.1619	0.1590	0.1634
Fe ₂ O ₃	0.0150	0.0150	0.0150	0.0147	0.0151
CaO	0.1224	0.1224	0.1224	0.1202	0.1235
Li ₂ O	0.0500	0.0500	0.0500	0.0491	0.0505
SnO ₂	0.0450	0.0450	0.0450	0.0442	0.0454
ZnO	0.0100	0.0100	0.0100	0.0098	0.0101
ZrO ₂	0.0650	0.0400	0.0350	0.0638	0.0656
V ₂ O ₅	0.0125	0.0125	0.0125	0.0300	0.0126
Cl	0.0047	0.0047	0.0047	0.0046	0.0047
Cr ₂ O ₃	0.0031	0.0031	0.0031	0.0030	0.0031
K ₂ O	0.0000	0.0000	0.0000	0.0000	0.0000
MgO	0.0350	0.0350	0.0350	0.0344	0.0352
P ₂ O ₅	0.0151	0.0151	0.0151	0.0148	0.0152
F	0.0071	0.0071	0.0071	0.0070	0.0072
SO ₃	0.0182	0.0182	0.0182	0.0179	0.0093
First/Second Melt Temp (°C)	1150/1200	1200	1200/1200	1200/1200	1250/1300
First/Second Melt Time (min)	70/65	60	60/60	65/65	60/60

To help incorporate the salt into the glass, the first modification involved increasing B₂O₃ mass fraction to 0.085, decreasing ZrO₂ mass fraction to 0.04, and melting at 1200°C for 60 min. This also formed a glass-ceramic with streaks of darker color and some yellow particles on top of the glass and in the crucible, as shown in Figure 3.43.



Figure 3.43. Photograph of Glass New-OL-116208 1st Modification Melted at 1200°C for 60 min

Because there was less salt present on the surface of this glass, the second modification involved further increasing B₂O₃ mass fraction to 0.09, decreasing ZrO₂ mass fraction to 0.035, and melting at 1200°C for 60 min. This formed a glass-ceramic again with phase separation and a very yellowish color as shown in Figure 3.44.



Figure 3.44. Photograph of Glass New-OL-116208 2nd Modification Melted at 1200°C for 60 min (plastic disk is 12 cm diameter)

The third modification increased V_2O_5 mass fraction to 0.03, decreased other components proportionately, and was melted at 1200°C for 60 min. This melt was very similar to the original composition with slightly less salts present, as shown in Figure 3.46. None of these modifications were successful in incorporating the segregated salt into the glass. As discussed in Section 3.12.2 below, a final modified composition was selected based on determining the sulfur solubility in the glass. The sulfur composition was substituted for the target SO_3 value, and the mass fractions of the remaining components were normalized so the mass fractions of all components (including SO_3) summed to unity. The modified glass composition was then batched, melted, and used as the final composition (Table 3.20).



Figure 3.45. Photograph of Glass New-OL-116208 Original Composition Melted at 1200°C for 65 min (plastic disk is 12 cm diameter)



Figure 3.46. Photograph of Glass New-OL-116208 3rd Modification Melted at 1200°C for 65 min

3.11.8 New-OL-127708

When melted at 1350°C for 60 min, the original composition of the New-OL-127708 glass formed a glass-ceramic with a layer of tan crystals on the crucible bottom, as shown in Figure 3.47. XRD analysis revealed crystalline inclusions to be tin oxide as shown in Figure 3.48.

Therefore, for the first modification shown in Table 3.21, the Na₂O mass fraction was increased by 0.025, the Al₂O₃ mass fraction was decreased by 0.025, and the batch was melted at 1300°C for 90 min. This melt produced a green opaque glass with white particles throughout the glass (which visually appeared to be SnO₂), as shown in Figure 3.49.

Table 3.21. Composition Modifications Made to Glass New-OL-127708

Component	Glass Oxide Mass Fractions				
	Original	1 st Mod	2 nd Mod	3 rd Mod	Final
SiO ₂	0.4700	0.4700	0.4700	0.4601	0.4651
Al ₂ O ₃	0.1344	0.1094	0.1094	0.1094	0.1094
B ₂ O ₃	0.1375	0.1375	0.1375	0.1375	0.1375
Na ₂ O	0.1000	0.1250	0.1250	0.1300	0.1300
Fe ₂ O ₃	0.0150	0.0150	0.0150	0.0150	0.0150
CaO	0.0030	0.0030	0.0030	0.0030	0.0030
Li ₂ O	0.0201	0.0201	0.0201	0.0250	0.0250
SnO ₂	0.0500	0.0500	0.0500⁽¹⁾	0.0500⁽¹⁾	0.0450⁽¹⁾
ZnO	0.0100	0.0100	0.0100	0.0100	0.0100
ZrO ₂	0.0000	0.0000	0.0000	0.0000	0.0000
V ₂ O ₅	0.0000	0.0000	0.0000	0.0000	0.0000
Cl	0.0006	0.0006	0.0006	0.0006	0.0006
Cr ₂ O ₃	0.0004	0.0004	0.0004	0.0004	0.0004
K ₂ O	0.0150	0.0150	0.0150	0.0150	0.0150
MgO	0.0350	0.0350	0.0350	0.0350	0.0350
P ₂ O ₅	0.0020	0.0020	0.0020	0.0020	0.0020
F	0.0009	0.0009	0.0009	0.0009	0.0009
SO ₃	0.0061	0.0061	0.0061	0.0061	0.0061
First/Second Melt Temp (°C)	1250/1350	1300/1300	1300	1300/1300	1300
First/Second Melt Time (min)	70/60	65/90	67	60/NR	62

(1) The tin was added as tin oxalate instead of tin oxide.

NR = Not recorded



Figure 3.47. Photograph of Glass New-OL-127708 Original Composition Melted at 1350°C for 60 min (plastic disk is 12 cm diameter)

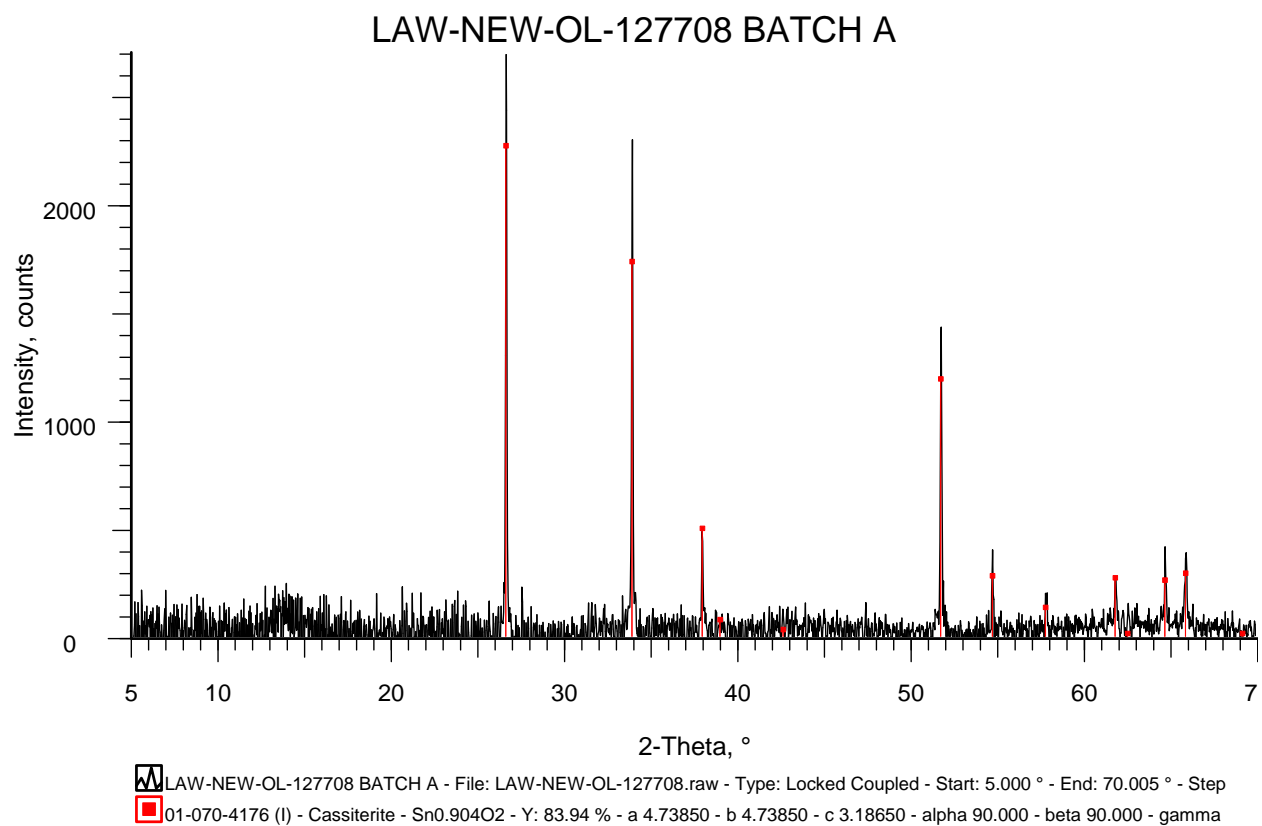


Figure 3.48. XRD Pattern of Original New-OL-127708 Composition



Figure 3.49. Photograph of Glass New-OL-127708 after 1st Modification Melted at 1300°C for 90 min (plastic disk is 12 cm diameter)

Because it visually appeared that the SnO_2 was still not dissolving into the glass, the same glass composition as modification #1 was used for modification #2, except tin oxalate was substituted for tin oxide, and the modified composition was melted at 1300°C for 60 min. This melt also had a layer of undissolved particles on the crucible bottom and a frothy surface layer.

In the third modification, tin oxalate remained the same, Na_2O mass fraction was increased to 0.13, Li_2O mass fraction was increased to 0.025, and SiO_2 was decreased to compensate for the additions. Melting temperature continued at 1300°C for 60 min. No crystals or undissolved particles were visible in the glass as shown in Figure 3.50, but under the microscope, some crystals were observed.

Because not many crystals were present in the 3rd modification melt, the composition for the 4th and final modification was only changed slightly by reducing the tin oxalate mass fraction to 0.045, increasing the SiO_2 to compensate, and continuing to melt at 1300°C for 60 min. This produced a glass (Figure 3.51) with only a few undissolved particles on the bottom of the crucible which were believed would melt into the glass with another melt. Therefore, this became the final composition of this glass.



Figure 3.50. Photograph of Glass New-OL-127708 after 3rd Modification Melted at 1300°C for 60 min (plastic disk is 12 cm diameter)



Figure 3.51. Photograph of Glass New-OL-127708 Final Composition Melted at 1300°C for 60 min (plastic disk is 12 cm diameter)

3.12 Matrix Glasses with Salt Segregation

As discussed in Sections 3.11.6 and 3.11.7, two of the glasses (New-OL-108249 and New-OL-116208) in this matrix had excess sulfur salt that did not dissolve into the glass. Therefore, the sulfur salts were washed from the ground glass to determine the sulfur amount incorporated in the glass during the melting process. To conduct the sulfur washing, the glass was milled for 2 min and then sieved through a 60 mesh sieve. Next, the powder was washed twice with DIW, once with 0.75 wt% HNO₃, once again with DIW, and finally with 100% ethanol. The glass powder was then dried at 95°C, and lastly re-melted. Sulfur concentration in the last glass re-melt was analytically measured by x-ray fluorescence (XRF). A new glass containing the measured SO₃ concentration was batched and melted for testing. The following sections describe the results of each of these glasses.

3.12.1 New-OL-108249

The original composition of this glass formed a glass with a segregated salt layer on the surface and extensive phase separation throughout (Figure 3.39) when melted at 1150°C, then crushed and re-melted at 1200°C. This glass was then ground and washed as described above and re-melted at 1150°C for 60 min. This melt produced a pea green glass with yellow sulfur salts throughout as seen in Figure 3.52. The sulfate wash as described above was repeated, the glass powder dried and re-melted at 1100°C for 60 min. This still produced sulfur streaks and possible crystals throughout the glass. This glass was then ground a third time and re-melted at 1300°C for 60 min and produced a glass with some streaks of both green and yellow throughout the top layer shown in Figure 3.53.

The sulfur content of the last melted glass was measured by XRF and found to be 0.89 wt%. Then, the composition of the glass was renormalized using this value for SO₃, with the final renormalized composition listed in Table 3.19. The glass was melted twice at 1300°C for 60 min each melt, and produced an emerald green glass as seen in Figure 3.54. This composition was used as the matrix glass. An overview of the sulfate wash and re-melt process is shown in Table 3.22.



Figure 3.52. Photograph of Glass New-OL-108249 1st Melt after 1st Sulfur Washing Melted at 1150°C for 60 min



Figure 3.53. Photograph of Glass New-OL-108249 2nd Melt (1300°C for 60 min) after 2nd Sulfur Washing (plastic disk is 12 cm diameter)

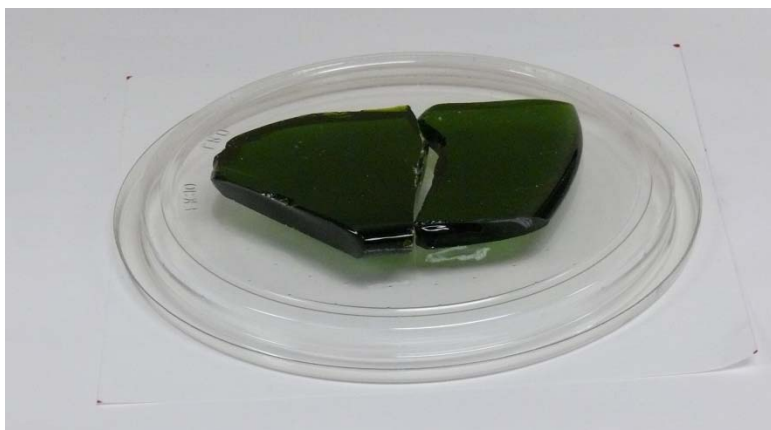


Figure 3.54. Photograph of Glass New-OL-108249 Final Modified Composition Melted at 1300°C for 60 min (plastic disk is 12 cm diameter)

Table 3.22. Glass New-OL-108249 Sulfate Washing

	Original Melt	First Wash and Melt	Second Wash and Melt	Modified Composition Melt
First/Second Melt Temp. (°C)	1150/1200	1150	1100/1300	1300/1300
First/Second Melt Time (min)	65/65	60	60/60	60/60
SO ₃ Wash before melt	No	Yes	Yes	No

3.12.2 New-OL-116208

When melted at 1200°C, the original composition of this glass formed a glass-ceramic with salt segregation all over the surface, as shown in Figure 3.45. This glass was then ground and washed as described in Section 3.12 and re-melted at 1200°C for 60 min. This melt produced a pea green glass with yellow sulfur salts throughout, as seen in Figure 3.55. The sulfur wash as described in Section 3.12 was repeated, and the glass powder was dried and re-melted at 1200°C for 60 min.

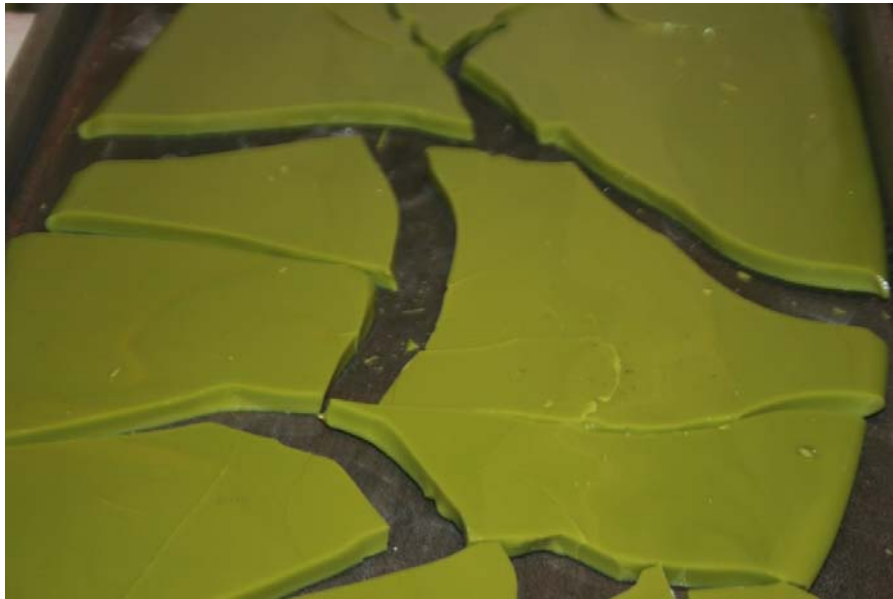


Figure 3.55. Photograph of Glass New-OL-116208 Melt after 1st Sulfate Washing Melted at 1200°C for 60 min

The sulfur content of the glass was then measured by XRF at 0.93 wt%. Then, the composition of the glass was renormalized using this value for SO₃, with the final renormalized composition listed in Table 3.20. This composition was melted at 1300°C for 80 min, and then ground and melted again at 1300°C for 60 min. It produced an opaque, greenish-yellow glass (Figure 3.56) with an amorphous black layer on the surface quenched by the stainless steel pour plate. The cloudy, opaque, green glass resulted from many submicron crystals that formed upon cooling. Because there were no sulfur salts present, this was chosen to be the final composition for this glass and all further testing on this glass used this composition. An overview of the entire sulfate wash and re-melt process is shown in Table 3.23.



Figure 3.56. Photograph of Glass New-OL-116208 Final Composition after Final Pour Melted at 1300°C for 60 min (plastic disk is 12 cm diameter)

Table 3.23. Glass New-OL-116208 Sulfate Washing

	Original Melt	First Wash and Melt	Second Wash and Melt	Modified Composition Melt
First/Second Melt Temp. (°C)	1150/1200	1200	1200	1300/1300
First/Second Melt Time (min)	70/65	60	60	80/60
SO ₃ Wash before melt	No	Yes	Yes	No

4.0 Summary

The objective of the task in this report was to generate data on different LAW glass compositions to ultimately support the development, validation, and implementation of glass property models that are capable of achieving high waste loading for the full region of Hanford LAW compositions. To extend the models beyond our current knowledge space, a new enhanced LAW EGCR was developed. Fifteen LAW glass components selected for variation in the experimental work, including an “Others” component mix. Certain components were chosen for variation in the experimental work for specific reasons. The components SnO₂ and ZrO₂ were included because they can decrease the VHT response. The components V₂O₅ and Li₂O were included because they can increase the SO₃ retention in the glass. Finally, the components ZnO and Cr₂O₃ were included because they can decrease refractory corrosion. The concentration range of K₂O was set to a relatively narrow range (0 to 1.5 wt%), which covered 98% of the glass projected to be produced at Hanford rather than the full range that extends above 5 wt%.

There were four of the outer-layer matrix glasses that needed some modification to their composition and/or melt temperature to form homogeneous glasses. Two more of the outer-layer matrix glasses needed to have tin oxalate added instead of tin oxide but maintained their original composition. And two others needed to have their SO₃ decreased to avoid segregated salt phases.

All of the sums of measured oxides for the study glasses fall within the interval of 96 to 101 wt%. For components present at more than 5 wt% of a glass, the measured chemical compositions were within 10% of the targeted compositions. The analyzed values of B₂O₃, Cl, F, and SO₃ were somewhat scattered. Some Cl, F, and SO₃ volatilization is likely, but the scatter in the measured values makes it difficult to quantify. Other than this observation, there was no indication of significant volatilization.

The Al₂O₃ concentration of glass EWG-LAW-ORP-LD1(3) was about 45% higher than the targeted value with B₂O₃, CaO, Na₂O, SiO₂, ZnO, and ZrO₂ below their targeted values. Upon further inspection, we determined that the incorrect aluminum source had been batched into the glass giving it a different composition than what was targeted. Therefore, based on the compositional analysis of these glasses, we concluded that the targeted compositions are adequate for use in future work to develop property-composition models except for the EWG-LAW-ORP-LD1(3). This glass composition was modified from the target composition to what was actually used.

For the tin to be soluble, a few glasses were prepared using tin oxalate instead of tin oxide. Because oxalate is a reducing agent, an effort was made to determine how much of the iron in these glasses was affected. A variety of glasses were analyzed including ones with tin oxalate and with tin oxide, along with ones with and without iron. The glass (New-IL-456) using SnO₂ was not reduced as expected. Two of the three glasses with iron and using tin oxalate were reduced. It is unclear at this time why the other glass (New-OL-45748) with tin oxalate and iron was not reduced. This does show that using tin oxalate most likely will result in obtaining a reduced glass.

During CCC treatment, several of the glasses seemed to form a heavy layer of crystals around the crucible walls. Several different methods were used for the CCC treatment including crucibles of different sizes and different materials of construction. When a quartz crucible was used, the glass could be CCC treated without forming a layer of crystallization. Therefore, this method was used for all such glasses.

The predicted glass density based on the model was higher than the measured density for all but two of the LAW Phase 1 glass compositions. Although the glass viscosity measured data versus the predicted viscosity data produced reasonably straight lines, they did not fall on the viscosity model measured versus predicted line and under-predicted the actual measured values (with a roughly constant offset). The EC at

1150°C at 1 kHz was used because this is the EC frequency used in the EC model and is above the frequency dependent regime for these melts. The previously published EC model did not fit this data well because it over-predicted the EC in all but three instances. Therefore, new models for all of these properties are needed to represent the property-composition relationships over the LAW enhanced glass composition region as the previous models were developed over a different LAW glass composition region.

In measuring the crystal fraction of the glasses by holding them at 950 to 1150°C for 24 ±2 hours, 10 glasses had either no crystals present or insufficient crystals to perform XRD analysis. Fifteen glasses contained cassiterite (SnO₂), and four glasses contained baddeleyite (ZrO₂). In three glasses, when the temperature was increased to 1150°C in selected glasses, the cassiterite was still present indicating the difficulty in getting it to re-dissolve after it forms in the melt.

PCT data showed that seven of the study glasses have NR values for boron (NR [B]) and sodium (NR [Na]) that are higher than the WTP contract limit of 2 g/m² for both the quenched and CCC heat treatments. These glasses are New-IL-42295, New-OL-17130, New-IL-5255, New-OL-14844, New-OL-80309, New-OL-116208 (SO₃ Mod) and New-OL-90780. Another four glasses have PCT values higher than the WTP PCT contract limit only for the CCC-treatment (New-IL-166731, New-OL-15493, New-OL-65959 (Mod), and New-OL-108249 (SO₃ Mod). This was anticipated and valuable to develop models that can accurately predict PCT responses at the limit. Glass New-IL-42295 had higher PCT values for the quenched glass than for the CCC glass.

Fourteen of the thirty-six glasses failed the VHT with a corrosion rate of >50 g/m²/d. This was anticipated and valuable to develop models that can accurately predict VHT responses at the limit. The glasses tested appeared to perform either extremely well or extremely poor with only four glasses near the limit.

5.0 References

- Aloy A, R Soshnikov, AV Trofimenko, JD Vienna, ML Elliott, and EW Holtzscheiter. 2006. "Improved Loading of Sulfate-Limited Waste in Glass." *Waste Management 2006*, Tucson, Arizona.
- ASTM. "Standard Test Methods for Determining Chemical Durability of Nuclear, Hazardous, and Mixed Waste Glasses and Multiphase Glass Ceramics: The Product Consistency Test (PCT)." ASTM C1285, ASTM International, West Conshohocken, Pennsylvania.
- ASTM. "Standard Test Method for Measuring Waste Glass or Glass Ceramic Durability by Vapor Hydration Test." ASTM C1663, ASTM International, West Conshohocken, Pennsylvania.
- ASTM. "Standard Test Method for Determining Liquidus Temperature of Immobilized Waste Glasses and Simulated Waste Glasses." ASTM C1720, ASTM International, West Conshohocken, Pennsylvania.
- Cooley SK, GF Piepel, H Gan, WK Kot, and IL Pegg. 2003. "A Two-Stage Layered Mixture Experiment Design for a Nuclear Waste Glass Application—Part 1." *2003 Proceedings of the American Statistical Association*, pp. 1036-1043, American Statistical Association, Alexandria, Virginia.
- Cooley SK, GF Piepel, H Gan, WK Kot, and IL Pegg. 2003. "A Two-Stage Layered Mixture Experiment Design for a Nuclear Waste Glass Application—Part 2." *2003 Proceedings of the American Statistical Association*, pp. 1044-1051, American Statistical Association, Alexandria, Virginia.
- Crum, JV, TB Edwards, RL Russell, PJ Workman, MJ Schweiger, RF Schumacher, DE Smith, DK Peeler, and JD Vienna. 2012. "DWPF Startup Frit Viscosity Measurement Round Robin Results," *Journal of the American Ceramic Society* 95(7):2196-2205.
- DOE. 2000. *Design, Construction, and Commissioning of the Hanford Tank Waste Treatment and Immobilization Plant*. Contract DE-AC27-01RV14136, as amended, U.S. Department of Energy, Office of River Protection, Richland, Washington.
- DOE. 2012. Memorandum, "Enhanced WTP Glass Composition Envelope Development," to C. Swan, Inter-Entity Work Order M0ORV00020, October 18, 2012, U.S. Department of Energy, Office of River Protection, Richland, Washington.
- Fox, KM, TB Edwards, WT Riley, and DR Best. 2015a. *Chemical Composition Analysis and Product Consistency Tests to Support Enhanced Hanford Waste Glass Models: Results for the August and October 2014 LAW Glasses*. SRNL-STI-2015-00226, Rev. 0, Westinghouse Savannah River Company, Aiken, South Carolina.
- Fox, KM, TB Edwards, WT Riley, and DR Best. 2015b. *Chemical Composition Analysis and Product Consistency Tests to Support Enhanced Hanford Waste Glass Models: Results for the January, March and April 2015 LAW Glasses*. SRNL-STI-2015-00436, Rev. 0, Westinghouse Savannah River Company, Aiken, South Carolina.
- Fox, KM, TB Edwards, WT Riley, and ME Caldwell. 2017. *Sulfur Solubility Testing and Characterization of LAW Phase 1 Matrix Glasses*. SRNL-STI-2017-00708, Rev. 0, Westinghouse Savannah River Company, Aiken, South Carolina.

Hrma P, GF Piepel, MJ Schweiger, DE Smith, DS Kim, PE Redgate, JD Vienna, CA Lopresti, DB Simpson, DK Peeler, and MH Langowski. 1994. *Property/Composition Relationships for Hanford High-Level Waste Glasses Melting at 1150 °C*. PNL-10359, Pacific Northwest National Laboratory, Richland, Washington.

Jantzen CM, NE Bibler, DC Beam, CL Crawford, and MA Pickett. 1993. *Characterization of the Defense Waste Processing Facility (DWPF) Environmental Assessment (EA) Glass Standard Reference Material (U)*. WSRC-TR-92-346, Rev. 1, Westinghouse Savannah River Company, Aiken, South Carolina.

Kim DS, JD Vienna, PR Hrma, MJ Schweiger, J Matyas, JV Crum, DE Smith, GJ Sevigny, WC Buchmiller, JS Tixier, JD Yeager, and KB Belew. 2003. *Development and Testing of ICV Glasses for Hanford LAW*. PNNL-14351, Pacific Northwest National Laboratory, Richland, Washington.

Kim DS and JD Vienna. 2012. *Preliminary ILAW Formulation Algorithm Description*. 24590-LAW-RPT-RT-04-0003, Rev. 1, River Protection Project, Hanford Tank Waste Treatment and Immobilization Plant, Richland, Washington.

Matlack KS, M Chaudhuri, H Gan, IS Muller, WK Kot, W Gong, and IL Pegg. 2005a. *Glass Formulation Testing to Increase Sulfate Incorporation*. VSL-04R4960-1, Vitreous State Laboratory, The Catholic University of America, Washington, D.C.

Matlack KS, W Gong, and IL Pegg. 2005b. *Glass Formulation Testing to Increase Sulfate Volatilization from Melter*. VSL-04R4970-1, Vitreous State Laboratory, The Catholic University of America, Washington, D.C.

Matlack KS, W Gong, IS Muller, I Joseph, and IL Pegg. 2006a. *LAW Envelope C Glass Formulation Testing to Increase Waste Loading*. VSL-05R5900-1, Vitreous State Laboratory, The Catholic University of America, Washington, D.C.

Matlack KS, W Gong, IS Muller, I Joseph, and IL Pegg. 2006b. *LAW Envelope A and B Glass Formulations Testing to Increase Waste Loading*. VSL-06R6900-1, Vitreous State Laboratory, The Catholic University of America, Washington, D.C.

Matlack KS, I Joseph, W Gong, IS Muller, and IL Pegg. 2007. *Enhanced LAW Glass Formulation Testing*. VSL-07R1130-1, Vitreous State Laboratory, The Catholic University of America, Washington, D.C.

Matlack KS, I Joseph, W Gong, IS Muller, and IL Pegg. 2009. *Glass Formulation Development and Dm10 Melter Testing with ORP LAW Glasses*. VSL-09R1510-2, Vitreous State Laboratory, The Catholic University of America, Washington, D.C.

Mellinger GB and JL Daniel. 1984. *Approved Reference and Testing Materials for Use in Nuclear Waste Management Research and Development Programs*. PNL-4955-2, Pacific Northwest Laboratory, Richland, Washington.

Muller IS, G Diener, I Joseph, and IL Pegg. 2004. *Proposed Approach for Development of LAW Glass Formulation Correlation: VSL-04L4460-1, Rev. 2*. ORP-56326, Catholic University of America, Washington, D.C.

Muller IS, KS Matlack, H Gan, I Joseph, and IL Pegg. 2010. *Waste Loading Enhancements for Hanford LAW Glasses: VSL-10r1790-1*. ORP-48578, Vitreous State Laboratory, The Catholic University of America, Washington, D.C.

Muller IS, WK Kot, HK Pasioka, K Gilbo, FC Perez-Cardenas, I Joseph, and IL Pegg. 2012. *Compilation and Management of Orp Glass Formulation Database*. VSL-12R2470-1, Vitreous State Laboratory, The Catholic University of America, Washington, D.C.

Muller IS, M Chaudhuri, IL Pegg, and I Joseph. 2013a. *Test Plan: Improved High-Alkali Low-Activity Waste Formulations*. VSL-13T3290-1, Vitreous State Laboratory, The Catholic University of America, Washington, D.C.

Muller IS, IL Pegg, and I Joseph. 2013b. *Test Plan: Enhanced LAW Glass Property-Composition Models, Phase 2*. VSL-13T3050-1, Vitreous State Laboratory, The Catholic University of America, Washington, D.C.

Peeler DK and P Hrma. 1994. "Predicting Liquid Immiscibility in Multicomponent Nuclear Waste Glasses." *Ceramics Transactions* 45:219-229.

Petkus LL. 2003. "Low Activity Container Centerline Cooling Data," to C.A. Musick, CCN: 074181, October 16, 2003, River Protection Project, Hanford Tank Waste Treatment and Immobilization Plant, Richland, Washington.

Piepel GF, CM Anderson, and PE Redgate. 1993. "Response Surface Designs for Irregularly-Shaped Regions" (Parts 1, 2, and 3). *1993 Proceedings of the Section on Physical and Engineering Sciences*, 205-227, American Statistical Association, Alexandria, Virginia.

Piepel GF, SK Cooley, and B Jones. 2005. "Construction of a 21-Component Layered Mixture Experiment Design Using a New Mixture Coordinate-Exchange Algorithm". *Quality Engineering* 17:579-594.

Piepel GF, SK Cooley, IS Muller, H Gan, I Joseph, and IL Pegg. 2007. *ILAW PCT, VHT, Viscosity, and Electrical Conductivity Model Development*. VSL-07R1240-4, Rev. 0, Vitreous State Laboratory, The Catholic University of America, Washington, D.C.

Piepel GF, SK Cooley, A Heredia-Langner, SM Landmesser, WK Kot, H Gan, and IL Pegg. 2008. *IHLW PCT, Spinel T_{1%}, Electrical Conductivity, and Viscosity Model Development*. VSL-07R1240-4, Rev. 0, Vitreous State Laboratory, The Catholic University of America, Washington, D.C.

Piepel GF, SK Cooley, JD Vienna, and JV Crum. 2015. "Designing a Mixture Experiment when the Components are Subject to a Nonlinear Multiplecomponent Constraint," *Quality Engineering*. DOI: 10.1080/08982112.2015.1086003.

Piepel GF, SK Cooley, JD Vienna, and JV Crum. 2016. *Experimental Design for Hanford Low-Activity Waste Glasses with High Waste Loading*. PNNL-24391, Rev. 1, Pacific Northwest National Laboratory, Richland, Washington.

Schweiger MJ. 2014. *Glass Development Lab Procedure: Glass Batching and Melting*. GDL-GBM-1, Rev. 1, Pacific Northwest National Laboratory, Richland, Washington.

Stucki JW. 1981. The quantitative assay of minerals for Fe²⁺ and Fe³⁺ using 1,10-phenanthroline. II. A photochemical method. *Soil Science Society of America Journal*, 45, 638-641.

Vienna, JD, P Hrma, A Jiricka, DE Smith, TH Lorier, IA Reamer, and RL Schultz. 2001. *Hanford Immobilized LAW Product Acceptance Testing: Tanks Focus Area Results*. PNNL-13744, Pacific Northwest National Laboratory, Richland, Washington.

Vienna, JD, WC Buchmiller, JV Crum, DD Graham, DS Kim, BD Macisaac, MJ Schweiger, DK Peeler, TB Edwards, IA Reamer, and RJ Workman. 2002. *Glass Formulation Development for INEEL Sodium-Bearing Waste*. PNNL-14050, Pacific Northwest National Laboratory, Richland, Washington.

Vienna, JD, DS Kim, and DK Peeler. 2003a. "Glass Formulation for INEEL Sodium Bearing Waste." *Ceramic Transactions* 143:169-176.

Vienna JD, DS Kim, and P Hrma. 2003b. "Interim Models Developed to Predict Key Hanford Waste Glass Properties Using Composition." *Ceramic Transactions* 143:151-157.

Vienna JD, DS Kim, MJ Schweiger, P Hrma, J Matyas, JV Crum, and DE Smith. 2004a. "Preliminary Glass Development and Testing for in-Container Vitrification of Hanford Low-Activity Waste," *Ceramic Transactions*, 97(10), 261-268, American Ceramic Society, Westerville, Ohio.

Vienna JD, P Hrma, WC Buchmiller, and JS Ricklefs. 2004b. *Preliminary Investigation of Sulfur Loading in Hanford LAW Glass*. PNNL-14649, Pacific Northwest National Laboratory, Richland, Washington.

Vienna JD, DS Kim, IS Muller, GF Piepel, and AA Kruger. 2014. "Toward Understanding the Effect of Low-Activity Waste Glass Composition on Sulfur Solubility." *Journal of the American Ceramic Society* 97(10):3135-3142.

Weier DR and GF Piepel. 2003. *Methodology for Adjusting and Normalizing Analyzed Glass Composition*. PNWD-3260, Battelle Pacific Northwest Division, Richland, Washington.

Appendix A
Analyzed Glass Compositions

Appendix A

Analyzed Glass Compositions

The data in this section compares the targeted glass compositions with the analyzed glass compositions and their percent differences. There appeared to be overall agreement in all samples and the targeted compositions are adequate for use in future work to develop property-composition models except for LAW-ORP-LD1(3). This glass was mis-batched and needs to have the composition changed to match the analyzed composition.

Table A.1. Comparison of Targeted and Analyzed LAW Phase 1 Enhanced Glass Compositions

Glass ID	New-IL-456			New-IL-1721			New-IL-5253			New-IL-5255		
	Targeted (wt%)	Analyzed (wt%)	% Diff	Targeted (wt%)	Analyzed (wt%)	% Diff	Targeted (wt%)	Analyzed (wt%)	% Diff	Targeted (wt%)	Analyzed (wt%)	% Diff
Al ₂ O ₃	6.25	6.27	0.3	6.25	6.30	0.8	6.25	6.17	-1.2	6.25	6.12	-2.1
B ₂ O ₃	8.00	7.97	-0.4	11.75	11.63	-1.0	11.75	11.13	-5.3	11.75	11.18	-4.8
CaO	9.00	8.75	-2.8	2.75	2.77	0.6	2.75	2.69	-2.3	2.75	2.68	-2.7
Cl	0.12	0.08	-37.9	0.31	0.20	-35.6	0.12	0.062	-48.3	0.12	0.07	-43.5
Cr ₂ O ₃	0.08	<0.15	--	0.21	0.22	3.7	0.08	<0.15	--	0.08	<0.15	--
Cs ₂ O	--	--	--	--	--	--	--	--	--	--	--	--
F	0.18	0.13	-28.2	0.47	0.36	-23.9	0.18	0.13	-25.7	0.18	0.14	-24.6
Fe ₂ O ₃	1.25	1.28	2.3	1.25	1.23	-1.5	1.25	1.24	-0.6	1.25	1.24	-1.1
K ₂ O	0.20	0.21	4.8	1.00	1.02	1.9	0.20	0.23	14.6	0.20	0.23	14.7
Li ₂ O	3.50	3.39	-3.3	3.50	3.38	-3.4	3.50	3.30	-5.7	3.50	3.25	-7.1
MgO	2.50	2.25	-10.1	0.50	0.49	-1.8	2.50	2.21	-11.6	2.50	2.20	-11.9
Na ₂ O	15.00	15.06	0.4	16.45	16.75	1.8	15.00	14.66	-2.3	18.00	17.46	-3.0
NiO	--	--	--	--	--	--	--	--	--	--	--	--
P ₂ O ₅	0.38	0.34	-10.2	1.01	1.02	0.9	0.38	0.37	-2.5	0.38	0.37	-3.4
PbO	--	--	--	--	--	--	--	--	--	--	--	--
SiO ₂	43.15	43.80	1.5	43.25	43.86	1.4	39.75	39.79	0.1	36.75	36.58	-0.5
SO ₃	0.40	0.38	-4.3	1.30	1.12	-13.9	1.30	0.95	-26.8	1.30	1.17	-10.2
SnO ₂	3.50	3.48	-0.5	3.50	3.22	-8.0	3.50	3.43	-1.9	3.50	3.44	-1.7
V ₂ O ₅	3.00	2.95	-1.8	3.00	2.88	-3.9	3.00	2.91	-3.2	3.00	2.90	-3.5
ZnO	2.00	2.01	0.7	2.00	1.96	-2.1	4.00	3.73	-6.9	4.00	3.70	-7.4
ZrO ₂	1.50	1.44	-4.3	1.50	1.54	2.7	4.50	4.33	-3.7	4.50	4.34	-3.6
Total	100.01	99.93	-0.1	100.00	99.94	-0.1	100.01	97.49	-2.5	100.01	97.19	-2.8

Table A.1. Comparison of Targeted and Analyzed LAW Phase 1 Enhanced Glass Compositions (cont.)

Glass ID	New-IL-42295			New-IL-70316			New-IL-87749			New-IL-93907		
	Targeted (wt%)	Analyzed (wt%)	% Diff	Targeted (wt%)	Analyzed (wt%)	% Diff	Targeted (wt%)	Analyzed (wt%)	% Diff	Targeted (wt%)	Analyzed (wt%)	% Diff
Al ₂ O ₃	6.25	6.26	0.2	6.25	6.14	-1.7	11.50	11.16	-3.0	11.50	10.87	-5.4
B ₂ O ₃	11.75	11.54	-1.8	8.00	7.67	-4.1	8.00	7.76	-3.0	11.75	10.81	-8.0
CaO	2.75	2.74	-0.4	9.00	8.64	-4.0	9.00	8.75	-2.8	2.75	2.65	-3.6
Cl	0.12	0.08	-34.6	0.12	0.06	-48.5	0.12	0.07	-39.6	0.12	0.06	-47.5
Cr ₂ O ₃	0.08	<0.15	--	0.08	<0.15	--	0.08	<0.15	--	0.08	<0.15	--
Cs ₂ O	--	--	--	--	--	--	--	--	--	--	--	--
F	0.18	0.14	-24.9	0.18	0.13	-29.4	0.18	0.13	-27.8	0.18	0.13	-29.4
Fe ₂ O ₃	1.25	1.28	2.3	1.25	1.24	-0.8	1.25	1.21	-3.2	1.25	1.24	-1.0
K ₂ O	0.20	0.23	14.0	1.00	1.05	4.6	1.00	1.02	2.2	1.00	1.06	6.1
Li ₂ O	3.50	3.35	-4.2	3.50	0.93	-6.7	3.50	3.31	-5.6	3.50	3.21	-8.3
MgO	2.50	2.22	-11.3	2.50	2.21	-11.8	0.50	0.46	-7.7	0.50	0.48	-4.5
Na ₂ O	17.48	17.83	2.0	20.23	19.98	-1.2	17.49	17.69	1.2	15.12	14.56	-3.7
NiO	--	--	--	--	--	--	--	--	--	--	--	--
P ₂ O ₅	0.38	0.36	-6.2	0.38	0.35	-9.1	0.38	0.35	-9.2	0.38	0.35	-9.1
PbO	--	--	--	--	--	--	--	--	--	--	--	--
SiO ₂	42.42	42.95	1.2	38.72	38.51	-0.5	37.41	37.33	-0.2	43.25	42.25	-2.3
SO ₃	0.40	0.40	-0.6	1.30	1.24	-4.9	0.40	0.41	1.7	1.13	0.91	-19.2
SnO ₂	1.00	1.00	0.3	3.50	3.47	-1.0	2.70	2.59	-4.0	3.50	3.42	-2.4
V ₂ O ₅	3.00	2.91	-2.9	3.00	2.91	-3.2	3.00	2.84	-5.4	0.50	0.50	-0.8
ZnO	2.00	1.99	-0.7	2.00	1.98	-1.2	2.00	1.95	-2.6	2.00	1.95	-2.3
ZrO ₂	4.75	4.63	-2.6	1.50	1.44	-4.3	1.50	1.39	-7.2	1.50	1.43	-4.8
Total	100.01	100.03	0.0	100.01	98.07	-1.9	100.01	98.56	-1.5	100.01	96.02	-4.0

Table A.1. Comparison of Targeted and Analyzed LAW Phase 1 Enhanced Glass Compositions (cont.)

Glass ID	New-IL-94020			New-IL-103151			New-IL-151542			New-IL-166697		
	Targeted (wt%)	Analyzed (wt%)	% Diff	Targeted (wt%)	Analyzed (wt%)	% Diff	Targeted (wt%)	Analyzed (wt%)	% Diff	Targeted (wt%)	Analyzed (wt%)	% Diff
Al ₂ O ₃	11.50	11.06	-3.8	6.25	6.01	-3.8	6.25	6.03	-3.6	11.25	10.78	-4.2
B ₂ O ₃	8.00	7.66	-4.3	8.00	7.41	-7.3	9.74	9.12	-6.4	10.22	9.79	-4.2
CaO	3.53	3.55	0.7	2.75	2.77	0.7	9.00	8.78	-2.4	2.75	2.69	-2.3
Cl	0.12	0.05	-56.0	0.12	0.08	-36.7	0.31	0.17	-46.0	0.31	0.18	-41.2
Cr ₂ O ₃	0.08	<0.15	--	0.08	<0.15	--	0.21	0.22	2.5	0.21	0.21	0.2
Cs ₂ O	--	--	--	--	--	--	--	--	--	--	--	--
F	0.18	0.13	-28.1	0.18	0.14	-23.6	0.47	0.34	-28.7	0.47	0.36	-23.2
Fe ₂ O ₃	1.25	1.24	-0.5	1.25	1.29	3.1	1.25	1.28	2.4	1.25	1.22	-2.6
K ₂ O	0.20	0.22	10.1	1.00	1.10	9.8	0.20	0.23	12.5	1.00	1.01	0.8
Li ₂ O	3.50	3.27	-6.5	1.00	0.91	-9.3	1.00	0.91	-8.9	3.50	3.31	-5.4
MgO	2.50	2.16	-13.4	2.50	2.26	-9.6	2.50	2.27	-9.1	0.50	0.49	-1.5
Na ₂ O	15.00	15.30	2.0	22.49	23.29	3.5	17.37	18.27	5.2	17.49	17.86	2.1
NiO	--	--	--	--	--	--	--	--	--	--	--	--
P ₂ O ₅	0.38	0.36	-4.7	0.38	0.37	-3.7	1.01	1.03	1.5	1.01	1.03	1.8
PbO	--	--	--	--	--	--	--	--	--	--	--	--
SiO ₂	43.25	42.25	-2.3	41.84	40.38	-3.5	39.39	39.31	-0.2	36.75	37.55	2.2
SO ₃	1.02	0.79	-22.2	1.17	1.22	4.6	1.30	1.07	-17.9	1.29	1.10	-14.9
SnO ₂	3.50	3.42	-2.4	2.50	2.60	4.1	3.50	3.39	-3.1	3.50	3.25	-7.1
V ₂ O ₅	0.50	0.49	-1.4	3.00	3.02	0.7	3.00	3.00	0.0	3.00	2.87	-14.9
ZnO	4.00	3.74	-6.4	4.00	3.87	-3.2	2.00	2.02	1.1	4.00	3.69	-7.8
ZrO ₂	1.50	1.42	-5.4	1.50	1.49	-0.5	1.50	1.55	3.5	1.50	1.53	2.2
Total	100.01	97.27	-2.7	100.01	98.36	-1.7	100.00	98.97	-1.0	100.00	98.90	-1.1

Table A.1. Comparison of Targeted and Analyzed LAW Phase 1 Enhanced Glass Compositions (cont.)

Glass ID	New-IL-166731			New-OL-8445			New-OL-8788(Mod)			New-OL-14844		
	Targeted (wt%)	Analyzed (wt%)	% Diff	Targeted (wt%)	Analyzed (wt%)	% Diff	Targeted (wt%)	Analyzed (wt%)	% Diff	Targeted (wt%)	Analyzed (wt%)	% Diff
Al ₂ O ₃	11.50	11.12	-3.3	12.41	12.13	-2.3	12.35	12.42	0.6	3.50	3.51	0.1
B ₂ O ₃	9.31	9.00	-3.3	13.75	13.57	-1.3	6.00	6.18	3.0	6.15	5.75	-6.5
CaO	2.75	2.76	0.2	12.24	11.73	-4.1	0.05	0.11	124	12.24	12.31	0.6
Cl	0.31	0.15	-51.5	0.47	0.29	-37.6	0.47	0.32	-31.7	0.47	0.14	-70.5
Cr ₂ O ₃	0.21	0.22	2.7	0.31	0.32	4.0	0.31	0.32	3.2	0.31	0.31	-1.2
Cs ₂ O	--	--	--	--	--	--	--	--	--	--	--	--
F	0.47	0.34	-27.7	0.71	0.51	-28.5	0.71	0.53	-25.3	0.71	0.42	-41.3
Fe ₂ O ₃	0.50	0.53	5.8	--	--	--	1.50	1.54	2.7	--	--	--
K ₂ O	0.20	0.21	6.2	1.50	1.56	4.0	1.50	1.53	2.2	1.50	1.38	-7.8
Li ₂ O	3.50	3.27	-6.7	2.01	1.91	-5.2	2.50	2.44	-2.2	5.00	4.68	-6.5
MgO	2.50	2.18	-12.8	3.50	2.98	-15.0	3.50	3.14	-10.3	3.50	2.95	-15.8
Na ₂ O	18.02	18.54	2.9	10.00	9.62	-3.8	13.00	12.59	-3.2	15.51	15.74	1.5
NiO	--	--	--	--	--	--	--	--	--	--	--	--
P ₂ O ₅	1.01	1.04	3.4	1.51	1.42	-6.2	1.51	1.47	-2.6	1.51	1.35	-10.5
PbO	--	--	--	--	--	--	--	--	--	--	--	--
SiO ₂	36.75	37.22	1.3	34.00	34.66	1.9	46.00	47.49	3.2	34.00	35.09	3.2
SO ₃	1.27	1.01	-20.3	0.10	<0.25	--	0.10	<0.25	--	0.10	<0.19	--
SnO ₂	3.20	2.95	-8.0	--	--	--	--	--	--	--	--	--
V ₂ O ₅	3.00	2.90	-3.3	--	--	--	--	--	--	4.00	3.81	-4.8
ZnO	4.00	3.74	-6.4	1.00	1.01	1.1	5.00	4.94	-1.3	5.00	4.51	-9.8
ZrO ₂	1.50	1.55	3.5	6.50	6.15	-5.3	5.50	5.36	-2.6	6.50	5.97	-8.2
Total	100.00	98.73	-1.3	100.01	98.55	-1.5	100.00	101.44	1.4	100.00	98.32	-1.7

Table A.1. Comparison of Targeted and Analyzed LAW Phase 1 Enhanced Glass Compositions (cont.)

Glass ID	New-OL-15493			New-OL-17130			New-OL-45748 (with tin oxalate)			New-OL-54017(with tin oxalate)		
Component	Targeted (wt%)	Analyzed (wt%)	% Diff	Targeted (wt%)	Analyzed (wt%)	% Diff	Targeted (wt%)	Analyzed (wt%)	% Diff	Targeted (wt%)	Analyzed (wt%)	% Diff
Al ₂ O ₃	3.50	3.57	1.9	3.50	3.49	-0.3	13.85	13.72	-1.0	3.50	3.68	5.0
B ₂ O ₃	6.00	5.94	-1.0	13.75	13.07	-5.0	6.00	6.21	3.4	6.00	6.21	3.6
CaO	12.24	12.00	-1.9	1.65	1.59	-3.8	12.24	12.58	2.7	11.17	10.60	-5.1
Cl	0.06	0.03	-59.2	0.47	0.33	-29.7	0.47	0.24	-49.4	0.06	0.04	-33.3
Cr ₂ O ₃	0.04	<0.15	--	0.31	0.32	4.0	0.31	0.31	0.0	0.04	0.06	-50.0
Cs ₂ O	--	--	--	--	--	--	--	--	--	--	--	--
F	0.09	0.06	-38.3	0.71	0.49	-31.8	0.71	0.51	-28.6	0.09	0.06	-36.7
Fe ₂ O ₃	--	--	--	1.50	1.50	-0.1	1.50	1.52	1.3	1.50	1.55	3.2
K ₂ O	1.50	1.50	-0.2	--	--	--	--	--	--	--	--	--
Li ₂ O	--	--	--	5.00	4.73	-5.5	5.00	4.96	-0.8	--	--	--
MgO	3.50	2.98	-15.0	--	--	--	--	--	--	3.50	3.18	-9.1
Na ₂ O	25.51	26.49	3.8	16.50	16.08	-2.6	11.40	11.65	2.2	15.00	14.73	-1.8
NiO	--	--	--	--	--	--	--	--	--	--	--	--
P ₂ O ₅	0.20	<0.23	--	1.51	1.50	-0.4	1.51	1.43	-5.3	0.20	0.20	0.0
PbO	--	--	--	--	--	--	--	--	--	--	--	--
SiO ₂	39.25	39.26	0.0	47.00	46.53	-1.0	34.00	34.98	2.9	47.00	48.30	2.8
SO ₃	0.10	<0.25	--	0.10	<0.25	--	0.10	<0.25	--	0.10	<0.25	--
SnO ₂	3.00	2.95	-1.7	3.00	3.00	-0.1	5.00	4.68	-6.5	5.00	4.43	-11.4
V ₂ O ₅	4.00	3.87	-3.4	4.00	3.93	-1.8	2.91	2.98	2.4	1.85	1.81	-2.2
ZnO	1.00	1.01	1.0	1.00	1.01	0.7	5.00	5.07	1.4	5.00	4.92	-1.7
ZrO ₂	--	--	--	--	--	--	--	--	--	--	--	--
Total	99.99	100.75	0.76	100.00	98.22	-1.78	100.00	101.49	1.49	99.99	100.47	0.48

Table A.1. Comparison of Targeted and Analyzed LAW Phase 1 Enhanced Glass Compositions (cont.)

Glass ID	New-OL-57284			New-OL-62380			New-OL-62909(Mod)			New-OL-65959(Mod)		
	Targeted (wt%)	Analyzed (wt%)	% Diff	Targeted (wt%)	Analyzed (wt%)	% Diff	Targeted (wt%)	Analyzed (wt%)	% Diff	Targeted (wt%)	Analyzed (wt%)	% Diff
Al ₂ O ₃	3.50	3.59	2.6	3.50	3.49	-0.4	12.35	12.24	-0.9	13.85	13.56	-2.1
B ₂ O ₃	13.75	13.37	-2.8	13.75	12.60	-8.4	8.90	9.01	1.2	13.05	13.09	0.3
CaO	2.98	2.90	-2.7	12.24	11.95	-2.4	12.24	12.37	1.0	--	0.05	--
Cl	0.47	0.35	-26.6	0.11	0.03	-69.1	0.47	0.22	-52.8	0.06	0.03	-43.3
Cr ₂ O ₃	0.31	0.32	2.9	0.08	<0.15	--	0.31	0.30	-4.5	0.04	0.05	25.0
Cs ₂ O	--	--	--	--	--	--	--	--	--	--	--	--
F	0.71	0.50	-30.0	0.71	0.10	-85.6	0.71	0.55	-22.3	0.09	0.06	-28.9
Fe ₂ O ₃	--	--	--	1.50	1.48	-1.1	--	--	--	--	--	--
K ₂ O	1.50	1.62	8.0	1.50	1.48	-1.6	--	--	--	--	--	--
Li ₂ O	--	--	--	--	--	--	2.50	2.40	-4.0	5.00	4.89	-2.3
MgO	--	--	--	--	--	--	3.50	3.51	0.3	3.50	3.13	-10.6
Na ₂ O	14.01	14.06	0.4	14.01	13.78	-1.6	13.00	13.47	3.6	16.50	16.01	-3.0
NiO	--	--	--	--	--	--	--	--	--	--	--	--
P ₂ O ₅	1.51	1.39	-7.7	0.37	0.35	-5.6	1.51	1.45	-4.0	0.20	0.19	-5.0
PbO	--	--	--	--	--	--	--	--	--	--	--	--
SiO ₂	47.00	46.90	-0.2	34.00	34.02	0.0	33.50	34.39	2.7	34.50	35.03	1.5
SO ₃	0.10	<0.25	--	0.10	<0.25	--	0.10	<0.25	--	0.10	<0.25	--
SnO ₂	--	--	--	4.50	4.41	-2.0	4.41	4.22	-4.3	4.50	4.25	-5.6
V ₂ O ₅	4.00	4.00	0.0	2.66	2.56	-3.9	--	--	--	3.60	3.53	-1.9
ZnO	5.00	4.73	-5.3	5.00	4.52	-9.6	1.00	0.96	-0.4	5.00	4.89	-2.2
ZrO ₂	5.16	4.96	-3.9	6.50	6.15	-5.4	5.50	4.88	-11.2	--	--	--
Total	100.00	99.60	-0.40	100.53	97.69	-2.84	100.00	100.66	0.66	99.99	99.40	-0.59

Table A.1. Comparison of Targeted and Analyzed LAW Phase 1 Enhanced Glass Compositions (cont.)

Glass ID	New-OL-80309			New-OL-90780			New-OL-100210			New-OL-108249(SO ₃ Mod)		
	Targeted (wt%)	Analyzed (wt%)	% Diff	Targeted (wt%)	Analyzed (wt%)	% Diff	Targeted (wt%)	Analyzed (wt%)	% Diff	Targeted (wt%)	Analyzed (wt%)	% Diff
Al ₂ O ₃	3.50	3.56	1.6	13.85	13.56	-2.1	3.50	3.52	0.5	12.03	12.13	0.8
B ₂ O ₃	13.75	13.82	0.5	13.75	13.34	-3.0	6.00	5.75	-4.2	6.04	6.21	2.9
CaO	--	0.03	--	--	--	--	1.89	1.87	-1.2	10.07	9.53	-5.4
Cl	0.06	0.04	-28.3	0.47	0.25	-47.4	0.47	0.35	-26.2	0.47	0.29	-37.7
Cr ₂ O ₃	0.04	0.05	25.0	0.31	0.32	2.0	0.31	0.32	4.0	0.31	0.32	3.2
Cs ₂ O	--	--	--	--	--	--	--	--	--	--	--	--
F	0.09	0.07	-25.6	0.71	0.53	-25.3	0.71	0.57	-19.7	0.71	0.58	-18.2
Fe ₂ O ₃	1.50	1.49	0.7	--	--	--	--	--	--	1.51	1.58	4.6
K ₂ O	1.50	1.49	0.7	1.50	1.58	5.4	--	--	--	1.51	1.50	0.2
Li ₂ O	5.00	4.84	-3.2	5.00	4.82	-3.7	--	--	--	5.03	4.99	-0.8
MgO	3.50	3.07	-12.3	3.50	2.99	-14.5	3.50	3.11	-11.0	--	0.07	--
Na ₂ O	15.10	14.46	-4.3	15.51	15.40	-0.7	26.00	27.43	5.5	15.61	15.17	-2.9
NiO	--	--	--	--	--	--	--	--	--	--	--	--
P ₂ O ₅	0.20	0.19	-5.0	1.51	1.49	-1.2	1.51	1.51	-0.1	1.52	1.47	-3.3
PbO	--	--	--	--	--	--	--	--	--	--	--	--
SiO ₂	34.00	34.39	1.1	34.25	34.55	0.9	47.00	46.58	-0.9	34.23	35.67	4.2
SO ₃	1.75	1.63	-6.9	1.64	1.28	-21.9	0.91	0.95	3.9	0.89	0.90	1.1
SnO ₂	4.50	4.28	-4.9	3.00	2.94	-1.9	3.20	3.34	4.3	5.03	4.59	-8.8
V ₂ O ₅	4.00	3.87	-3.3	4.00	3.87	-3.3	--	--	--	--	--	--
ZnO	5.00	4.81	-3.8	1.00	1.01	1.0	5.00	4.78	-4.3	5.03	4.91	-2.4
ZrO ₂	6.50	5.85	-10.1	--	--	--	--	--	--	--	--	--
Total	99.99	97.93	-2.06	100.00	98.34	-1.66	100.00	100.87	0.87	99.99	100.23	0.24

Table A.1. Comparison of Targeted and Analyzed LAW Phase 1 Enhanced Glass Compositions (cont.)

Glass ID	New-OL-116208(SO ₃ Mod)			New-OL-122817			New-OL-127708(Mod)			EWG-LAW-Centroid-1		
	Targeted (wt%)	Analyzed (wt%)	% Diff	Targeted (wt%)	Analyzed (wt%)	% Diff	Targeted (wt%)	Analyzed (wt%)	% Diff	Targeted (wt%)	Analyzed (wt%)	% Diff
Al ₂ O ₃	3.53	3.62	2.5	3.50	3.55	1.5	10.94	10.91	-0.3	9.00	8.73	-3.1
B ₂ O ₃	6.05	6.11	1.0	6.00	5.96	-0.7	13.75	13.91	1.2	10.00	9.70	-3.0
CaO	12.35	11.68	-5.5	12.24	11.98	-2.1	0.30	0.31	3.3	5.50	5.34	-2.9
Cl	0.47	0.29	-39.4	0.47	0.27	-42.1	0.06	0.03	-51.7	0.21	0.11	-49.6
Cr ₂ O ₃	0.31	0.32	3.2	0.31	0.32	2.4	0.04	0.05	25.0	0.14	<0.15	--
Cs ₂ O	--	--	--	--	--	--	--	--	--	--	--	--
F	0.72	0.59	-18.5	0.71	0.47	-34.0	0.09	0.05	-41.1	0.32	0.23	-26.8
Fe ₂ O ₃	1.51	1.53	1.3	1.50	1.52	1.0	1.50	1.51	0.7	1.00	1.01	1.0
K ₂ O	--	--	--	1.50	1.59	5.8	1.50	1.53	1.3	0.40	0.45	12.9
Li ₂ O	5.05	4.89	-3.2	--	--	--	2.50	2.45	-2.0	2.00	1.87	-6.6
MgO	3.53	3.44	-2.6	--	--	--	3.50	3.16	-9.7	1.50	1.41	-6.3
Na ₂ O	16.34	15.74	-3.7	18.60	19.28	3.6	13.00	12.51	-3.8	19.00	19.51	2.7
NiO	--	--	--	--	--	--	--	--	--	--	--	--
P ₂ O ₅	1.52	1.44	-5.3	1.51	1.48	-1.9	0.20	0.18	-10.0	0.68	0.63	-7.8
PbO	--	--	--	--	--	--	--	--	--	--	--	--
SiO ₂	34.31	35.67	4.0	44.17	43.21	-2.2	46.51	47.87	2.9	39.55	39.31	-0.6
SO ₃	0.93	0.98	5.4	1.49	1.28	-14.0	0.61	<0.25	--	0.70	0.59	-15.6
SnO ₂	4.54	4.49	-1.1	3.00	3.08	2.7	4.50	4.27	-5.1	2.00	2.07	3.5
V ₂ O ₅	1.26	1.26	0.0	4.00	3.96	-1.0	--	--	--	2.00	2.04	1.8
ZnO	1.01	0.97	-4.0	1.00	1.04	3.5	1.00	0.96	-4.0	3.00	2.92	-2.6
ZrO ₂	6.56	6.06	-7.6	--	--	--	--	--	--	3.00	2.94	-2.0
Total	99.99	99.19	-0.80	100.00	99.49	-0.51	100.00	100.26	0.26	100.00	99.00	-1.0

Table A.1. Comparison of Targeted and Analyzed LAW Phase 1 Enhanced Glass Compositions (cont.)

Glass ID	EWG-LAW-Centroid-2			LAW-ORP-LD1(1)			LAW-ORP-LD1(2)			LAW-ORP-LD1(3)		
Component	Targeted (wt%)	Analyzed (wt%)	% Diff	Targeted (wt%)	Analyzed (wt%)	% Diff	Targeted (wt%)	Analyzed (wt%)	% Diff	Targeted (wt%)	Analyzed (wt%)	% Diff
Al ₂ O ₃	9.00	8.82	-2.0	10.15	9.82	-1.7	10.15	10.04	-1.1	10.15	14.73	45.1
B ₂ O ₃	10.00	9.71	-2.9	12.04	11.52	-3.3	12.04	12.13	0.8	12.04	11.59	-3.7
CaO	5.50	5.32	-3.3	8.01	7.58	-5.3	8.01	7.55	-5.7	8.01	7.17	-10.5
Cl	0.21	0.14	-33.5	0.33	0.17	-47.3	0.33	0.17	-47.6	0.33	0.16	-50.9
Cr ₂ O ₃	0.14	0.15	5.4	0.50	0.50	-0.5	0.50	0.48	-4.0	0.50	0.49	-2.0
Cs ₂ O	--	--	--	0.13	--	--	0.13	--	--	0.13	--	--
F	0.32	0.25	-22.7	0.17	0.12	-31.6	0.17	0.12	-27.1	0.17	0.12	-31.8
Fe ₂ O ₃	1.00	1.06	5.5	1.00	0.99	-1.0	1.00	1.02	2.0	1.00	0.98	-2.0
K ₂ O	0.40	0.47	16.8	0.16	0.19	17.4	0.16	0.17	6.3	0.16	0.19	18.8
Li ₂ O	2.00	1.89	-5.4	--	--	--	--	--	--	--	--	--
MgO	1.50	1.41	-6.0	1.00	0.92	-8.1	1.00	0.96	-4.0	1.00	1.02	2.0
Na ₂ O	19.00	19.85	4.5	20.98	20.66	-1.5	20.98	20.25	-3.5	20.98	19.31	-8.0
NiO	--	--	--	0.04	--	--	0.04	--	--	0.04	--	--
P ₂ O ₅	0.68	0.65	-4.6	0.29	0.28	-2.4	0.29	0.27	-6.9	0.29	0.28	-3.4
PbO	--	--	--	0.01	--	--	0.01	--	--	0.01	--	--
SiO ₂	39.55	40.06	1.3	37.14	37.06	-0.2	37.14	37.87	2.0	37.14	36.15	-2.7
SO ₃	0.70	0.71	1.4	1.06	0.99	-6.4	1.06	0.82	-22.6	1.06	0.90	-15.1
SnO ₂	2.00	2.08	4.1	--	--	--	--	--	--	--	--	--
V ₂ O ₅	2.00	2.06	3.1	1.00	0.99	-1.2	1.00	0.96	-4.1	1.00	0.97	-3.0
ZnO	3.00	2.98	-0.7	3.00	2.86	-4.8	3.00	2.92	-2.7	3.00	2.75	-8.3
ZrO ₂	3.00	3.00	0.1	3.00	2.89	-3.5	3.00	2.84	-5.4	3.00	2.82	-2.7
Total	100.00	100.60	0.60	99.83	97.88	-1.95	99.83	99.43	-0.40	99.83	100.47	0.64

Appendix B
Viscosity Data

Appendix B

Viscosity Data

This appendix contains the measured viscosity data for each of the glasses in this matrix. The spindle factor was generated during equipment calibration and was calculated by the following equation:

$$\text{S.F.} = a(\text{speed})^2 + b(\text{speed}) + c \quad (\text{B.1})$$

where the *speed* is the rotations per minute (rpms) of the spindle measuring the viscosity and *a*, *b*, and *c* are fit parameters. For the calibration used to calculate viscosity of glasses in this study, the parameters are: *a* = 0.0002163, *b* = -0.03861 and *c* = 10.05.

The plots shown in this appendix are fitted to the Arrhenius equation

$$\ln(\eta) = A + \frac{B}{T_K} \quad (\text{B.2})$$

where *A* and *B* are independent of temperature and temperature (T_K) is in K ($T(^{\circ}\text{C}) + 273.15$). However, some of the plots showed curvature and would be better fit to the Vogel- Fulcher - Tamman (VFT) model

$$\ln(\eta) = E + \frac{F}{T_k - T_0} \quad (\text{B.3})$$

where *E*, *F*, and T_0 are temperature independent and composition dependent coefficients and T_K is the temperature in K ($T(^{\circ}\text{C}) + 273.15$). The intent of the figures and Arrhenius equation fits shown in this appendix are mainly to assess trends of the data and provide some observations about whether there may be sufficient curvature in the data to consider VFT fits in the subsequent work that will decide between fitting the data to the Arrhenius or VFT equations for the viscosity-temperature data for each glass that is being made in subsequent work.

There does appear to be some indication of possible small curvature in several of the viscosity plots because the middle data points are slightly below the fitted line, and end points are slightly above the fitted line. The curvature is still slight but the Arrhenius equation may not be adequate for all glasses. For the glasses with the largest curvature, the curved fit is also shown in the plots.

B.1 Glass New-IL-456 Viscosity Data

Table B.1. Viscosity Data for Glass New-IL-456

Setpoint, °C	Measured Temp., °C	Viscosity, Pa·s	$1/(T+273.15) \times 10,000, K^{-1}$	$\ln \eta, Pa \cdot s$
1150	1138	2.528	7.086	0.927
1050	1041	5.420	7.609	1.690
950	943	19.540	8.223	2.972
1150	1135	2.545	7.102	0.934
1250	1234	1.240	6.635	0.215
1150	1140	2.649	7.076	0.974

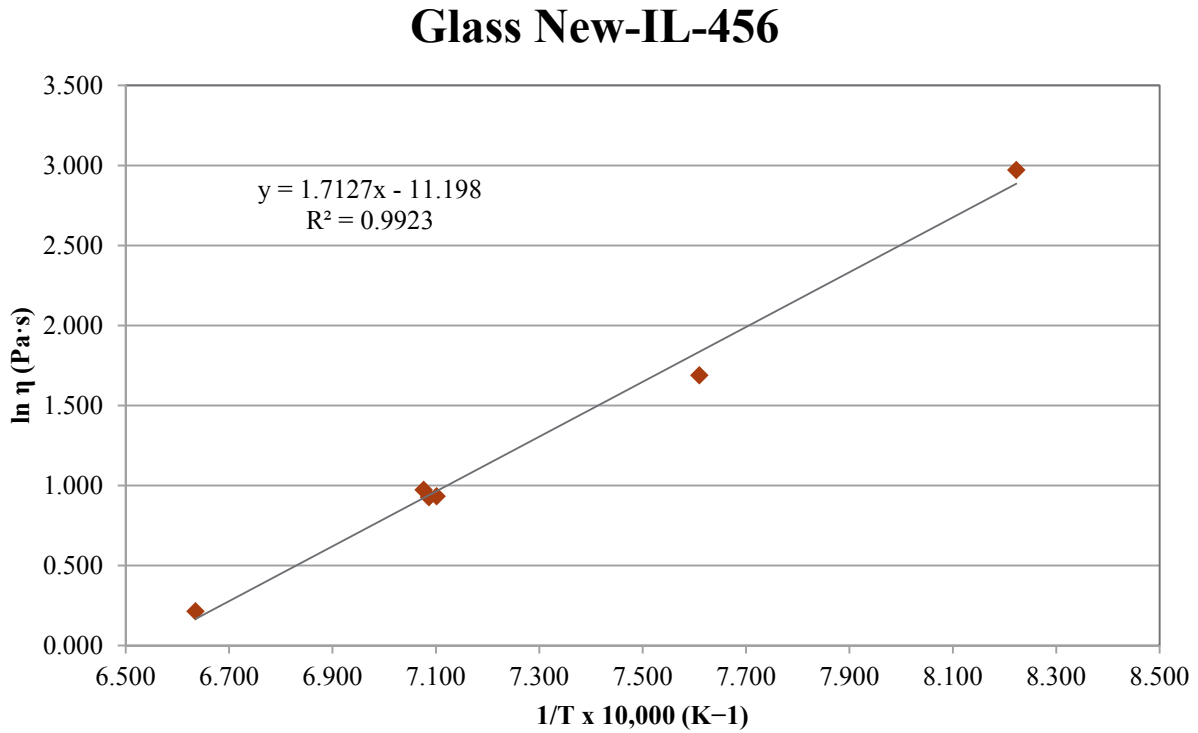


Figure B.1. Viscosity-Temperature Data and Arrhenius Equation Fit for Glass New-IL-456

B.2 Glass New-IL-1721 Viscosity Data

Table B.2. Viscosity Data for Glass New-IL-1721

Setpoint, °C	Measured Temp., °C	Viscosity, Pa·s	$1/(T+273.15) \times 10,000, K^{-1}$	$\ln \eta, Pa \cdot s$
1150	1138	2.808	7.086	1.032
1050	1041	5.615	7.609	1.725
950	943	18.770	8.223	2.932
1150	1135	2.808	7.102	1.032
1250	1234	1.473	6.635	0.387
1150	1140	2.983	7.076	1.093

Glass New-IL-1721

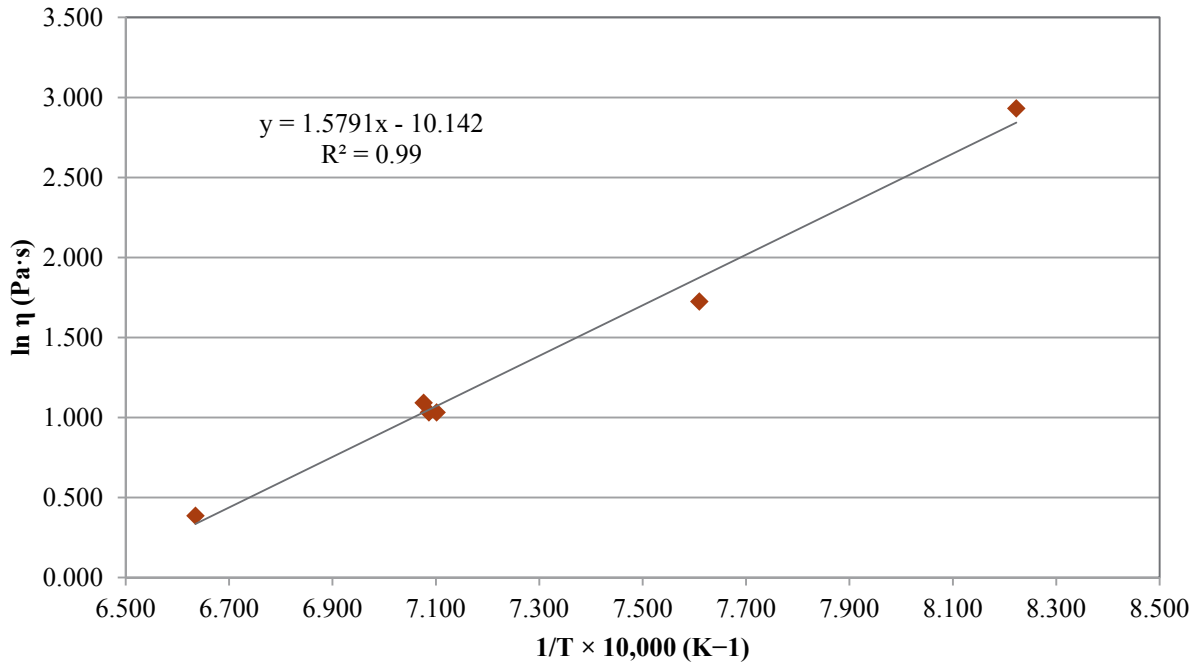


Figure B.2. Viscosity-Temperature Data and Arrhenius Equation Fit for Glass New-IL-1721

B.3 Glass New-IL-5253 Viscosity Data

Table B.3. Viscosity Data for Glass New-IL-5253

Setpoint, °C	Measured Temp., °C	Viscosity, Pa·s	$1/(T+273.15) \times 10,000, K^{-1}$	$\ln \eta, Pa \cdot s$
1150	1138	2.552	7.086	0.937
1050	1041	5.516	7.609	1.708
950	943	20.724	8.223	3.031
1150	1135	2.558	7.102	0.939
1250	1234	1.296	6.635	0.259
1150	1140	2.696	7.076	0.992

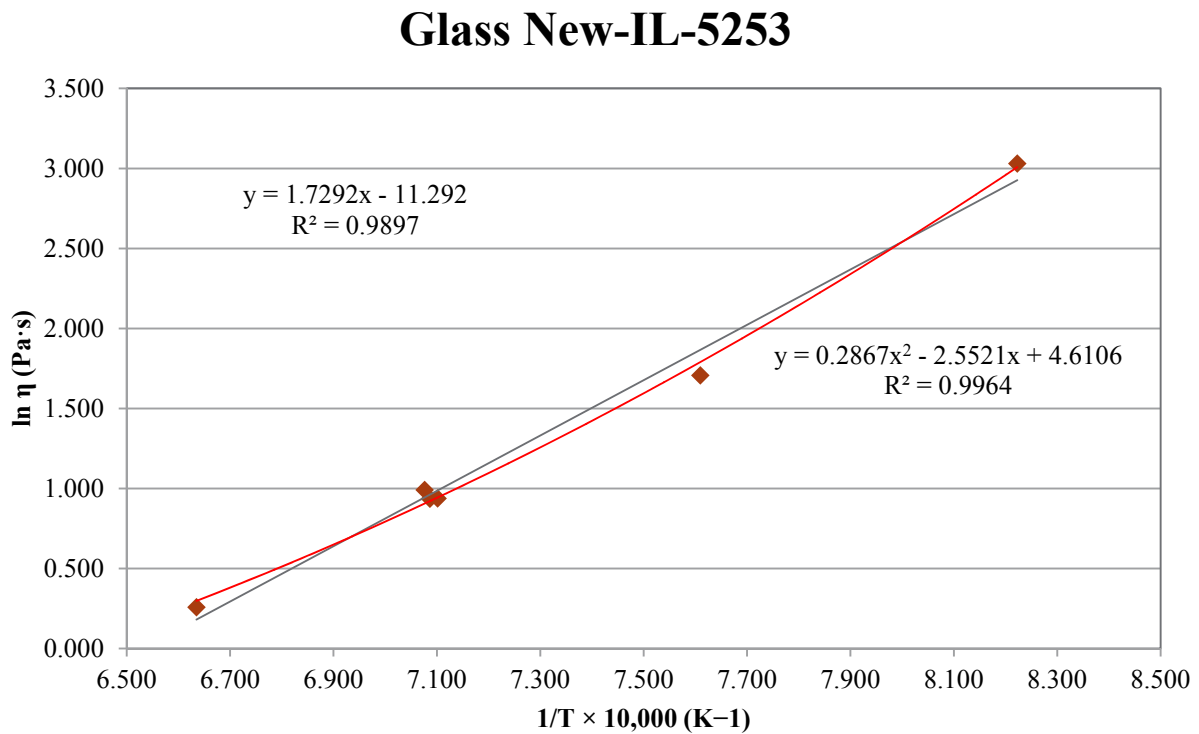


Figure B.3. Viscosity-Temperature Data and Arrhenius Equation Fit for Glass New-IL-5253

B.4 Glass New-IL-5255 Viscosity Data

Table B.4. Viscosity Data for Glass New-IL-5255

Setpoint, °C	Measured Temp., °C	Viscosity, Pa·s	$1/(T+273.15) \times 10,000, K^{-1}$	$\ln \eta, Pa \cdot s$
1150	1137	1.473	7.091	0.387
1050	1041	3.764	7.609	1.325
950	943	9.402	8.223	2.241
1150	1135	1.497	7.102	0.403
1250	1235	0.755	6.631	-0.281
1150	1140	1.557	7.076	0.443

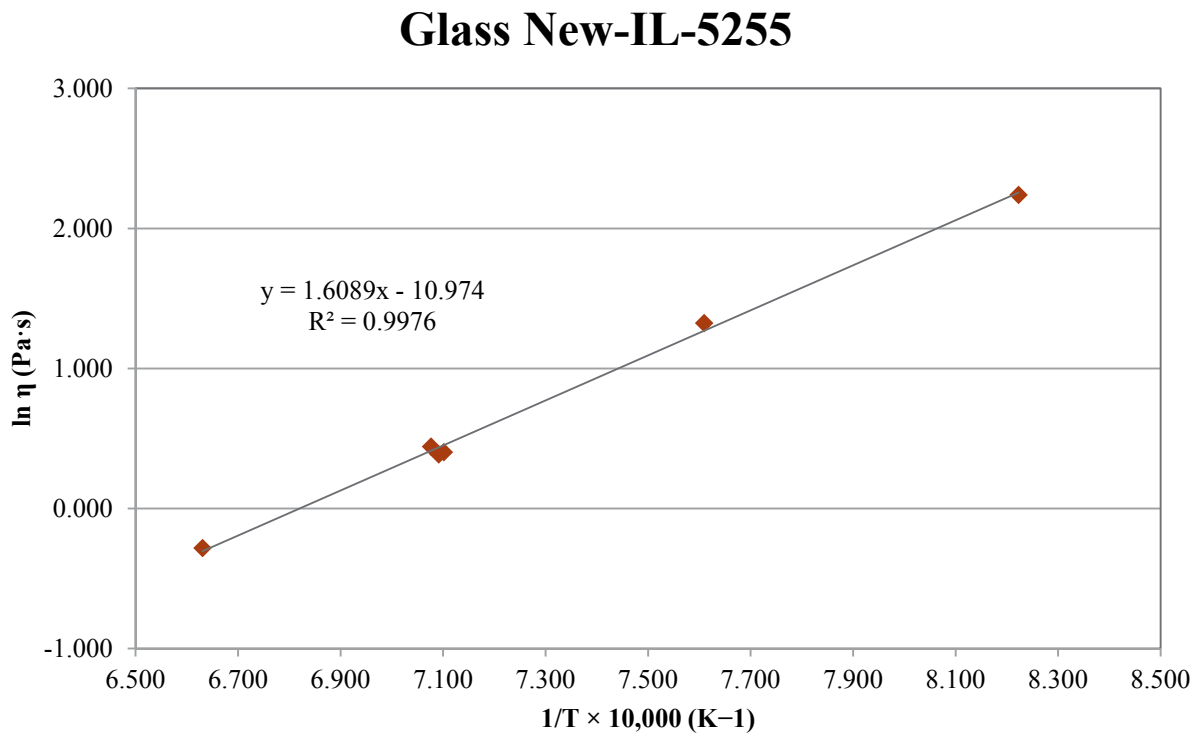


Figure B.4. Viscosity-Temperature Data and Arrhenius Equation Fit for Glass New-IL-5255

B.5 Glass New-IL-42295 Viscosity Data

Table B.5. Viscosity Data for Glass New-IL-42295

Setpoint, °C	Measured Temp., °C	Viscosity, Pa·s	$1/(T+273.15) \times 10,000, K^{-1}$	$\ln \eta, Pa \cdot s$
1150	1136	2.410	7.096	0.880
1050	1040	5.044	7.615	1.618
950	943	14.687	8.223	2.687
1150	1133	2.442	7.112	0.893
1250	1233	1.261	6.639	0.232
1150	1140	2.463	7.076	0.901

Glass New-IL-42995

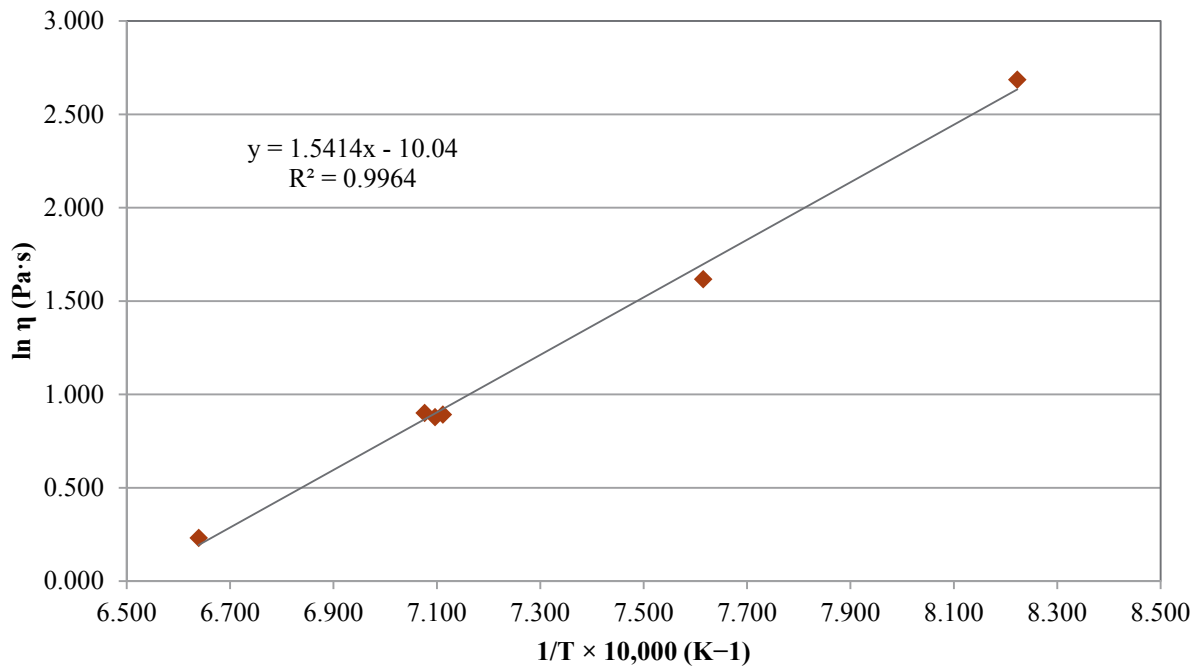


Figure B.5. Viscosity-Temperature Data and Arrhenius Equation Fit for Glass New-IL-42295

B.6 Glass New-IL-70316 Viscosity Data

Table B.6. Viscosity Data for Glass New-IL-70316

Setpoint, °C	Measured Temp., °C	Viscosity, Pa·s	$1/(T+273.15) \times 10,000, K^{-1}$	$\ln \eta, Pa \cdot s$
1150	1137	2.265	7.091	0.818
1050	1041	5.133	7.609	1.636
950	943	18.847	8.223	2.936
1150	1134	2.273	7.107	0.821
1250	1234	1.155	6.635	0.144
1150	1142	2.395	7.066	0.873

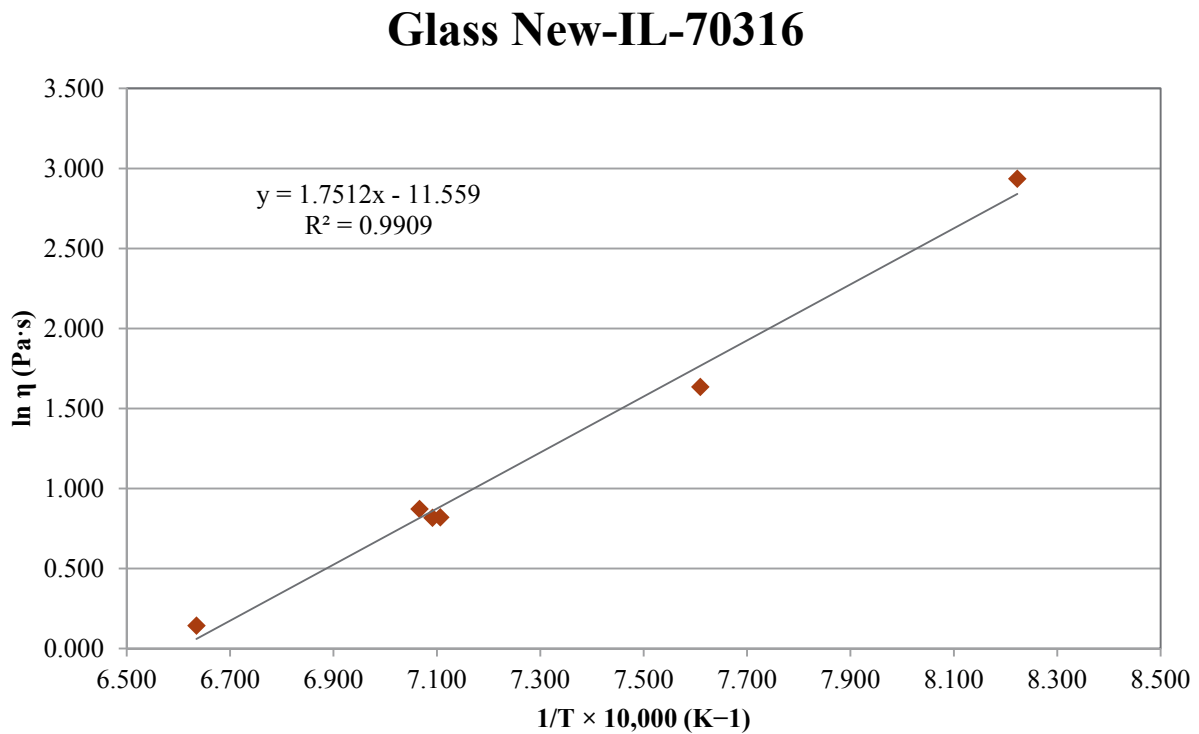


Figure B.6. Viscosity-Temperature Data and Arrhenius Equation Fit for Glass New-IL-70316

B.7 Glass New-IL-87749 Viscosity Data

Table B.7. Viscosity Data for Glass New-IL-87749

Setpoint, °C	Measured Temp., °C	Viscosity, Pa·s	$1/(T+273.15) \times 10,000, \text{K}^{-1}$	$\ln \eta, \text{Pa}\cdot\text{s}$
1150	1137	2.214	7.091	0.795
1050	1040	4.944	7.615	1.598
950	943	14.808	8.223	2.695
1150	1134	2.259	7.107	0.815
1250	1234	1.126	6.635	0.119
1150	1140	2.339	7.076	0.850

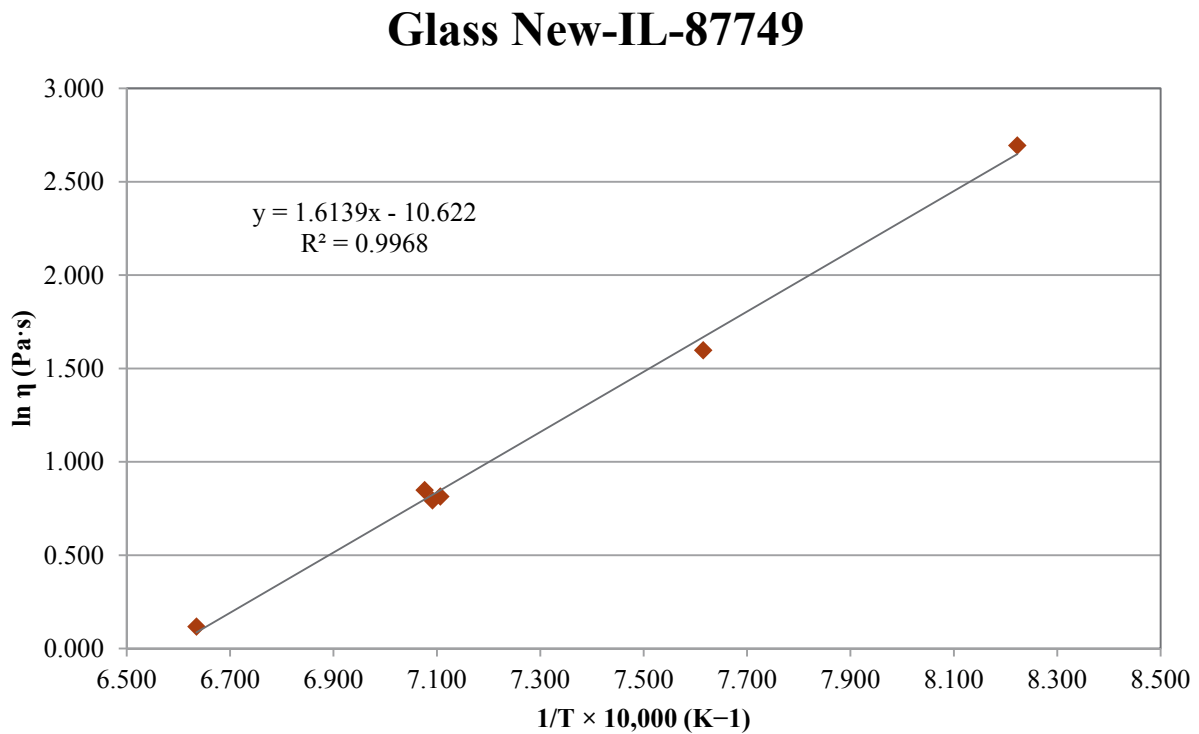


Figure B.7. Viscosity-Temperature Data and Arrhenius Equation Fit for Glass New-IL-87749

B.8 Glass New-IL-93907 Viscosity Data

Table B.8. Viscosity Data for Glass New-IL-93907

Setpoint, °C	Measured Temp., °C	Viscosity, Pa·s	$1/(T+273.15) \times 10,000, K^{-1}$	$\ln \eta, Pa \cdot s$
1150	1137	5.163	7.091	1.642
1050	1041	12.906	7.609	2.558
950	--	--	--	--
1150	1153	4.896	7.012	1.588
1250	1243	2.762	6.596	1.016
1150	1138	5.300	7.086	1.668

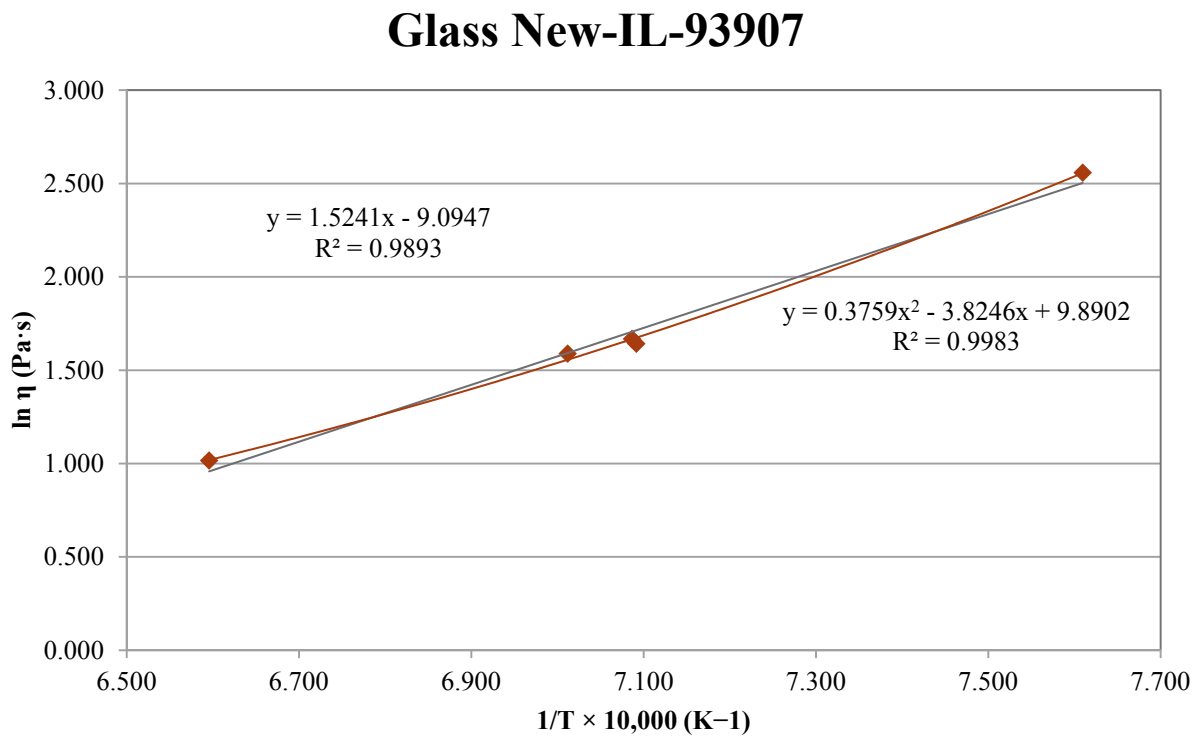


Figure B.8. Viscosity-Temperature Data and Arrhenius Equation Fit for Glass New-IL-93907

B.9 Glass New-IL-94020 Viscosity Data

Table B.9. Viscosity Data for Glass New-IL-94020

Setpoint, °C	Measured Temp., °C	Viscosity, Pa·s	$1/(T+273.15) \times 10,000, K^{-1}$	$\ln \eta, Pa \cdot s$
1150	1137	8.486	7.091	2.138
1050	1068	44.076	7.456	3.786
950	--	--	--	--
1150	1150	5.593	7.027	1.722
1250	1249	2.901	6.570	1.065
1150	1159	5.263	6.983	1.661

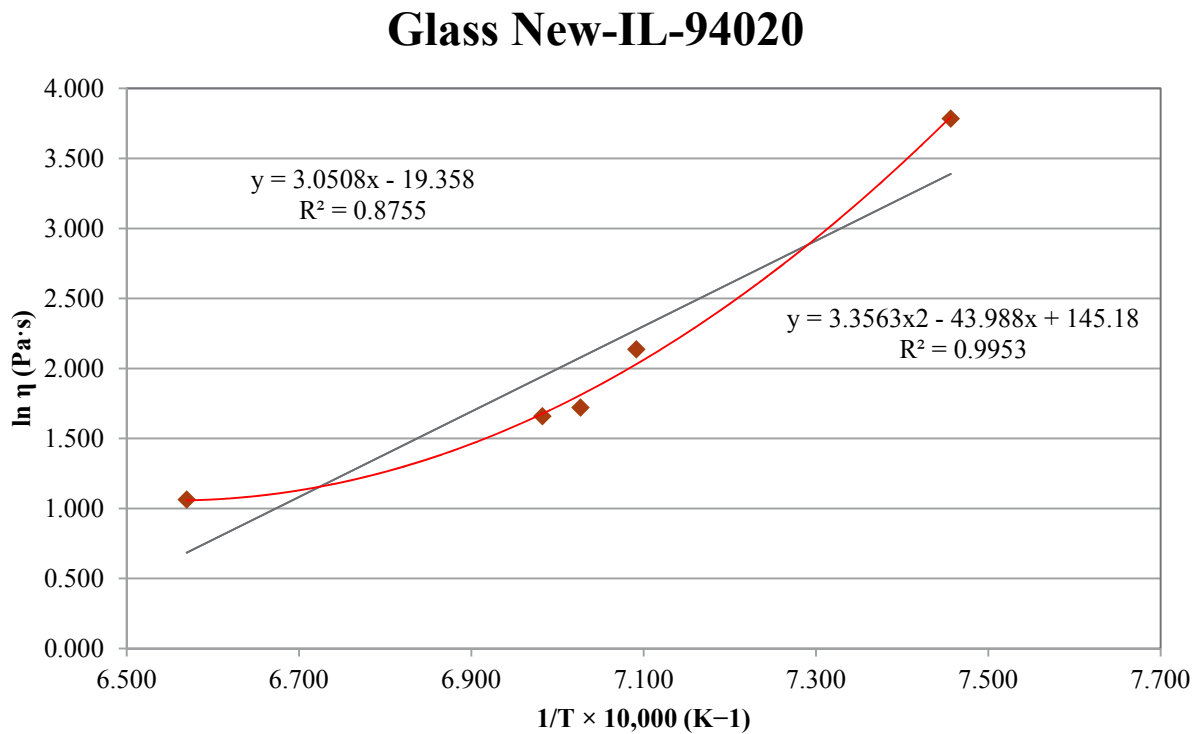


Figure B.9. Viscosity-Temperature Data and Arrhenius Equation Fit for Glass New-IL-94020

B.10 Glass New-IL-103151 Viscosity Data

Table B.10. Viscosity Data for Glass New-IL-103151

Setpoint, °C	Measured Temp., °C	Viscosity, Pa·s	$1/(T+273.15) \times 10,000, K^{-1}$	$\ln \eta, Pa \cdot s$
1150	1138	3.278	7.086	1.187
1050	1041	6.677	7.609	1.899
950	944	25.357	8.216	3.233
1150	1135	3.282	7.102	1.188
1250	1235	1.646	6.631	0.498
1150	1140	3.530	7.076	1.261

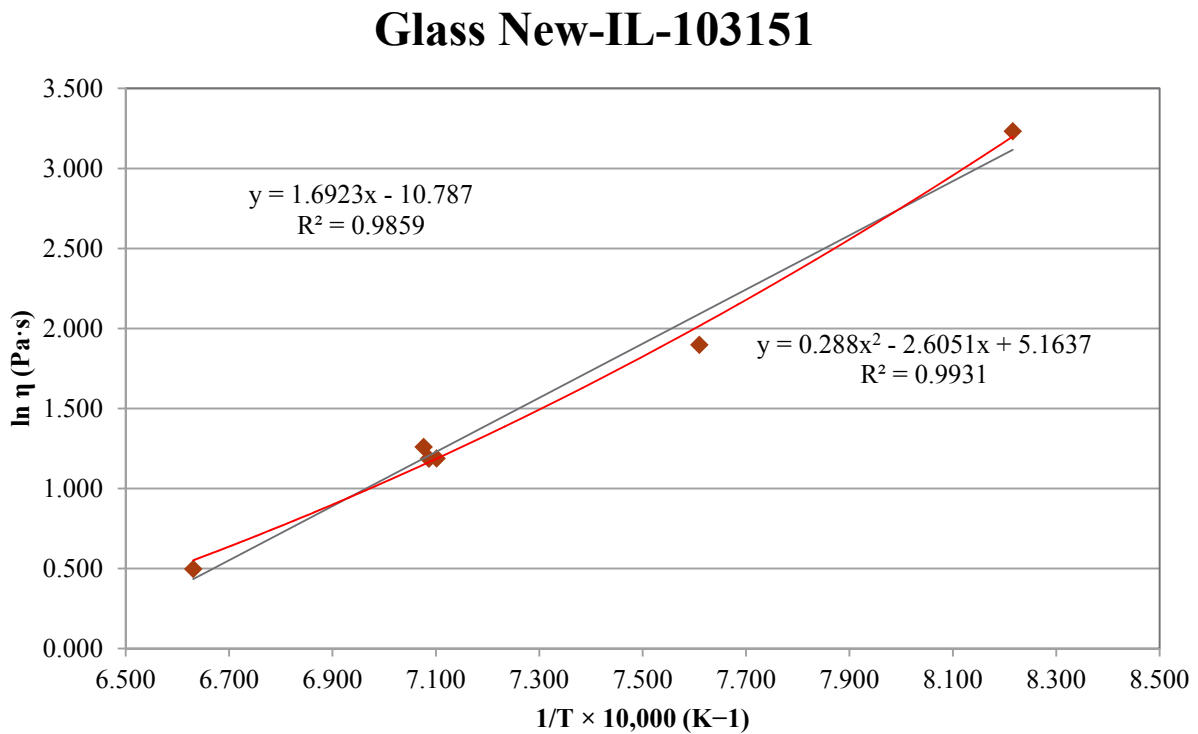


Figure B.10. Viscosity-Temperature Data and Arrhenius Equation Fit for Glass New-IL-103151

B.11 Glass New-IL-151542 Viscosity Data

Table B.11. Viscosity Data for Glass New-IL-151542

Setpoint, °C	Measured Temp., °C	Viscosity, Pa·s	$1/(T+273.15) \times 10,000, K^{-1}$	$\ln \eta, Pa \cdot s$
1150	1137	2.697	7.091	0.992
1050	1041	6.027	7.609	1.796
950	944	26.439	8.216	3.275
1150	1134	2.698	7.107	0.993
1250	1234	1.363	6.635	0.310
1150	1140	2.897	7.076	1.064

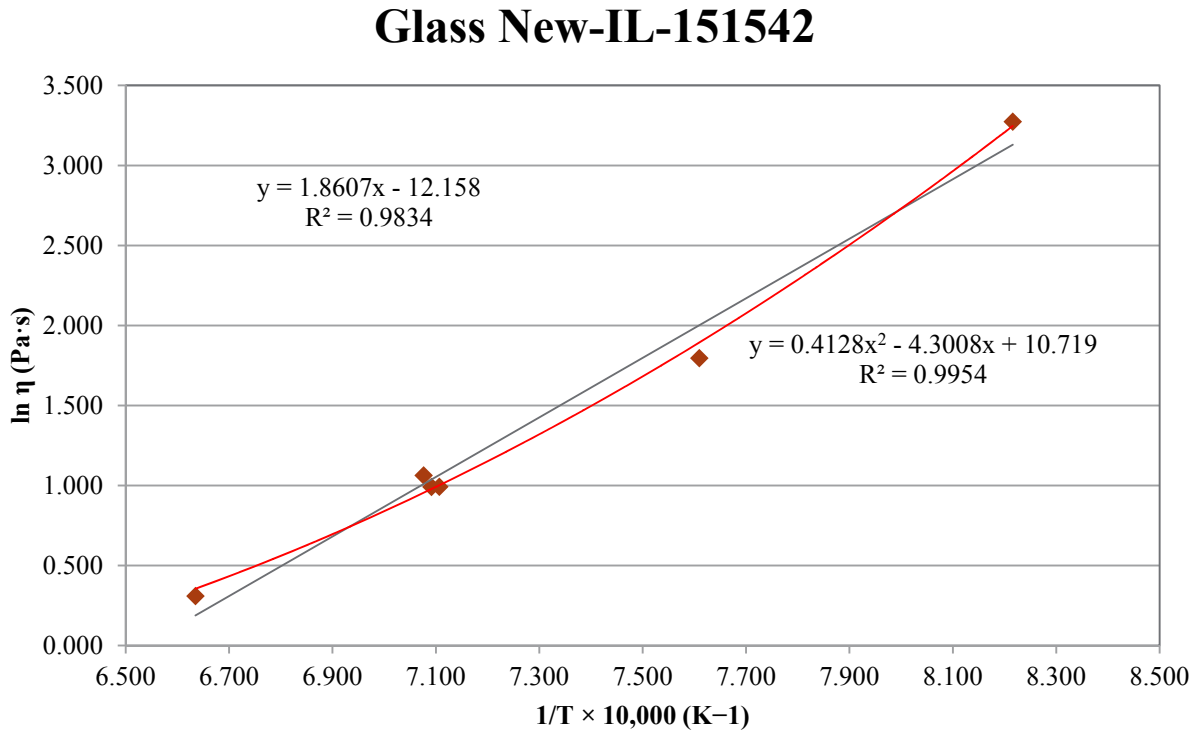


Figure B.11. Viscosity-Temperature Data and Arrhenius Equation Fit for Glass New-IL-151542

B.12 Glass New-IL-166697 Viscosity Data

Table B.12. Viscosity Data for Glass New-IL-166697

Setpoint, °C	Measured Temp., °C	Viscosity, Pa·s	$1/(T+273.15) \times 10,000, K^{-1}$	$\ln \eta, Pa \cdot s$
1150	1137	2.686	7.091	0.988
1050	1041	5.719	7.609	1.744
950	943	21.721	8.223	3.078
1150	1135	2.876	7.102	1.056
1250	1234	1.384	6.635	0.325
1150	1140	2.869	7.076	1.054

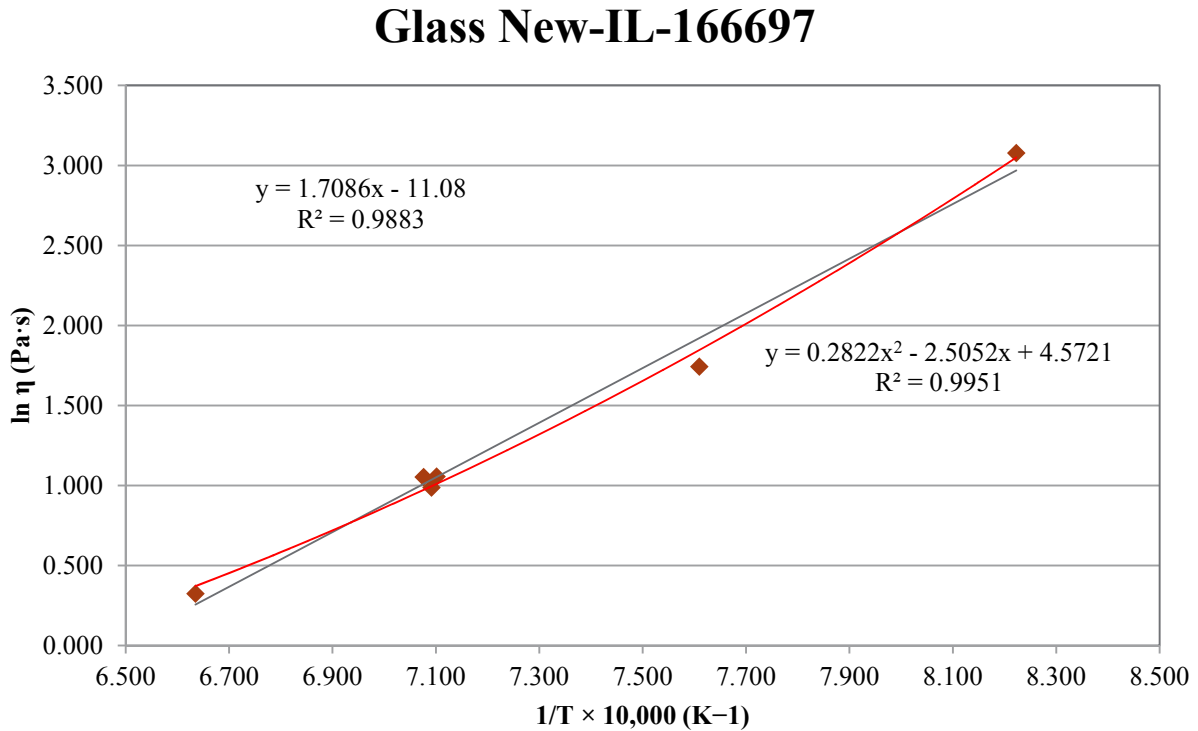


Figure B.12. Viscosity-Temperature Data and Arrhenius Equation Fit for Glass New-IL-166697

B.13 Glass New-IL-166731 Viscosity Data

Table B.13. Viscosity Data for Glass New-IL-166731

Setpoint, °C	Measured Temp., °C	Viscosity, Pa·s	$1/(T+273.15) \times 10,000, K^{-1}$	$\ln \eta, Pa \cdot s$
1150	1137	2.924	7.091	1.073
1050	1041	12.350	7.609	2.514
950	--	--	--	--
1150	1156	2.449	6.997	0.896
1250	1250	1.302	6.565	0.264
1150	1140	2.961	7.076	1.086

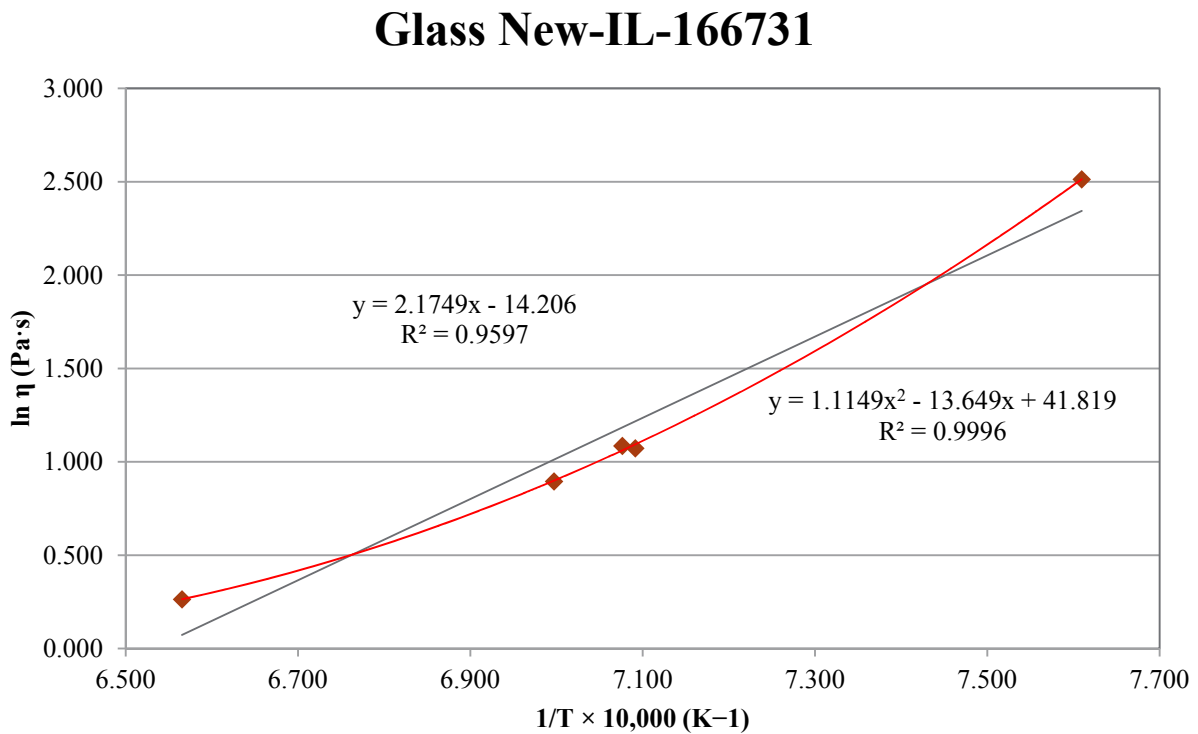


Figure B.13. Viscosity-Temperature Data and Arrhenius Equation Fit for Glass New-IL-166731

B.14 Glass New-OL-8445 Viscosity Data

Table B.14. Viscosity Data for Glass New-OL-8445

Setpoint, °C	Measured Temp., °C	Viscosity, Pa·s	$1/(T+273.15) \times 10,000, \text{K}^{-1}$	$\ln \eta, \text{Pa}\cdot\text{s}$
1150	1138	3.245	7.086	1.177
1050	1041	7.482	7.609	2.013
950	944	36.983	8.216	3.610
1150	1134	3.190	7.107	1.160
1250	1234	1.473	6.635	0.387
1150	1140	3.406	7.076	1.226

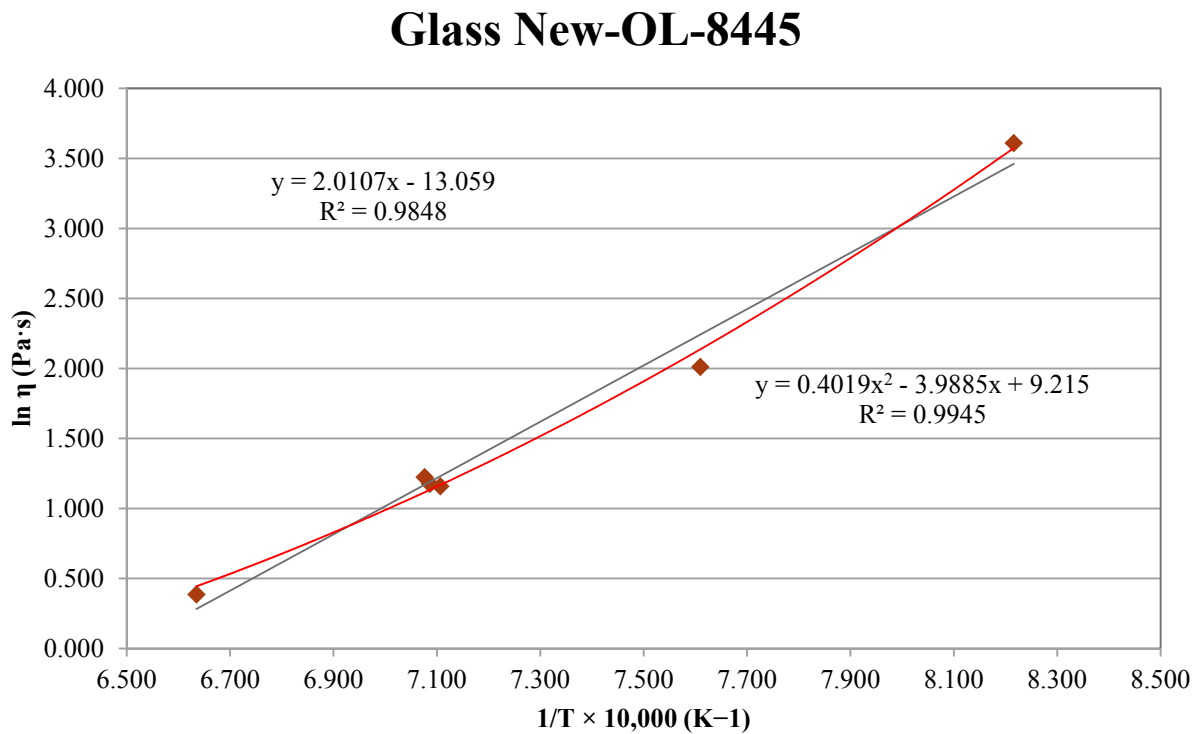


Figure B.14. Viscosity-Temperature Data and Arrhenius Equation Fit for Glass New-OL-8445

B.15 Glass New-OL-8788(Mod) Viscosity Data

Table B.15. Viscosity Data for Glass New-OL-8788(Mod)

Setpoint, °C	Measured Temp., °C	Viscosity, Pa·s	$1/(T+273.15) \times 10,000, K^{-1}$	$\ln \eta, Pa \cdot s$
1150	1138	28.911	7.086	3.364
1050	--	--	--	--
950	--	--	--	--
1150	1153	24.841	7.012	3.212
1250	1251	8.515	6.561	2.142
1150	1151	26.956	7.022	3.294

Glass New-OL-8788(Mod)

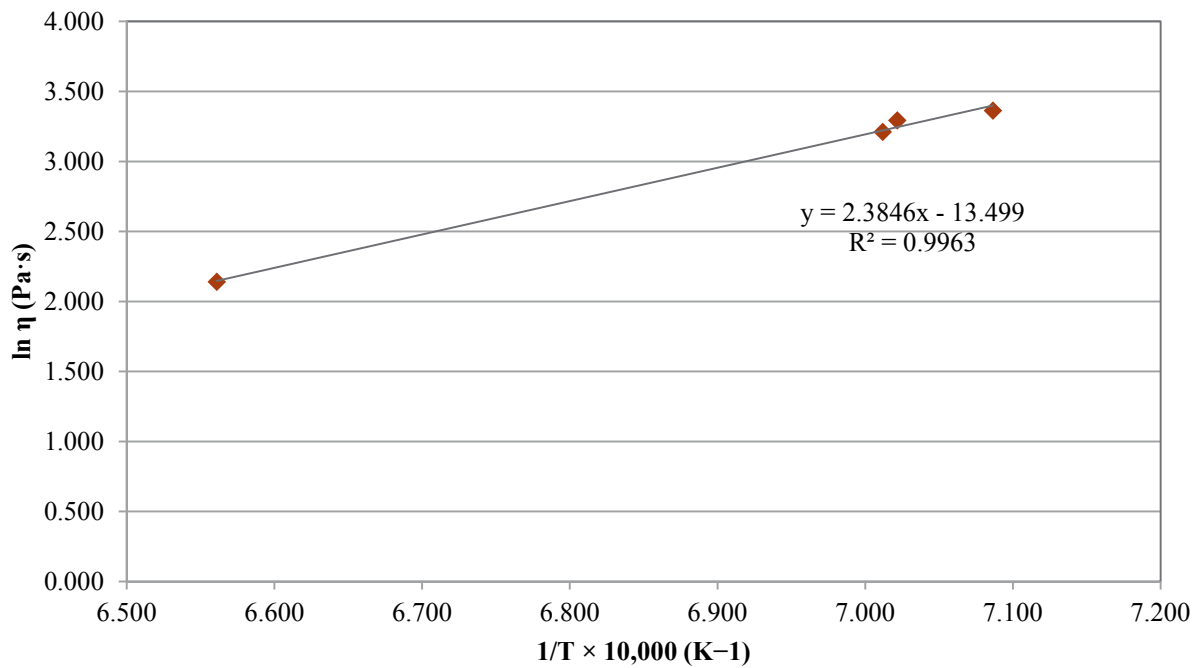


Figure B.15. Viscosity-Temperature Data and Arrhenius Equation Fit for Glass New-OL-8788(Mod)

B.16 Glass New-OL-14844 Viscosity Data

Table B.16. Viscosity Data for Glass New-OL-14844

Setpoint, °C	Measured Temp., °C	Viscosity, Pa·s	$1/(T+273.15) \times 10,000, \text{K}^{-1}$	$\ln \eta, \text{Pa}\cdot\text{s}$
1150	1138	0.489	7.086	-0.715
1050	1041	1.370	7.609	0.315
950	943	3.775	8.223	1.328
1150	1134	0.556	7.107	-0.587
1250	1234	0.253	6.635	-1.374
1150	1140	0.487	7.076	-0.719

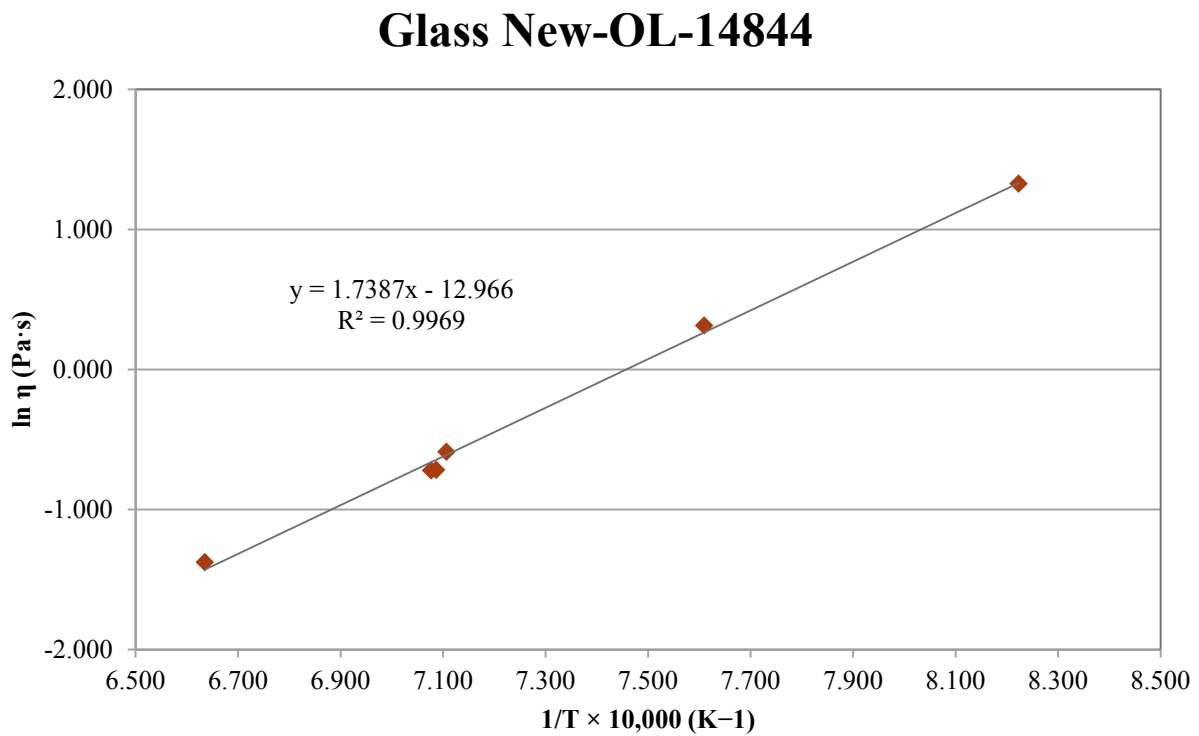


Figure B.16. Viscosity-Temperature Data and Arrhenius Equation Fit for Glass New-OL-14844

B.17 Glass New-OL-15493 Viscosity Data

Table B.17. Viscosity Data for Glass New-OL-15493

Setpoint, °C	Measured Temp., °C	Viscosity, Pa·s	$1/(T+273.15) \times 10,000, K^{-1}$	$\ln \eta, Pa \cdot s$
1150	1137	1.207	7.091	0.188
1050	1041	3.070	7.609	1.122
950	943	7.710	8.223	2.043
1150	1134	1.312	7.107	0.272
1250	1234	0.607	6.635	-0.499
1150	1140	1.298	7.076	0.261

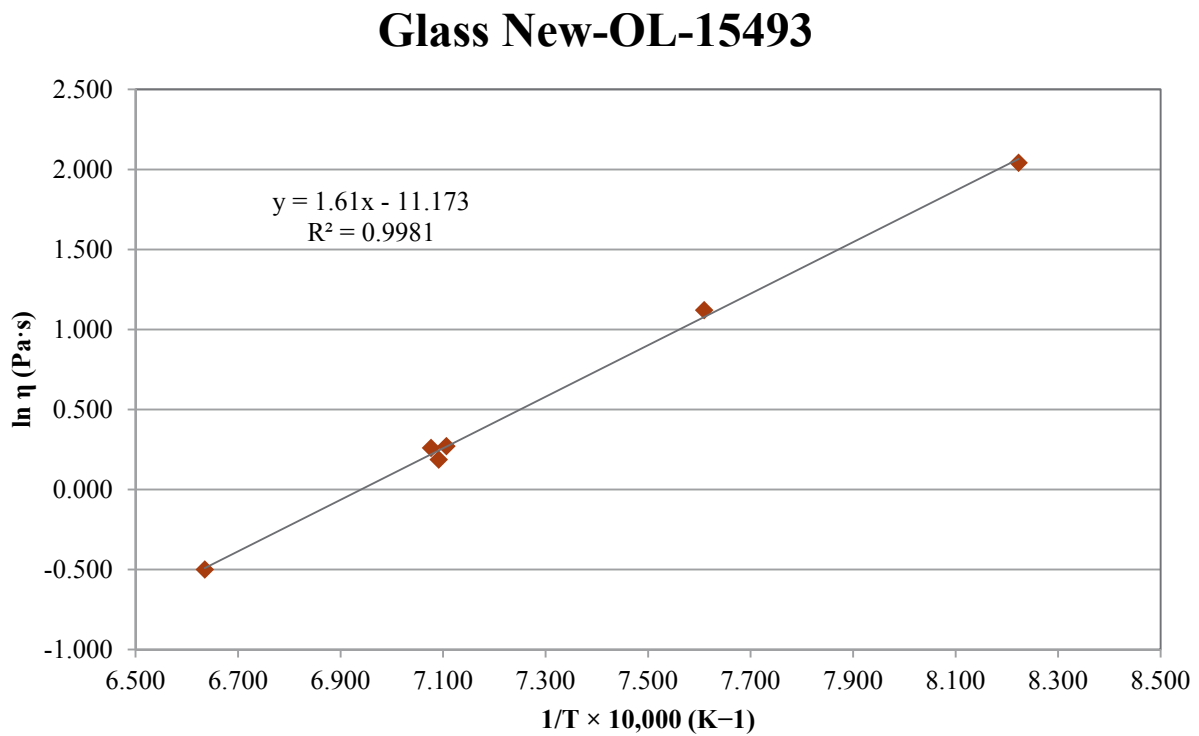


Figure B.17. Viscosity-Temperature Data and Arrhenius Equation Fit for Glass New-OL-15493

B.18 Glass New-OL-17130 Viscosity Data

Table B.18. Viscosity Data for Glass New-OL-17130

Setpoint, °C	Measured Temp., °C	Viscosity, Pa·s	$1/(T+273.15) \times 10,000, K^{-1}$	$\ln \eta, Pa \cdot s$
1150	1137	1.598	7.091	0.469
1050	1041	3.674	7.609	1.301
950	942	8.045	8.229	2.085
1150	1133	1.692	7.112	0.526
1250	1233	0.882	6.639	-0.126

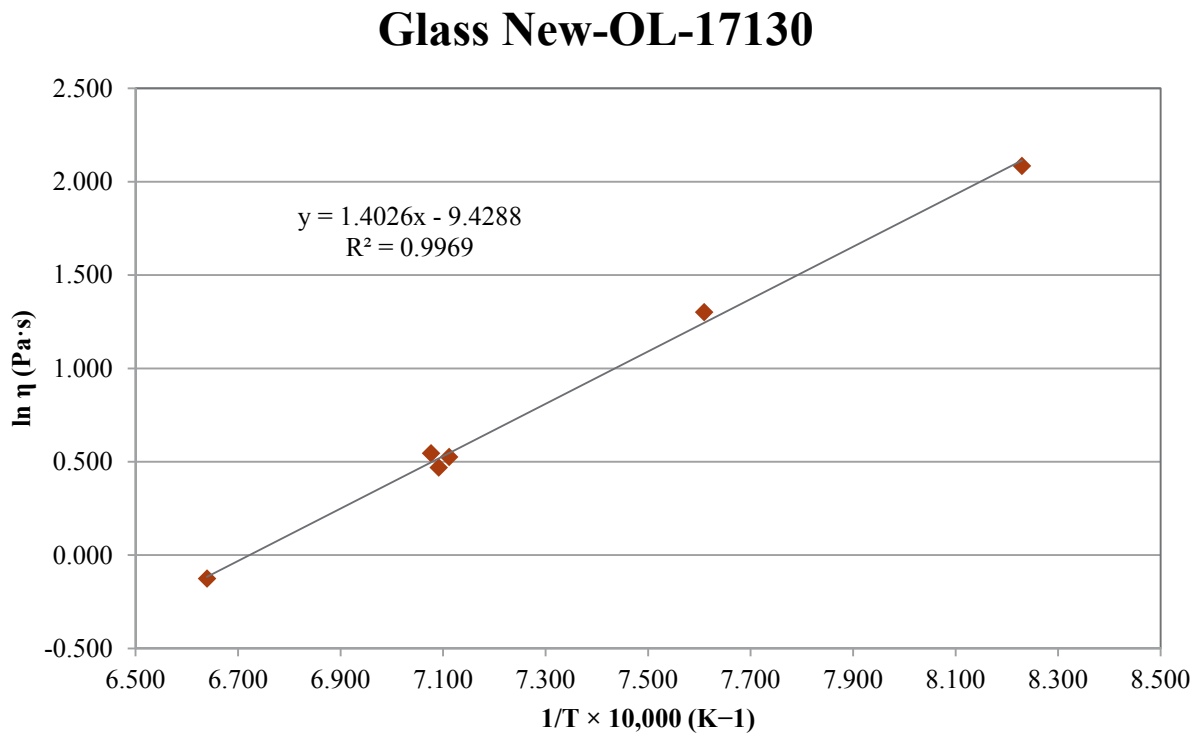


Figure B.18. Viscosity-Temperature Data and Arrhenius Equation Fit for Glass New-OL-17130

B.19 Glass New-OL-45748 (Sn Mod) Viscosity Data

Table B.19. Viscosity Data for Glass New-OL-45748 (Sn Mod)

Setpoint, °C	Measured Temp., °C	Viscosity, Pa·s	$1/(T+273.15) \times 10,000, K^{-1}$	$\ln \eta, Pa \cdot s$
1150	1137	3.057	7.091	1.117
1050	1042	7.248	7.604	1.981
950	945	32.956	8.209	3.495
1150	1133	3.104	7.112	1.133
1250	1233	1.475	6.639	0.389
1150	1141	3.546	7.071	1.266

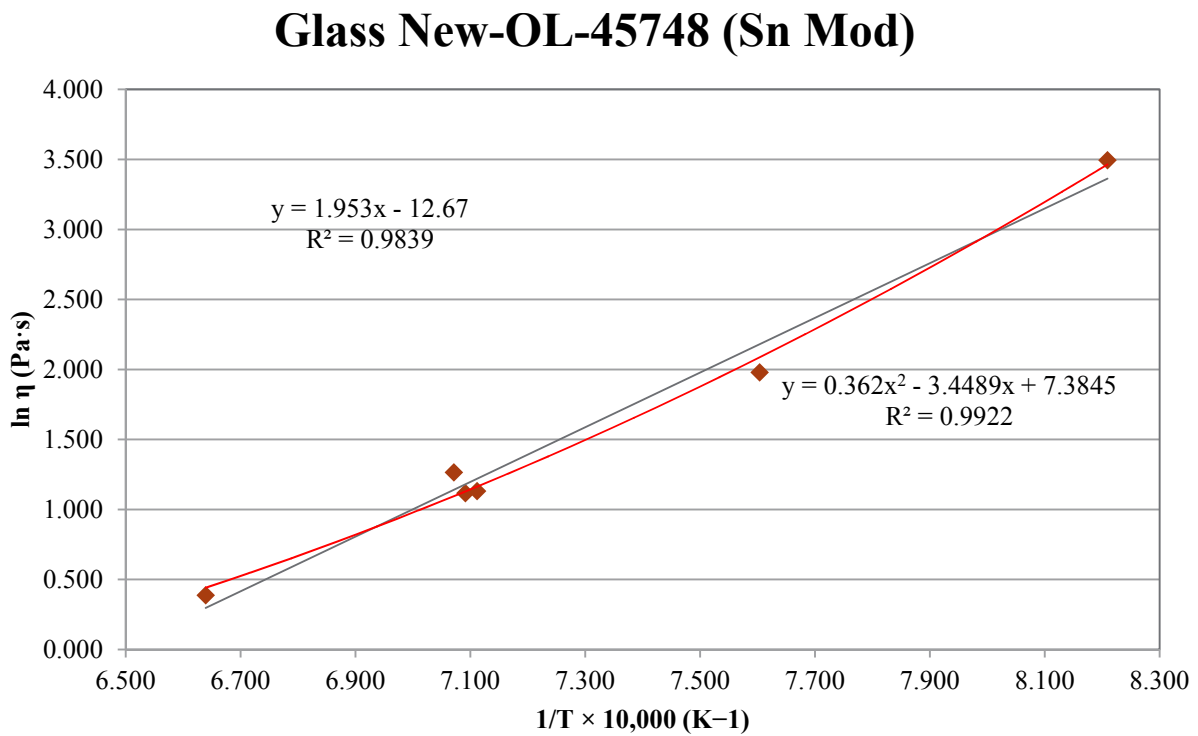


Figure B.19. Viscosity-Temperature Data and Arrhenius Equation Fit for Glass New-OL-45748 (Sn Mod)

B.20 Glass New-OL-54017 (Sn Mod) Viscosity Data

Table B.20. Viscosity Data for Glass New-OL-54017 (Sn Mod)

Setpoint, °C	Measured Temp., °C	Viscosity, Pa·s	$1/(T+273.15) \times 10,000, K^{-1}$	$\ln \eta, Pa \cdot s$
1150	1138	5.761	7.086	1.751
1050	1042	21.226	7.604	3.055
950	--	--	--	--
1150	1151	5.200	7.022	1.649
1250	1251	2.595	6.561	0.954
1150	1148	5.526	7.037	1.709

Glass New-OL-54017 (Sn Mod)

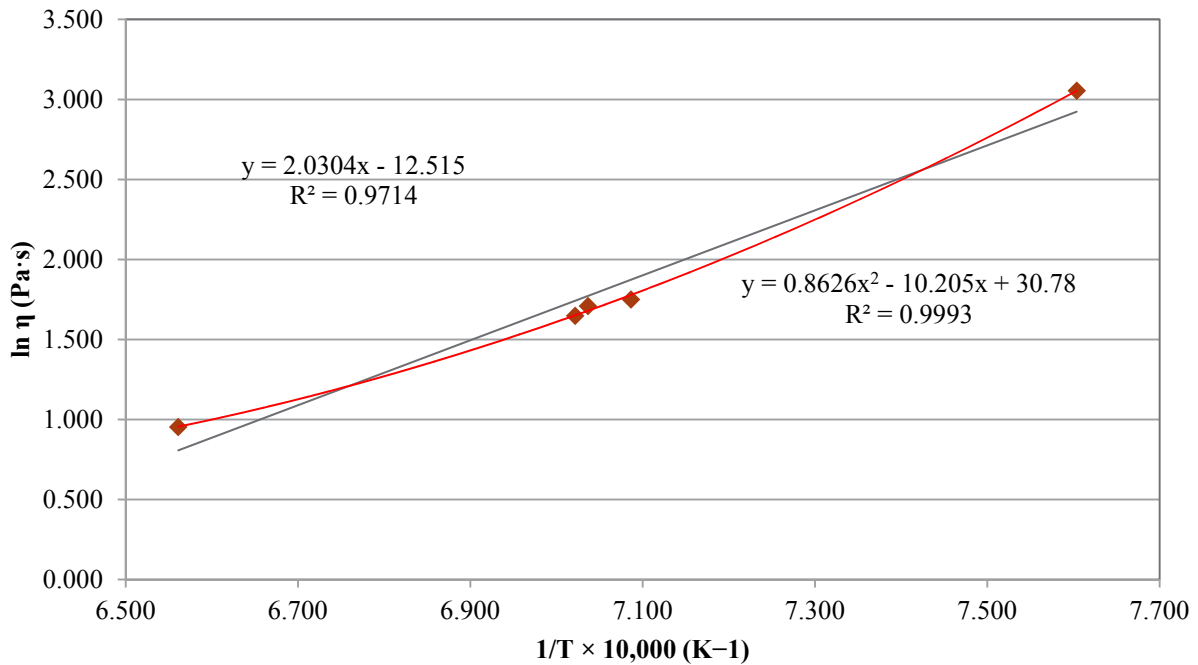


Figure B.20. Viscosity-Temperature Data and Arrhenius Equation Fit for Glass New-OL-54017 (Sn Mod)

B.21 Glass New-OL-57284 Viscosity Data

Table B.21. Viscosity Data for Glass New-OL-57284

Setpoint, °C	Measured Temp., °C	Viscosity, Pa·s	$1/(T+273.15) \times 10,000, K^{-1}$	$\ln \eta, Pa \cdot s$
1150	1138	8.361	7.086	2.124
1050	1041	31.233	7.609	3.441
950	--	--	--	--
1150	1152	7.259	7.017	1.982
1250	1245	4.301	6.587	1.459
1150	1143	8.336	7.061	2.121

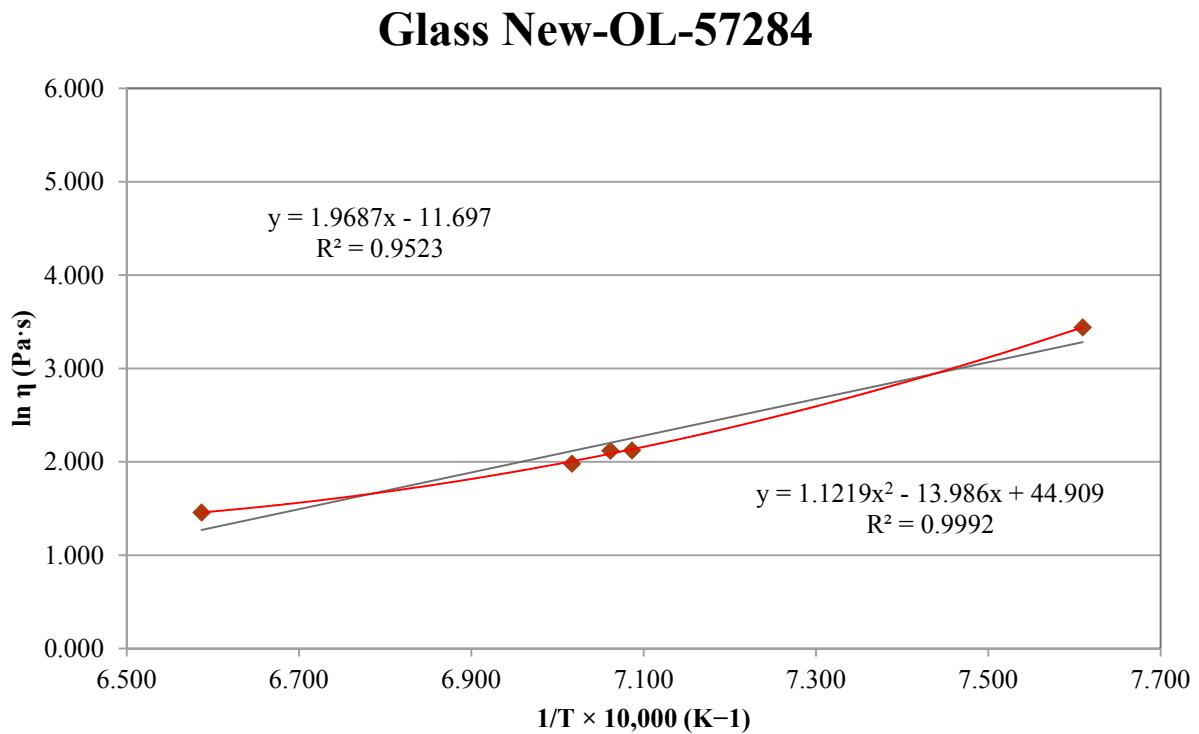


Figure B.21. Viscosity-Temperature Data and Arrhenius Equation Fit for Glass New-OL-57284

B.22 Glass New-OL-62380 Viscosity Data

Table B.22. Viscosity Data for Glass New-OL-62380

Setpoint, °C	Measured Temp., °C	Viscosity, Pa·s	$1/(T+273.15) \times 10,000, K^{-1}$	$\ln \eta, Pa \cdot s$
1150	1137	1.889	7.091	0.636
1050	1041	5.345	7.609	1.676
950	943	31.276	8.223	3.443
1150	1134	2.019	7.107	0.703
1250	1234	0.813	6.635	-0.207
1150	1140	2.049	7.076	0.717

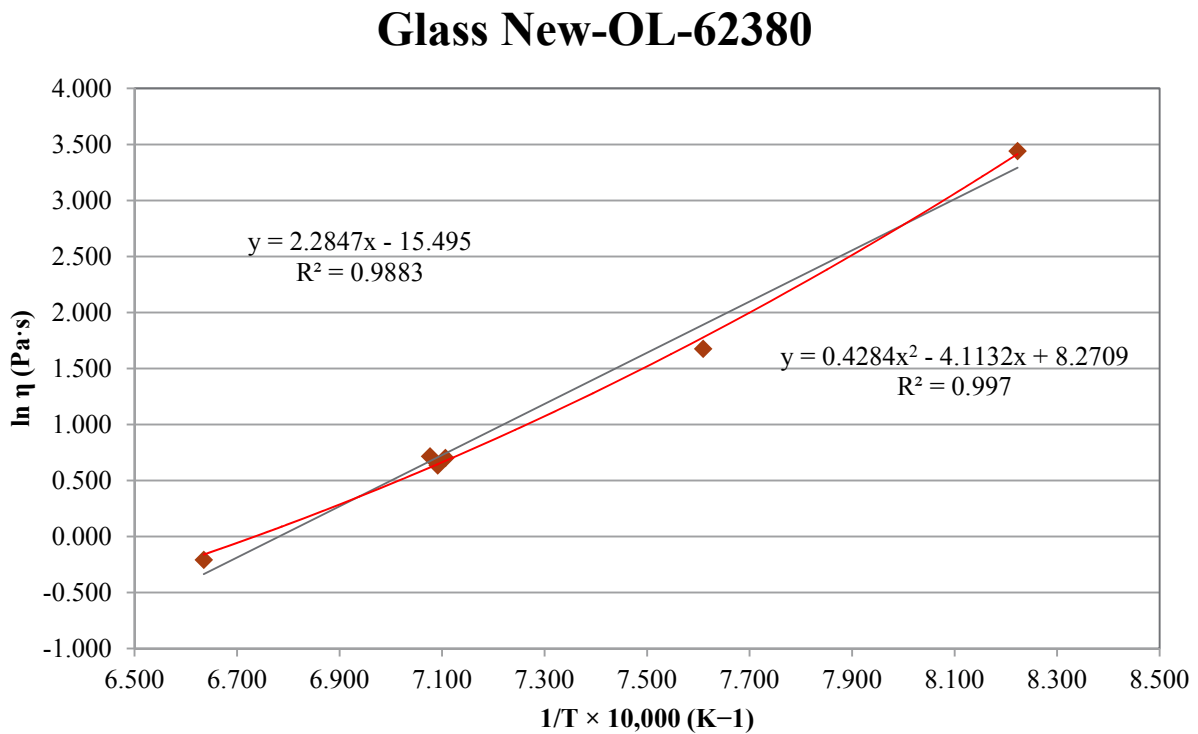


Figure B.22. Viscosity-Temperature Data and Arrhenius Equation Fit for Glass New-OL-62380

B.23 Glass New-OL-62909(Mod) Viscosity Data

Table B.23. Viscosity Data for Glass New-OL-62909(Mod)

Setpoint, °C	Measured Temp., °C	Viscosity, Pa·s	$1/(T+273.15) \times 10,000, K^{-1}$	$\ln \eta, Pa \cdot s$
1150	1137	4.905	7.091	1.590
1050	1042	23.766	7.604	3.168
950	--	--	--	--
1150	1151	4.074	7.022	1.405
1250	1246	1.395	6.583	0.333
1150	1149	5.021	7.032	1.614

Glass New-OL-62909 (Mod)

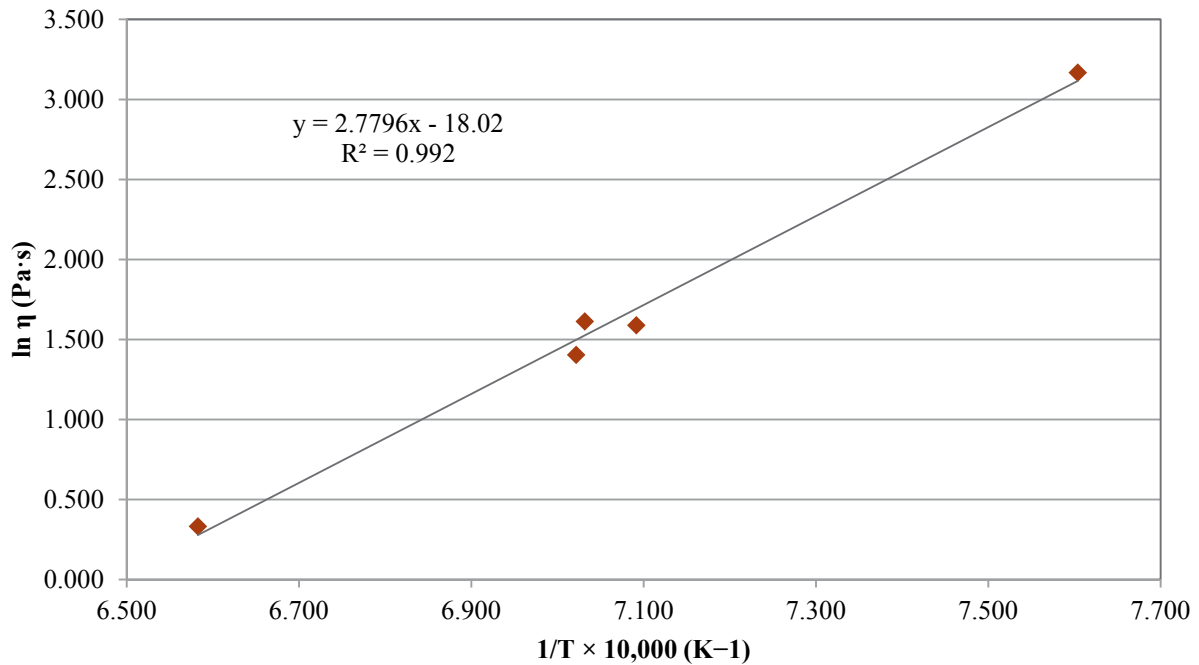


Figure B.23. Viscosity-Temperature Data and Arrhenius Equation Fit for Glass New-OL-62909(Mod)

B.24 Glass New-OL-65959(Mod) Viscosity Data

Table B.24. Viscosity Data for New-OL-65959(Mod)

Setpoint, °C	Measured Temp., °C	Viscosity, Pa·s	$1/(T+273.15) \times 10,000, K^{-1}$	$\ln \eta, Pa \cdot s$
1150	1127	1.595	7.142	0.467
1050	1033	4.672	7.656	1.542
950	938	13.984	8.257	2.638
1150	1121	1.534	7.173	0.428
1250	1224	0.873	6.679	-0.136
1150	1139	1.773	7.081	0.573

Glass New-OL-65959 (Mod)

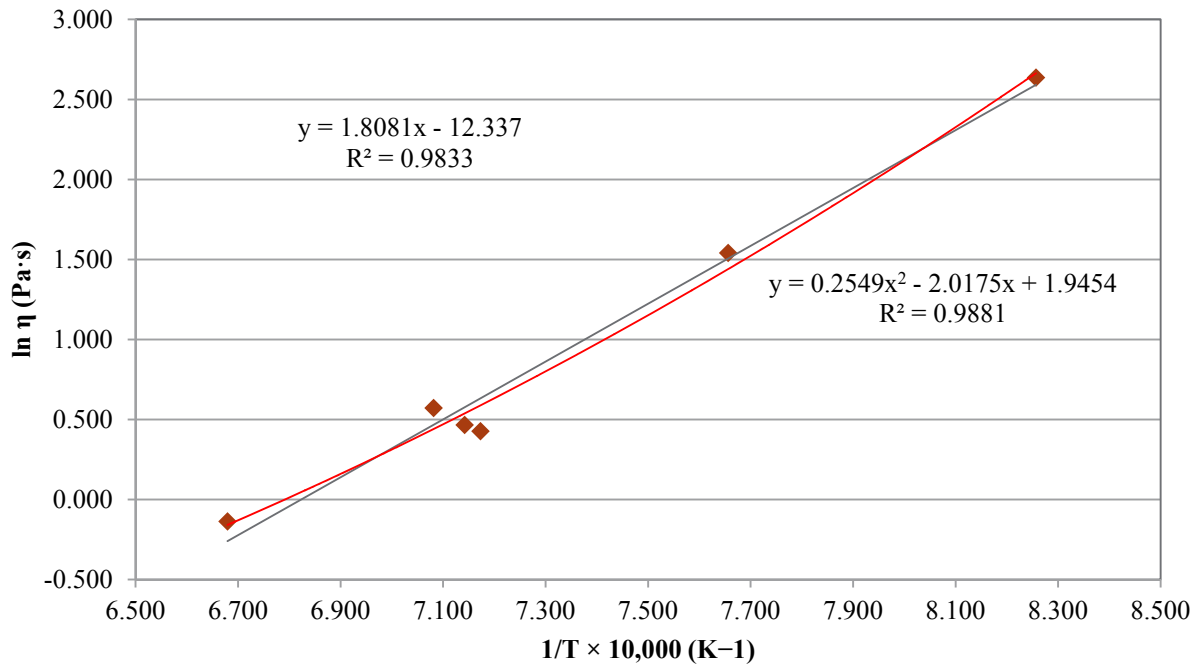


Figure B.24. Viscosity-Temperature Data and Arrhenius Equation Fit for Glass New-OL-65959(Mod)

B.25 Glass New-OL-80309 Viscosity Data

Table B.25. Viscosity Data for Glass New-OL-80309

Setpoint, °C	Measured Temp., °C	Viscosity, Pa·s	1/(T+273.15) × 10,000, K ⁻¹	ln η, Pa·s
1150	1138	0.889	7.086	-0.118
1050	1042	2.780	7.604	1.022
950	944	6.414	8.216	1.858
1150	1134	0.826	7.107	-0.191
1250	1234	0.398	6.635	-0.921
1150	1141	0.879	7.071	-0.129

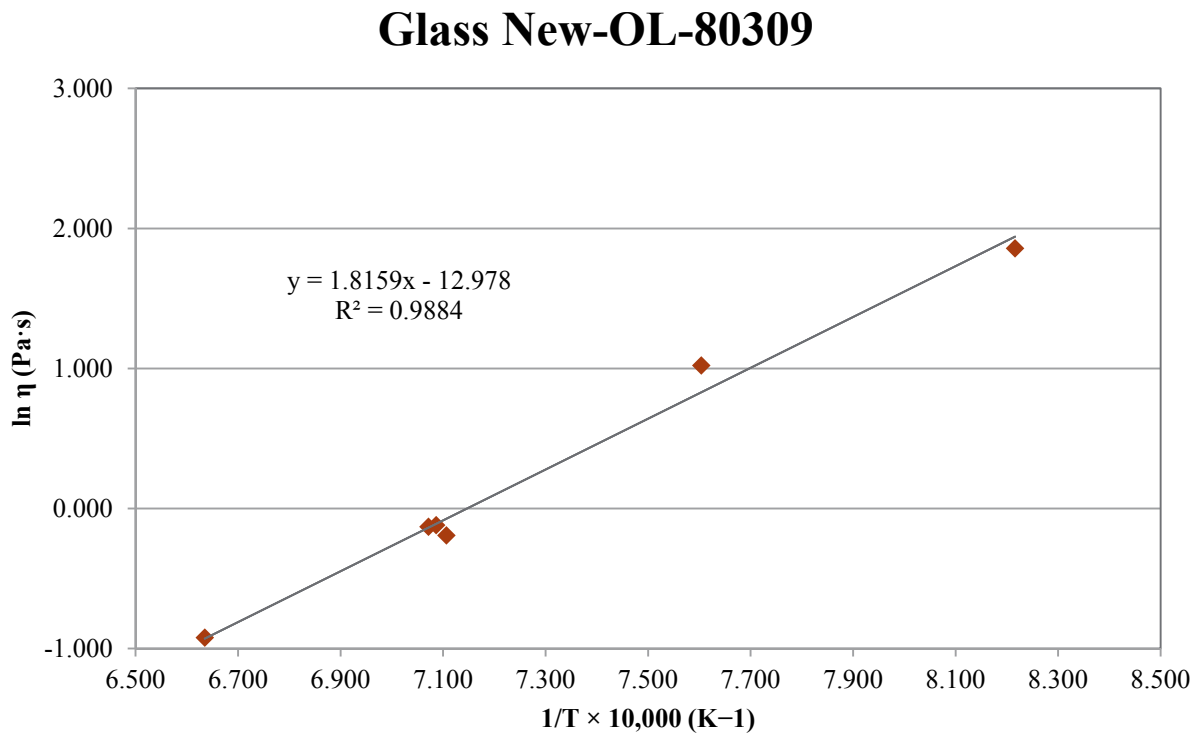


Figure B.25. Viscosity-Temperature Data and Arrhenius Equation Fit for Glass New-OL-80309

B.26 Glass New-OL-90780 Viscosity Data

Table B.26. Viscosity Data for Glass New-OL-90780

Setpoint, °C	Measured Temp., °C	Viscosity, Pa·s	$1/(T+273.15) \times 10,000, K^{-1}$	$\ln \eta, Pa \cdot s$
1150	1137	2.376	7.091	0.865
1050	1041	5.689	7.609	1.739
950	943	20.895	8.223	3.040
1150	1134	2.322	7.107	0.842
1250	1234	1.263	6.635	0.233
1150	1140	2.322	7.076	0.842

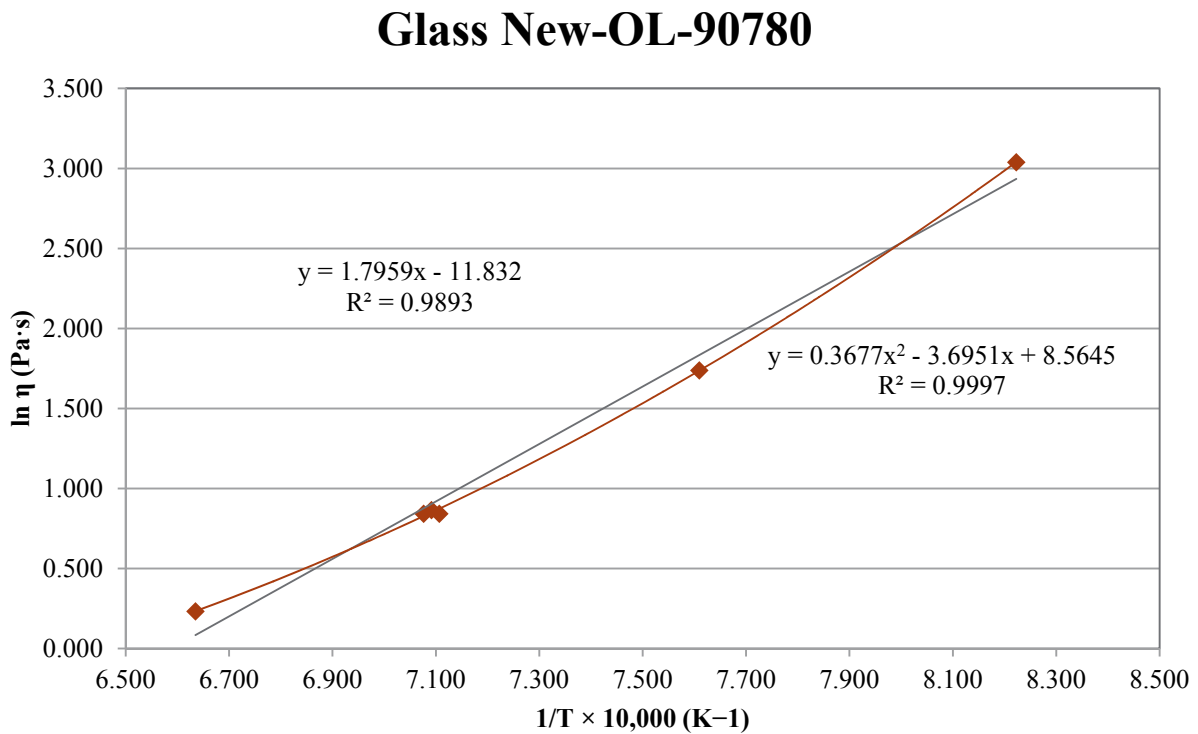


Figure B.26. Viscosity-Temperature Data and Arrhenius Equation Fit for Glass New-OL-90780

B.27 Glass New-OL-100210 Viscosity Data

Table B.27. Viscosity Data for Glass New-OL-100210

Setpoint, °C	Measured Temp., °C	Viscosity, Pa·s	$1/(T+273.15) \times 10,000, K^{-1}$	$\ln \eta, Pa \cdot s$
1150	1138	4.869	7.086	1.583
1050	1041	10.881	7.609	2.387
950	943	48.452	8.223	3.881
1150	1134	4.802	7.107	1.569
1250	1233	2.281	6.639	0.825
1150	1140	4.858	7.076	1.581

Glass New-OL-100210

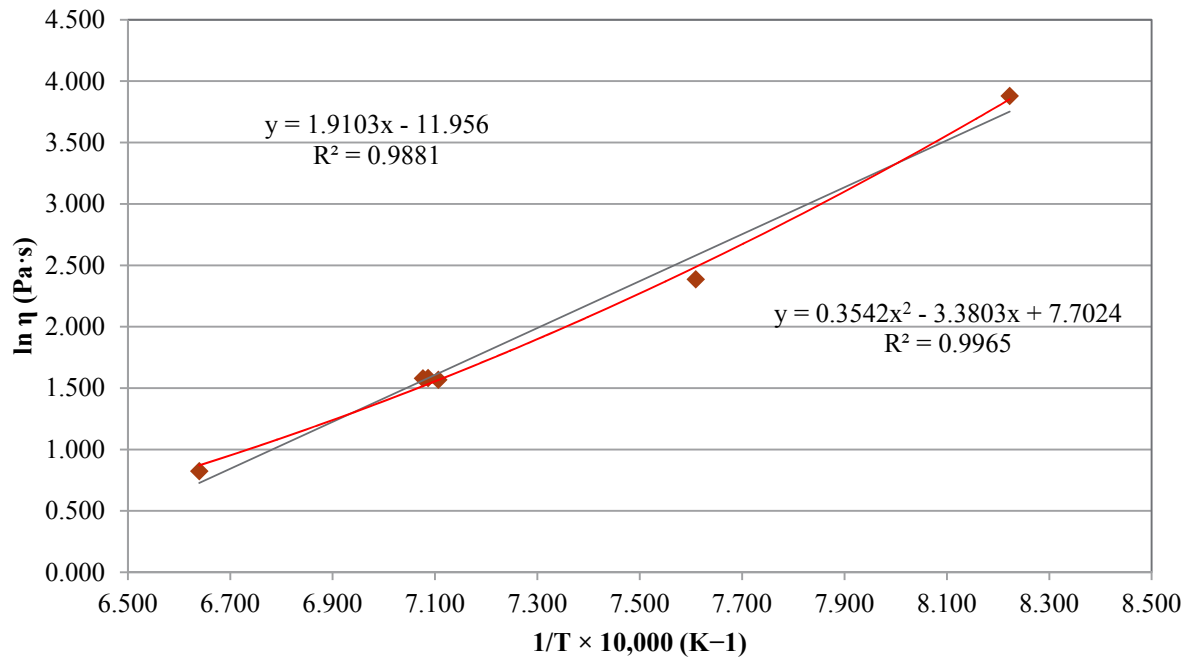


Figure B.27. Viscosity-Temperature Data and Arrhenius Equation Fit for Glass New-OL-100210

B.28 Glass New-OL-108249 (SO₃ Mod) Viscosity Data

Table B.28. Viscosity Data for Glass New-OL-108249 (SO₃ Mod)

Setpoint, °C	Measured Temp., °C	Viscosity, Pa·s	$1/(T+273.15) \times 10,000, K^{-1}$	$\ln \eta, Pa \cdot s$
1150	1130	2.437	7.127	0.891
1050	1037	5.770	7.633	1.753
950	941	25.191	8.236	3.226
1150	1123	2.049	7.163	0.717
1250	1226	0.724	6.670	-0.323
1150	--	--	--	--

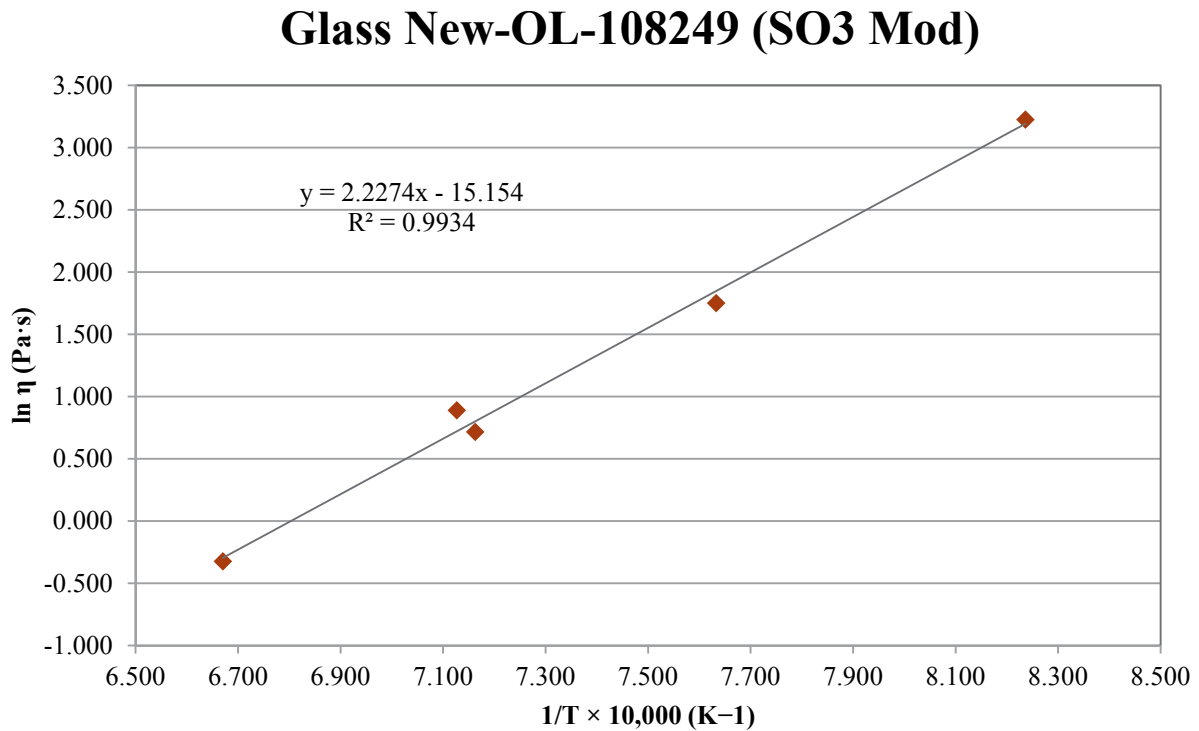


Figure B.28. Viscosity-Temperature Data and Arrhenius Equation Fit for Glass New-OL-108249 (SO₃ Mod)

B.29 Glass New-OL-116208 (SO₃ Mod) Viscosity Data

Table B.29. Viscosity Data for Glass New-OL-116208 (SO₃ Mod)

Setpoint, °C	Measured Temp., °C	Viscosity, Pa·s	1/(T+273.15) × 10,000, K ⁻¹	ln η, Pa·s
1150	1134	0.816	7.107	-0.203
1050	1038	2.203	7.627	0.790
950	942	10.334	8.229	2.335
1150	1130	0.807	7.127	-0.214
1250	1231	0.333	6.648	-1.100
1150	1138	0.878	7.086	-0.130

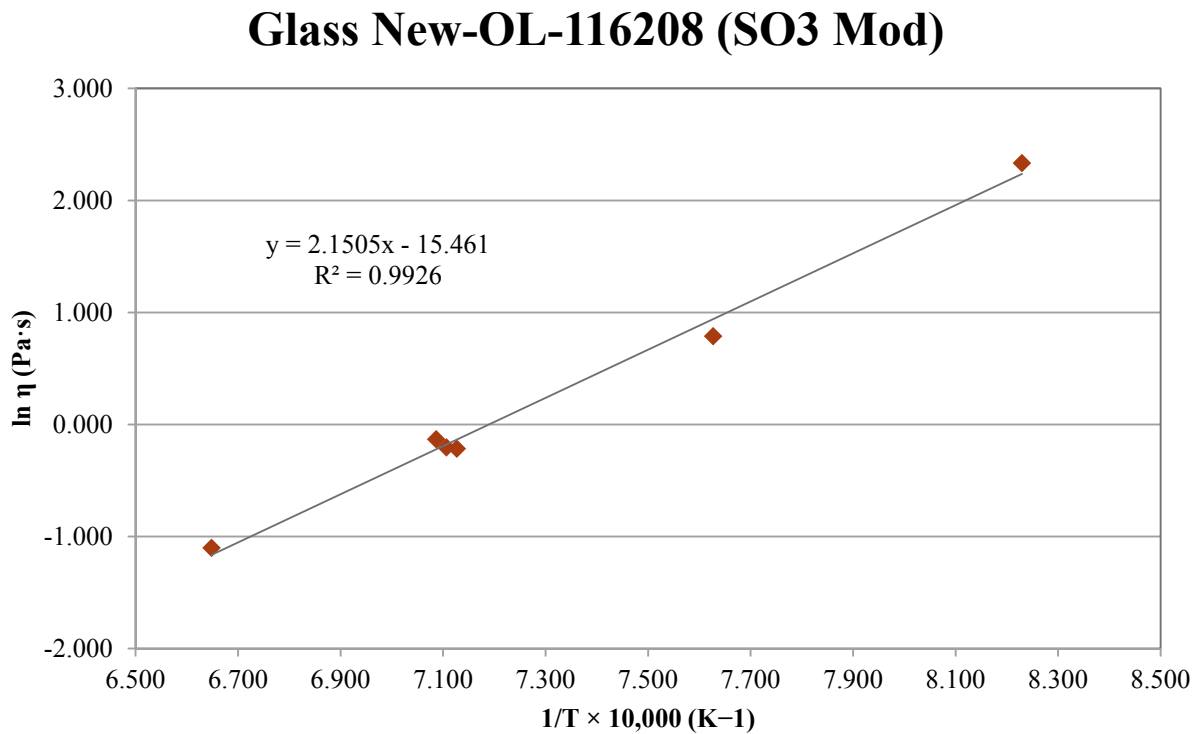


Figure B.29. Viscosity -Temperature Data and Arrhenius Equation Fit for Glass New-OL-116208 (SO₃ Mod)

B.30 Glass New-OL-122817 Viscosity Data

Table B.30. Viscosity Data for Glass New-OL-122817

Setpoint, °C	Measured Temp., °C	Viscosity, Pa·s	$1/(T+273.15) \times 10,000, K^{-1}$	$\ln \eta, Pa \cdot s$
1150	1138	3.839	7.086	1.345
1050	1041	8.621	7.609	2.154
950	--	--	--	--
1150	1154	3.435	7.007	1.234
1250	1235	1.867	6.631	0.624
1150	1140	4.192	7.076	1.433

Glass New-OL-122817

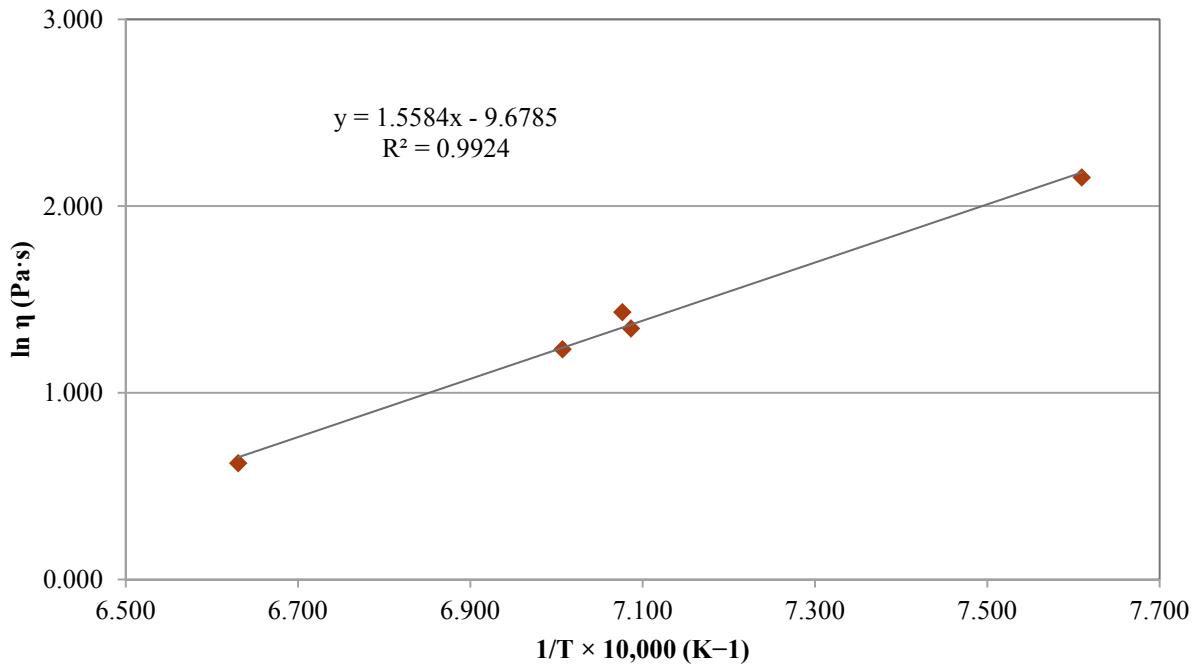


Figure B.30. Viscosity -Temperature Data and Arrhenius Equation Fit for Glass New-OL-122817

B.31 Glass New-OL-127708 (Mod) Viscosity Data

Table B.31. Viscosity Data for Glass New-OL-127708(Mod)

Setpoint, °C	Measured Temp., °C	Viscosity, Pa·s	$1/(T+273.15) \times 10,000, K^{-1}$	$\ln \eta, Pa \cdot s$
1150	1136	8.692	7.091	2.162
1050	1042	28.694	7.609	3.357
950	--	--	--	--
1150	1155	7.491	7.491	7.002
1250	1251	4.603	4.603	6.557
1150	--	--	--	--

Glass New-OL-127708 (Mod)

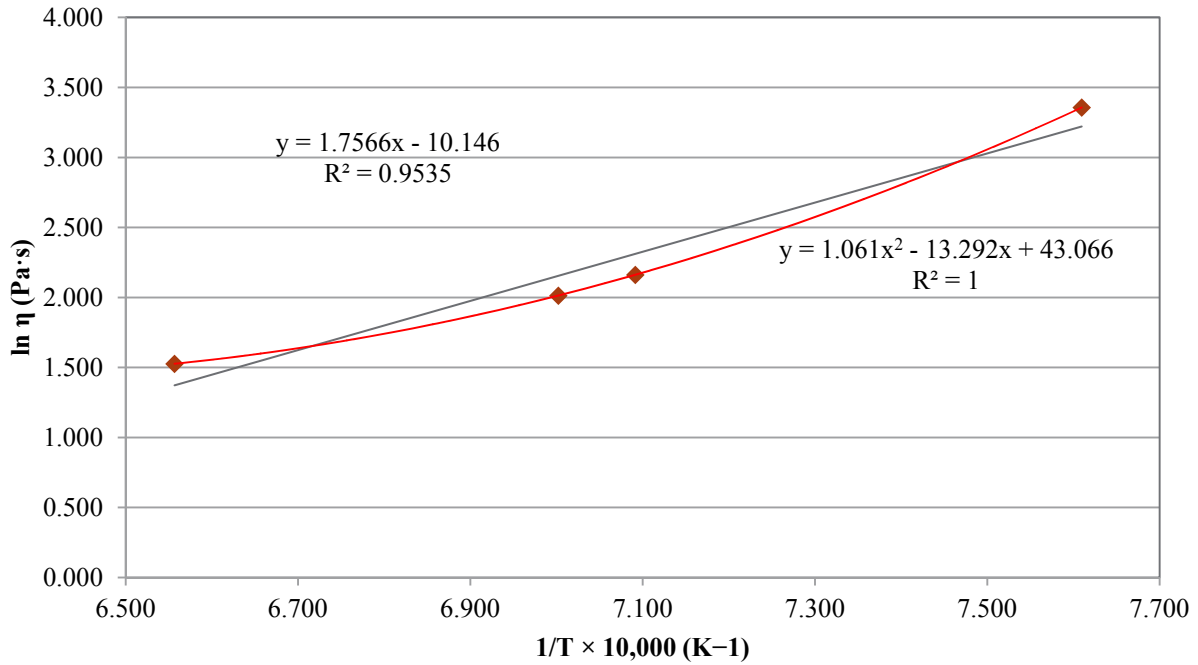


Figure B.31. Viscosity-Temperature Data and Arrhenius Equation Fit for Glass New-OL-127708(Mod)

B.32 Glass EWG-LAW-Centroid-1 Viscosity Data

Table B.32. Viscosity Data for Glass EWG-LAW-Centroid-1

Setpoint, °C	Measured Temp., °C	Viscosity, Pa·s	$1/(T+273.15) \times 10,000, K^{-1}$	$\ln \eta, Pa \cdot s$
1150	1137	3.089	7.091	1.128
1050	1041	6.396	7.609	1.856
950	943	24.556	8.223	3.201
1150	1134	3.161	7.107	1.151
1250	1234	1.626	6.635	0.486
1150	1140	3.413	7.076	1.228

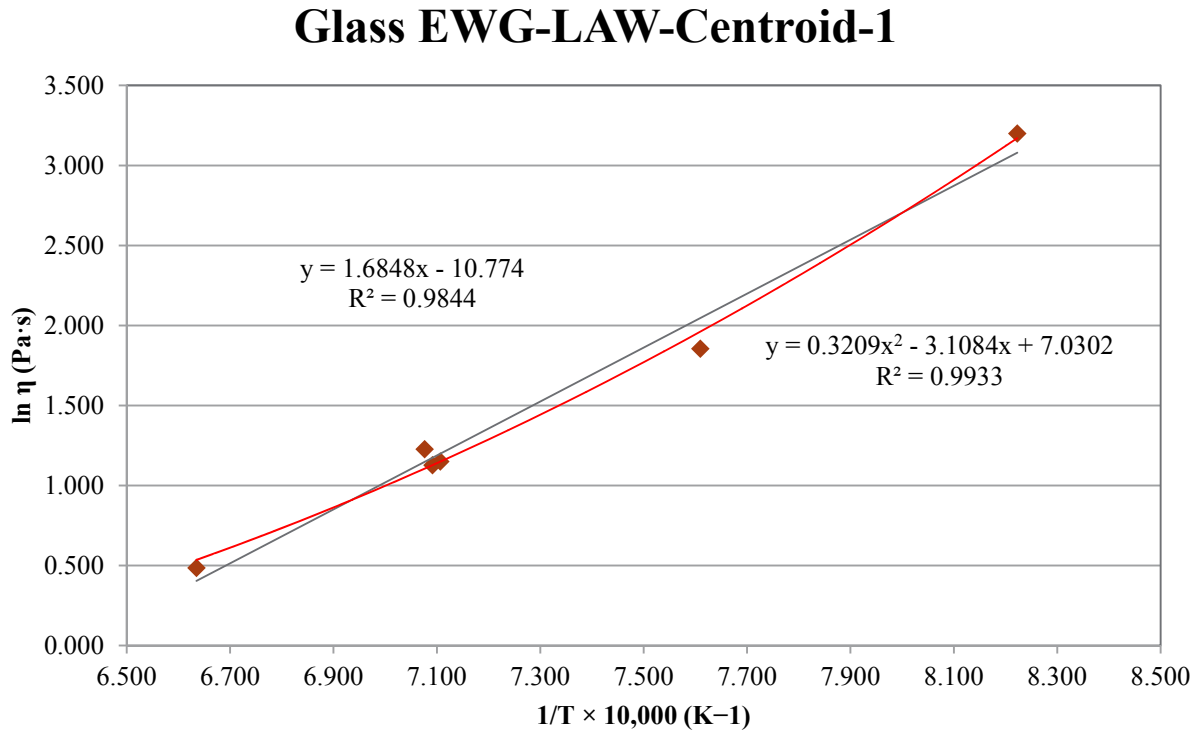


Figure B.32. Viscosity-Temperature Data and Arrhenius Equation Fit for Glass EWG-LAW-Centroid-1

B.33 Glass EWG-LAW-Centroid-2 Viscosity Data

Table B.33. Viscosity Data for Glass EWG-LAW-Centroid-2

Setpoint, °C	Measured Temp., °C	Viscosity, Pa·s	$1/(T+273.15) \times 10,000, K^{-1}$	$\ln \eta, Pa \cdot s$
1150	1136	3.124	7.096	1.139
1050	1040	6.345	7.615	1.848
950	943	24.256	8.223	3.189
1150	1133	3.113	7.112	1.136
1250	1233	1.563	6.639	0.447
1150	1139	3.305	7.081	1.195

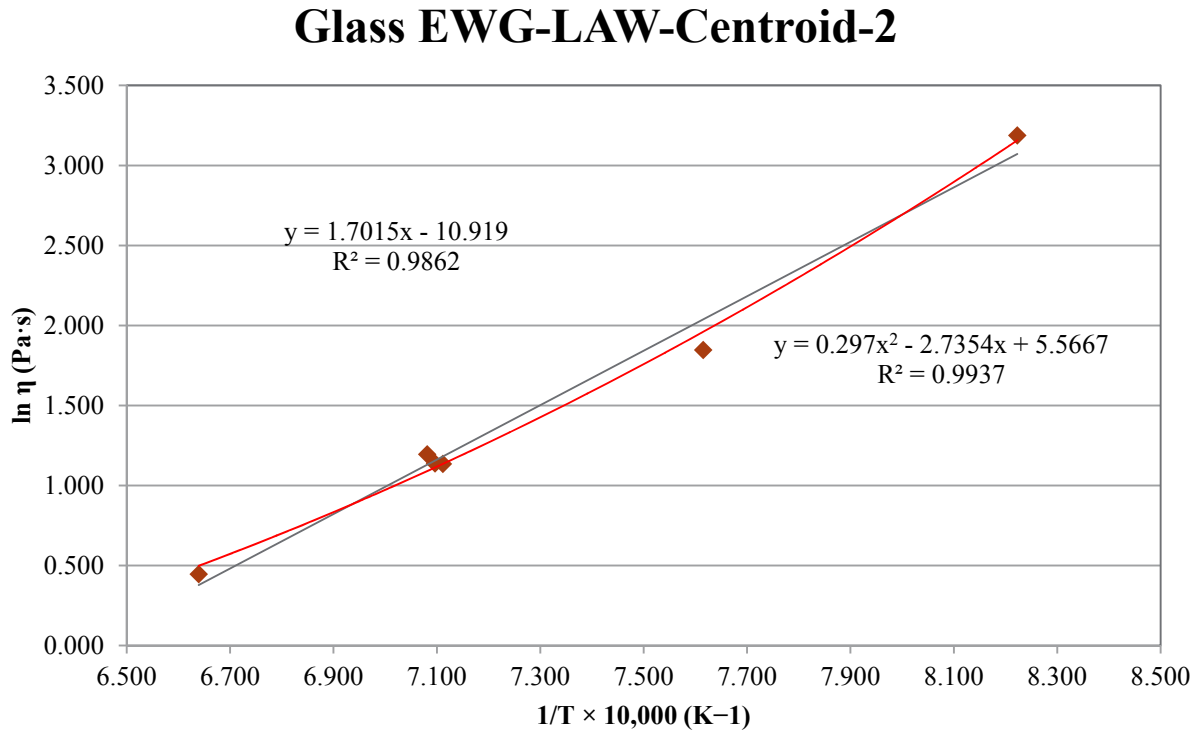


Figure B.33. Viscosity-Temperature Data and Arrhenius Equation Fit for Glass EWG-LAW-Centroid-2

B.34 Glass LAW-ORP-LD1-1 Viscosity Data

Table B.34. Viscosity Data for Glass LAW-ORP-LD1-1

Setpoint, °C	Measured Temp., °C	Viscosity, Pa·s	$1/(T+273.15) \times 10,000, K^{-1}$	$\ln \eta, Pa \cdot s$
1150	1137	3.292	7.091	1.191
1050	1041	6.977	7.609	1.943
950	943	29.978	8.223	3.400
1150	1134	3.366	7.107	1.214
1250	1234	1.619	6.635	0.482
1150	1141	3.497	7.071	1.252

Glass LAW-ORP-LD1-1

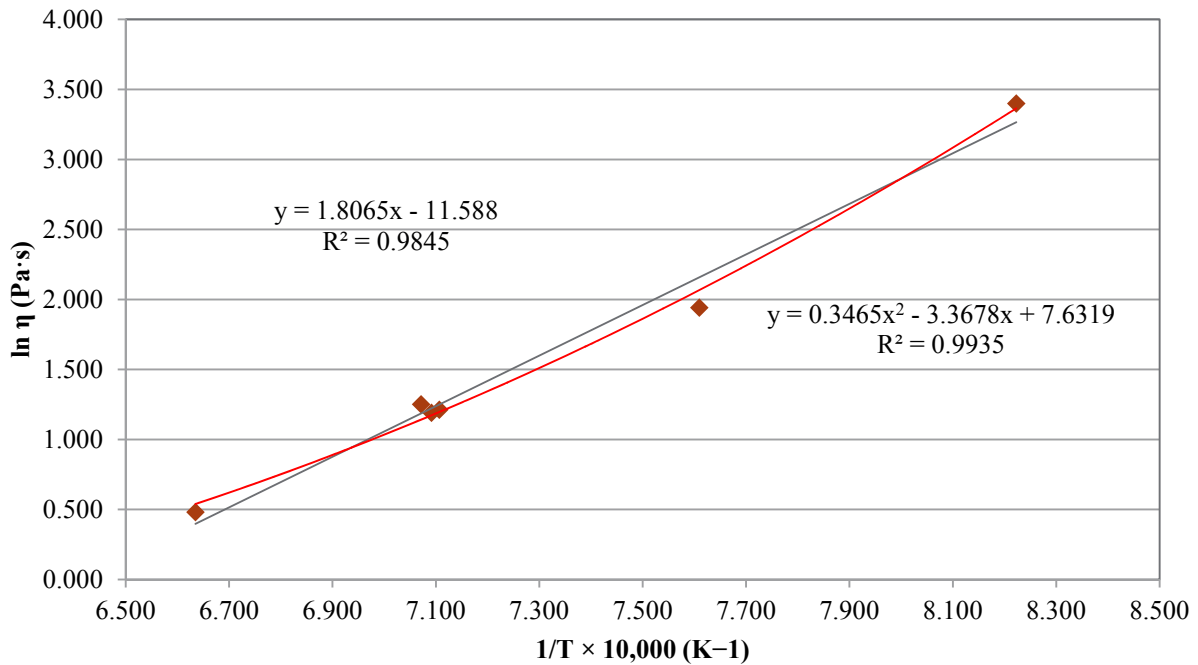


Figure B.34. Viscosity-Temperature Data and Arrhenius Equation Fit for Glass LAW-ORP-LD1-1

B.35 Glass LAW-ORP-LD1-2 Viscosity Data

Table B.35. Viscosity Data for Glass LAW-ORP-LD1-2

Setpoint, °C	Measured Temp., °C	Viscosity, Pa·s	$1/(T+273.15) \times 10,000, K^{-1}$	$\ln \eta, Pa \cdot s$
1150	1138	3.388	7.086	1.220
1050	1042	7.052	7.604	1.953
950	944	30.888	8.216	3.430
1150	1135	3.348	7.102	1.208
1250	1235	1.604	6.631	0.473
1150	1141	3.399	7.071	1.223

Glass LAW-ORP-LD1-2

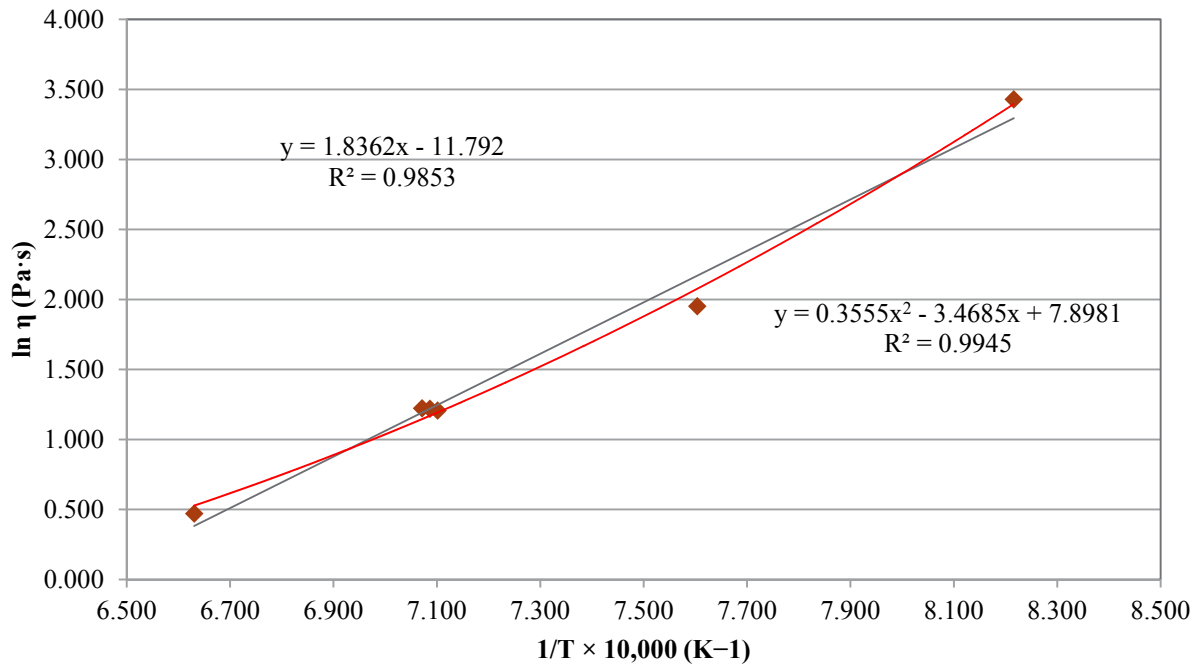


Figure B.35. Viscosity-Temperature Data and Arrhenius Equation Fit for Glass LAW-ORP-LD1-2

B.36 Glass LAW-ORP-LD1-3 Viscosity Data

Table B.36. Viscosity Data for Glass LAW-ORP-LD1-3

Setpoint, °C	Measured Temp., °C	Viscosity, Pa·s	$1/(T+273.15) \times 10,000, K^{-1}$	$\ln \eta, Pa \cdot s$
1150	1130	5.310	7.127	1.670
1050	1037	14.468	7.633	2.672
950	--	--	--	--
1150	1130	5.335	7.127	1.674
1250	1226	2.810	6.670	1.033
1150	1135	5.381	7.102	1.683

Glass LAW-ORP-LD1-3

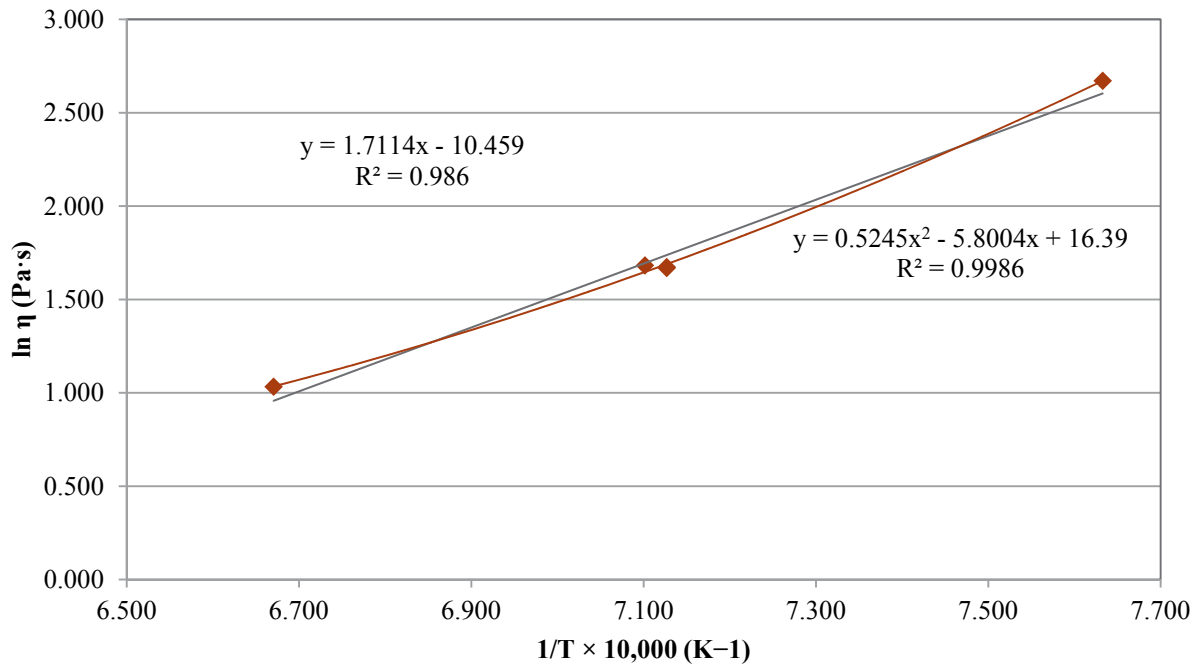


Figure B.36. Viscosity-Temperature Data and Arrhenius Equation Fit for Glass LAW-ORP-LD1-3

Appendix C

Electrical Conductivity Data

Appendix C

Electrical Conductivity Data

This appendix contains the measured electrical conductivity data for each of the glasses in this matrix.

The plots shown in this appendix are fitted to the Arrhenius equation, which is shown below:

$$\ln(\epsilon) = A + \frac{B}{T_K} \quad (\text{C.1})$$

where A and B are independent of temperature and temperature (T_K) is in K ($T(^{\circ}\text{C}) + 273.15$). However, some of the plots showed curvature and would be better fit to the Vogel -Fulcher-Tamman (VFT) model:

$$\ln(\epsilon) = E + \frac{F}{T_K - T_0} \quad (\text{C.2})$$

where E , F , and T_0 are temperature independent and composition dependent coefficients and T_K is in $^{\circ}\text{K}$ ($T(^{\circ}\text{C}) + 273.15$). The intent of the figures and Arrhenius equation fits shown in this appendix are mainly to assess trends of the data and provide some observations about whether there may be sufficient curvature in the data to consider VFT fits in the subsequent work that will decide between fitting the data to the Arrhenius or VFT equations for the electrical conductivity-temperature data for each glass that is being made.

There does appear to be some indication of possible small curvature in some of the electrical conductivity plots because the middle data points are slightly above the fitted line, and end points are slightly below the fitted line. The curvature is still slight but the Arrhenius equation may not be adequate for all glasses. For the glasses with the largest curvature, the curved fit is also shown in the plots.

C.1 Glass New-IL-456 Electrical Conductivity Data

Table C.1. Electrical Conductivity Data for Glass New-IL-456

Temperature, °C	Conductivity, S/m	$1/(T+273.15), K^{-1}$	$\ln \epsilon$ (S/m)
1237	46.16	0.00066	3.83
1139	34.65	0.00071	3.55
1139	34.63	0.00071	3.54
1040	23.61	0.00076	3.16
940	14.05	0.00082	2.64

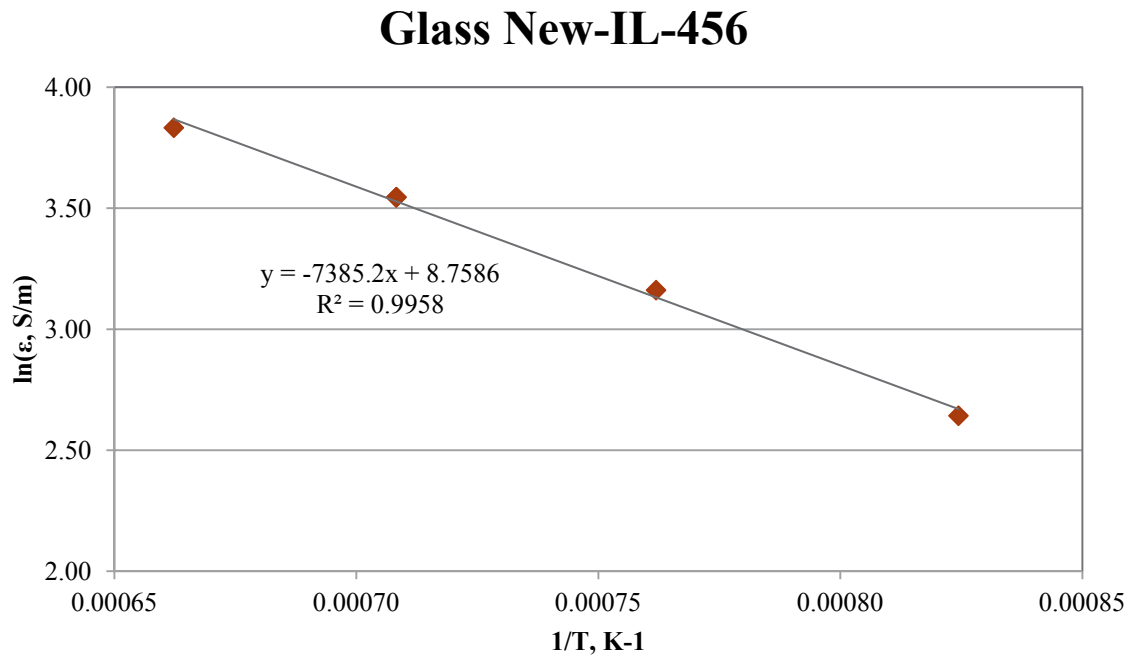


Figure C.1. Electrical Conductivity-Temperature Data and Arrhenius Equation Fit for Glass New-IL-456

C.2 Glass New-IL-1721 Electrical Conductivity Data

Table C.2. Electrical Conductivity Data for Glass New-IL-1721

Temperature, °C	Conductivity, S/m	1/(T+273.15), K ⁻¹	ln(ε, S/m)
1237	49.39	0.00066	3.90
1139	38.72	0.00071	3.66
1139	38.69	0.00071	3.66
1040	27.90	0.00076	3.33
941	18.21	0.00082	2.90
941	18.19	0.00082	2.90

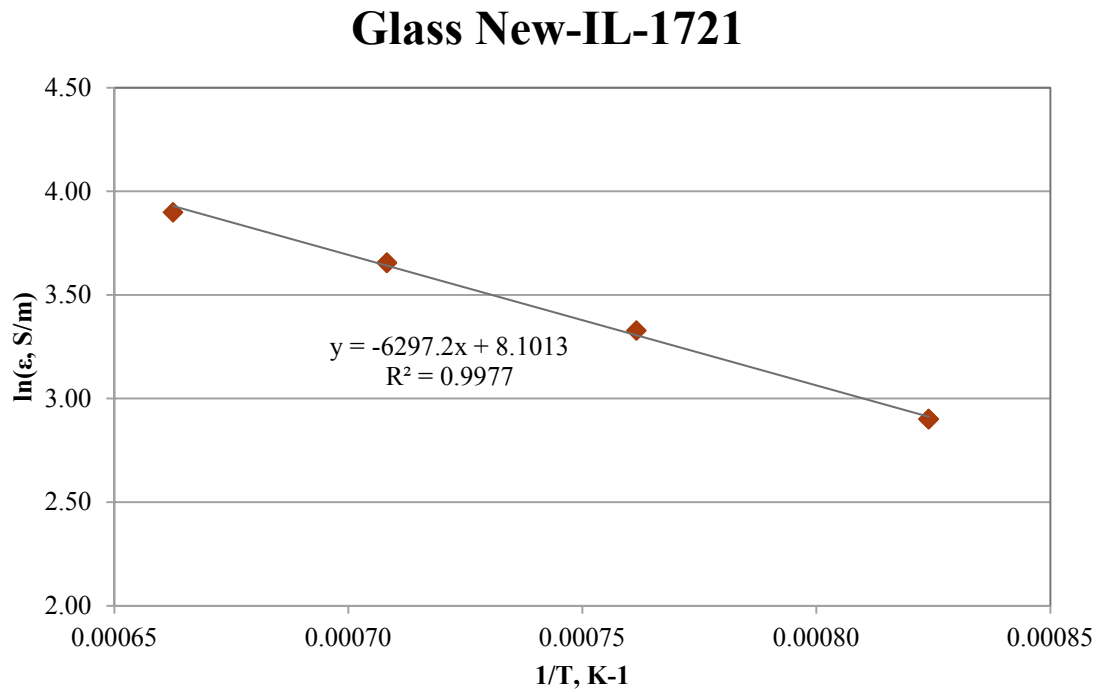


Figure C.2. Electrical Conductivity -Temperature Data and Arrhenius Equation Fit for Glass New-IL-1721

C.3 Glass New-IL-5253 Electrical Conductivity Data

Table C.3. Electrical Conductivity Data for Glass New-IL-5253

Temperature, °C	Conductivity, S/m	1/(T+273.15), K ⁻¹	ln(ε, S/m)
1236	46.03	0.00066	3.83
1139	36.29	0.00071	3.59
1041	26.08	0.00076	3.26
941	16.55	0.00082	2.81
941	16.56	0.00082	2.81

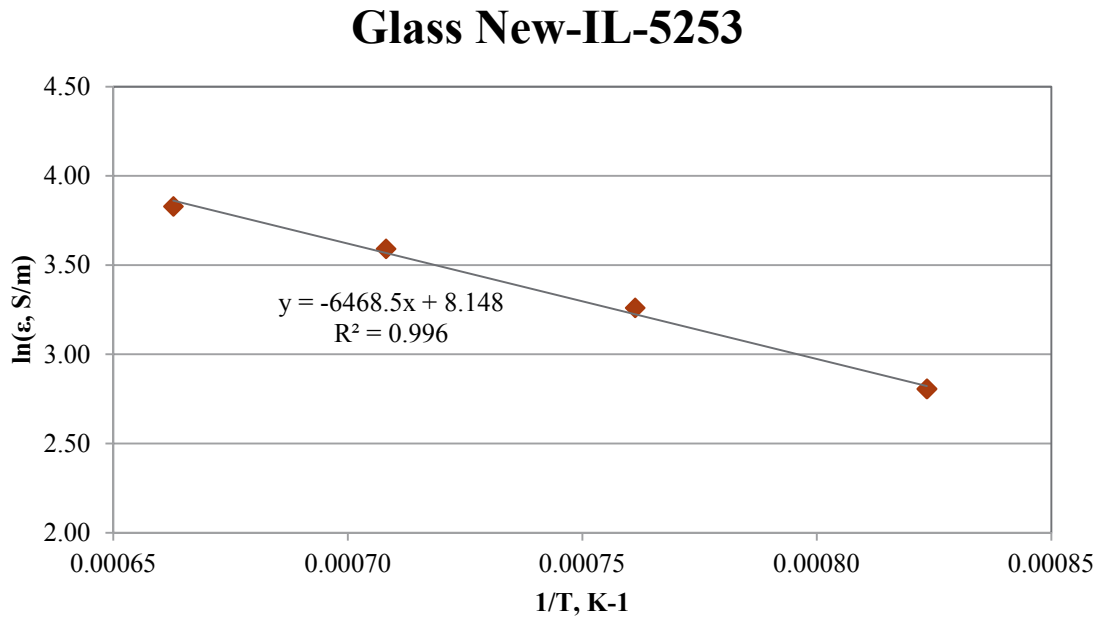


Figure C.3. Electrical Conductivity -Temperature Data and Arrhenius Equation Fit for Glass - New IL-5253

C.4 Glass New-IL-5255 Electrical Conductivity Data

Table C.4. Electrical Conductivity Data for Glass New-IL-5255

Temperature, °C	Conductivity, S/m	1/(T+273.15), K ⁻¹	ln(ϵ , S/m)
1236	60.42	0.00066	4.10
1140	48.77	0.00071	3.89
1040	36.50	0.00076	3.60
941	24.52	0.00082	3.20
941	24.53	0.00082	3.20

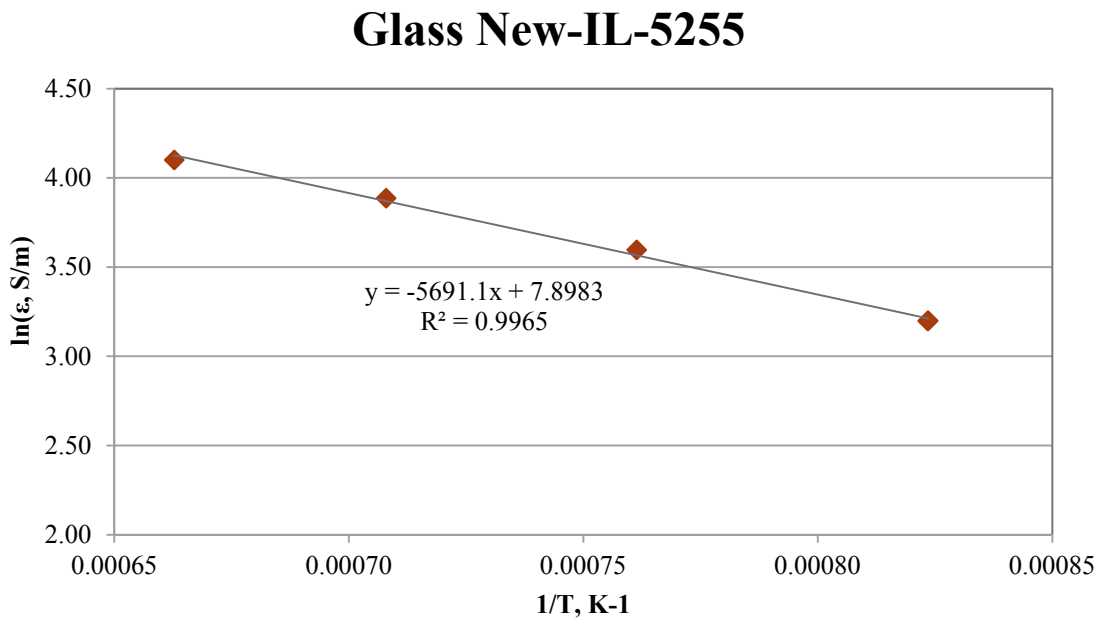


Figure C.4. Electrical Conductivity -Temperature Data and Arrhenius Equation Fit for Glass New-IL-5255

C.5 Glass New-IL-42295 Electrical Conductivity Data

Table C.5. Electrical Conductivity Data for Glass New-IL-42295

Temperature, °C	Conductivity, S/m	1/(T+273.15), K ⁻¹	ln(ε, S/m)
1237	55.75	0.00066	4.02
1237	55.74	0.00066	4.02
1140	44.51	0.00071	3.80
1140	44.49	0.00071	3.80
1041	33.02	0.00076	3.50
942	21.96	0.00082	3.09
942	21.96	0.00082	3.09

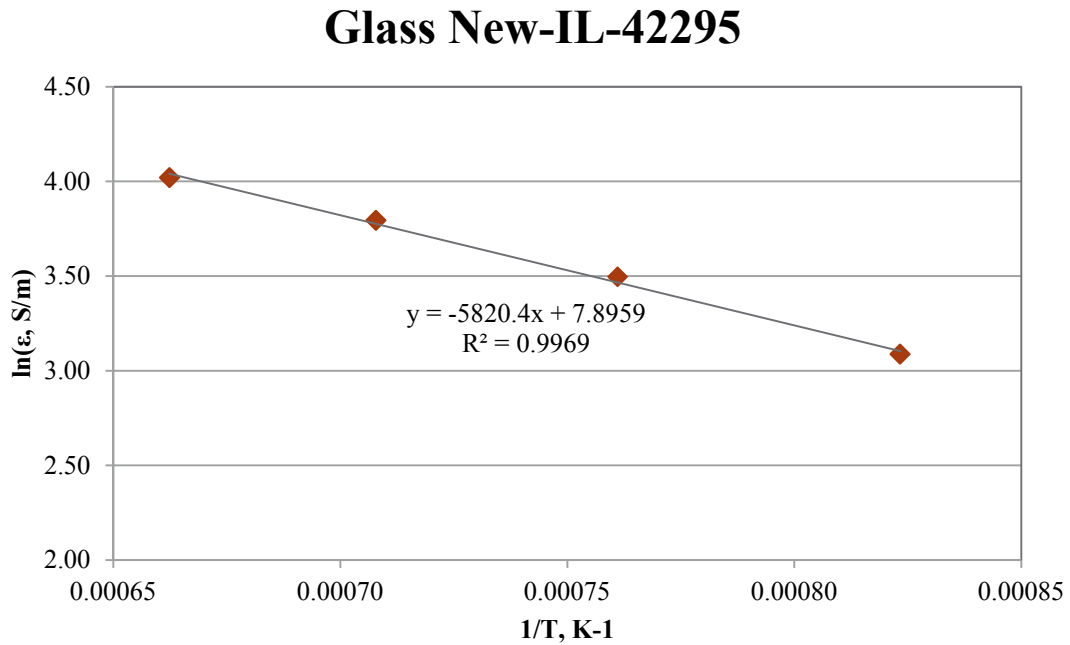


Figure C.5. Electrical Conductivity -Temperature Data and Arrhenius Equation Fit for Glass New-IL-42295

C.6 Glass New-IL-70316 Electrical Conductivity Data

Table C.6. Electrical Conductivity Data for Glass New-IL-70316

Temperature, °C	Conductivity, S/m	1/(T+273.15), K ⁻¹	ln(ε, S/m)
1239	48.74	0.00066	3.89
1239	48.81	0.00066	3.89
1141	38.00	0.00071	3.64
1042	27.08	0.00076	3.30
1042	27.08	0.00076	3.30
943	17.26	0.00082	2.85
943	17.26	0.00082	2.85

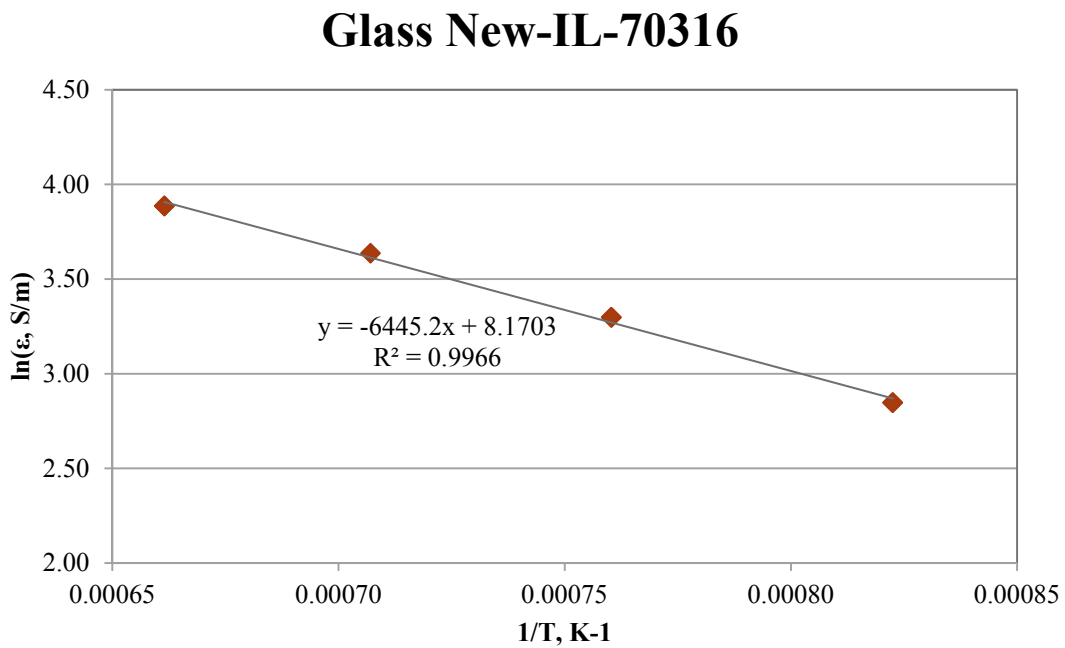


Figure C.6. Electrical Conductivity -Temperature Data and Arrhenius Equation Fit for Glass New-IL-70316

C.7 Glass New-IL-87749 Electrical Conductivity Data

Table C.7. Electrical Conductivity Data for Glass New-IL-87749

Temperature, °C	Conductivity, S/m	$1/(T+273.15), K^{-1}$	$\ln(\epsilon, S/m)$
1237	51.15	0.00066	3.93
1140	40.40	0.00071	3.70
1140	40.42	0.00071	3.70
1041	28.97	0.00076	3.37
942	18.48	0.00082	2.92

Glass New-IL-87749

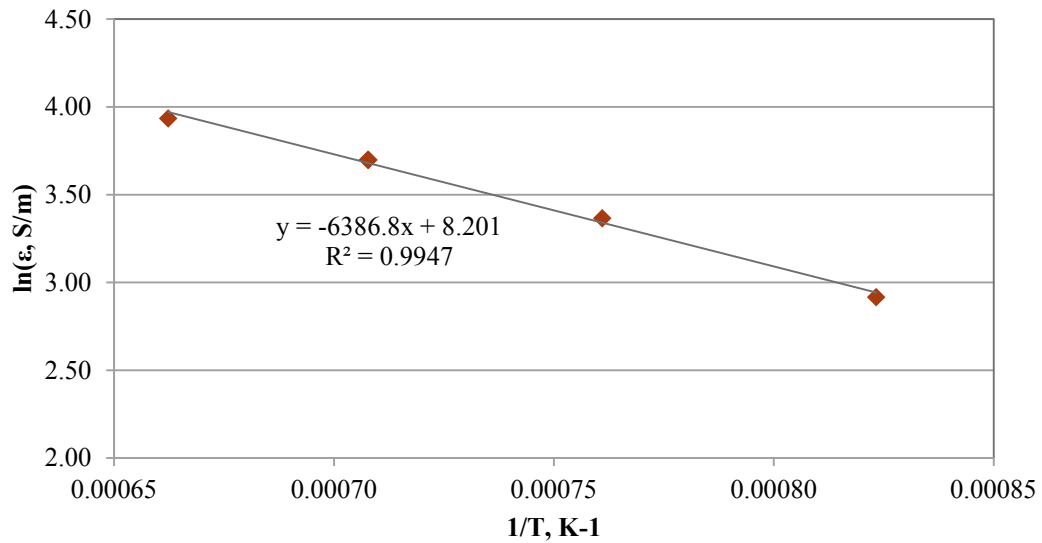


Figure C.7. Electrical Conductivity -Temperature Data and Arrhenius Equation Fit for Glass New-IL-87749

C.8 Glass New-IL-93907 Electrical Conductivity Data

Table C.8. Electrical Conductivity Data for Glass New-IL-93907

Temperature, °C	Conductivity, S/m	1/(T+273.15), K ⁻¹	ln(ε, S/m)
1236	42.94	0.00066	3.76
1138	33.05	0.00071	3.50
1138	32.99	0.00071	3.50
1040	23.24	0.00076	3.15
940	14.52	0.00082	2.68
940	14.49	0.00082	2.67

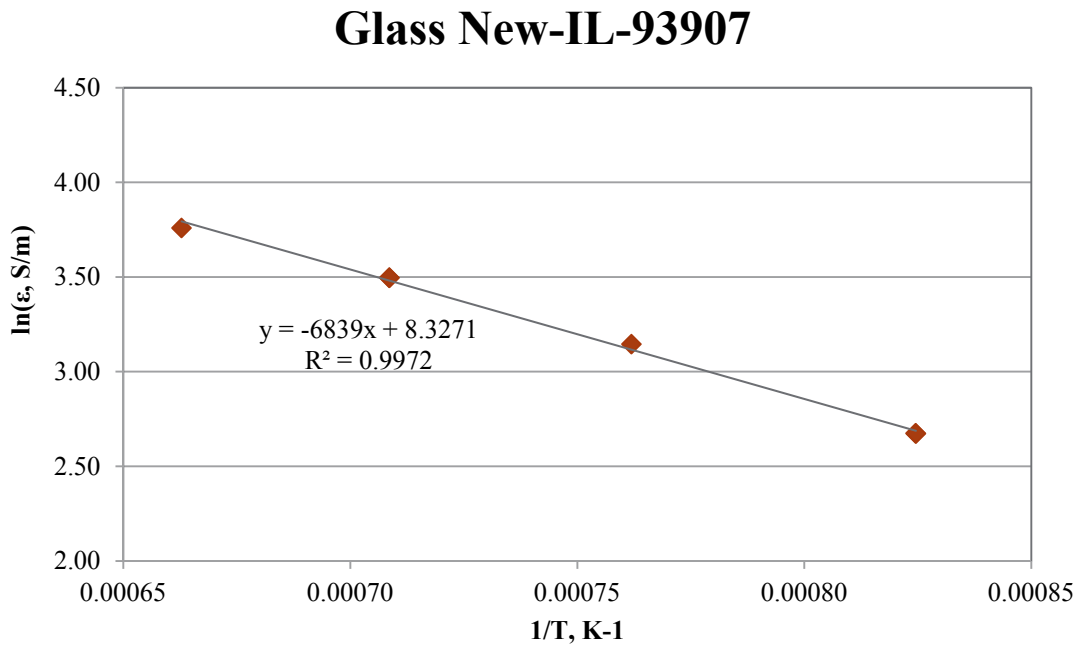


Figure C.8. Electrical Conductivity -Temperature Data and Arrhenius Equation Fit for Glass New-IL-93907

C.9 Glass New-IL-94020 Electrical Conductivity Data

Table C.9. Electrical Conductivity Data for Glass New-IL-94020

Temperature, °C	Conductivity, S/m	$1/(T+273.15), K^{-1}$	$\ln(\epsilon, S/m)$
1236	9.76	0.00066	2.28
1040	5.19	0.00076	1.65
941	7.14	0.00082	1.14

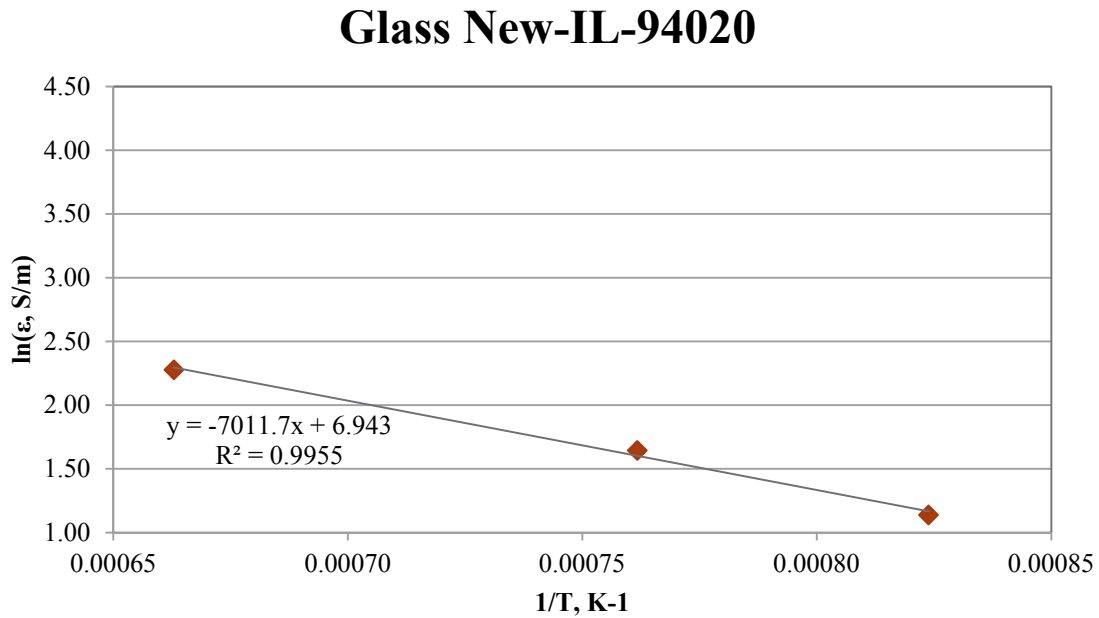


Figure C.9. Electrical Conductivity -Temperature Data and Arrhenius Equation Fit for Glass New-IL-94020

C.10 Glass New-IL-103151 Electrical Conductivity Data

Table C.10. Electrical Conductivity Data for Glass New-IL-103151

Temperature, °C	Conductivity, S/m	1/(T+273.15), K ⁻¹	ln(ϵ , S/m)
1237	55.37	0.00066	4.01
1237	55.42	0.00066	4.01
1139	44.88	0.00071	3.80
1041	34.08	0.00076	3.53
1041	34.08	0.00076	3.53
941	23.58	0.00082	3.16
941	23.60	0.00082	3.16

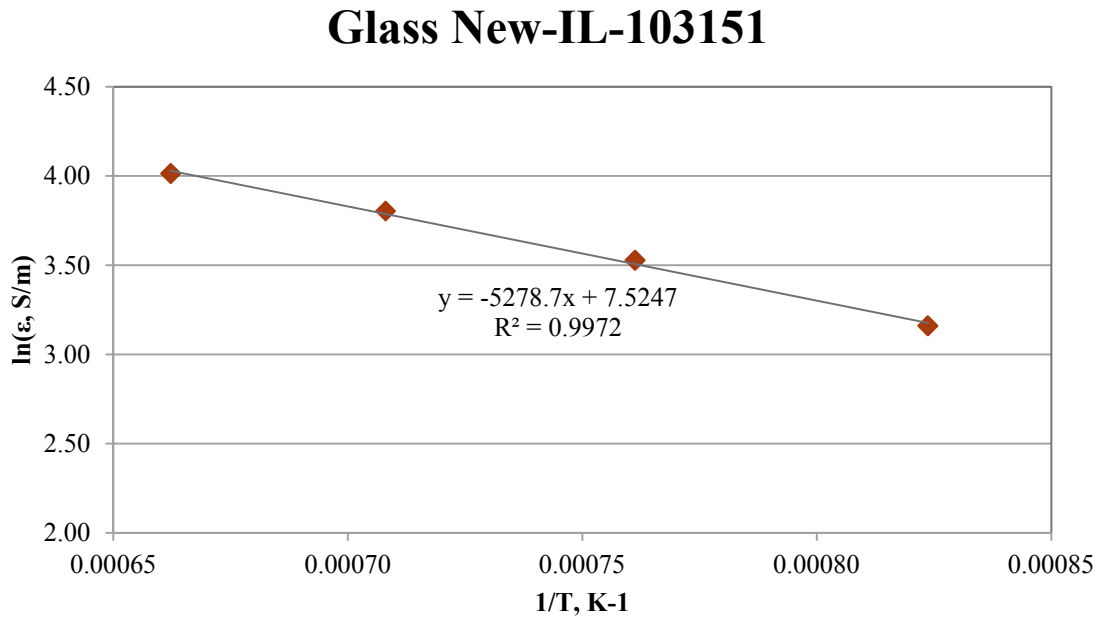


Figure C.10. Electrical Conductivity -Temperature Data and Arrhenius Equation Fit for Glass New-IL-103151

C.11 Glass New-IL-151542 Electrical Conductivity Data

Table C.11. Electrical Conductivity Data for Glass New-IL-151542

Temperature, °C	Conductivity, S/m	$1/(T+273.15), K^{-1}$	$\ln(\epsilon, S/m)$
1237	38.90	0.00066	3.66
1140	29.08	0.00071	3.37
1041	19.78	0.00076	2.98
1041	19.79	0.00076	2.99
942	11.87	0.00082	2.47
942	11.86	0.00082	2.47

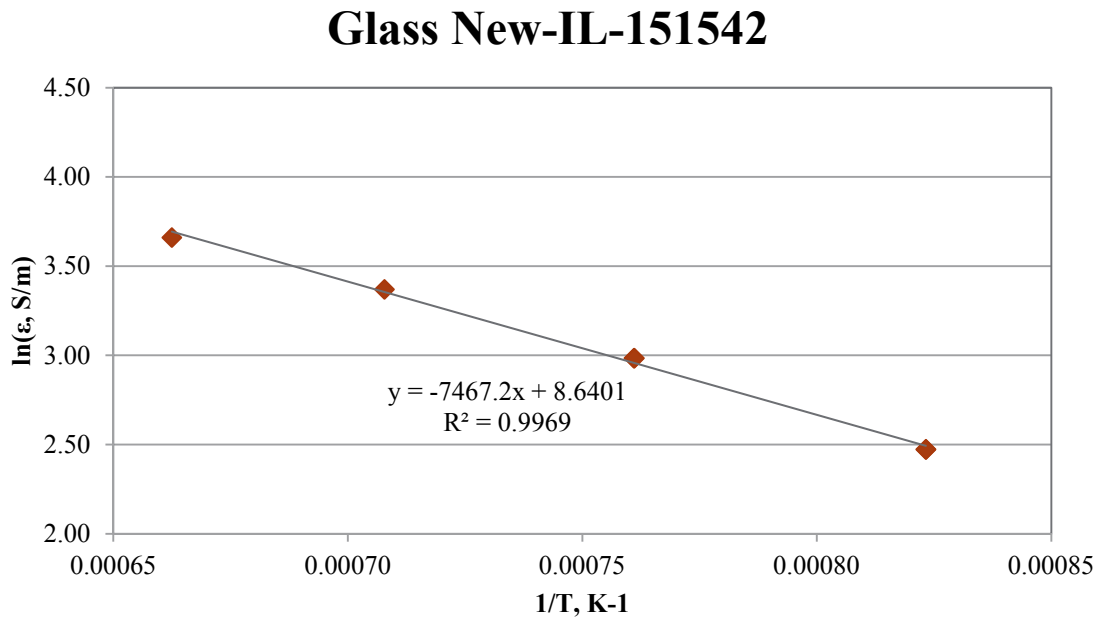


Figure C.11. Electrical Conductivity -Temperature Data and Arrhenius Equation Fit for Glass New-IL-151542

C.12 Glass New-IL-166697 Electrical Conductivity Data

Table C.12. Electrical Conductivity Data for Glass New-IL-166697

Temperature, °C	Conductivity, S/m	$1/(T+273.15), K^{-1}$	$\ln(\epsilon, S/m)$
1236	58.72	0.00066	4.07
1139	47.32	0.00071	3.86
1040	35.33	0.00076	3.56
942	23.97	0.00082	3.18
941	23.96	0.00082	3.18

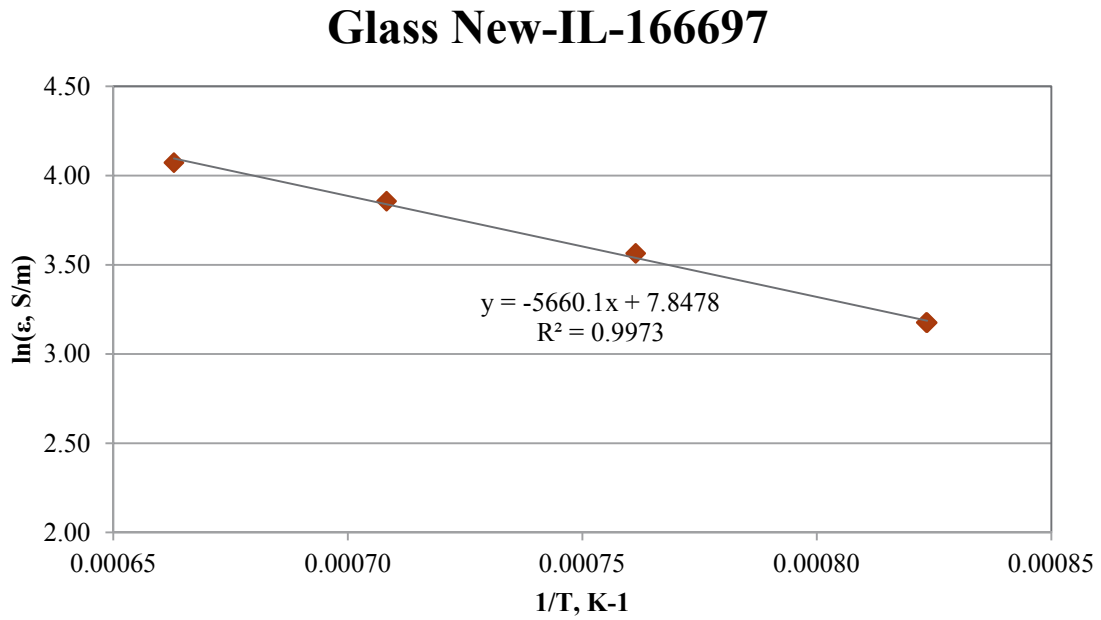


Figure C.12. Electrical Conductivity -Temperature Data and Arrhenius Equation Fit for Glass New-IL-166697

C.13 Glass New-IL-166731 Electrical Conductivity Data

Table C.13. Electrical Conductivity Data for Glass New-IL-166731

Temperature, °C	Conductivity, S/m	1/(T+273.15), K ⁻¹	ln(ε, S/m)
1235	54.88	0.00066	4.01
1235	54.81	0.00066	4.00
1138	43.91	0.00071	3.78
1138	43.95	0.00071	3.78
1038	32.43	0.00076	3.48
932	21.56	0.00083	3.07
932	21.57	0.00083	3.07

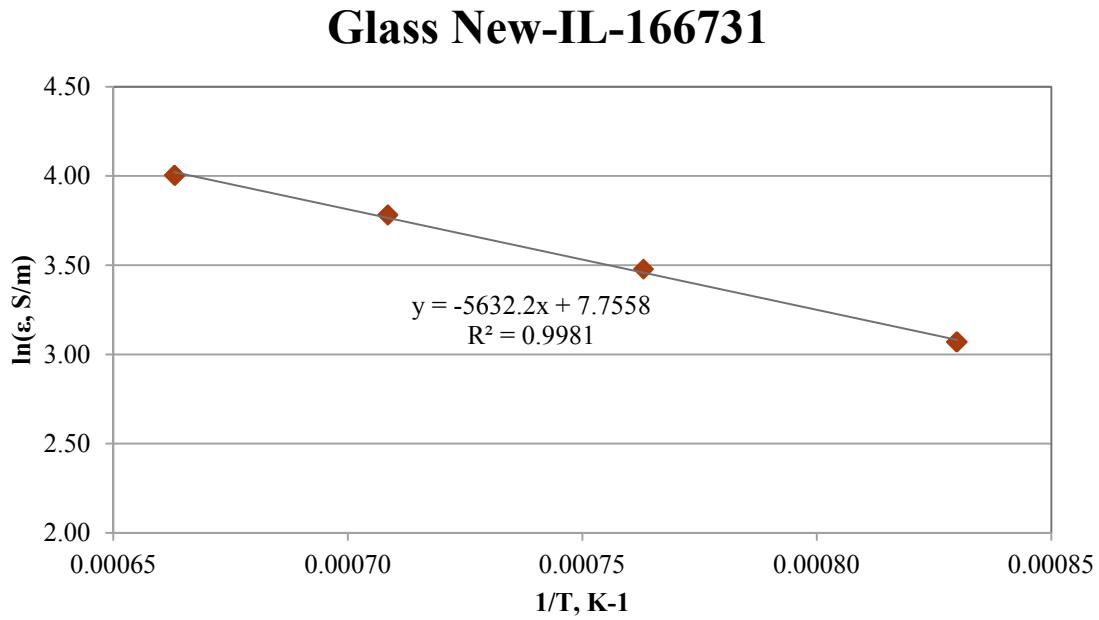


Figure C.13. Electrical Conductivity -Temperature Data and Arrhenius Equation Fit for Glass New-IL-166731

C.14 Glass New-OL-8445 Electrical Conductivity Data

Table C.14. Electrical Conductivity Data for Glass New-OL-8445

Temperature, °C	Conductivity, S/m	1/(T+273.15), K ⁻¹	ln(ϵ , S/m)
1237	22.63	0.00066	3.12
1237	22.62	0.00066	3.12
1139	14.85	0.00071	2.70
1040	8.48	0.00076	2.14
941	4.10	0.00082	1.41
941	4.10	0.00082	1.41

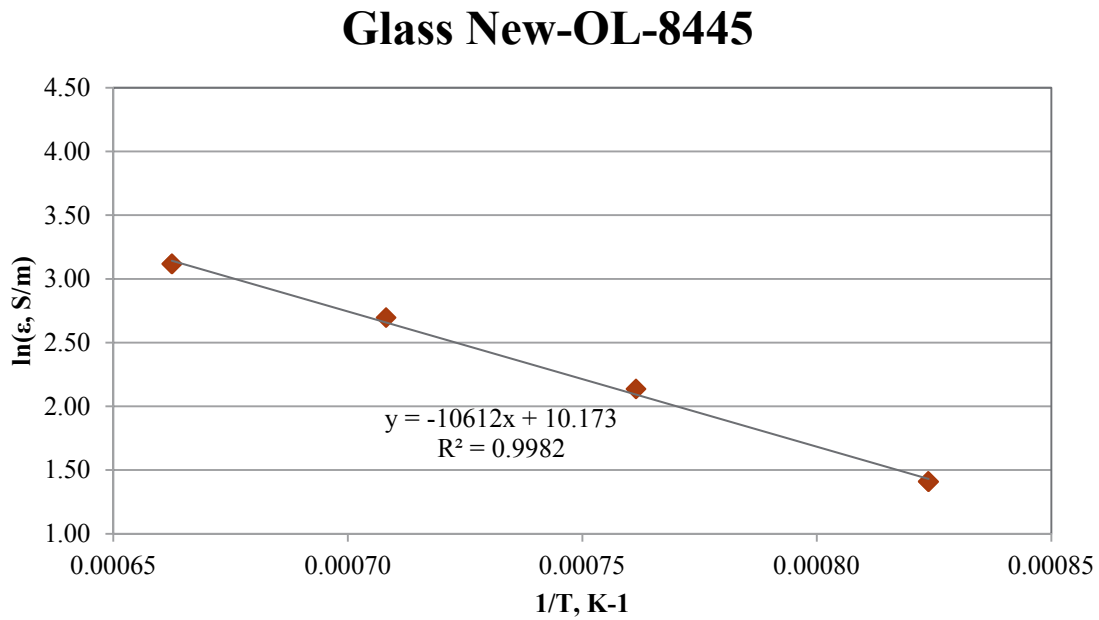


Figure C.14. Electrical Conductivity -Temperature Data and Arrhenius Equation Fit for Glass New-OL-8445

C.15 Glass New-OL-8788(Mod) Electrical Conductivity Data

Table C.15. Electrical Conductivity Data for Glass New-OL-8788(Mod)

Temperature, °C	Conductivity, S/m	1/(T+273.15), K ⁻¹	ln(ϵ , S/m)
1237	24.14	0.00066	3.18
1237	24.15	0.00066	3.18
1139	17.82	0.00071	2.88
1139	17.81	0.00071	2.88
1041	12.33	0.00076	2.51
942	7.59	0.00082	2.03
942	7.57	0.00082	2.02

Glass New-OL-8788(Mod)

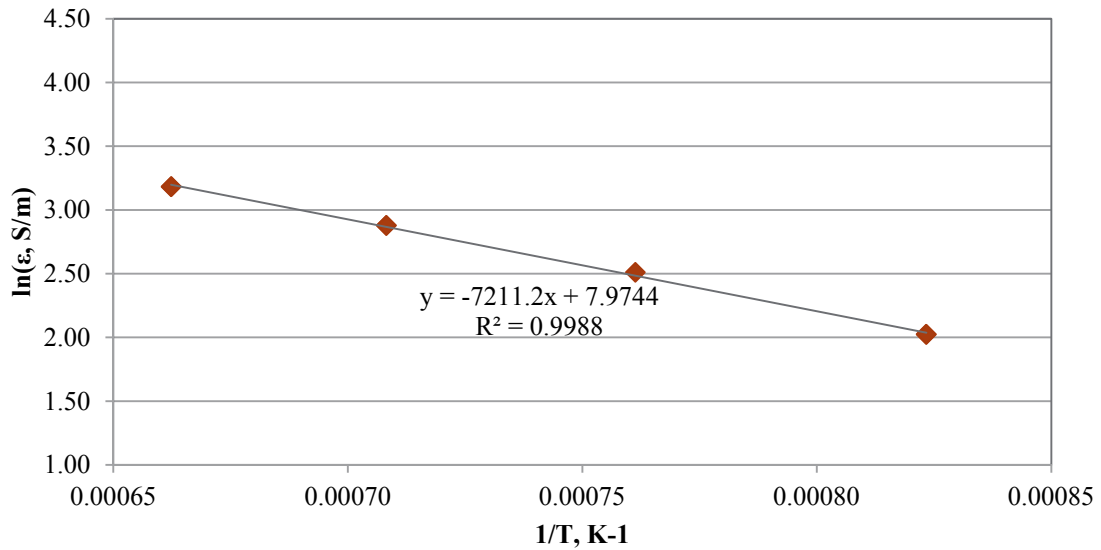


Figure C.15. Electrical Conductivity -Temperature Data and Arrhenius Equation Fit for Glass New-OL-8788(Mod)

C.16 Glass New-OL-14844 Electrical Conductivity Data

Table C.16. Electrical Conductivity Data for Glass New-OL-14844

Temperature, °C	Conductivity, S/m	$1/(T+273.15), K^{-1}$	$\ln(\epsilon, S/m)$
1236	66.22	0.00066	4.19
1140	52.18	0.00071	3.95
1042	40.84	0.00076	3.71
1042	40.82	0.00076	3.71
942	28.04	0.00082	3.33
942	28.02	0.00082	3.33

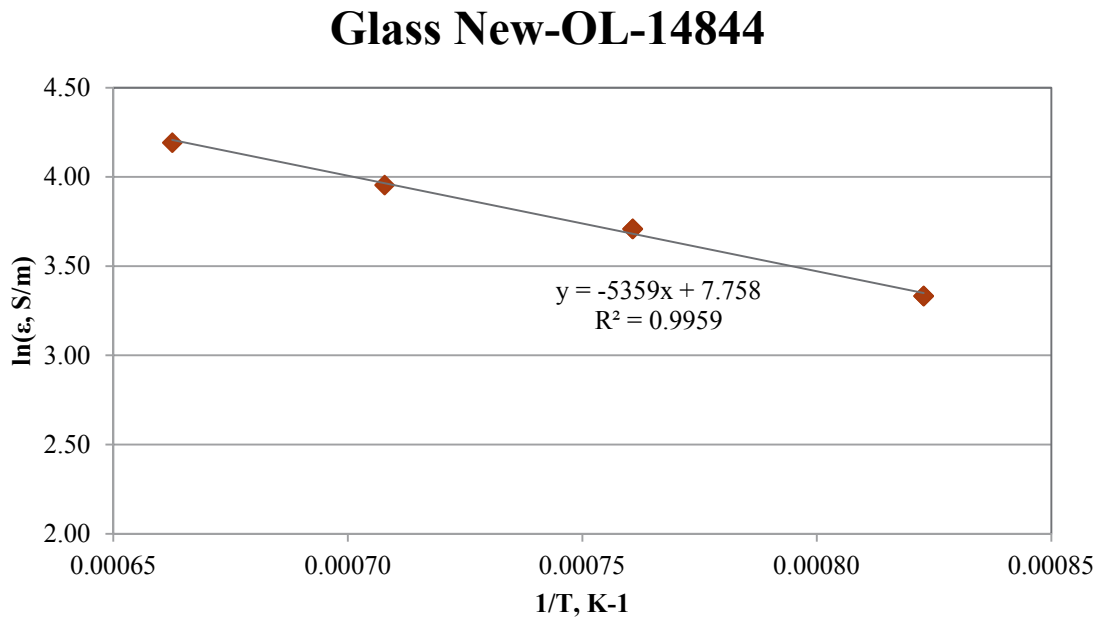


Figure C.16. Electrical Conductivity -Temperature Data and Arrhenius Equation Fit for Glass New-OL-14844

C.17 Glass New-OL-15493 Electrical Conductivity Data

Table C.17. Electrical Conductivity Data for Glass New-OL-15493

Temperature, °C	Conductivity, S/m	1/(T+273.15), K ⁻¹	ln(ε, S/m)
1239	67.28	0.00066	4.21
1142	54.57	0.00071	4.00
1043	41.54	0.00076	3.73
1043	41.47	0.00076	3.72
940	22.32	0.00082	3.11
940	22.26	0.00082	3.10

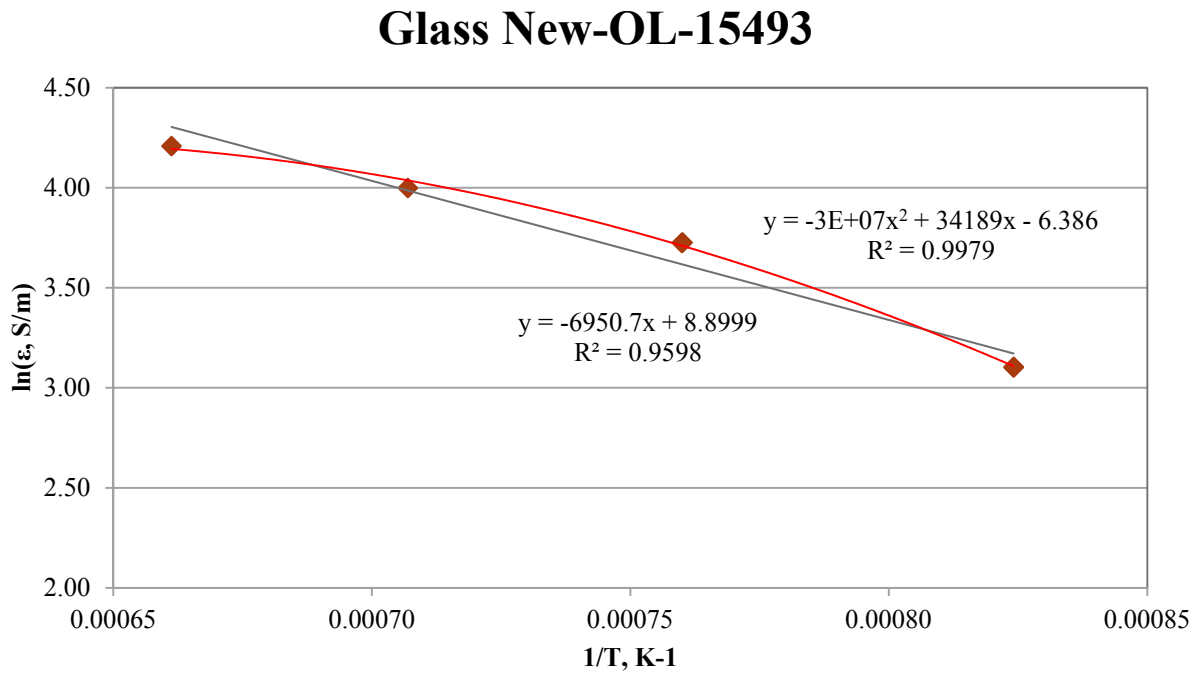


Figure C.17. Electrical Conductivity -Temperature Data and Arrhenius Equation Fit for Glass New-OL-15493

C.18 Glass New-OL-17130 Electrical Conductivity Data

Table C.18. Electrical Conductivity Data for Glass New-OL-17130

Temperature, °C	Conductivity, S/m	1/(T+273.15), K ⁻¹	ln(ϵ , S/m)
1236	59.02	0.00066	4.08
1139	47.45	0.00071	3.86
1040	35.83	0.00076	3.58
1040	35.82	0.00076	3.58
940	24.59	0.00082	3.20
940	24.60	0.00082	3.20

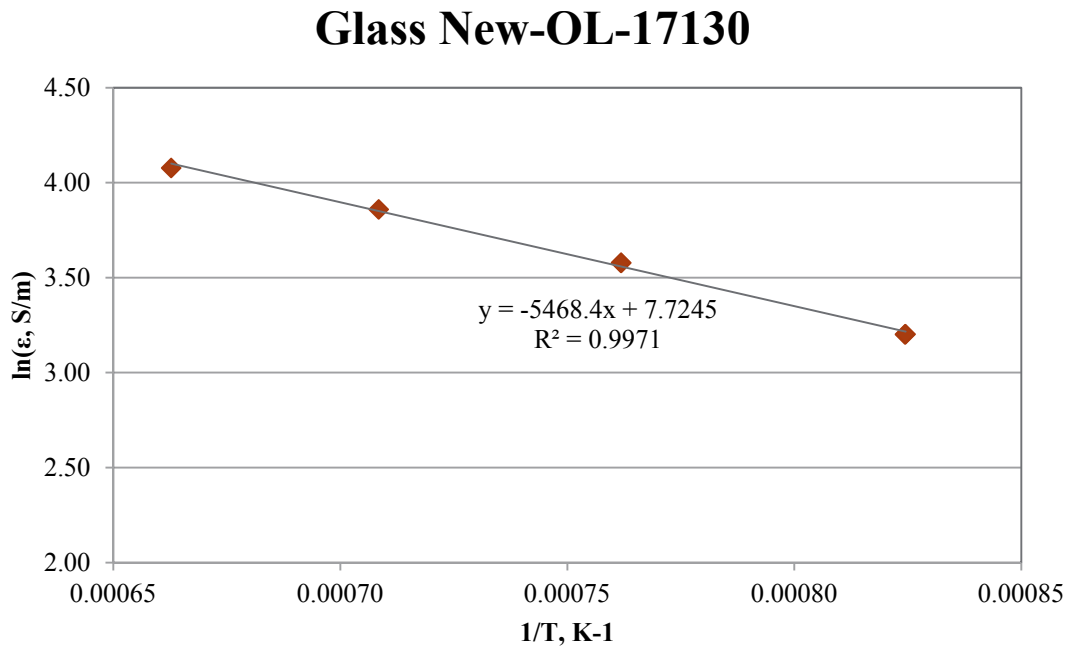


Figure C.18. Electrical Conductivity -Temperature Data and Arrhenius Equation Fit for Glass New-OL-17130

C.19 Glass New-OL-45748 (with Tin Oxalate) Electrical Conductivity Data

Table C.19. Electrical Conductivity Data for Glass New-OL-45748 (with tin oxalate)

Temperature, °C	Conductivity, S/m	1/(T+273.15), K ⁻¹	ln(ε, S/m)
1230	44.08	0.00067	3.79
1230	42.43	0.00067	3.75
1134	37.85	0.00071	3.63
1036	27.19	0.00076	3.30
1036	27.20	0.00076	3.30
938	17.05	0.00083	2.84
937	17.06	0.00083	2.84

Glass New-OL-45748 (with Tin Oxalate)

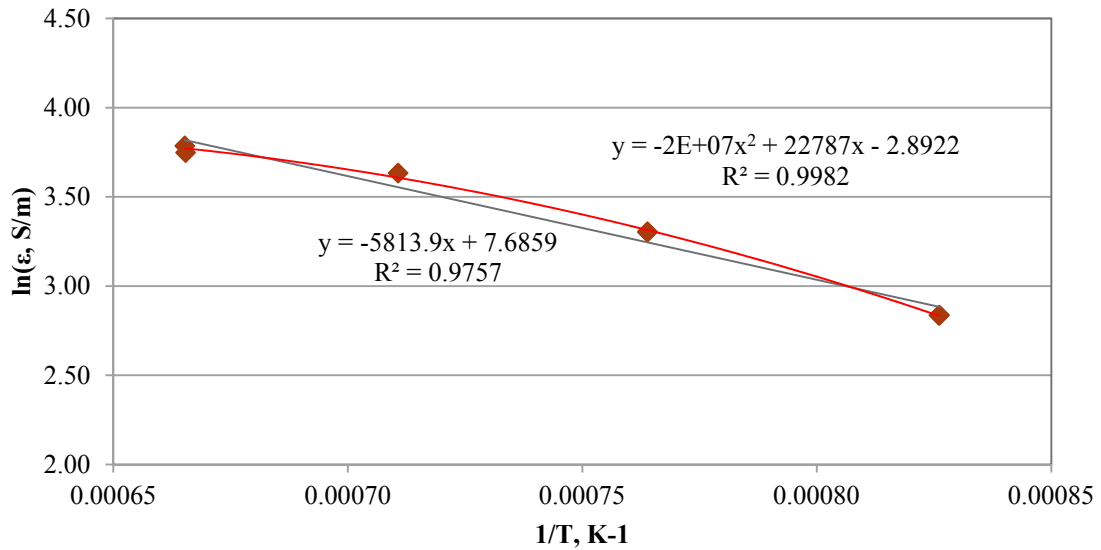


Figure C.19. Electrical Conductivity -Temperature Data and Arrhenius Equation Fit for Glass New-OL-45748 (with tin oxalate)

C.20 Glass New-OL-54017 (with tin oxalate) Electrical Conductivity Data

Table C.20. Electrical Conductivity Data for Glass New-OL-54017 (with tin oxalate)

Temperature, °C	Conductivity, S/m	1/(T+273.15), K ⁻¹	ln(ε, S/m)
1236	27.69	0.00066	3.32
1236	27.68	0.00066	3.32
1139	19.01	0.00071	2.95
1139	19.04	0.00071	2.95
1041	11.66	0.00076	2.46
1041	11.65	0.00076	2.46
942	6.12	0.00082	1.81
942	6.11	0.00082	1.81

Glass New-OL-54017 (with Tin Oxalate)

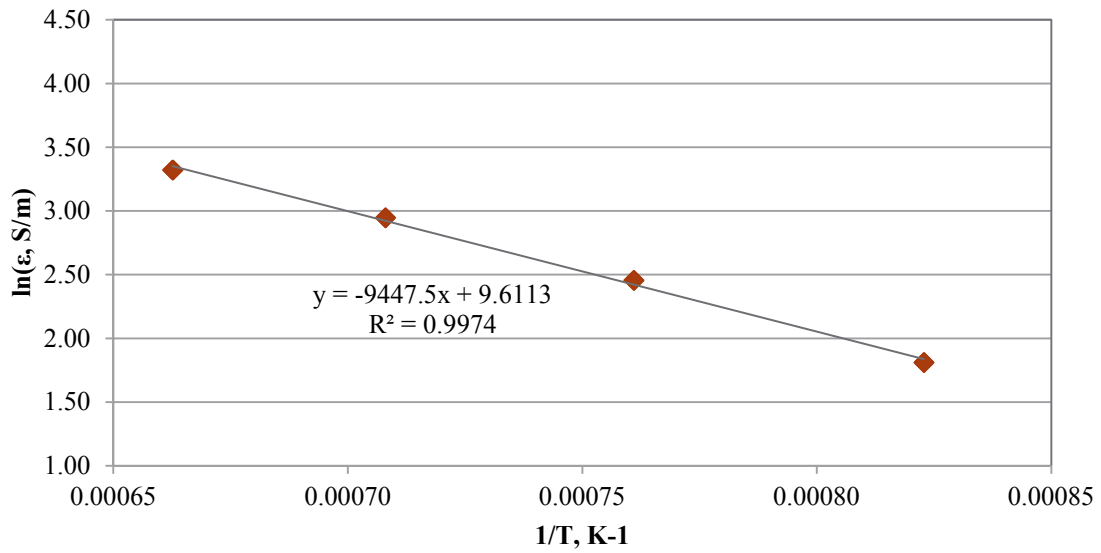


Figure C.20. Electrical Conductivity -Temperature Data and Arrhenius Equation Fit for Glass New-OL-54017 (with tin oxalate)

C.21 Glass New-OL-57284 Electrical Conductivity Data

Table C.21. Electrical Conductivity Data for Glass New-OL-57284

Temperature, °C	Conductivity, S/m	1/(T+273.15), K ⁻¹	ln(ϵ , S/m)
1239	20.08	0.00066	3.00
1238	20.03	0.00066	3.00
1141	14.68	0.00071	2.69
1043	9.78	0.00076	2.28
1043	9.79	0.00076	2.28
944	5.69	0.00082	1.74
944	5.70	0.00082	1.74

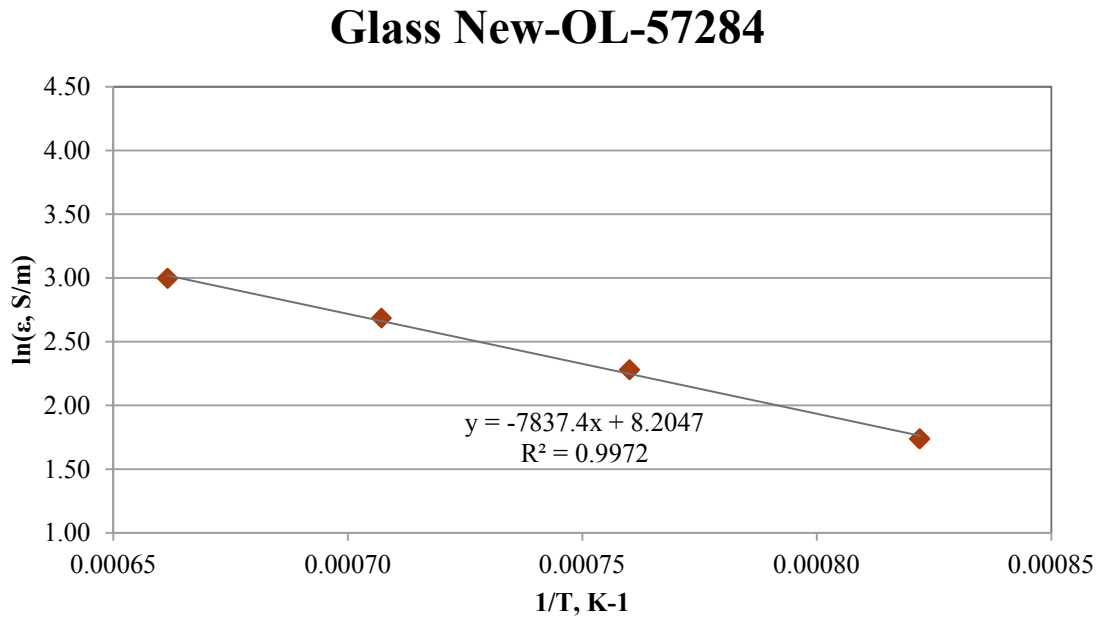


Figure C.21. Electrical Conductivity -Temperature Data and Arrhenius Equation Fit for Glass New-OL-57284

C.22 Glass New-OL-62380 Electrical Conductivity Data

Table C.22. Electrical Conductivity Data for Glass New-OL-62380

Temperature, °C	Conductivity, S/m	1/(T+273.15), K ⁻¹	ln(σ, S/m)
1238	18.76	0.00066	2.93
1141	15.60	0.00071	2.75
1141	15.56	0.00071	2.74
1042	10.31	0.00076	2.33
1042	10.31	0.00076	2.33
943	5.49	0.00082	1.70
943	5.50	0.00082	1.70

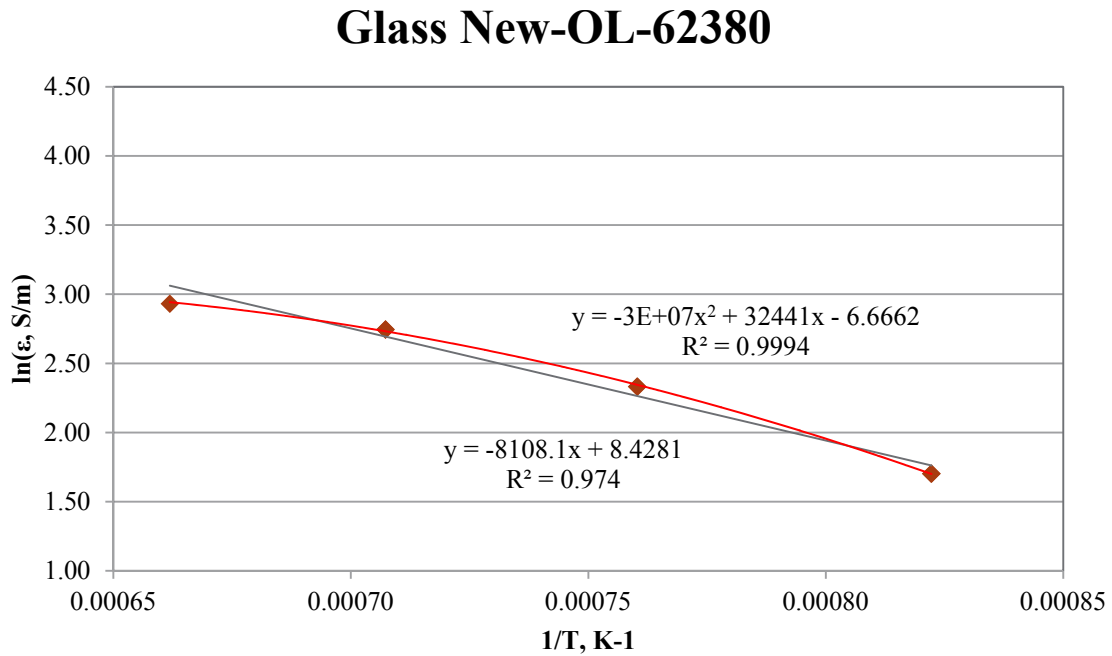


Figure C.22. Electrical Conductivity -Temperature Data and Arrhenius Equation Fit for Glass New-OL-62380

C.23 Glass New-OL-62909(Mod) Electrical Conductivity Data

Table C.23. Electrical Conductivity Data for Glass New-OL-62909(Mod)

Temperature, °C	Conductivity, S/m	1/(T+273.15), K ⁻¹	ln(ε, S/m)
1233	33.65	0.00066	3.52
1136	23.23	0.00071	3.15
1136	23.22	0.00071	3.15
1038	14.17	0.00076	2.65
1038	14.18	0.00076	2.65
939	7.39	0.00083	2.00
939	7.40	0.00083	2.00

Glass New-OL-62909(Mod)

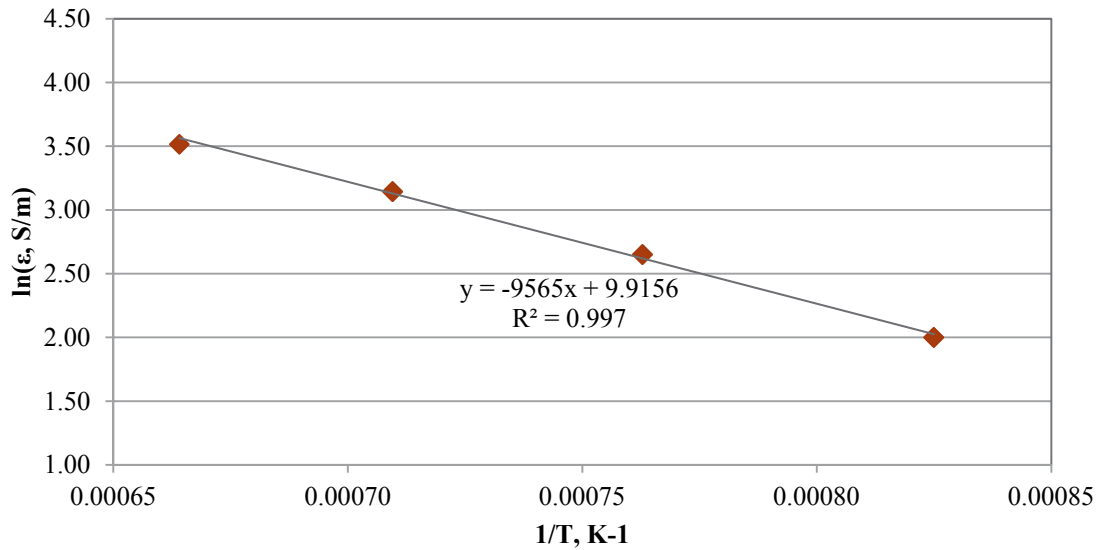


Figure C.23. Electrical Conductivity -Temperature Data and Arrhenius Equation Fit for Glass New-OL-62909(Mod)

C.24 Glass New-OL-65959(Mod) Electrical Conductivity Data

Table C.24. Electrical Conductivity Data for Glass New-OL-65959(Mod)

Temperature, °C	Conductivity, S/m	1/(T+273.15), K ⁻¹	ln(ε, S/m)
1239	54.78	0.00066	4.00
1142	46.27	0.00071	3.83
1142	46.31	0.00071	3.84
1044	36.68	0.00076	3.60
945	24.52	0.00082	3.20
944	24.38	0.00082	3.19

Glass New-OL-65959(Mod)

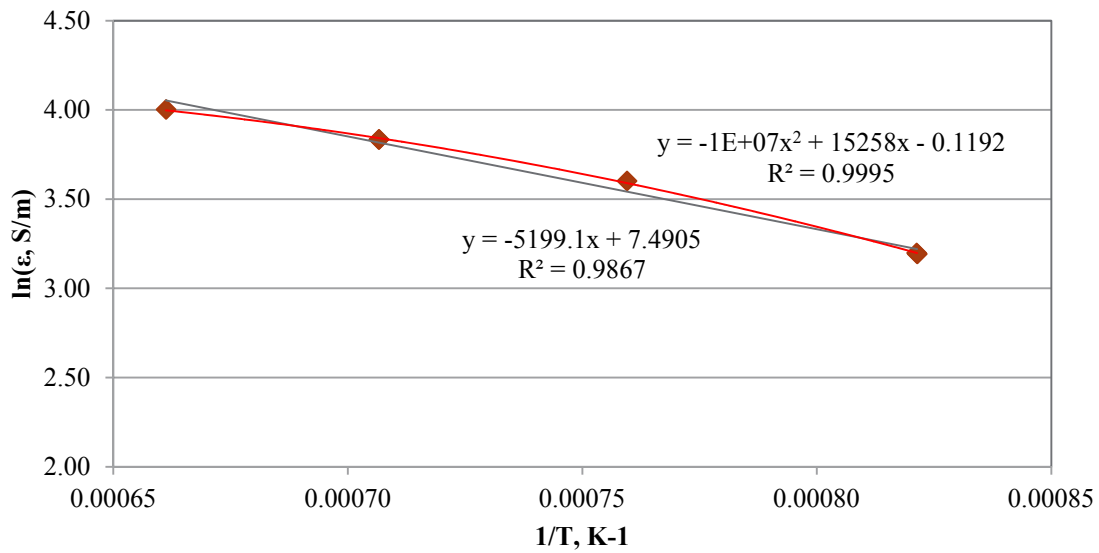


Figure C.24. Electrical Conductivity -Temperature Data and Arrhenius Equation Fit for Glass New-OL-65959(Mod)

C.25 Glass New-OL-80309 Electrical Conductivity Data

Table C.25. Electrical Conductivity Data for Glass New-OL-80309

Temperature, °C	Conductivity, S/m	1/(T+273.15), K ⁻¹	ln(ε, S/m)
1236	48.92	0.00066	3.89
1139	43.26	0.00071	3.77
1041	33.75	0.00076	3.52
1041	33.76	0.00076	3.52
942	23.67	0.00082	3.16
942	23.67	0.00082	3.16

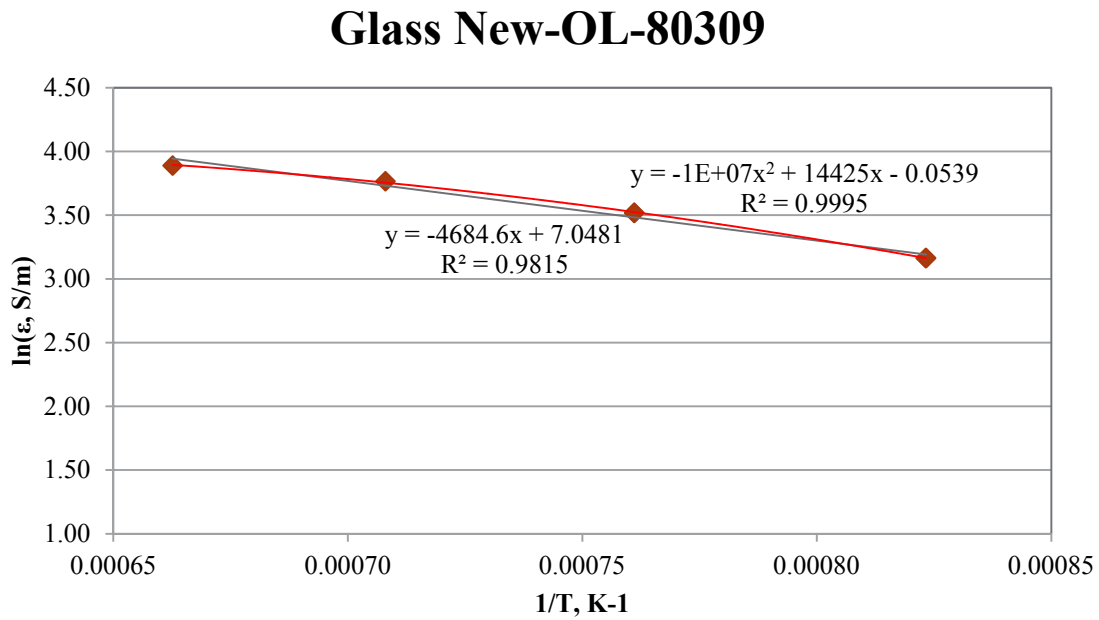


Figure C.25. Electrical Conductivity - Temperature Data and Arrhenius Equation Fit for Glass New-OL-80309

C.26 Glass New-OL-90780 Electrical Conductivity Data

Table C.26. Electrical Conductivity Data for Glass New-OL-90780

Temperature, °C	Conductivity, S/m	$1/(T+273.15), K^{-1}$	$\ln(\epsilon, S/m)$
1232	63.07	0.00067	4.14
1136	51.51	0.00071	3.94
1136	51.58	0.00071	3.94
1038	38.96	0.00076	3.66
939	26.97	0.00083	3.29
939	26.92	0.00083	3.29

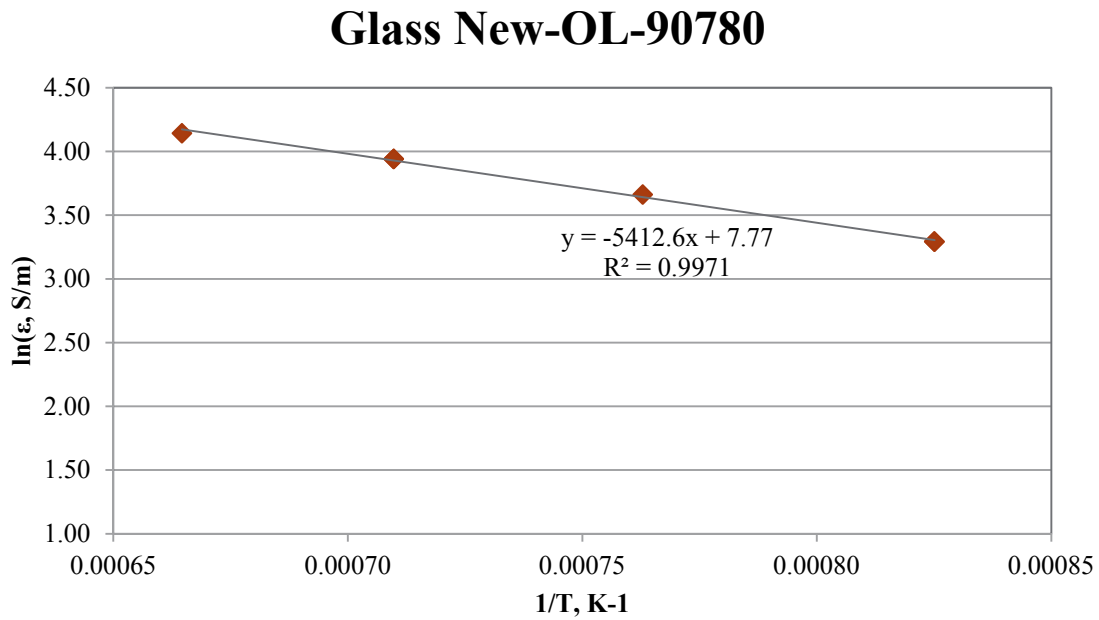


Figure C.26. Electrical Conductivity -Temperature Data and Arrhenius Equation Fit for Glass New-OL-90780

C.27 Glass New-OL-100210 Electrical Conductivity Data

Table C.27. Electrical Conductivity Data for Glass New-OL-100210

Temperature, °C	Conductivity, S/m	$1/(T+273.15), K^{-1}$	$\ln(\epsilon, S/m)$
1237	50.99	0.00066	3.93
1139	43.48	0.00071	3.77
1139	43.53	0.00071	3.77
1041	35.51	0.00076	3.57
1041	35.52	0.00076	3.57
942	26.79	0.00082	3.29
942	26.79	0.00082	3.29

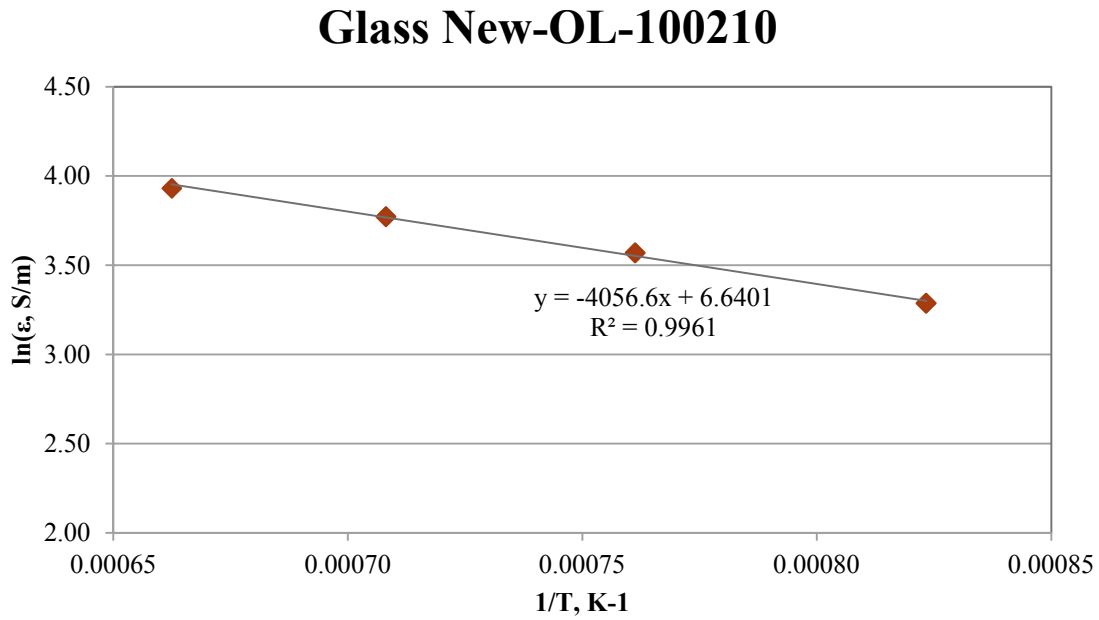


Figure C.27. Electrical Conductivity -Temperature Data and Arrhenius Equation Fit for Glass New-OL-100210

C.28 Glass New-OL-108249 (SO₃ Mod) Electrical Conductivity Data

Table C.28. Electrical Conductivity Data for Glass New-OL-108249 (SO₃ Mod)

Temperature, °C	Conductivity, S/m	1/(T+273.15), K ⁻¹	ln(ϵ , S/m)
1235	48.84	0.00066	3.89
1236	48.85	0.00066	3.89
1140	39.33	0.00071	3.67
1041	29.25	0.00076	3.38
942	19.39	0.00082	2.96
942	19.39	0.00082	2.96

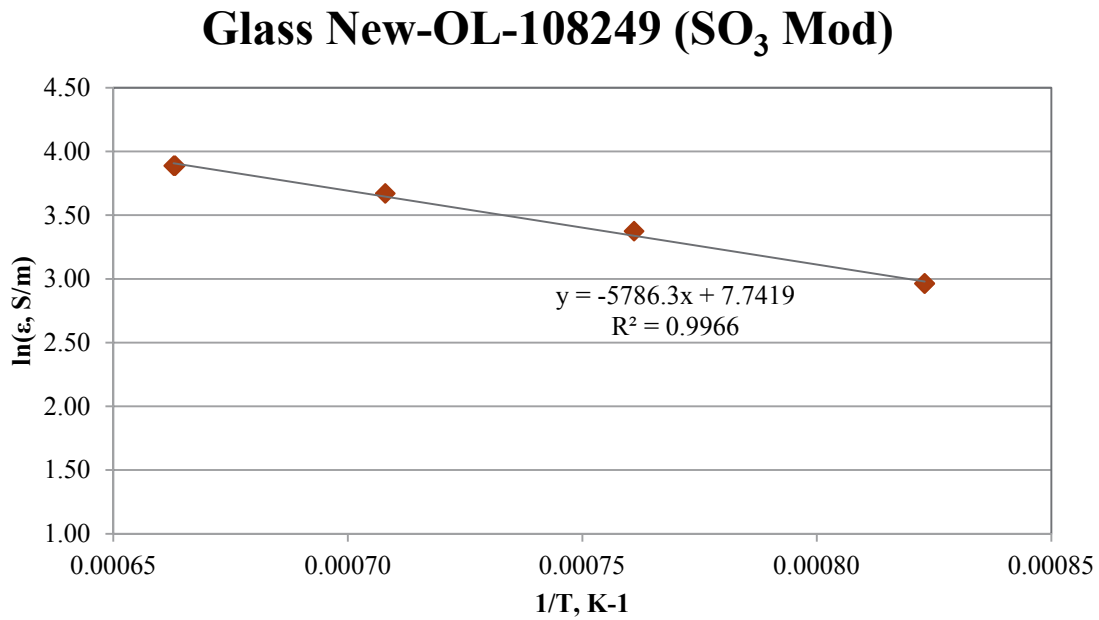


Figure C.28. Electrical Conductivity -Temperature Data and Arrhenius Equation Fit for Glass New-OL-108249 (SO₃ Mod)

C.29 Glass New-OL-116208 (SO₃ Mod) Electrical Conductivity Data

Table C.29. Electrical Conductivity Data for Glass New-OL-116208 (SO₃ Mod)

Temperature, °C	Conductivity, S/m	1/(T+273.15), K ⁻¹	ln(ϵ , S/m)
954	29.76	0.00082	3.39
944	29.60	0.00082	3.39
1056	43.04	0.00075	3.76
1044	42.86	0.00076	3.76
1236	64.91	0.00066	4.17
1236	64.86	0.00066	4.17
893	22.89	0.00086	3.13
892	22.87	0.00086	3.13

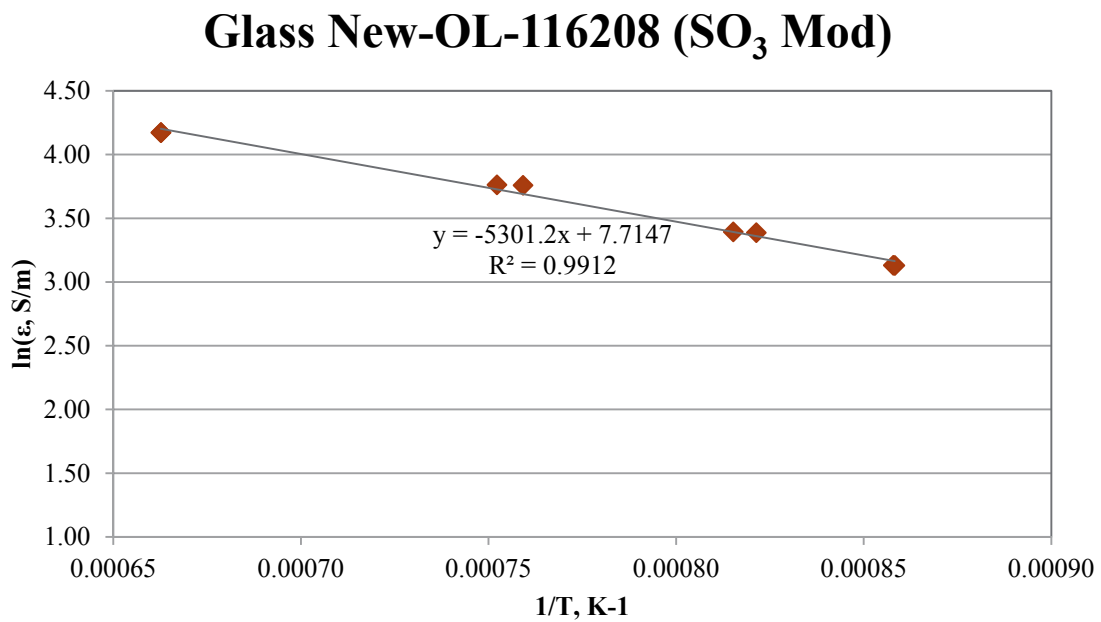


Figure C.29. Electrical Conductivity-Temperature Data and Arrhenius Equation Fit for Glass New-OL-116208 (SO₃ Mod)

C.30 Glass New-OL-122817 Electrical Conductivity Data

Table C.30. Electrical Conductivity Data for Glass New-OL-122817

Temperature, °C	Conductivity, S/m	1/(T+273.15), K ⁻¹	ln(σ, S/m)
1236	41.93	0.00066	3.74
1235	41.87	0.00066	3.73
1139	31.70	0.00071	3.46
1040	21.90	0.00076	3.09
1040	21.92	0.00076	3.09
941	13.47	0.00082	2.60
941	13.48	0.00082	2.60

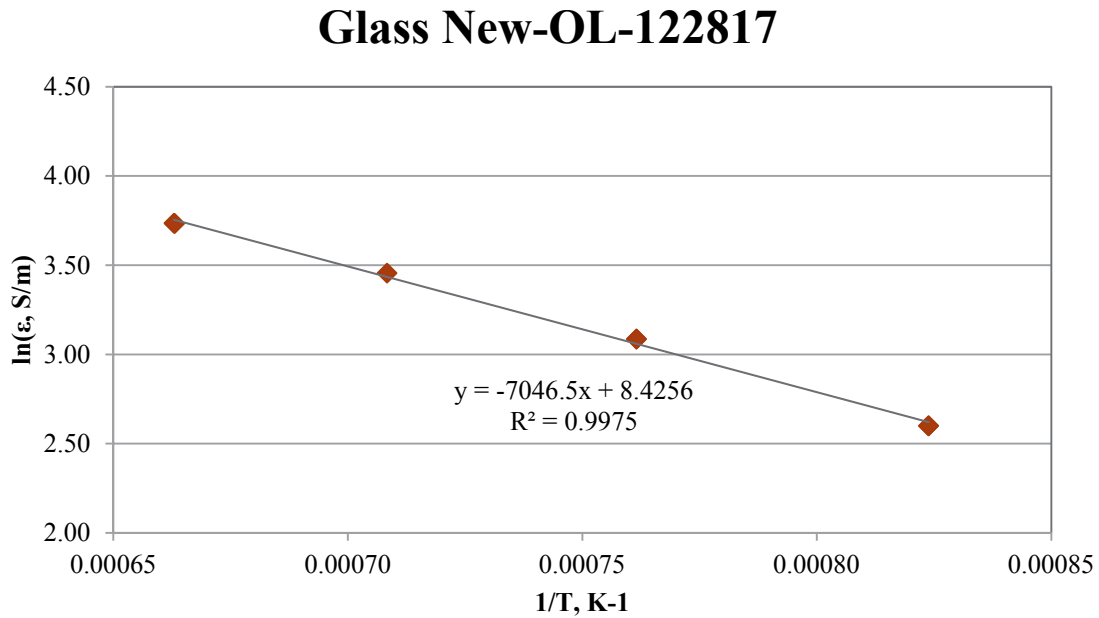


Figure C.30. Electrical Conductivity -Temperature Data and Arrhenius Equation Fit for Glass New-OL-122817

C.31 Glass New-OL-127708(Mod) Electrical Conductivity Data

Table C.31. Electrical Conductivity Data for Glass New-OL-127708(Mod)

Temperature, °C	Conductivity, S/m	$1/(T+273.15), K^{-1}$	$\ln(\epsilon, S/m)$
1236	31.14	0.00066	3.44
1139	23.15	0.00071	3.14
1040	15.77	0.00076	2.76
942	9.36	0.00082	2.24

Glass New-OL-127708(Mod)

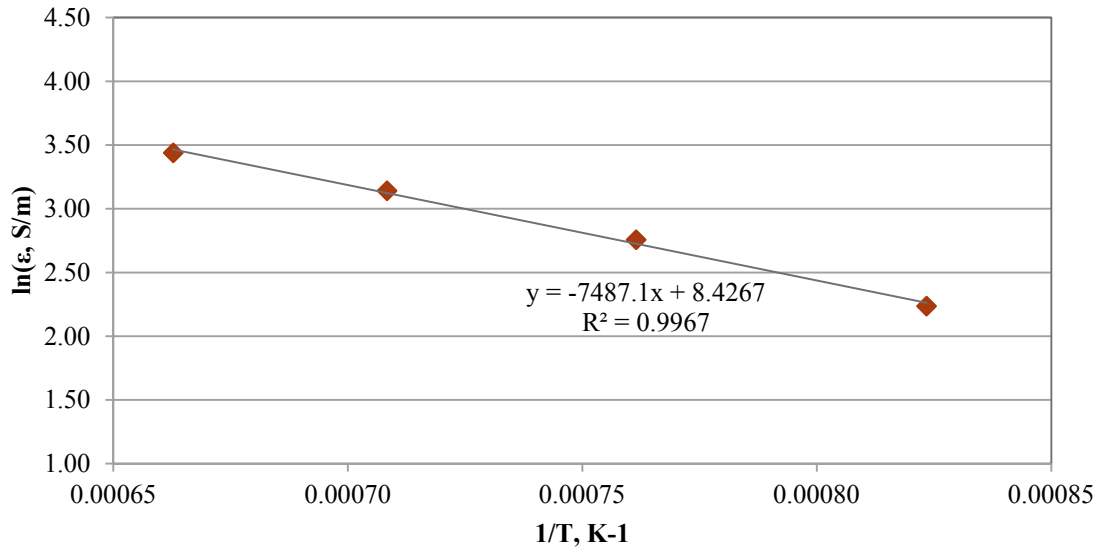


Figure C.31. Electrical Conductivity -Temperature Data and Arrhenius Equation Fit for Glass New-OL-127708(Mod)

C.32 Glass EWG-LAW-Centroid-1 Electrical Conductivity Data

Table C.32. Electrical Conductivity Data for Glass EWG-LAW-Centroid-1

Temperature, °C	Conductivity, S/m	1/(T+273.15), K ⁻¹	ln(ε, S/m)
1238	48.32	0.00066	3.88
1141	37.80	0.00071	3.63
1042	27.34	0.00076	3.31
943	17.65	0.00082	2.87
943	17.65	0.00082	2.87

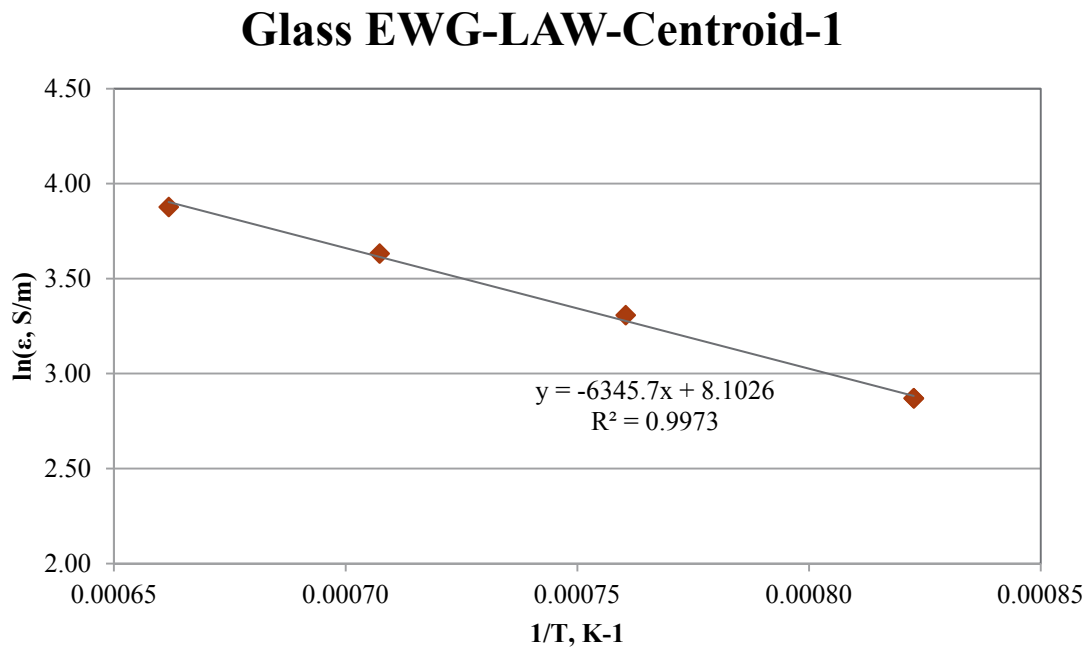


Figure C.32. Electrical Conductivity -Temperature Data and Arrhenius Equation Fit for Glass EWG-LAW-Centroid-1

C.33 Glass EWG-LAW-Centroid-2 Electrical Conductivity Data

Table C.33. Electrical Conductivity Data for Glass EWG-LAW-Centroid-2

Temperature, °C	Conductivity, S/m	1/(T+273.15), K ⁻¹	ln(ε, S/m)
1235	49.52	0.00066	3.90
1235	49.44	0.00066	3.90
1134	38.72	0.00071	3.66
1134	38.67	0.00071	3.66
1028	27.89	0.00077	3.33
1027	27.86	0.00077	3.33
919	17.71	0.00084	2.87
919	17.69	0.00084	2.87

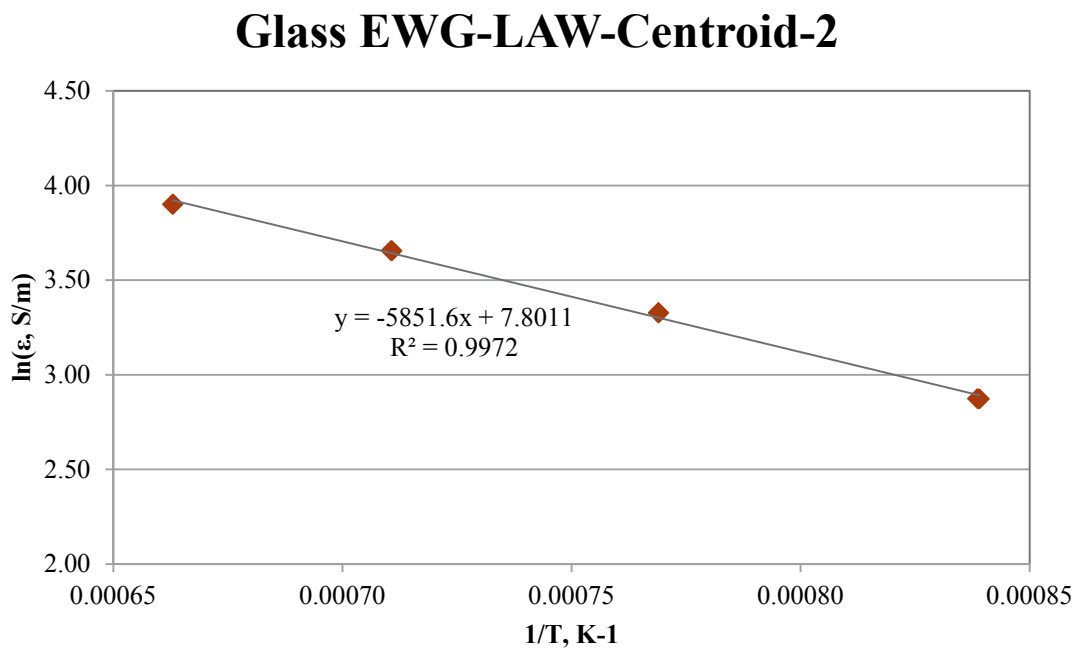


Figure C.33. Electrical Conductivity -Temperature Data and Arrhenius Equation Fit for Glass EWG-LAW-Centroid-2

C.34 Glass LAW-ORP-LD1-1 Electrical Conductivity Data

Table C.34. Electrical Conductivity Data for Glass LAW-ORP-LD1-1

Temperature, °C	Conductivity, S/m	1/(T+273.15), K ⁻¹	ln(ε, S/m)
1233	41.59	0.00066	3.73
1233	41.59	0.00066	3.73
1137	32.79	0.00071	3.49
1039	23.97	0.00076	3.18
940	15.78	0.00082	2.76
940	15.75	0.00082	2.76

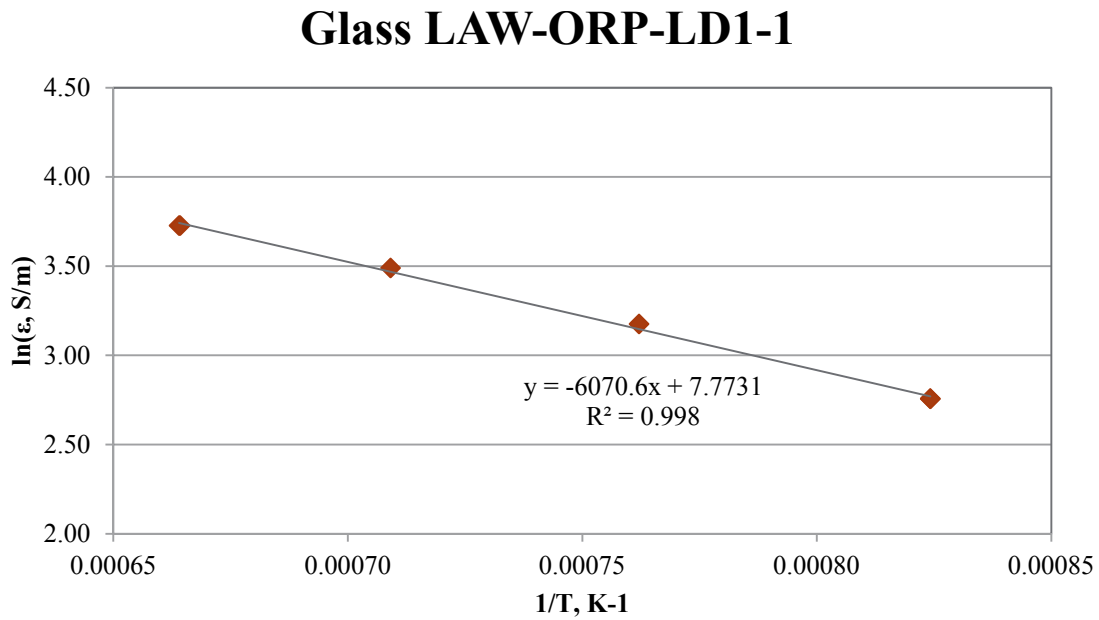


Figure C.34. Electrical Conductivity -Temperature Data and Arrhenius Equation Fit for Glass LAW-ORP-LD1-1

C.35 Glass LAW-ORP-LD1-2 Electrical Conductivity Data

Table C.35. Electrical Conductivity Data for Glass LAW-ORP-LD1-2

Temperature, °C	Conductivity, S/m	$1/(T+273.15), K^{-1}$	$\ln(\epsilon, S/m)$
1230	49.63	0.00067	3.90
1230	49.49	0.00067	3.90
1134	38.97	0.00071	3.66
1134	38.98	0.00071	3.66
1036	28.19	0.00076	3.34
1036	28.19	0.00076	3.34
938	18.25	0.00083	2.90
938	18.22	0.00083	2.90

Glass LAW-ORP-LD1-2

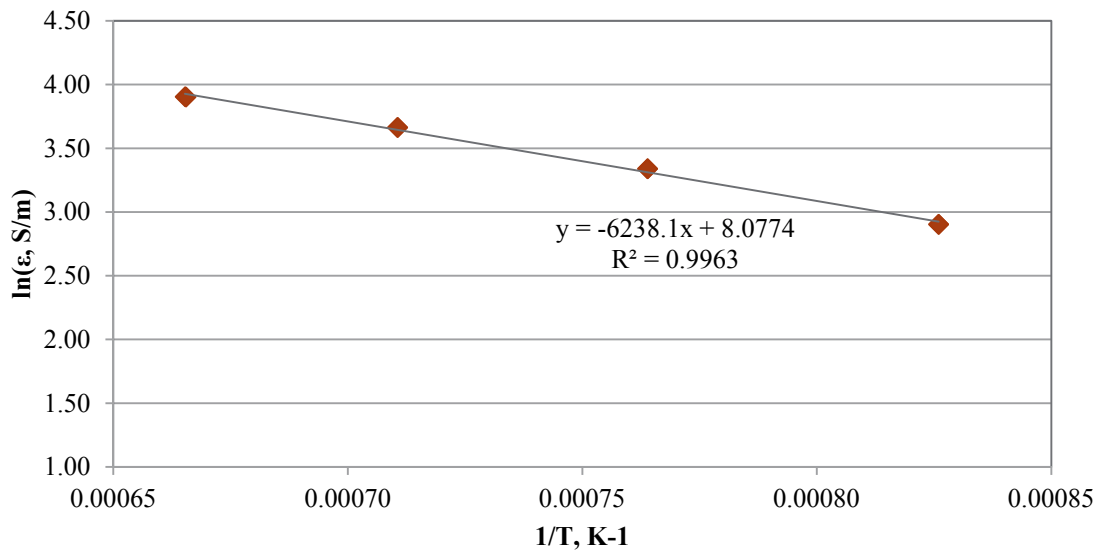


Figure C.35. Electrical Conductivity - Temperature Data and Arrhenius Equation Fit for Glass LAW-ORP-LD1-2

C.36 Glass LAW-ORP-LD1-3 Electrical Conductivity Data

Table C.36. Electrical Conductivity Data for Glass LAW-ORP-LD1-2

Temperature, °C	Conductivity, S/m	1/(T+273.15), K ⁻¹	ln(ε, S/m)
1233	41.04	0.00066	3.71
1137	31.76	0.00071	3.46
1038	22.59	0.00076	3.12
940	14.36	0.00083	2.66
940	14.37	0.00083	2.67

Glass LAW-ORP-LD1-3

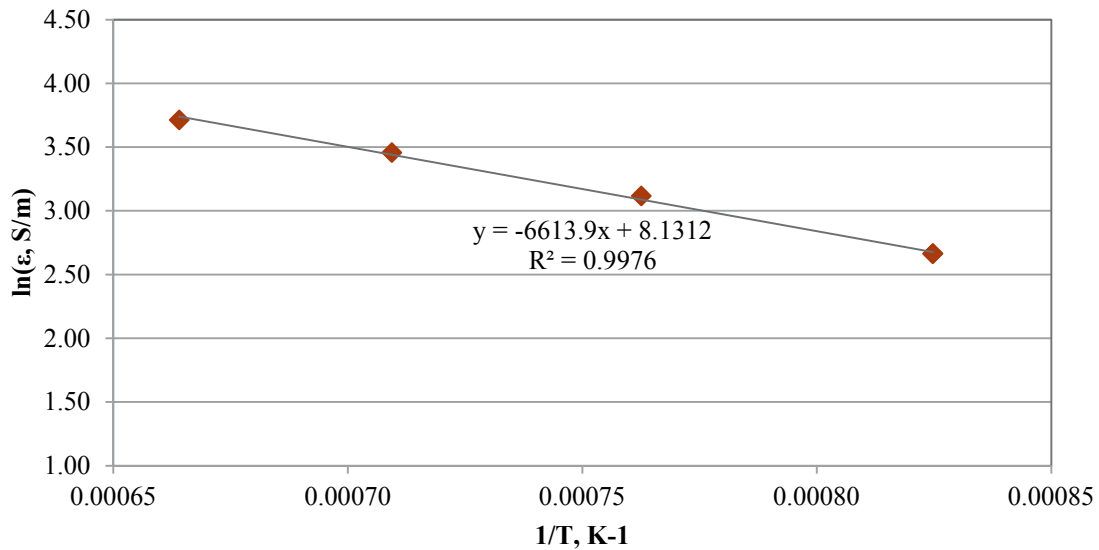


Figure C.36. Electrical Conductivity -Temperature Data and Arrhenius Equation Fit for Glass LAW-ORP-LD1-3

Appendix D

Canister Centerline Cooling Glass Photographs

Appendix D

Canister Centerline Cooled Glass Photographs

This appendix contains photos of glasses after they were canister centerline cooled (CCC) treated beginning at the glass melting temperature, which is indicated in the picture title. Each showed different responses to the CCC treatment as indicated by these photos.



Figure D.1. Photograph of Glass New-IL-456 after CCC Beginning at 1200°C



Figure D.2. Optical Micrograph of Glass New-IL-5253 Surface after CCC Beginning at 1150°C

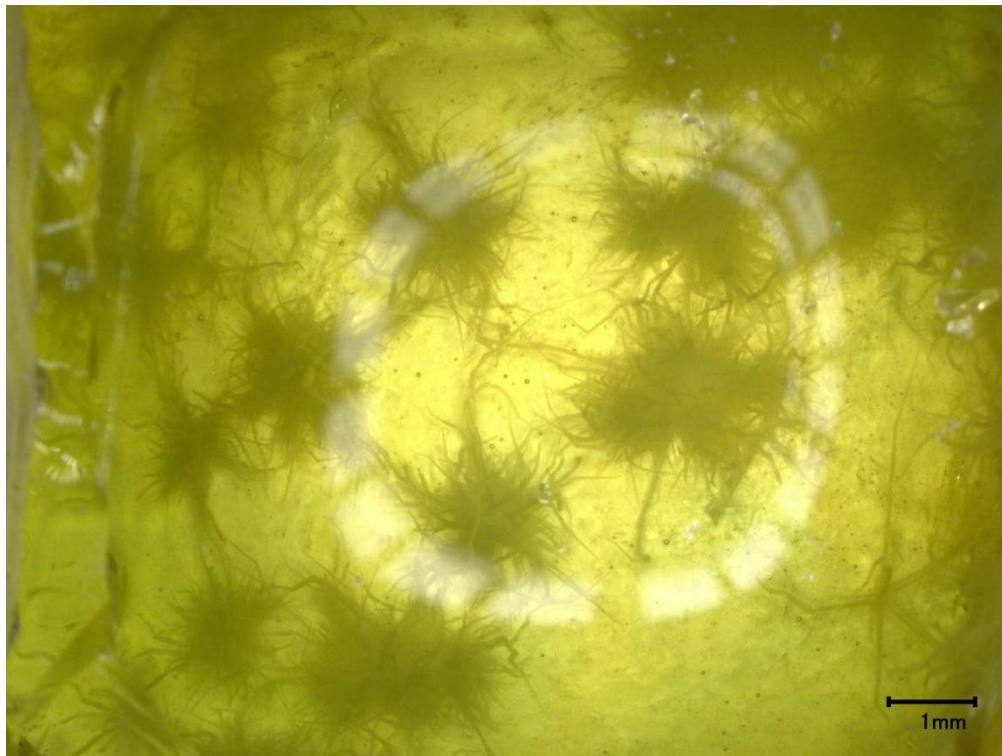


Figure D.3. Optical Micrograph of Glass New-IL-5255 after CCC Beginning at 1150°C

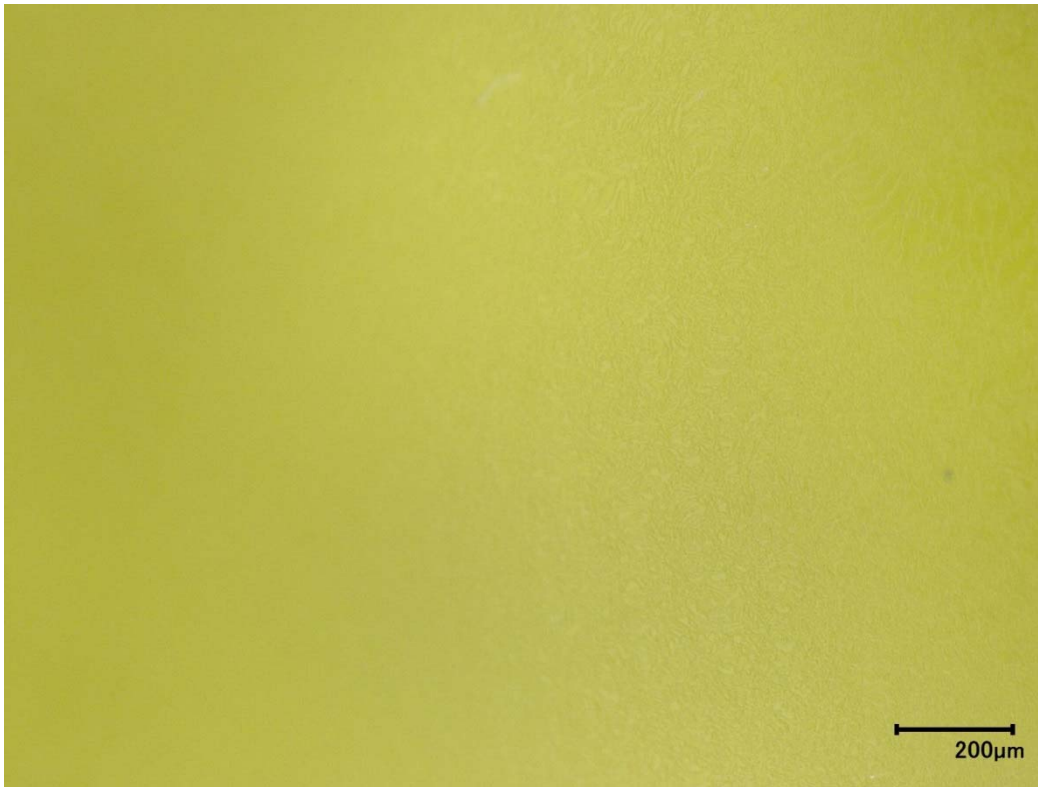


Figure D.4. Optical Micrograph of Glass New-IL-70316 after CCC Beginning at 1200°C



Figure D.5. Photograph of Glass New-IL-87749 after CCC Beginning at 1225°C from Pt Crucible (bottom) and Quartz Crucible (top)



Figure D.6. Photograph of Glass New-IL-93907 after CCC Beginning at 1150°C (1 cm cube glass)



Figure D.7. Photograph of Glass New-IL-94020 after CCC Beginning at 1300°C

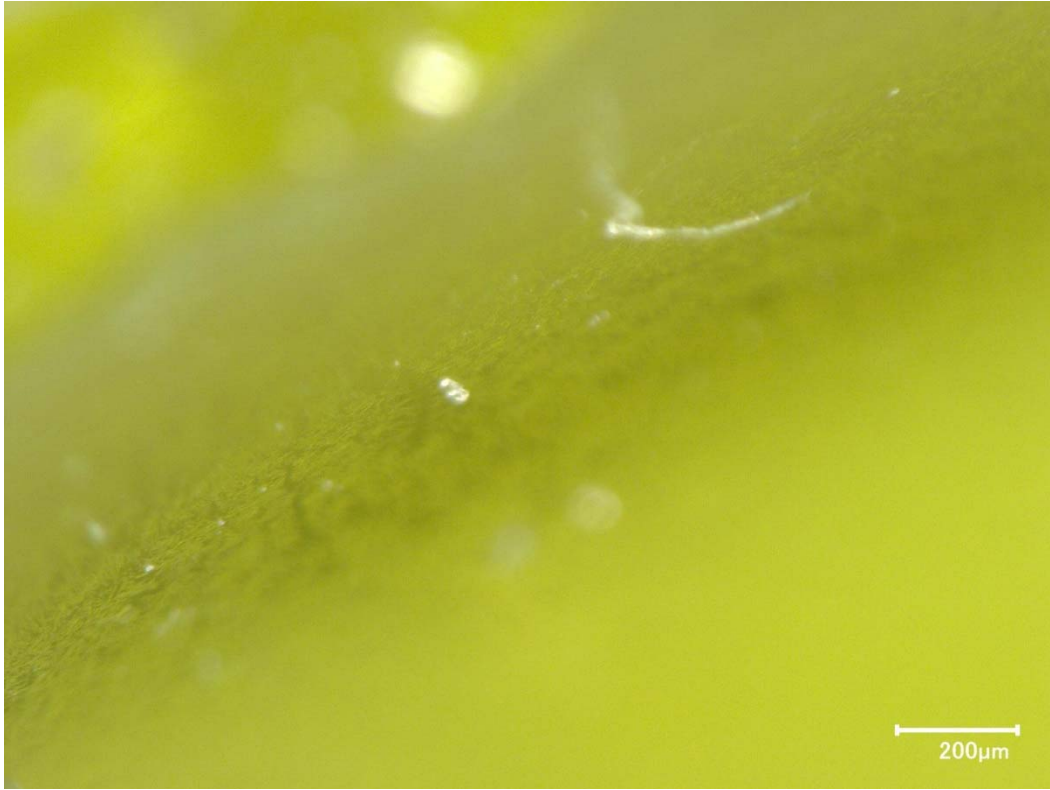


Figure D.8. Optical Micrograph of Glass New-IL-103151 after CCC Beginning at 1250°C

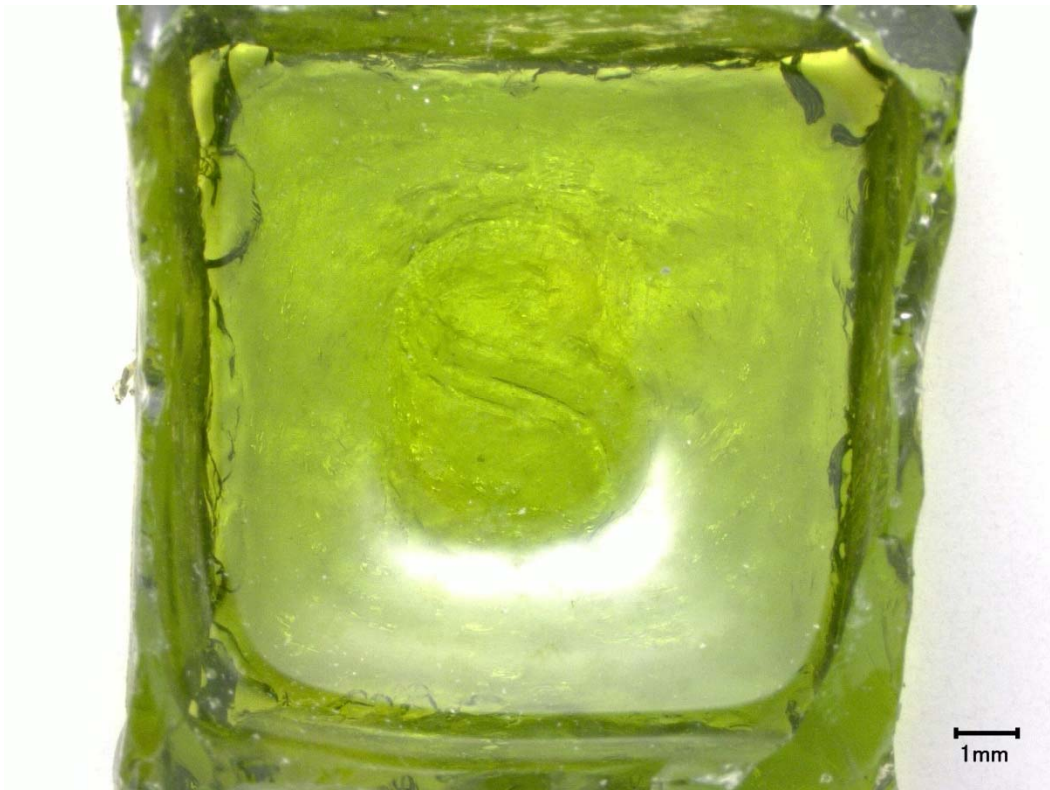


Figure D.9. Photograph of Glass New-IL-151542 after CCC Beginning at 1225°C



Figure D.10. Photograph of Glass New-IL-166697 after CCC Beginning at 1250°C from Pt Crucible 1 cm Cube (top) and Quartz Crucible (bottom)



Figure D.11. Photograph of New-IL-166731 after CCC Beginning at 1225°C from Pt Crucible (top) and Quartz Crucible (bottom)

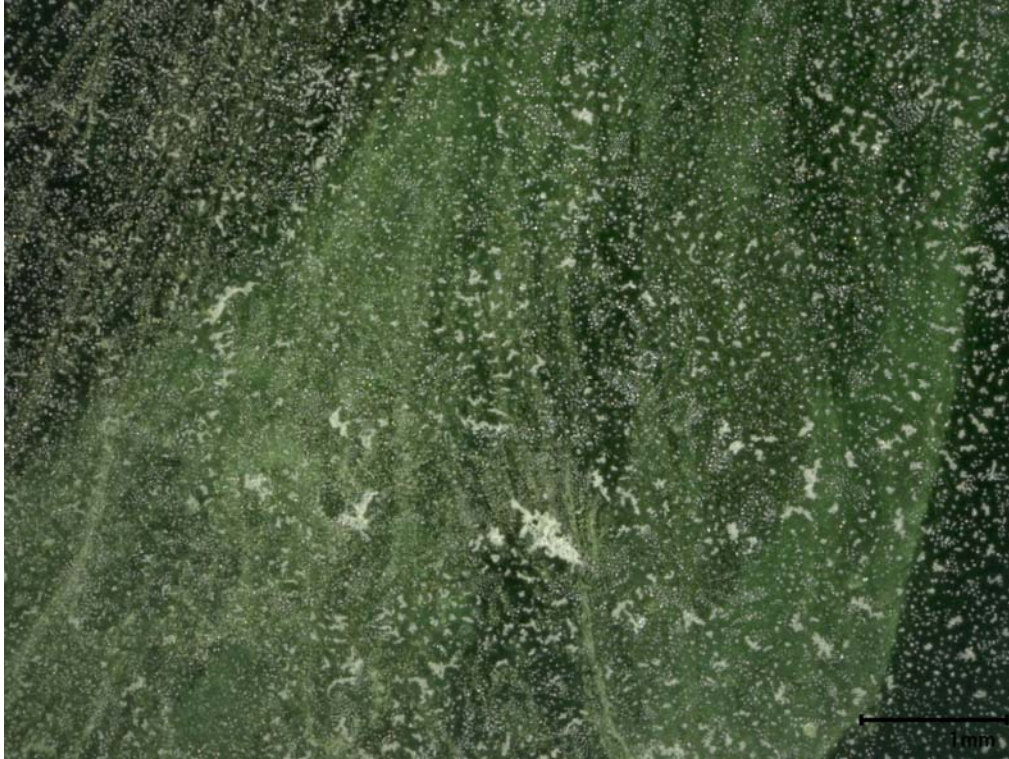


Figure D.12. Optical Micrograph of Glass New-OL-8445 after CCC Beginning at 1150°C



Figure D.13. Optical Micrograph of Glass New-OL-8788(Mod) after CCC Beginning at 1150°C

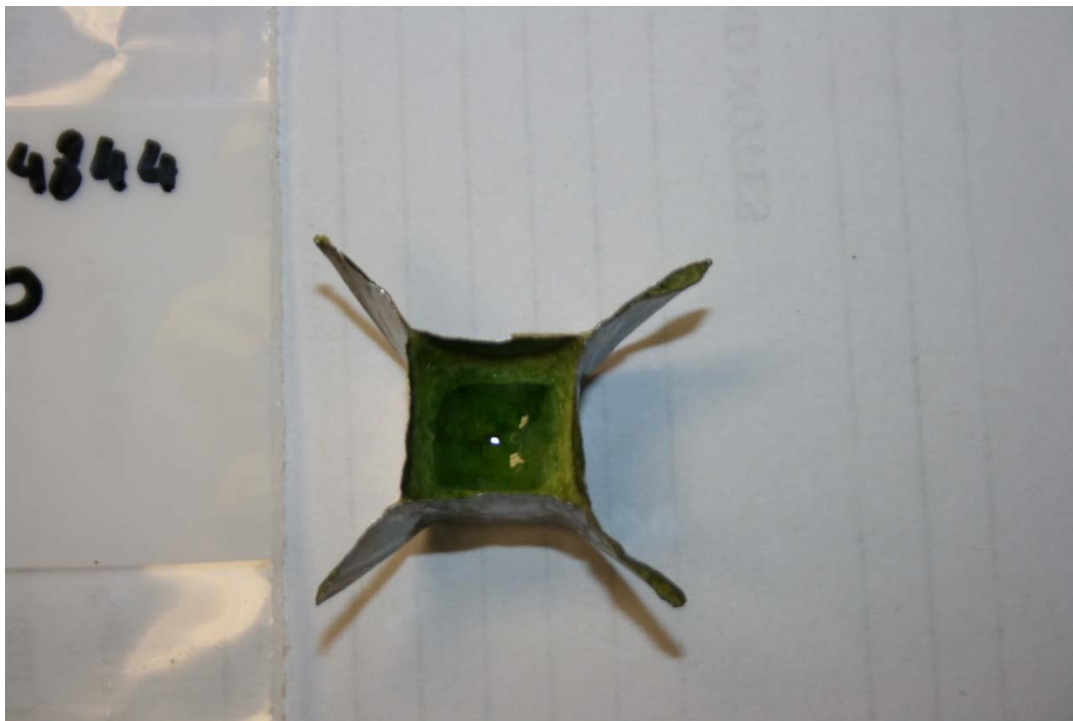


Figure D.14. Photograph of Glass New-OL-14844 after CCC Beginning at 1250°C (1 cm cube)

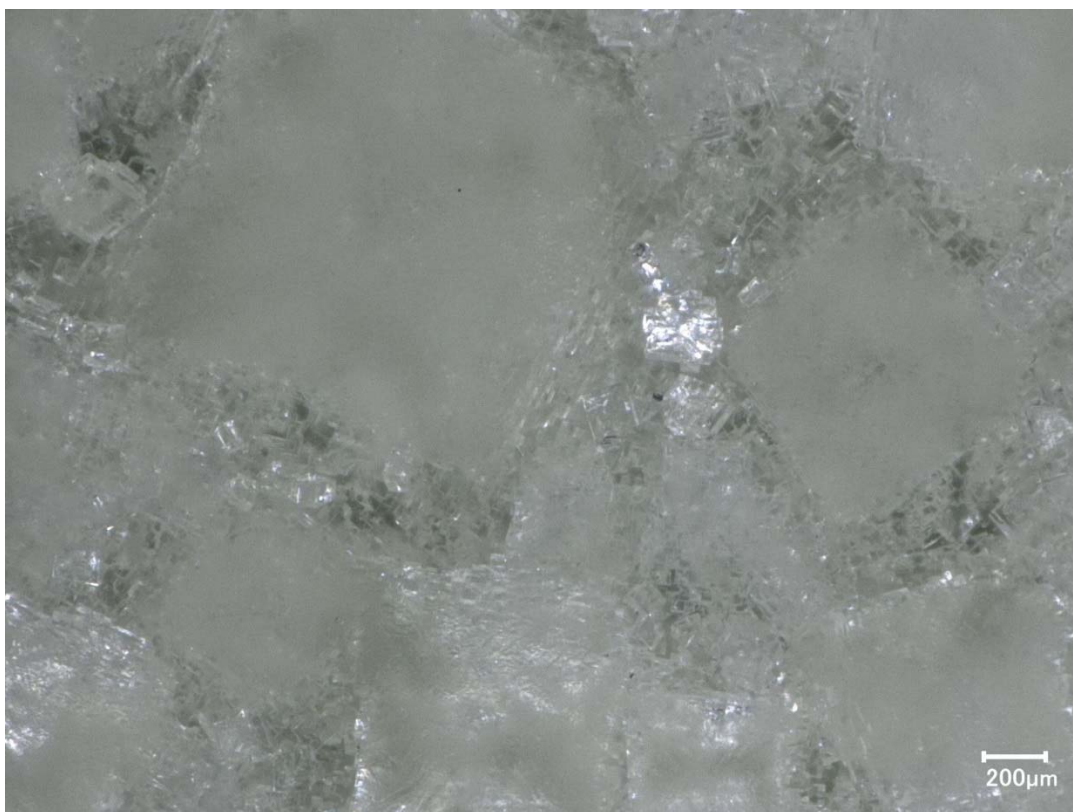


Figure D.15. Optical Micrograph of Glass New-OL-15493 after CCC Beginning at 1225°C



Figure D.16. Optical Micrograph of Glass New-OL-45748 (Sn Mod) after CCC Beginning at 1300°C

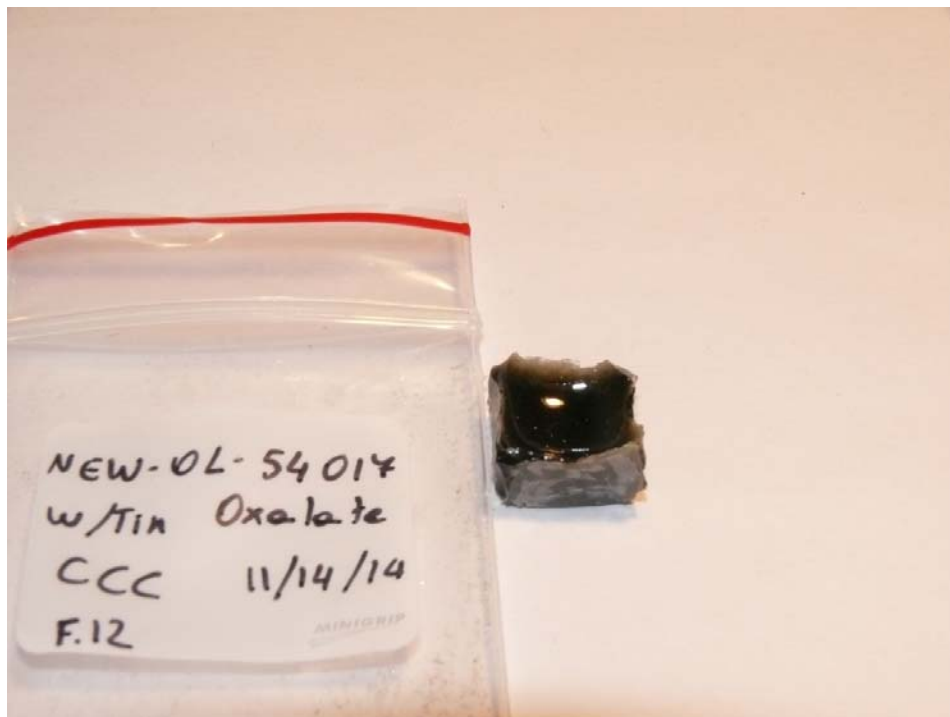


Figure D.17. Photograph of Glass New-OL-54017 (Sn Mod) after CCC Beginning at 1150°C (1 cm cube)



Figure D.18. Photograph of Glass New-OL-57284 after CCC Beginning at 1225°C

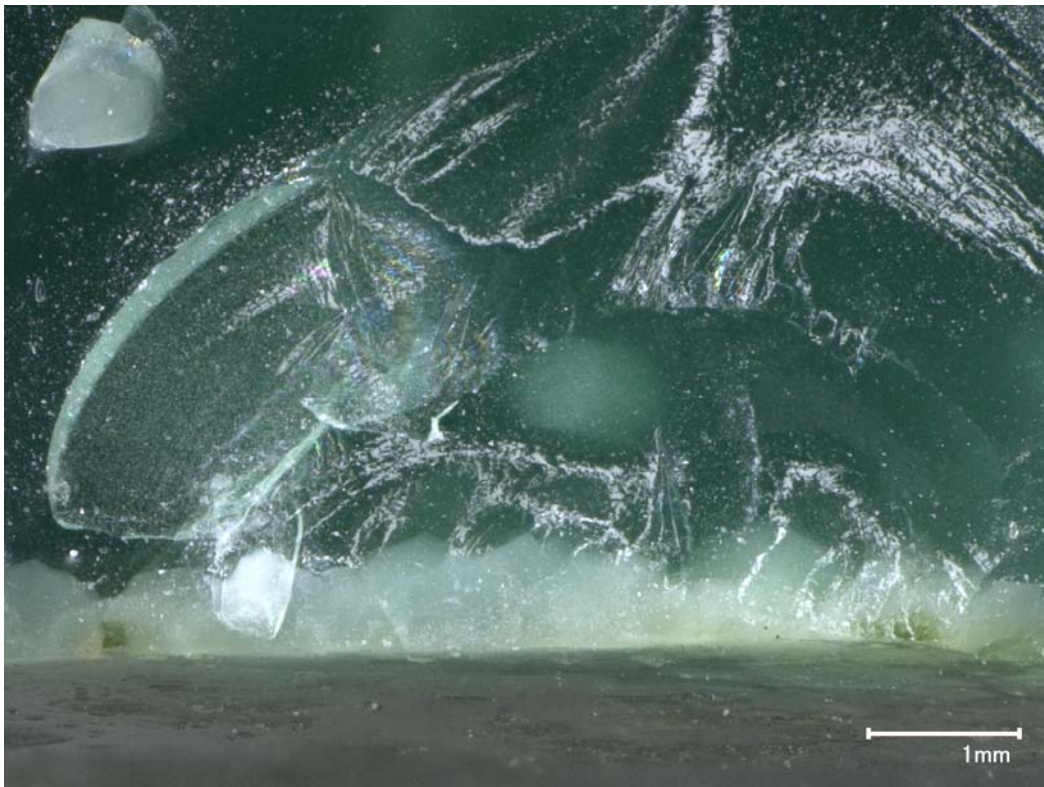


Figure D.19. Optical Micrograph of Glass New-OL-62909(Mod) after CCC Beginning at 1300°C



Figure D.20. Optical Micrograph of Glass New-OL-65959(Mod) after CCC Beginning at 1225°C

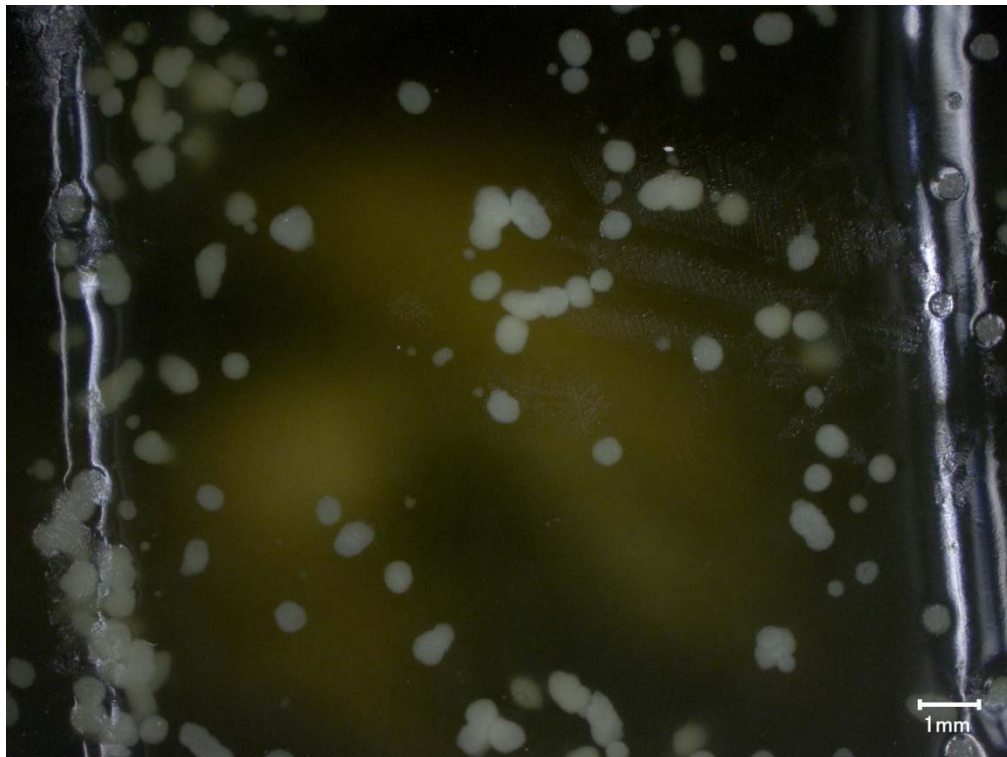


Figure D.21. Optical Micrograph of Glass New-OL-80309 after CCC Beginning at 1300°C



Figure D.22. Optical Micrograph of Glass New-OL-90780 after CCC Beginning at 1200°C

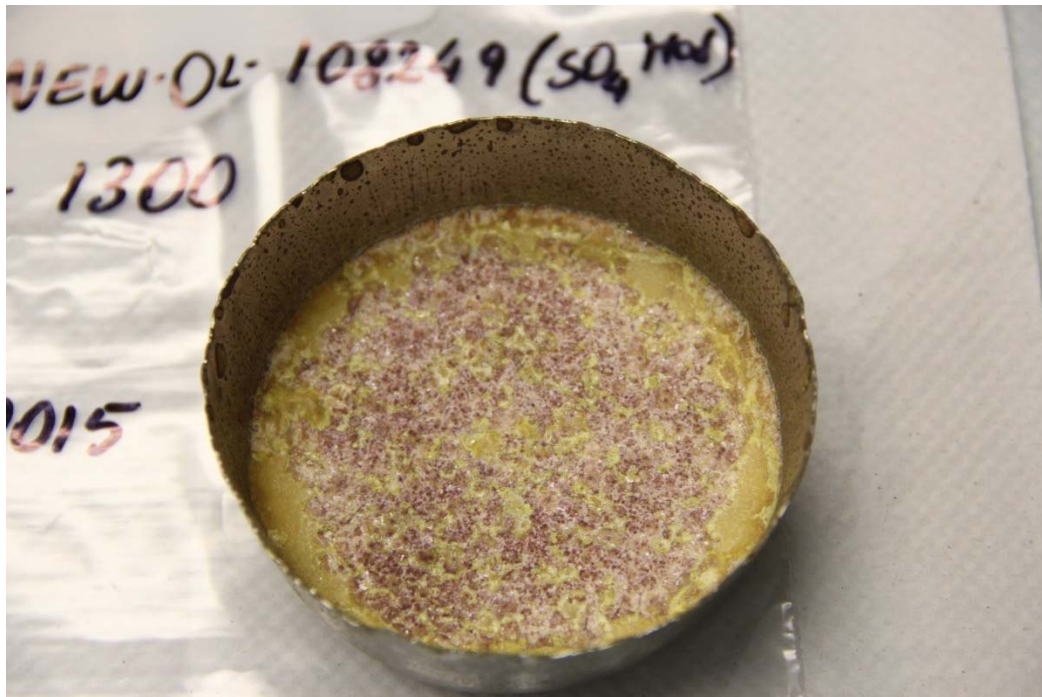


Figure D.23. Photograph of Glass New-OL-108249 (SO₃ Mod) after CCC Beginning at 1300°C



Figure D.24. Optical Micrograph of Glass New-OL-122817 after CCC Beginning at 1200°C



Figure D.25. Optical Micrograph of Glass New-OL-127708(Mod) after CCC Beginning at 1150°C

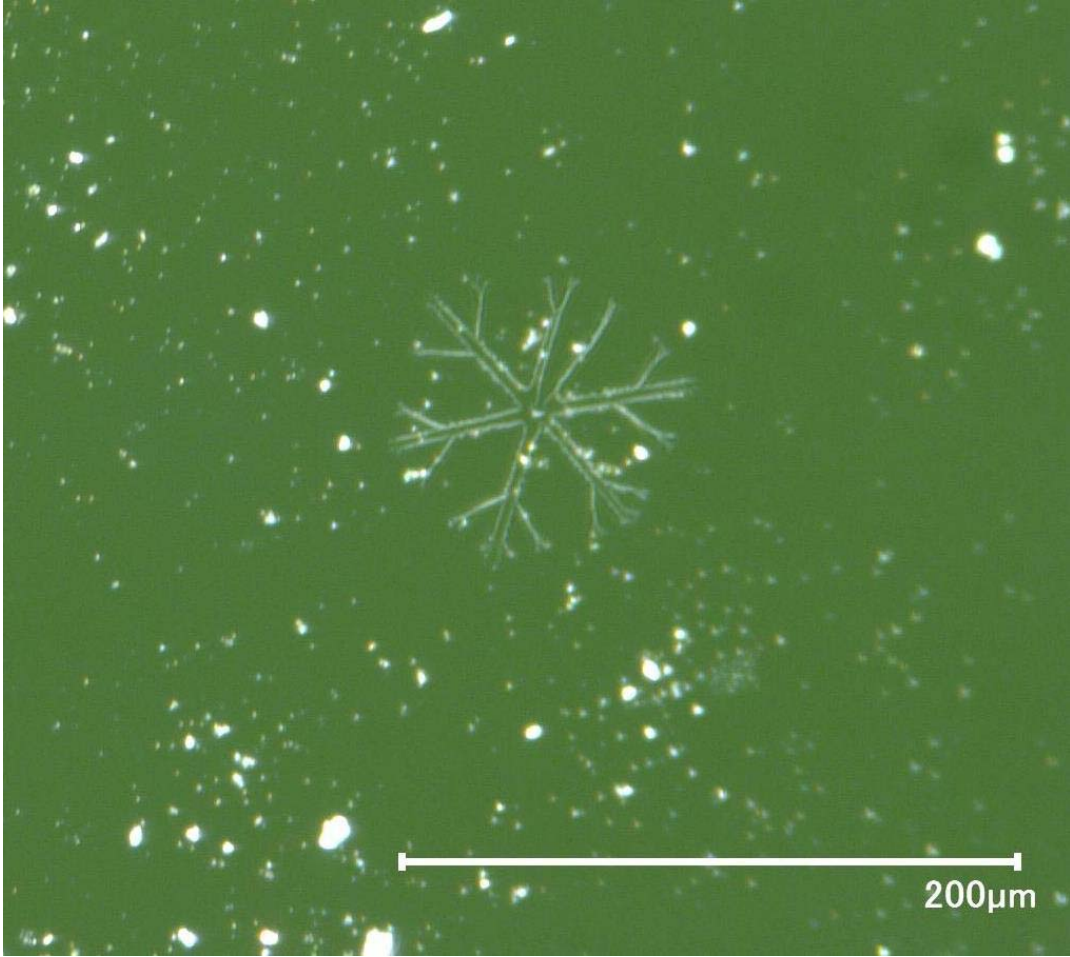


Figure D.26. Optical Micrograph of Glass LAW-Centroid-1 after CCC Beginning at 1150°C



Figure D.27. Photograph of LAW-ORP-LD1-1 after CCC Beginning at 1300°C from 1 cm cube Pt Crucible (top) and Quartz Crucible (bottom)



Figure D.28. Photograph of LAW-ORP-LD1-2 after CCC Beginning at 1300°C from Quartz Crucible



Figure D.29. Photograph of LAW-ORP-LD1-3 after CCC Beginning at 1300°C from Quartz Crucible

Appendix E

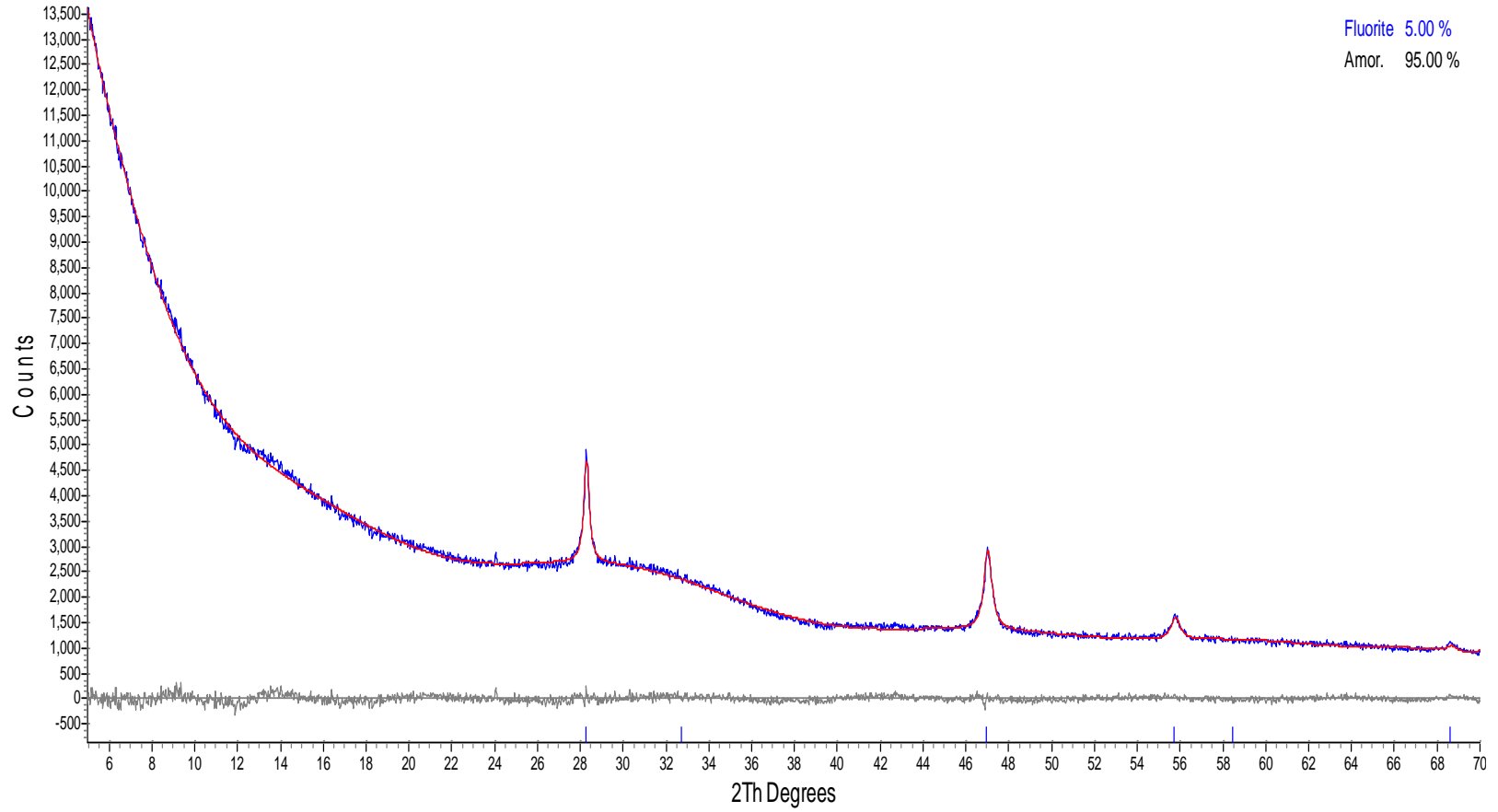
X-Ray Diffraction Spectra of Canister Centerline Cooling Treated Glasses

Appendix E

X-Ray Diffraction Spectra of Canister Centerline Cooling Treated Glasses

This appendix shows the x-ray diffraction (XRD) spectra of these glasses after CCC treatment. These glasses all responded very differently to the CCC treatment from remaining amorphous to developing quite a few crystals of various kinds as shown by the following plots. Some glasses did not contain enough crystals to perform XRD and therefore are not included in the appendix.

NEW-IL-5255-CCC-XRD.raw_1



E.2

Figure E.1. XRD Spectrum of CCC-Treated Glass New-IL-5255

NEW-IL-70316-CCC-Cc.raw_1

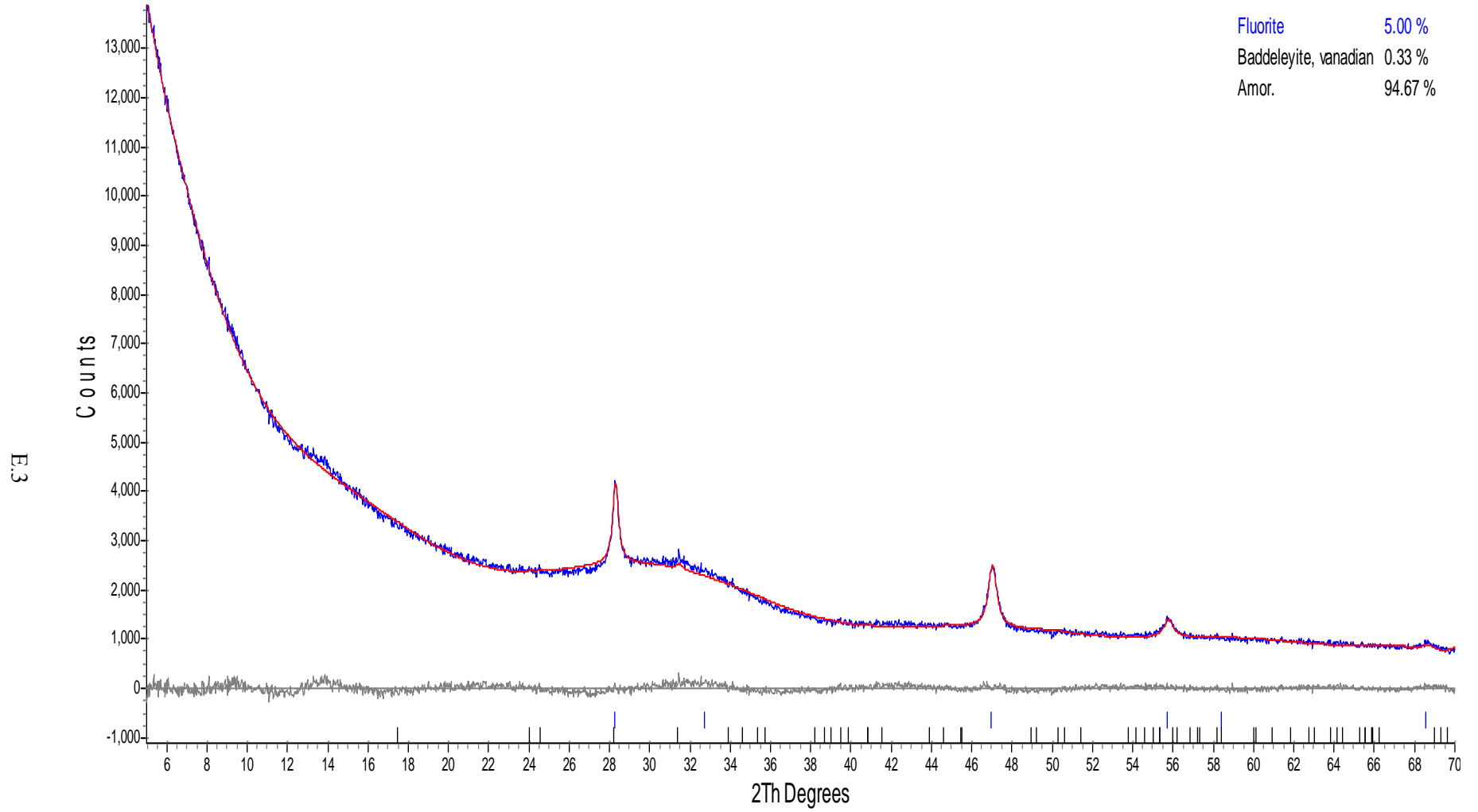


Figure E.2. XRD Spectrum of CCC-Treated Glass New-IL-70316

NEW-IL-94020-CCC-Cc.raw_1

Fluorite 5.01 %
Cassiterite 1.27 %
Amor. 93.73 %

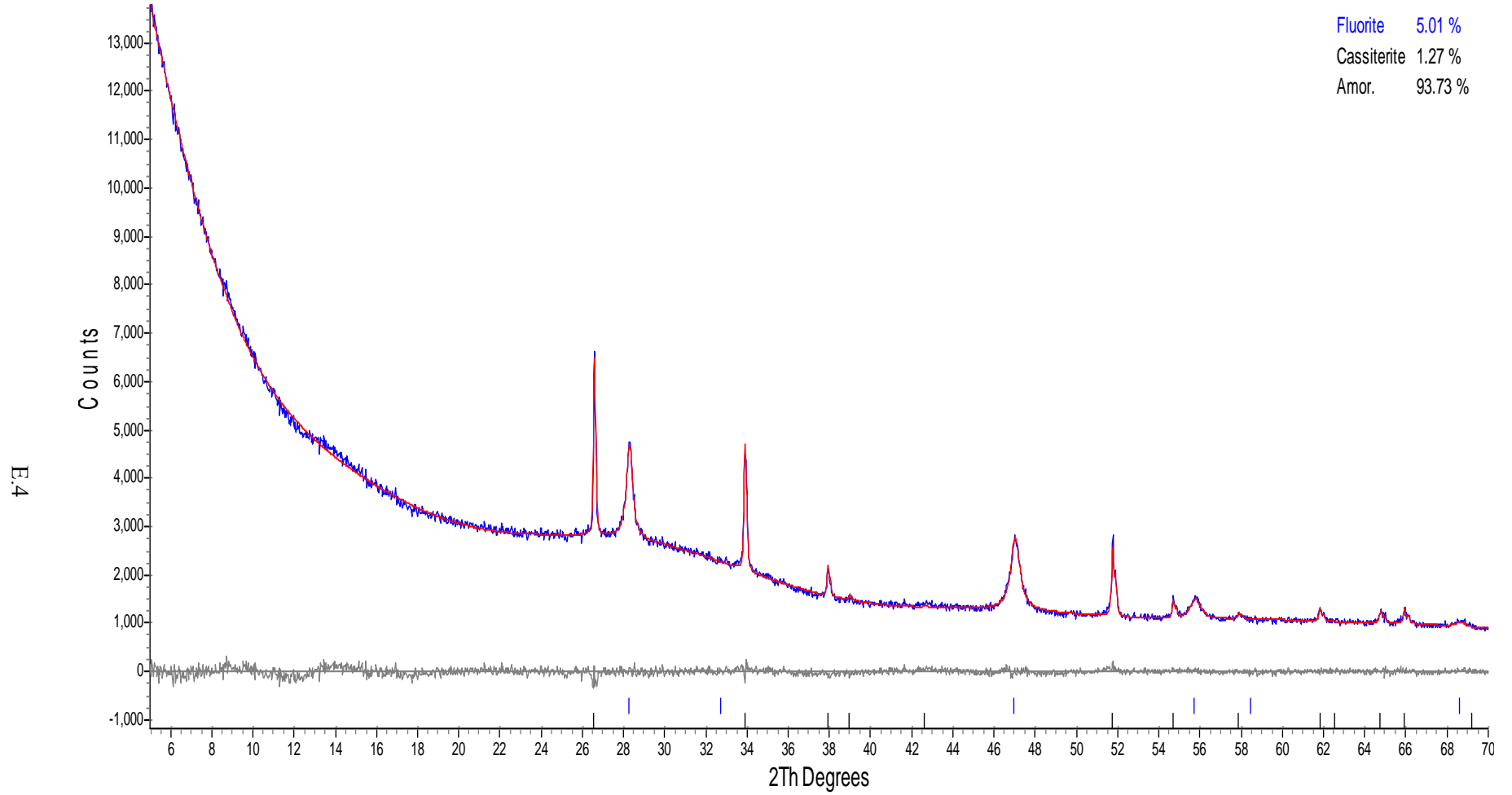


Figure E.3. XRD Spectrum of CCC-Treated Glass New-IL-94020

NEW-IL-166697-CCC-Cc.raw_1

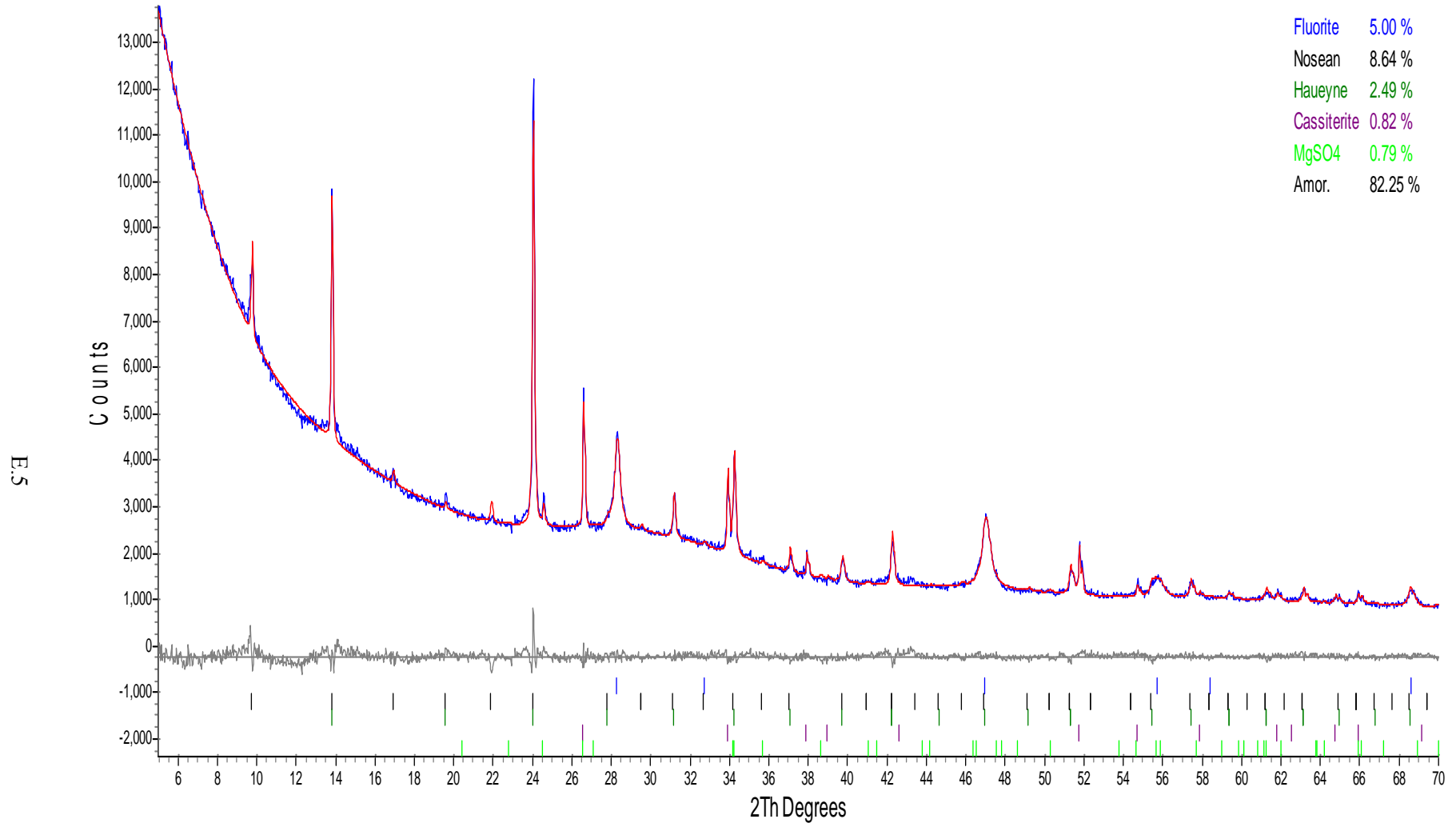


Figure E.4. XRD Spectrum of CCC-Treated Glass New-IL-166697

LAW-NEW-OL-166731-CCC-Cc.raw_1

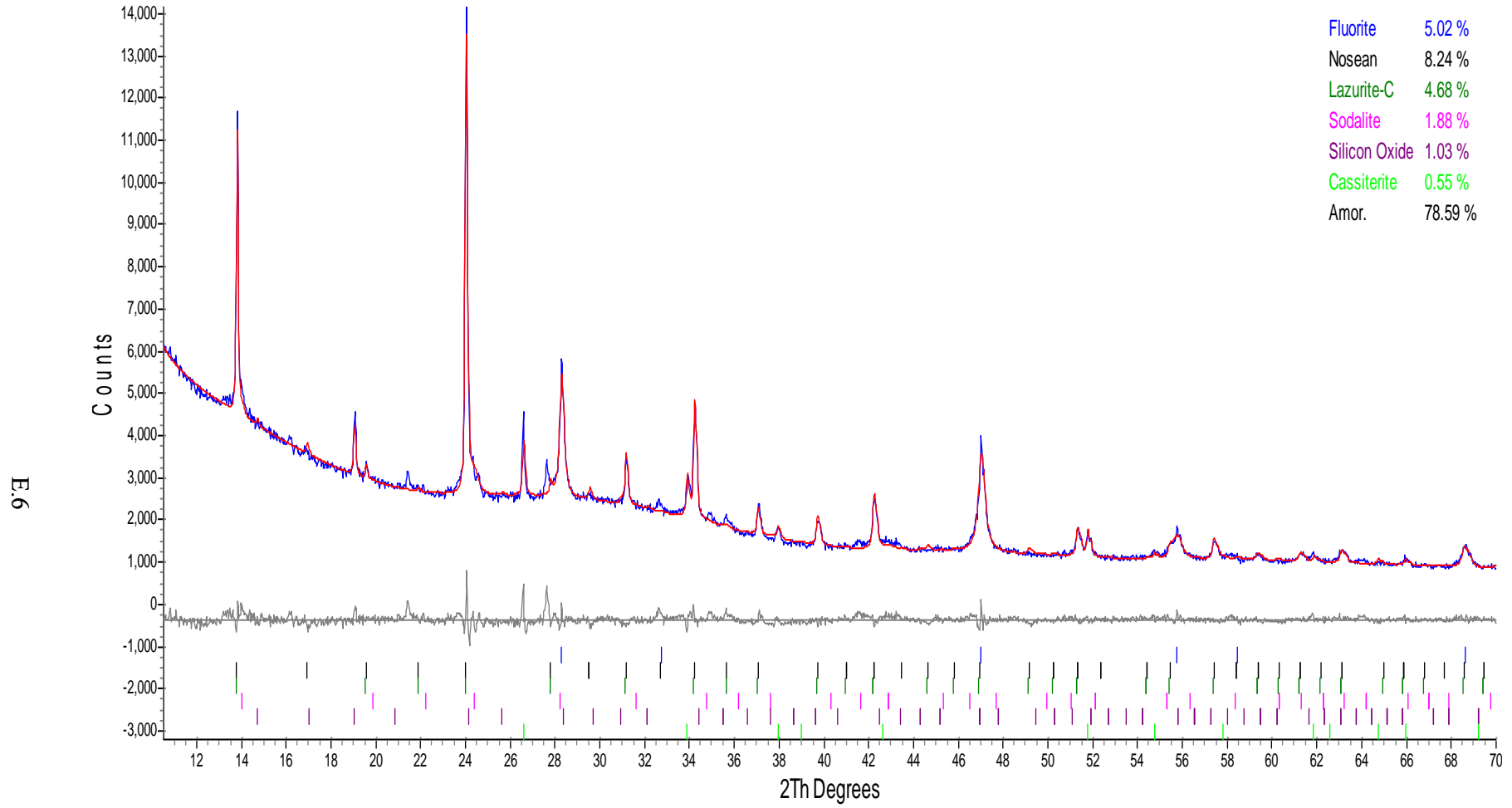


Figure E.5. XRD Spectrum of CCC-Treated Glass New-IL-166731

LAW-NEW-OL-8445-CCC-Cc.raw_1

Fluorite 5.01 %
Amor. 94.99 %

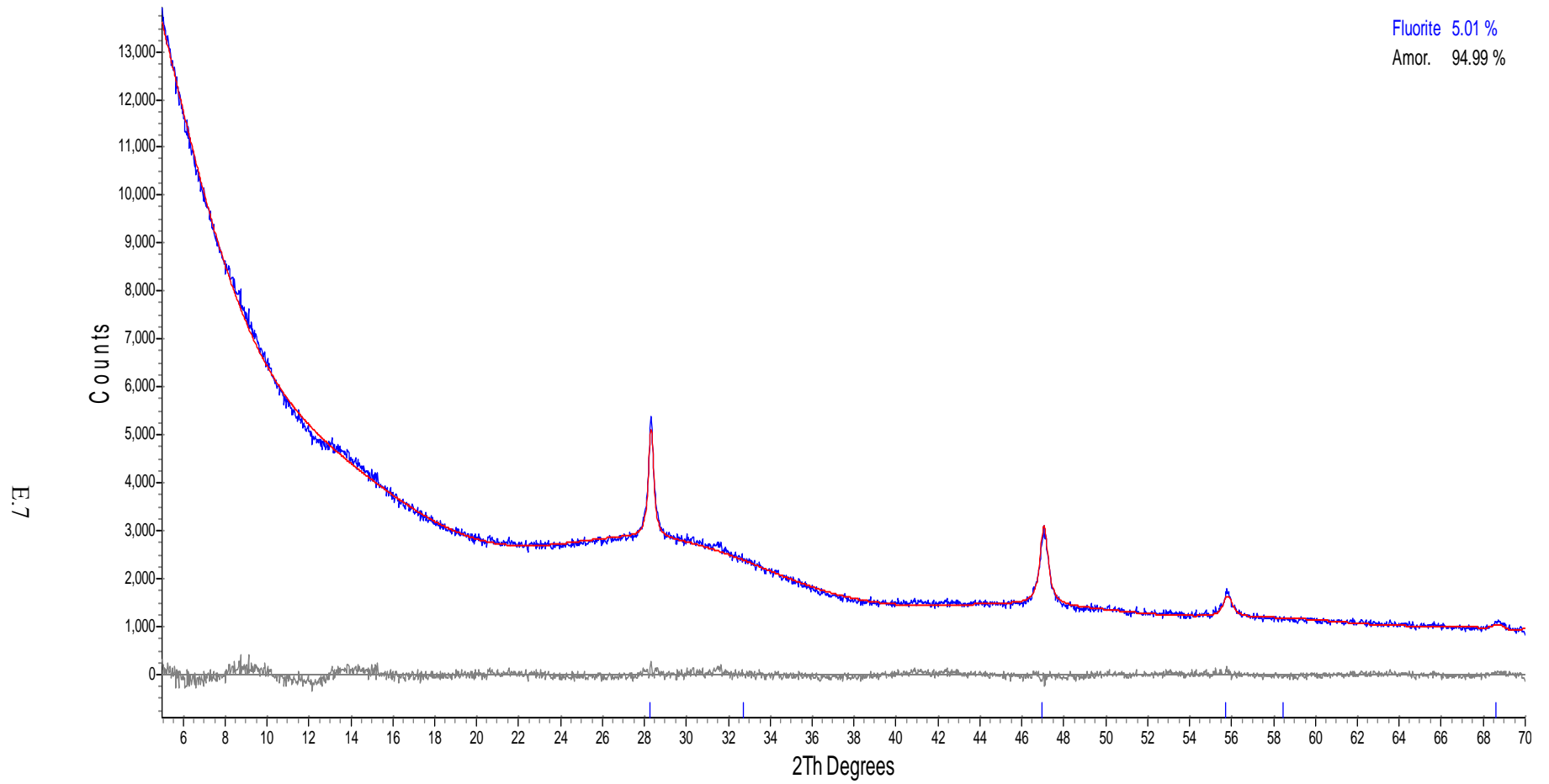


Figure E.6. XRD Spectrum of CCC-Treated Glass New-OL-8445

NEW-OL-8788Mod-CCC-Cc.raw_1

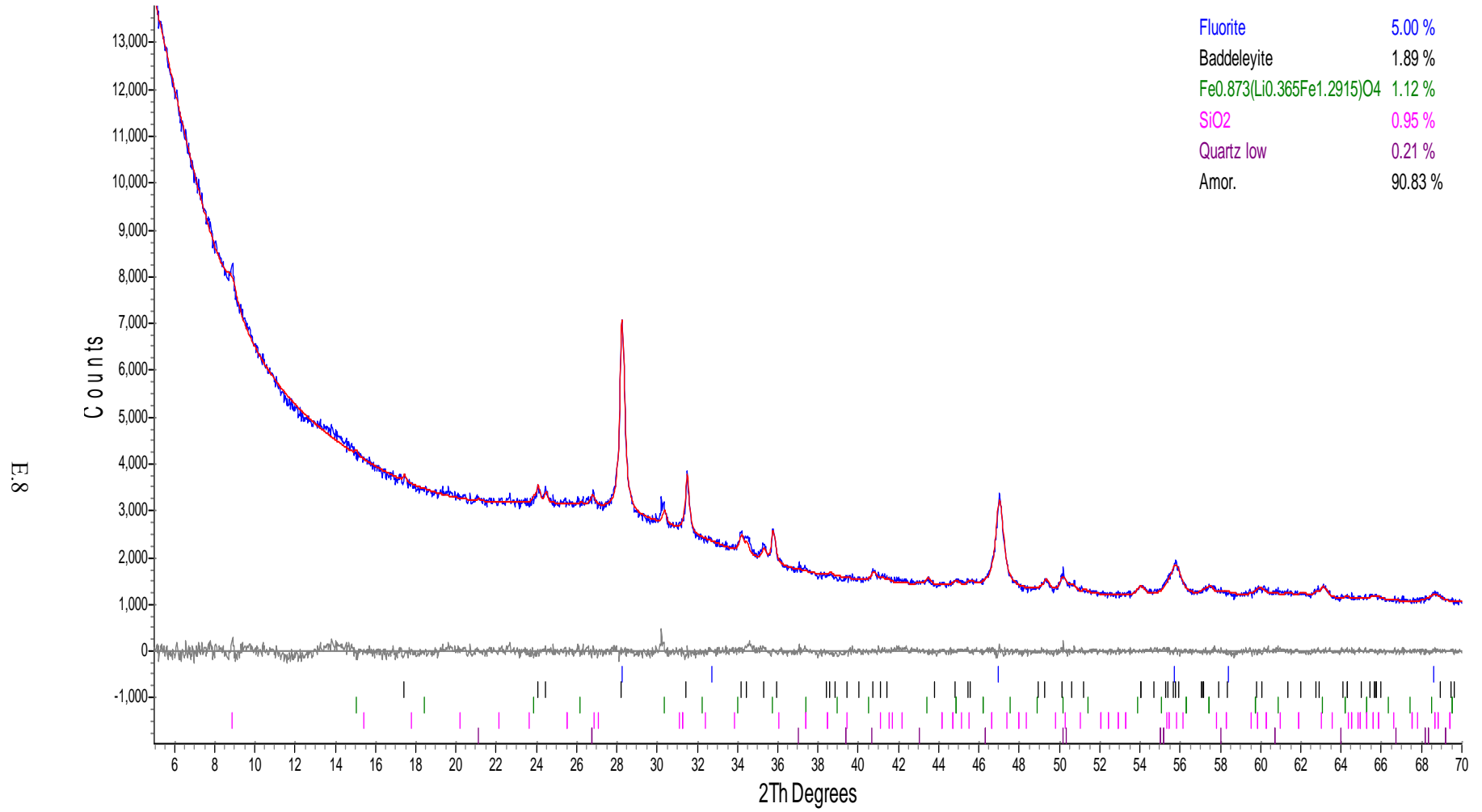


Figure E.7. XRD Spectrum of CCC-Treated Glass New-OL-8788(Mod)

NEW-OL-14844-CCC-Cc.raw_1

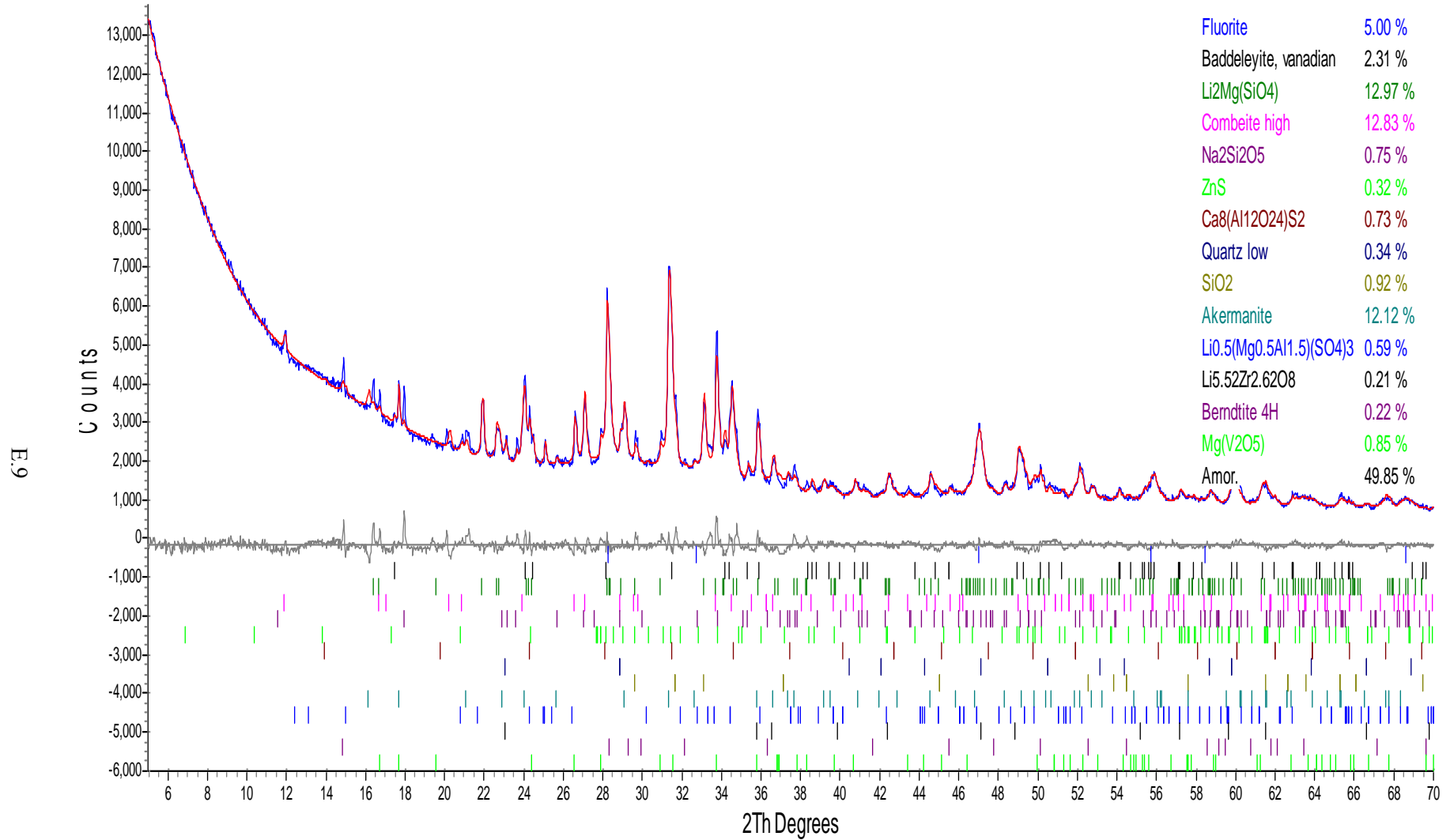


Figure E.8. XRD Spectrum of CCC-Treated Glass New-OL-14844

LAW-NEW-OL-15493-CCC-Cc.raw_1

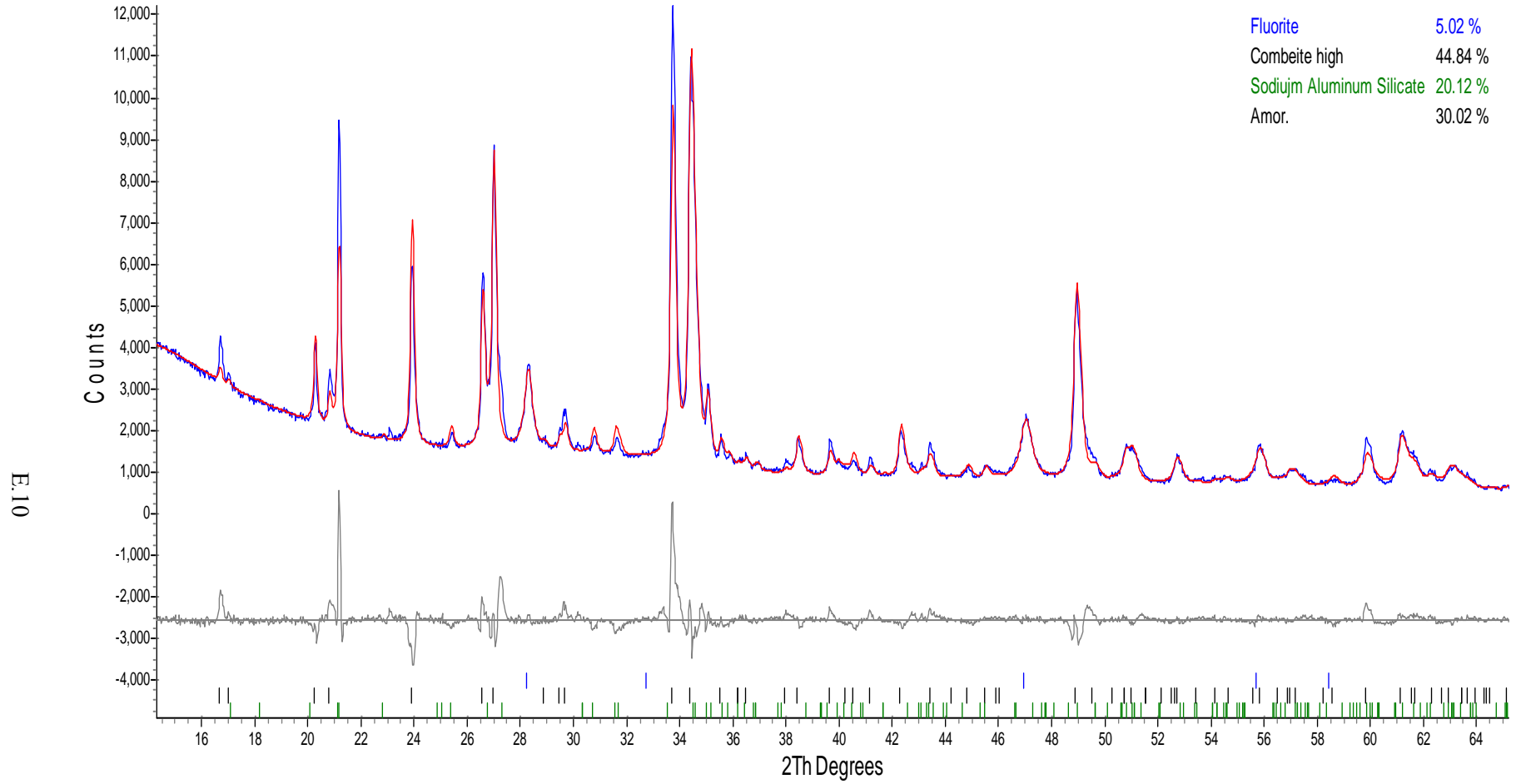


Figure E.9. XRD Spectrum of CCC-Treated Glass New-OL-15493

NEW-OL-45748wTinOxalate-CCC-Cc.raw_1

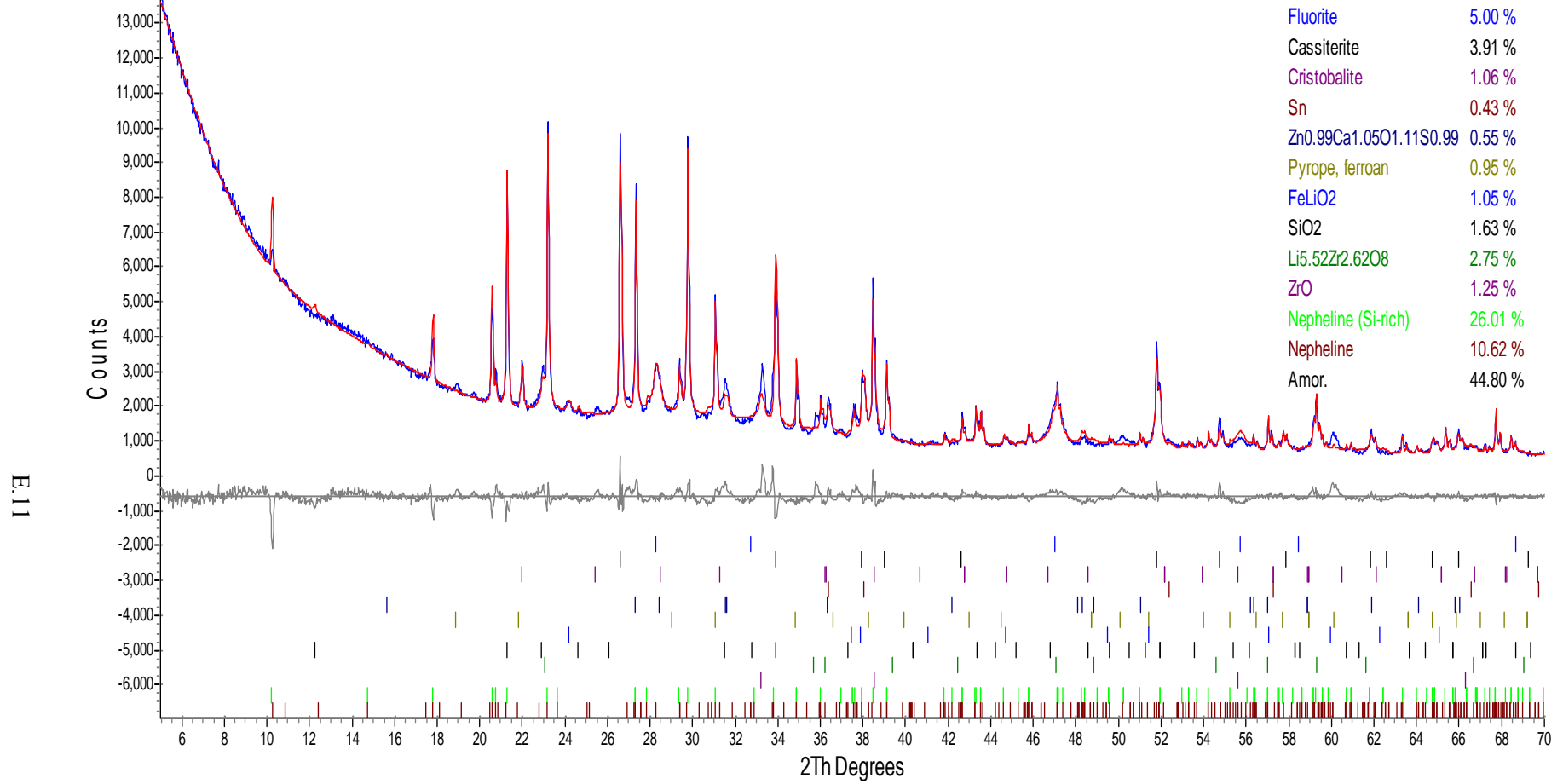


Figure E.10. XRD Spectrum of CCC-Treated Glass New-OL-45748 (Sn Mod)

LAW-NEW-OL-57284-CCC-Cc.raw_1

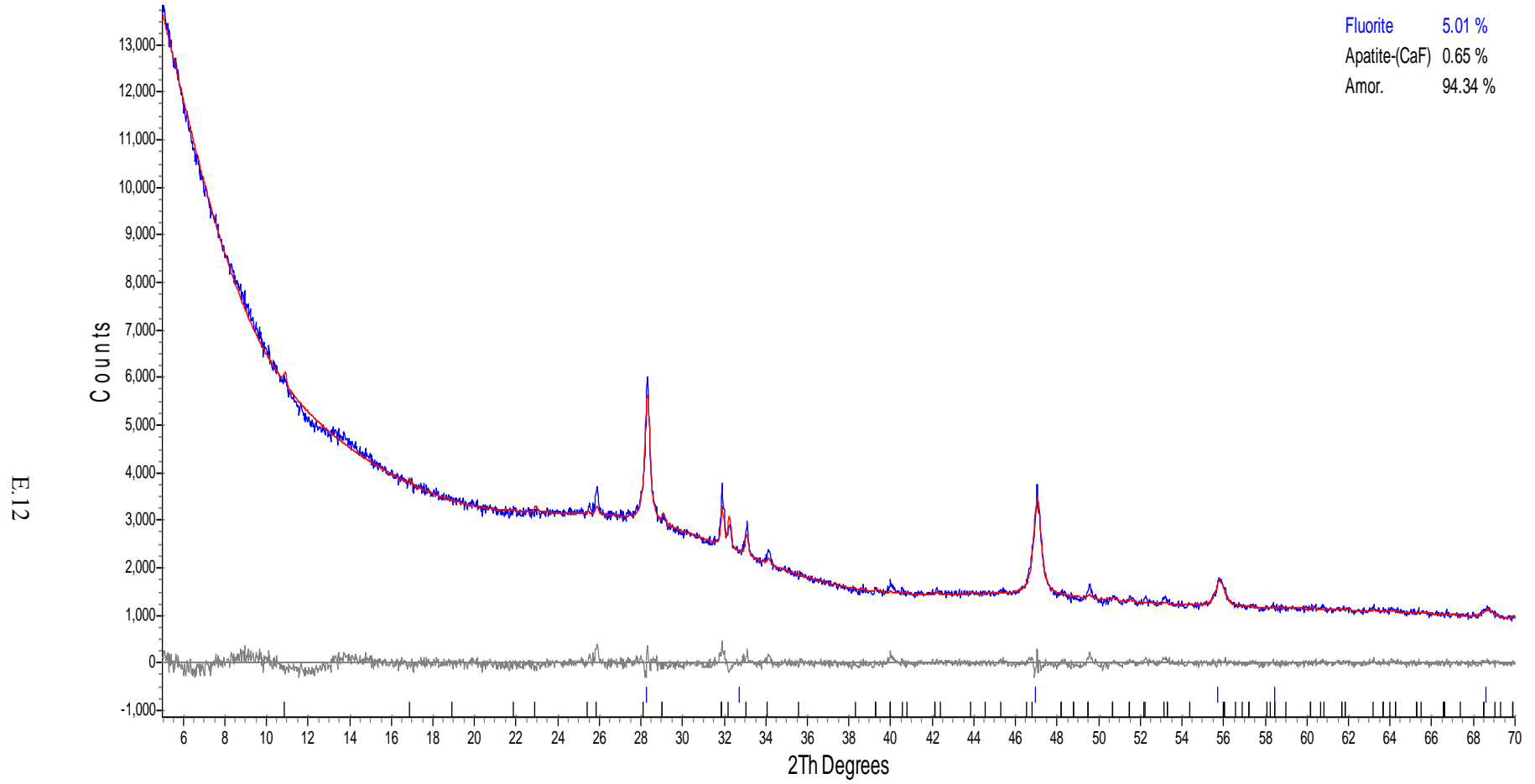


Figure E.11. XRD Spectrum of CCC-Treated Glass New-OL-57284

NEW-OL-62909-CCC-Cc.raw_1

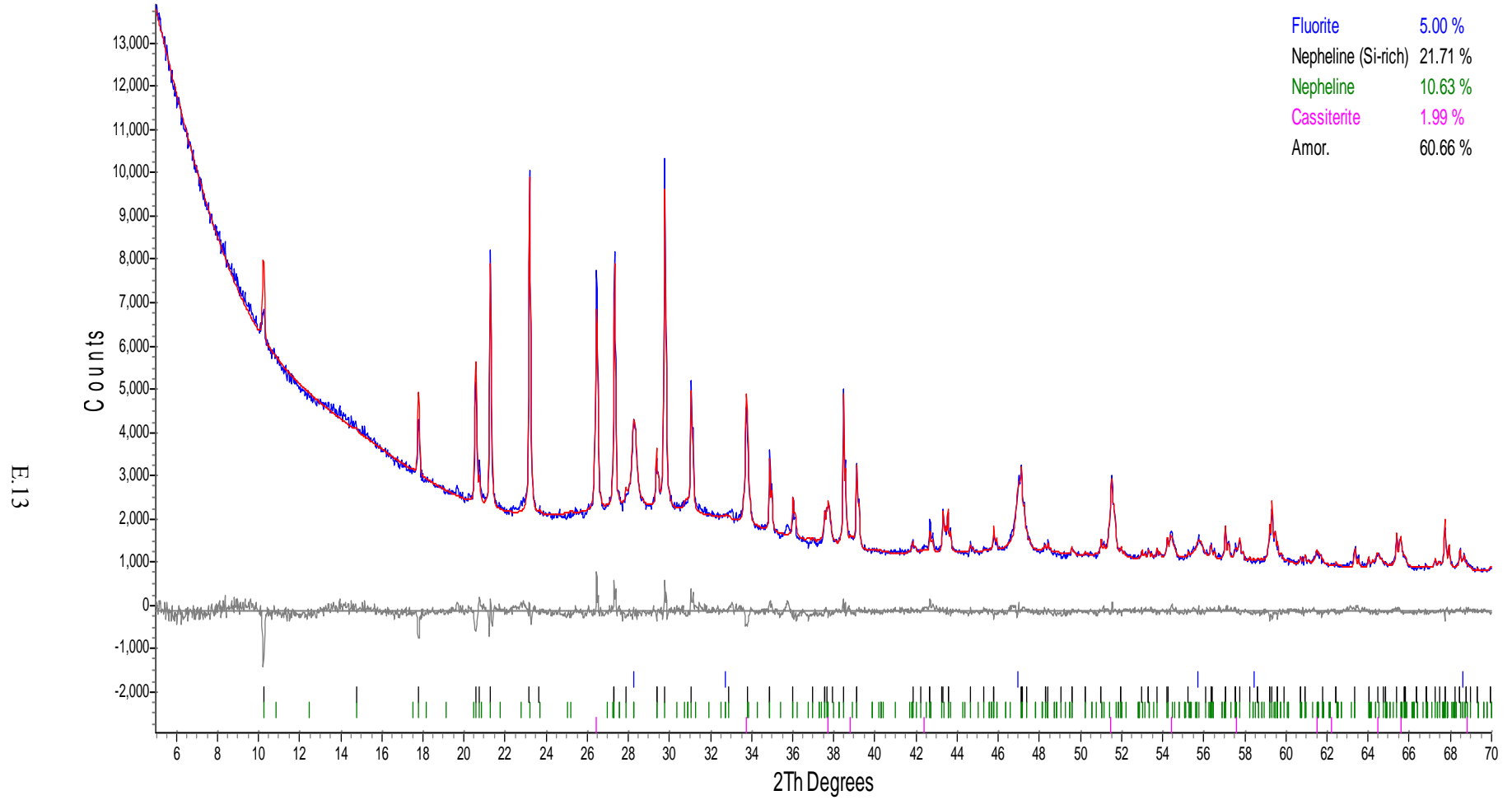
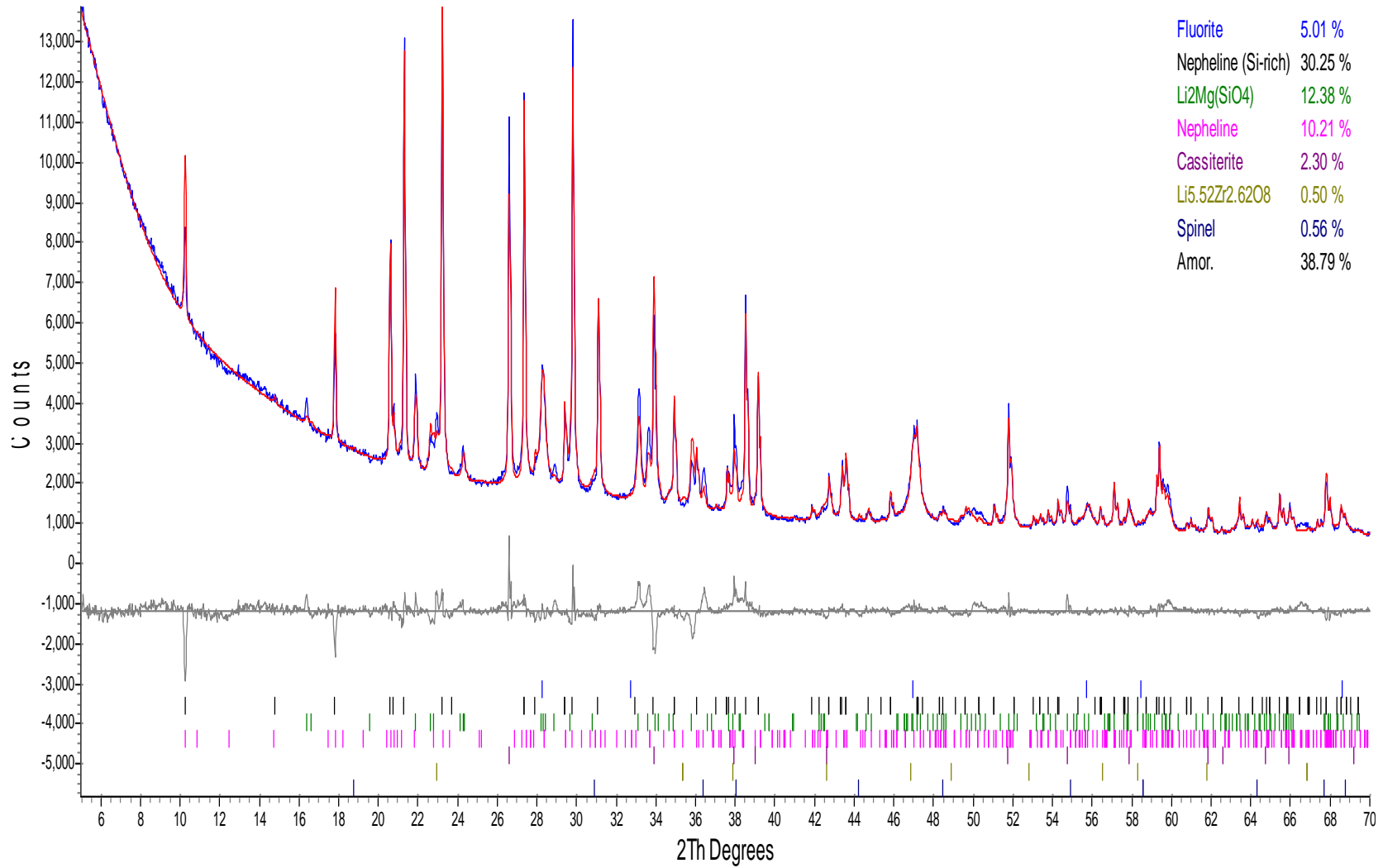


Figure E.12. XRD Spectrum of CCC-Treated Glass New-OL-62909(Mod)

NEW-OL-659559-CCC-Cc.raw_1



E.14

Figure E.13. XRD Spectrum of CCC-Treated Glass New-OL-65959(Mod)

NEW-OL-80309-CCC-Cc.raw_1

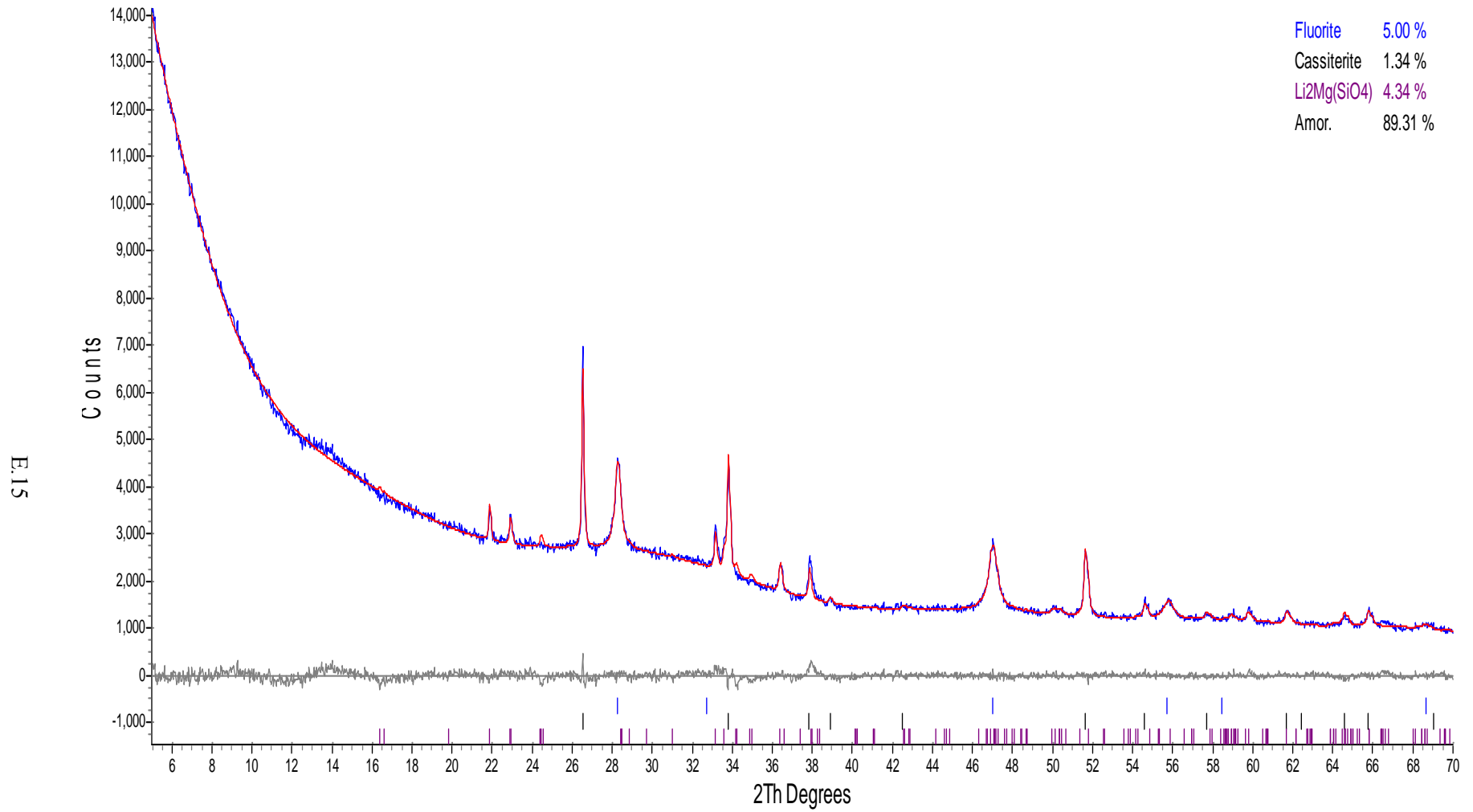


Figure E.14. XRD Spectrum of CCC-Treated Glass New-OL-80309

LAW-NEW-OL-90780-CCC-Cc.raw_1

E.16

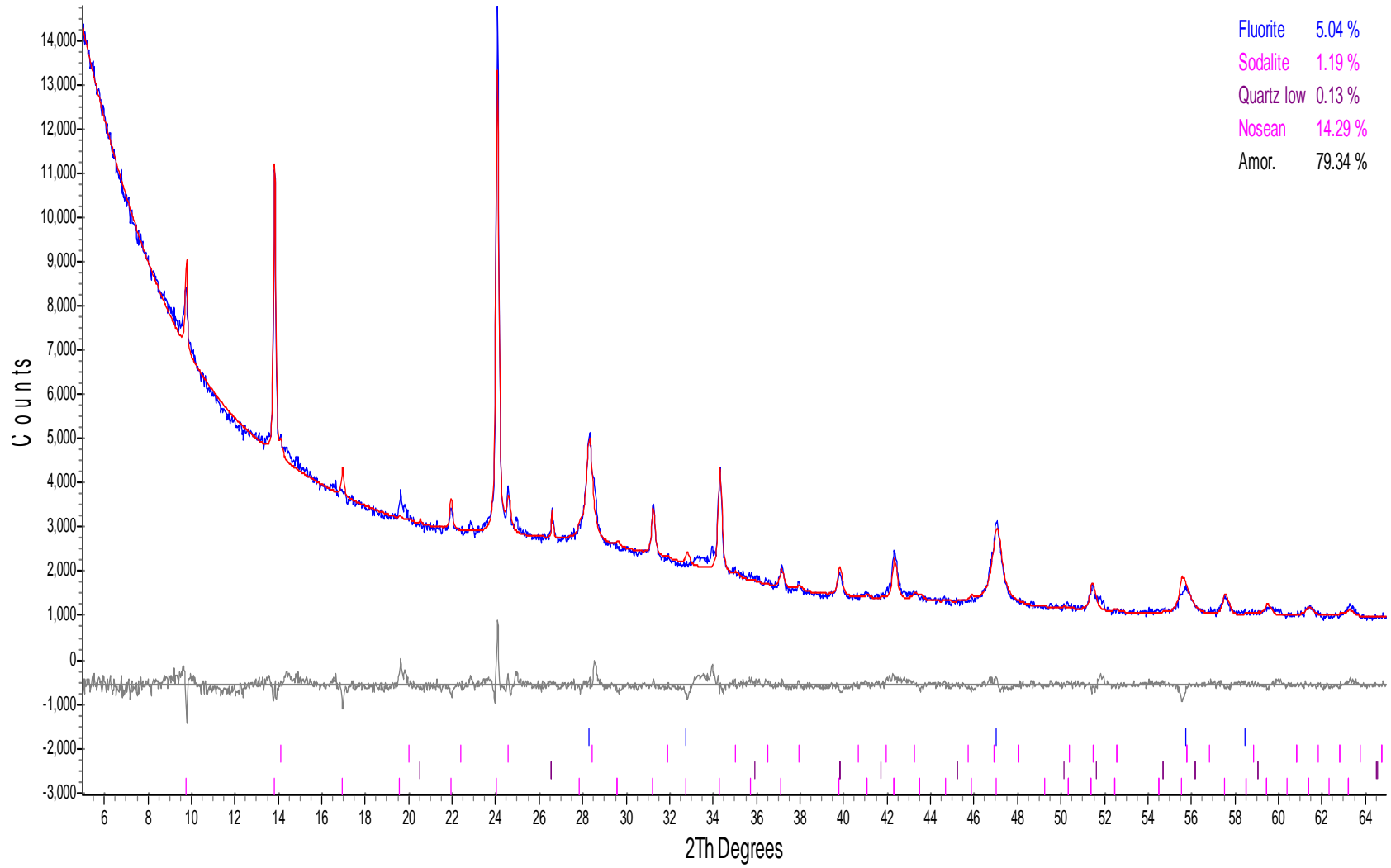


Figure E.15. XRD Spectrum of CCC-Treated Glass New-OL-90780

LAW-ORP-LDI(1)-CCC-Cc-1cm.raw_1

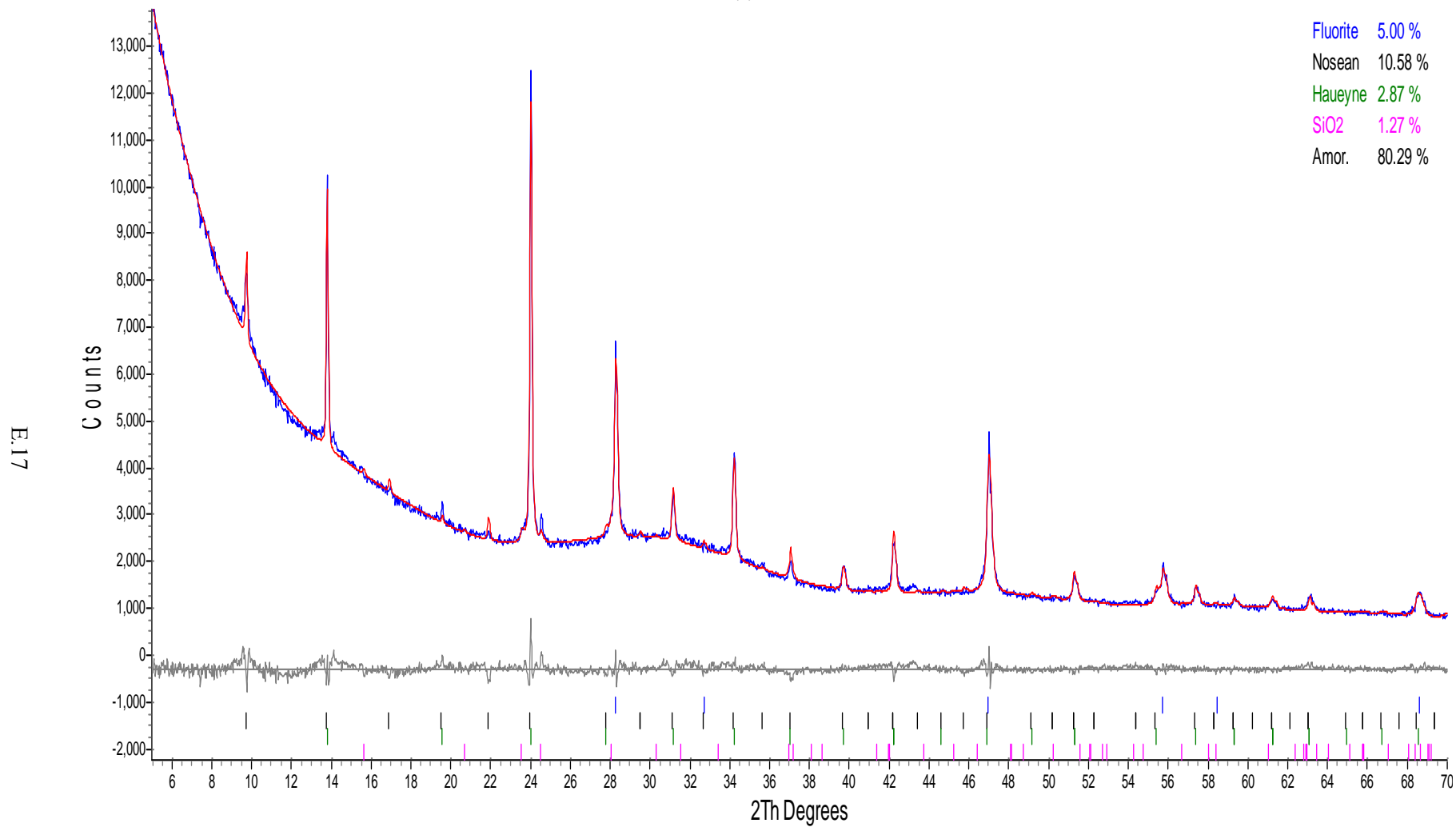


Figure E.16. XRD Spectrum of CCC-Treated Glass LAW-ORP-LDI-1

LAW-ORP-LDI(2)-CCC-Cc-1cm.raw_1

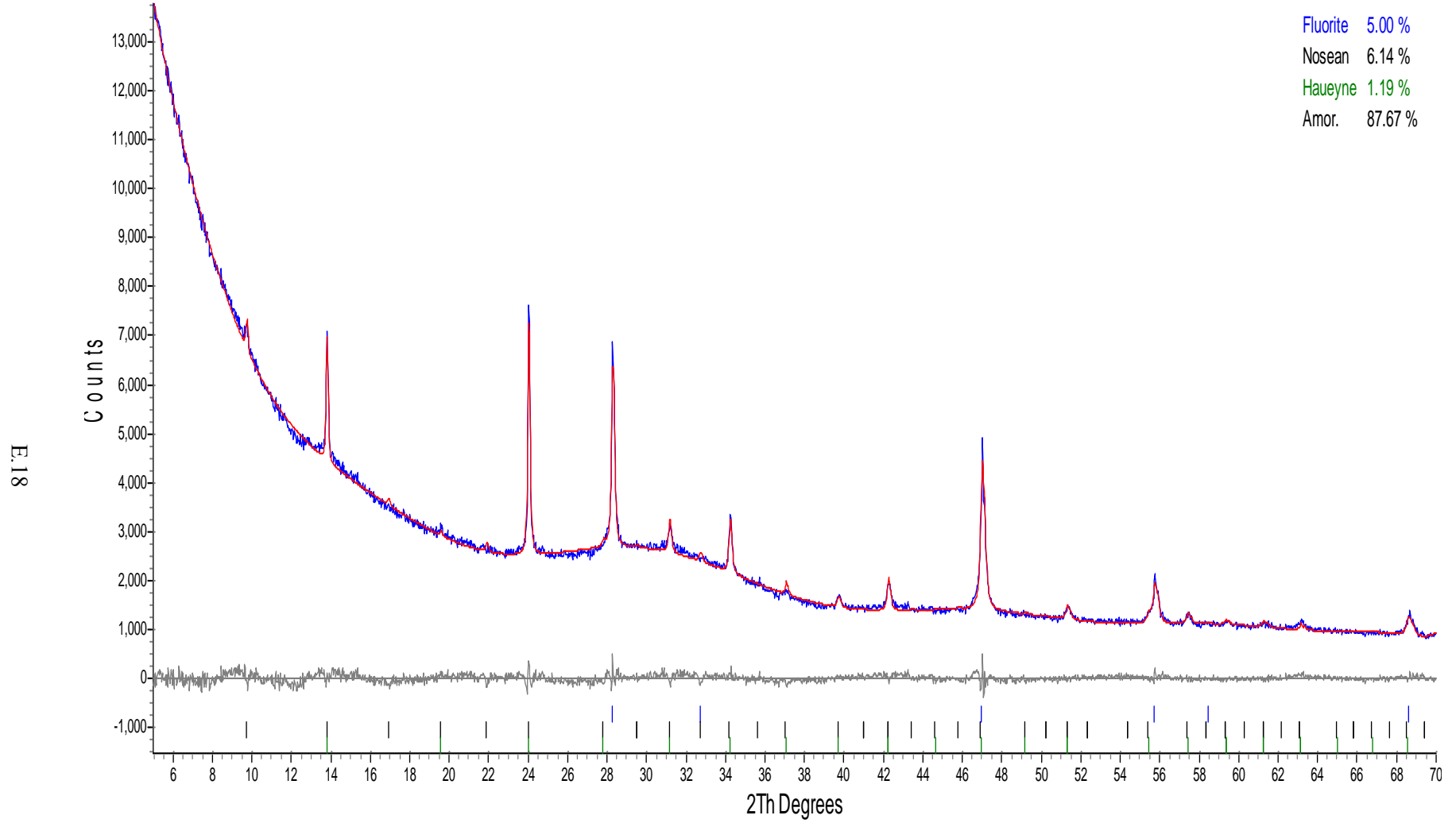


Figure E.17. XRD Spectrum of CCC-Treated Glass LAW-ORP-LD1-2

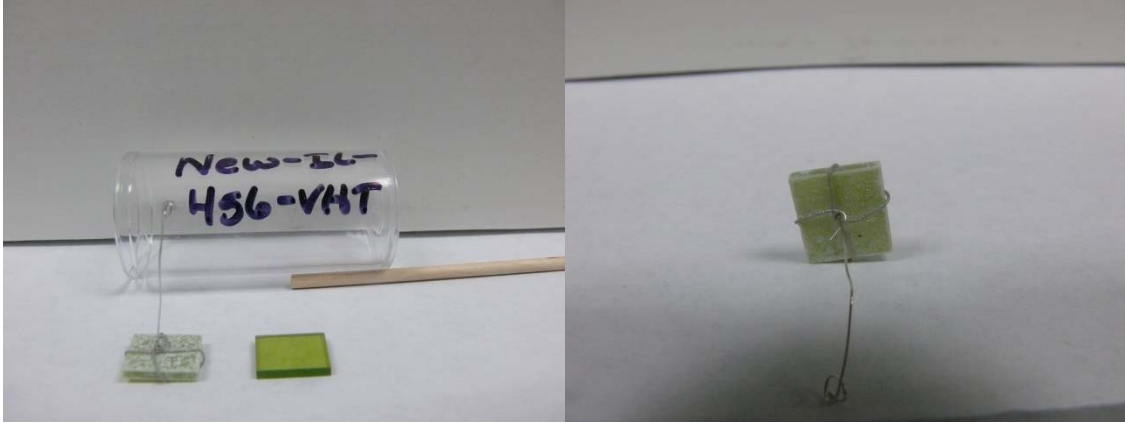
Appendix F

Vapor Hydration Test Results

Appendix F

Vapor Hydration Test Results

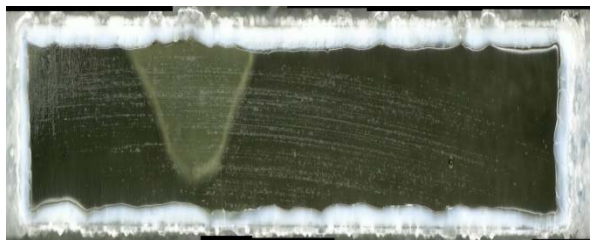
This appendix shows photos of the vapor hydration test (VHT) samples both before and after testing. The glasses tested performed either extremely well or extremely poor with only four glasses near the corrosion rate limit. These photos show the variation in corrosion with the samples.



a) Photo of glass square (1 cm) after and before VHT b) Photo of glass square (1 cm) after VHT



c) Micrograph of glass surface after VHT



d) Micrograph of glass cross section after VHT

Figure F.1. Glass New-IL-456 after VHT for 24 Days



Figure F.2. Photo of Glass New-IL-456 after VHT for 7 Days (left) and before VHT (right) (1 cm square)



a) Photo of glass square (1 cm) after and before VHT b) Photo of glass square (1 cm square) after VHT



c) Micrograph of glass surface after VHT

Figure F.3. Glass New-IL-1721 after VHT for 24 Days



a) Photo of glass square (1 cm) after VHT

b) Micrograph of glass surface after VHT



c) Micrograph of glass cross section after VHT

Figure F.4. Glass New-IL-1721 after VHT for 7 Days



a) Photo of glass square after (left) and before (right) VHT



b) Photo of glass square after VHT

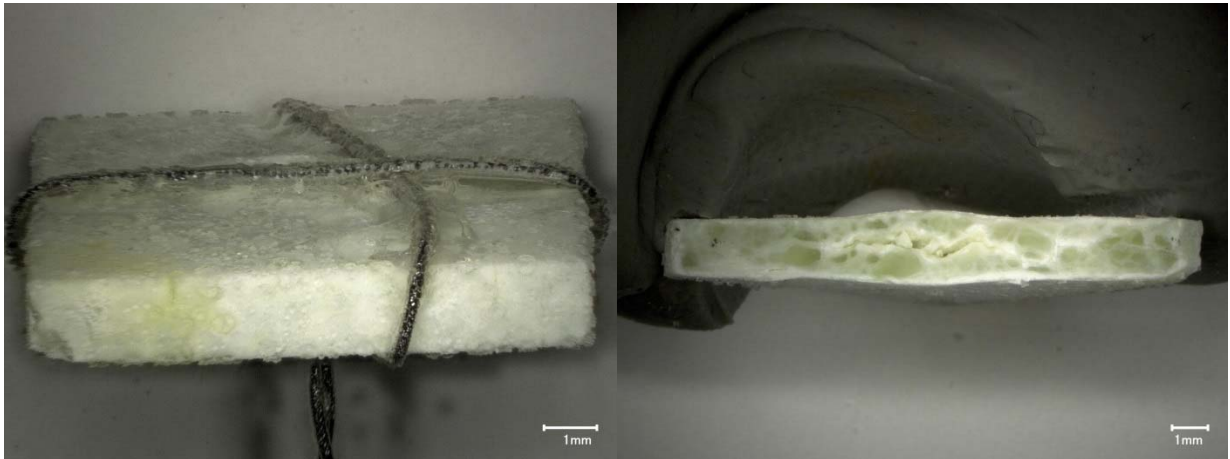


c) Micrograph of glass cross section after VHT

Figure F.5. Glass New-IL-5253 after VHT for 24 Days



a) Photo of glass square (1 cm) after and before VHT b) Photo of glass square (1 cm) after VHT

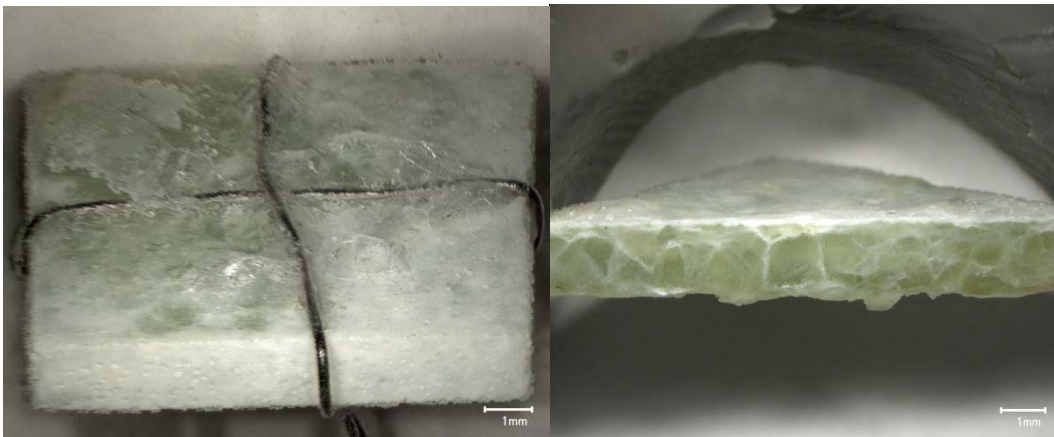


c) Micrograph of glass square after VHT d) Micrograph of glass cross section after VHT

Figure F.6. Glass New-IL-5255 after VHT for 24 Days



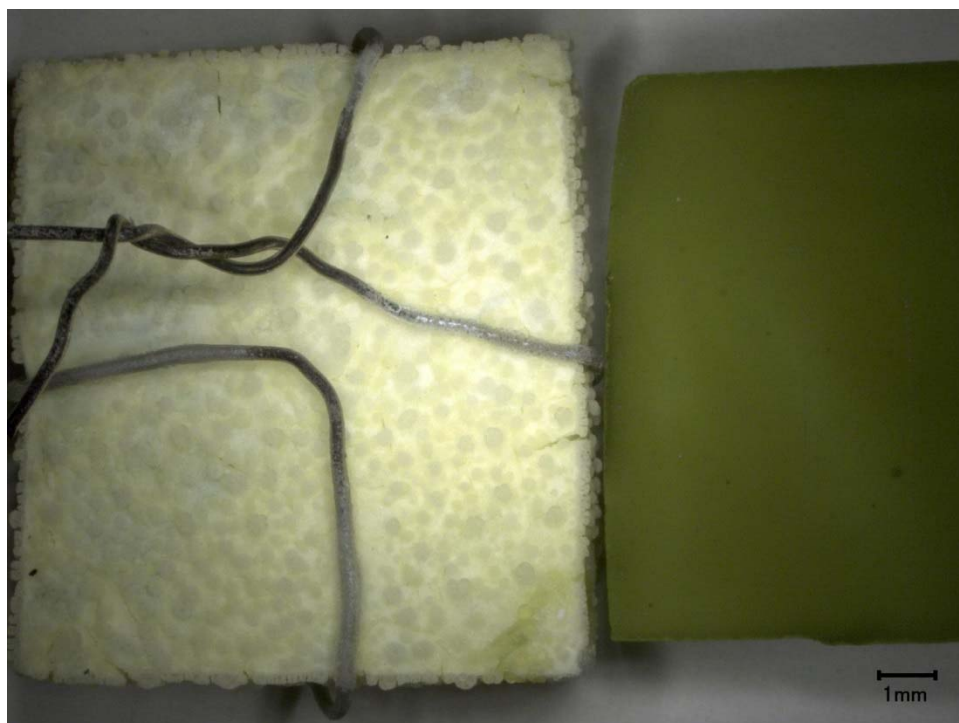
a) Photo of glass square after (left) and before (right) VHT



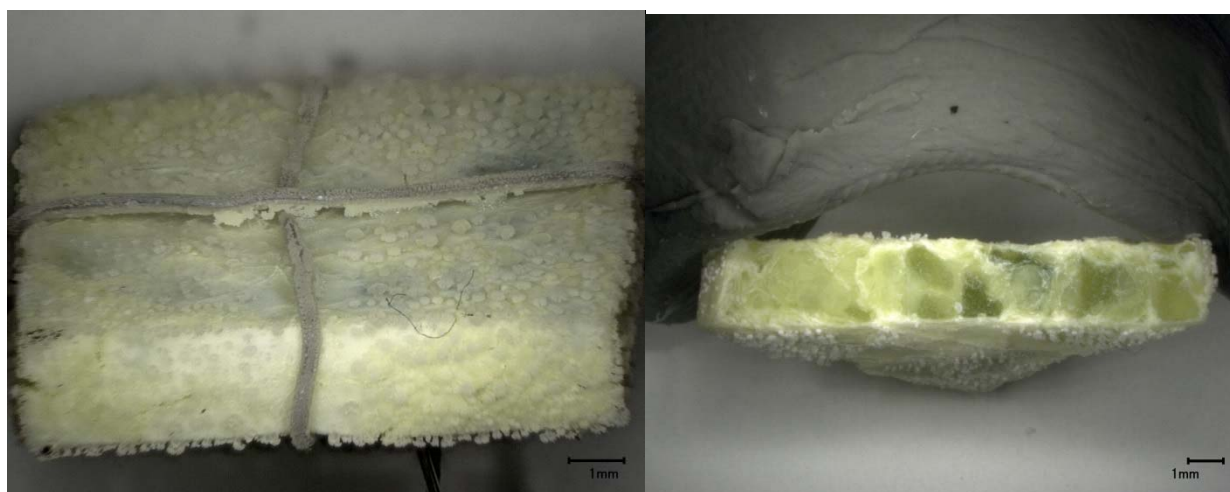
b) Photo of glass square after VHT

c) Micrograph of glass cross section after VHT

Figure F.7. Glass New-IL-5255 after VHT for 7 Days



a) Photo of glass square after (left) and before (right) VHT



b) Photo of glass square (1 cm) after VHT c) Micrograph of glass cross section after VHT

Figure F.8. Glass New-IL-42295 after VHT after 24 Days



a) Photo of glass square after (left) and before (right) VHT



b) Photo of glass square after VHT



c) Micrograph of glass cross section after VHT

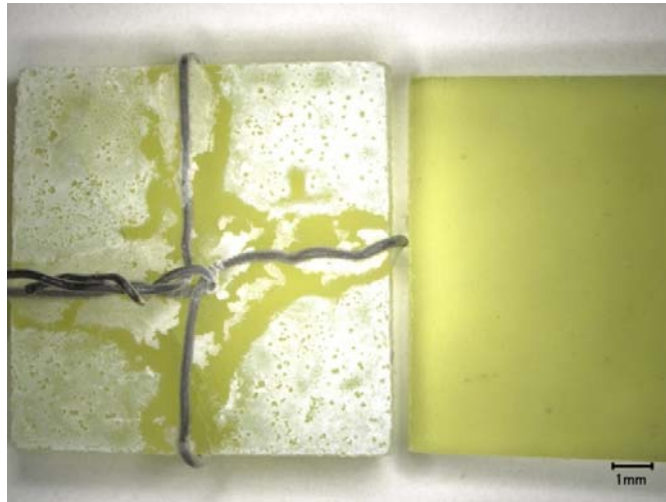
Figure F.9. Glass New-IL-42295 after VHT after 7 Days



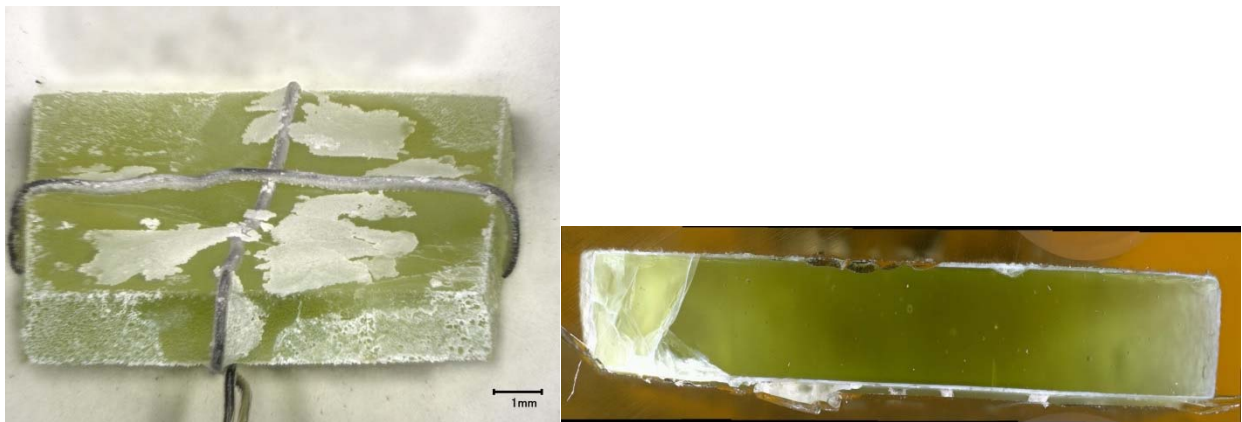
a) Photo of glass square after VHT

b) Micrograph of glass cross section after VHT

Figure F.10. Glass New-IL-70316 after VHT for 24 Days



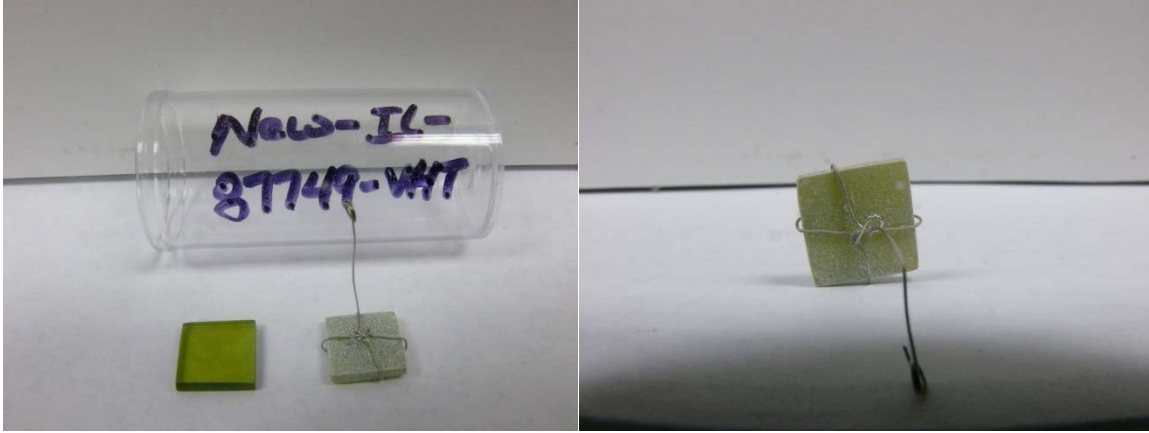
a) Photo of glass square after (left) and before (right) VHT



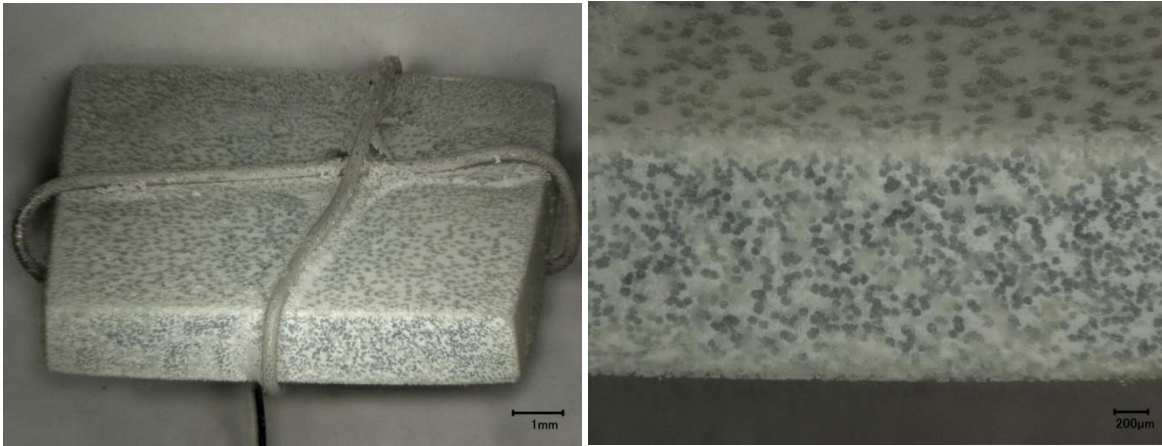
b) Photo of glass square after VHT

c) Micrograph of glass cross section after VHT

Figure F.11. Glass New-IL-70316 after VHT for 7 Days

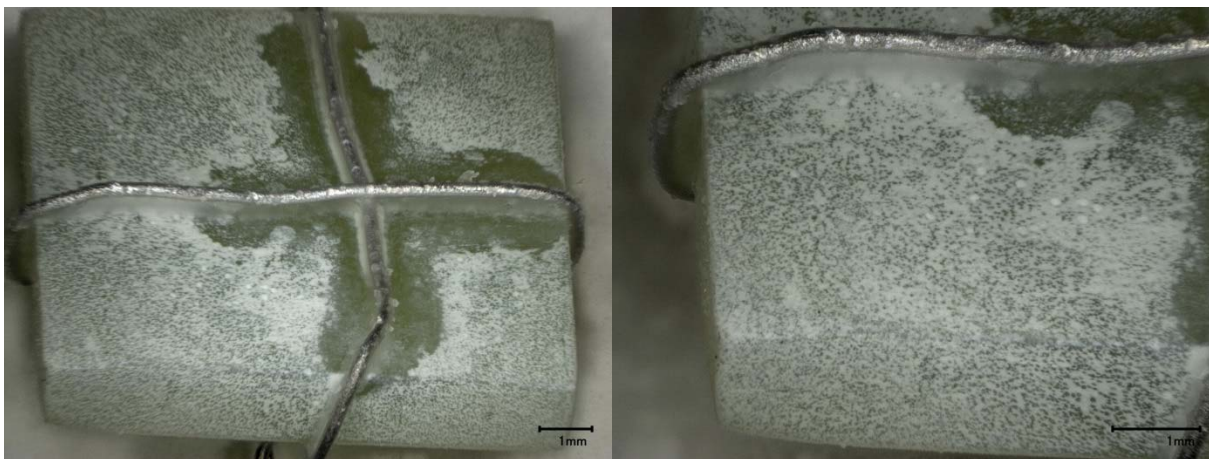


a) Photo of glass square (1 cm) before (left) and after (right) VHT b) Photo of glass square (1 cm) after VHT



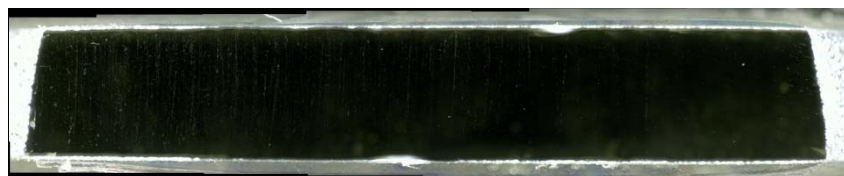
c) Micrograph of glass square after VHT d) Micrograph of glass surface after VHT

Figure F.12. Glass New-IL-87749 after VHT for 24 Days



a) Micrograph of glass square after VHT

b) Micrograph of glass surface after VHT



c) Micrograph of glass cross section after VHT

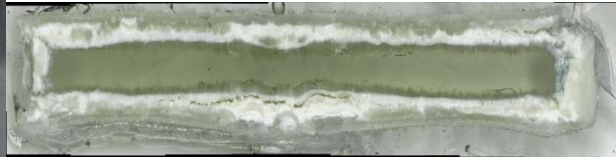
Figure F.13. Glass New-IL-87749 after VHT for 7 Days



a) Photo of glass square after (left) and before (right) VHT

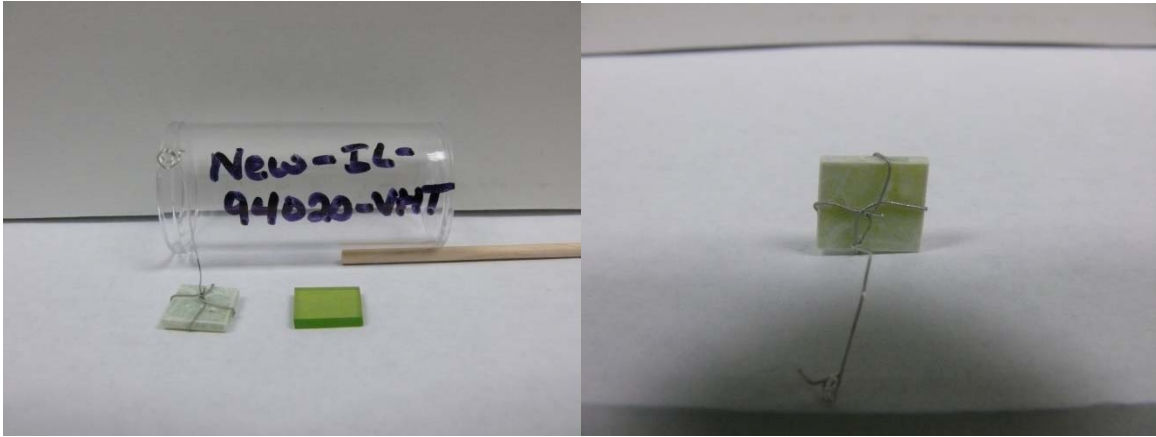


b) Micrograph of glass square after VHT

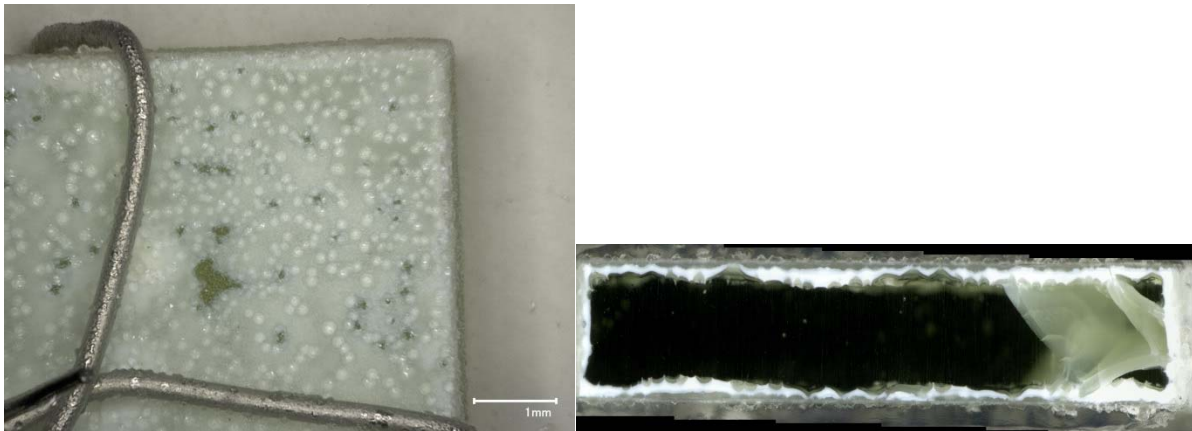


c) Micrograph of glass cross section after VHT

Figure F.14. Glass New-IL-93907 after VHT for 24 Days



a) Photo of glass square (1 cm) after (left) and before (right) VHT b) Photo of glass square (1 cm) after VHT



c) Micrograph of glass surface after VHT d) Micrograph of glass cross section after VHT

Figure F.15. Glass New-IL-94020 after VHT for 24 Days



a) Photo of glass square (1 cm) before (left) and after (right) VHT b) Photo of glass square (1 cm) after VHT



c) Micrograph of glass square after VHT

d) Micrograph of glass cross section after VHT

Figure F.16. Glass New-IL-103151 after VHT for 24 Days



a) Photo of glass square after (left) and before (right) VHT

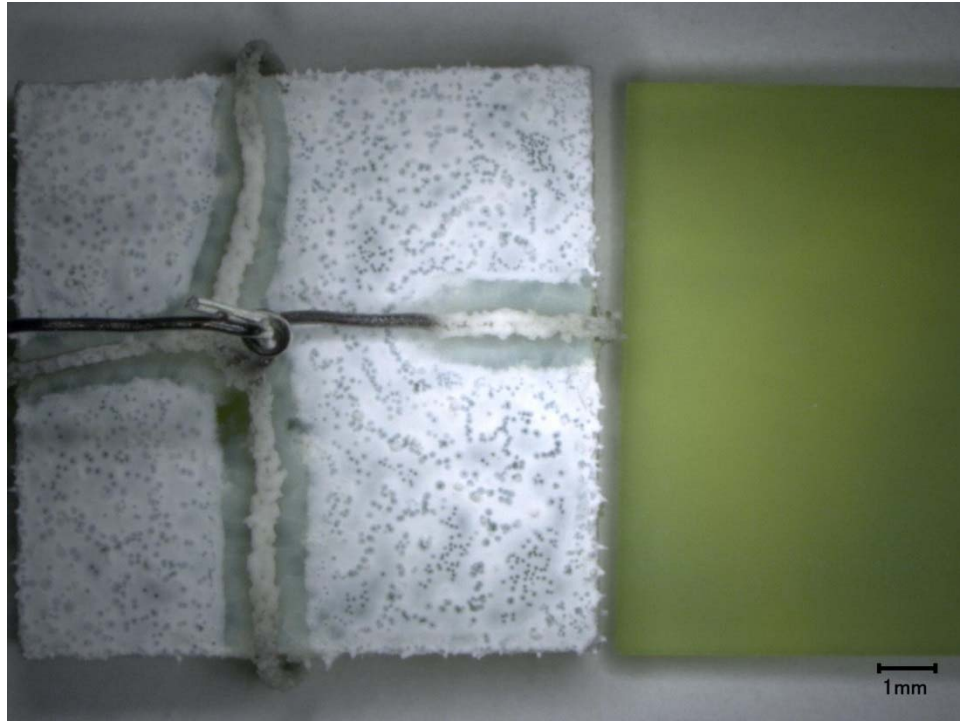


b) Micrograph of glass square after VHT



c) Micrograph of glass cross section after VHT

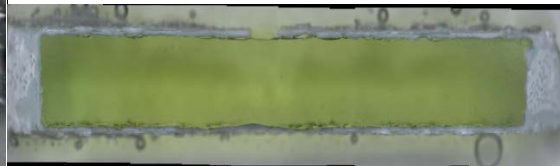
Figure F.17. Glass New-IL-103151 after VHT for 7 Days



a) Photo of glass square after (left) and before (right) VHT



b) Micrograph of glass square after VHT



c) Micrograph of glass cross section after VHT

Figure F.18. Glass New-IL-151542 after VHT for 24 Days



a) Micrograph of glass square after VHT

b) Micrograph of glass surface after VHT

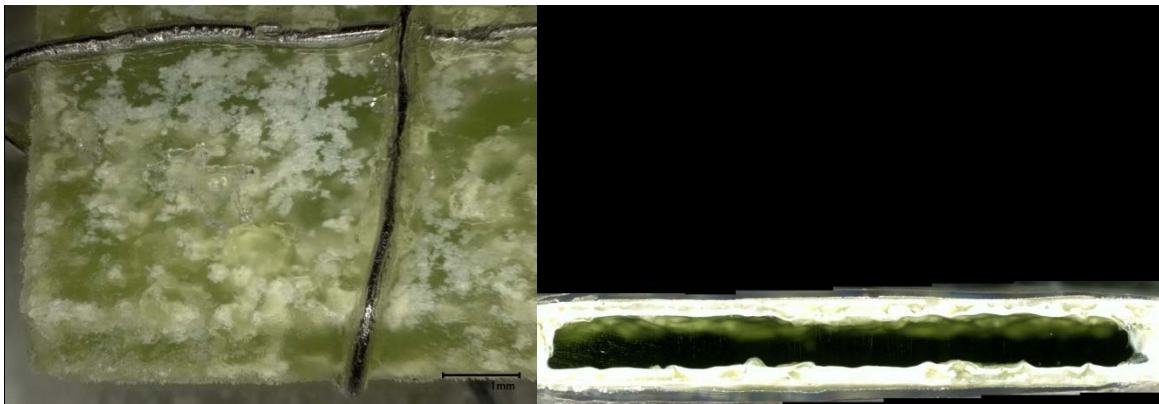


c) Micrograph of glass cross section after VHT

Figure F.19. Glass New-IL-166697 after VHT for 24 Days



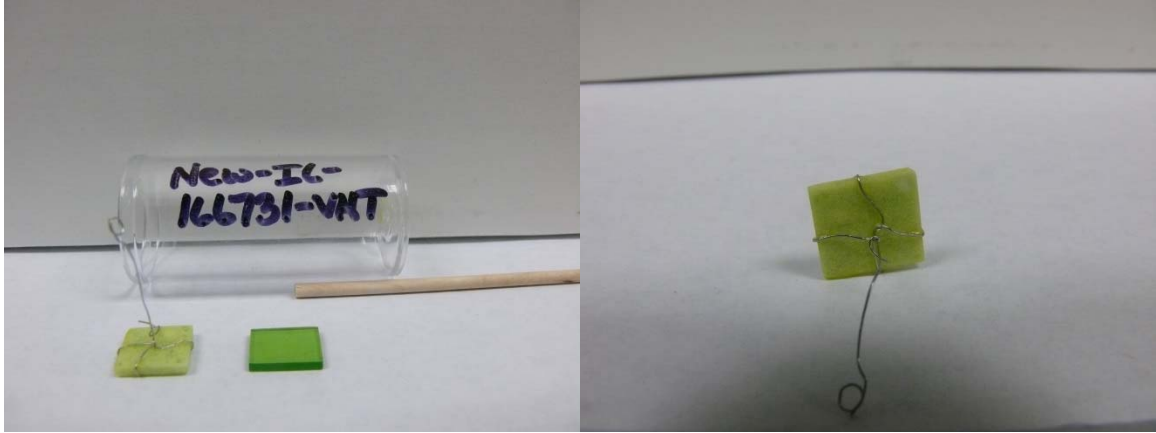
a) Micrograph of glass square after VHT



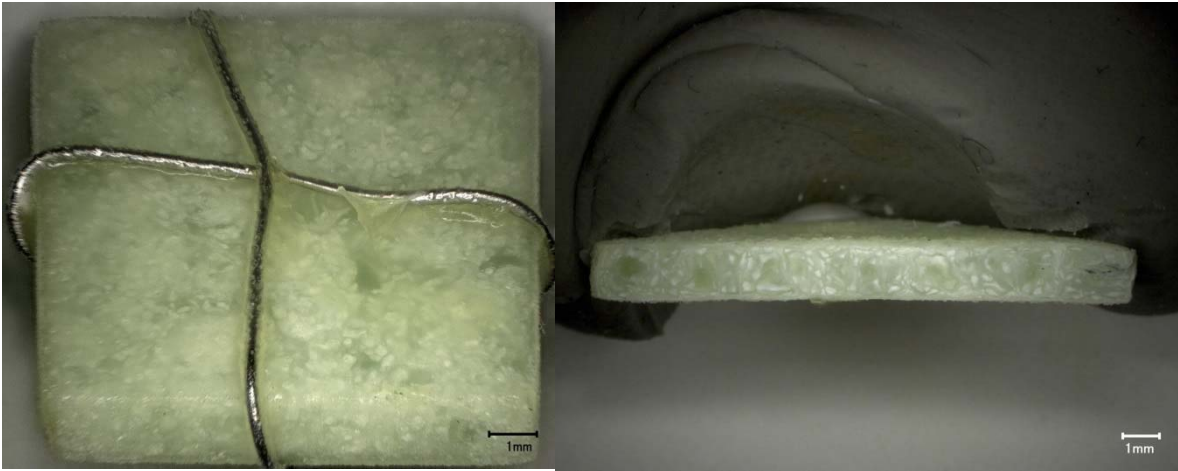
b) Micrograph of glass surface after VHT

c) Micrograph of glass cross section after VHT

Figure F.20. Glass New-IL-166697 after VHT for 7 Days



a) Photo of glass square (1 cm) after (left) and before (right) VHT b) Photo of glass square (1 cm) after VHT



c) Micrograph of glass square after VHT d) Micrograph of glass cross section after VHT

Figure F.21. Glass New-IL-166731 after VHT for 24 Days



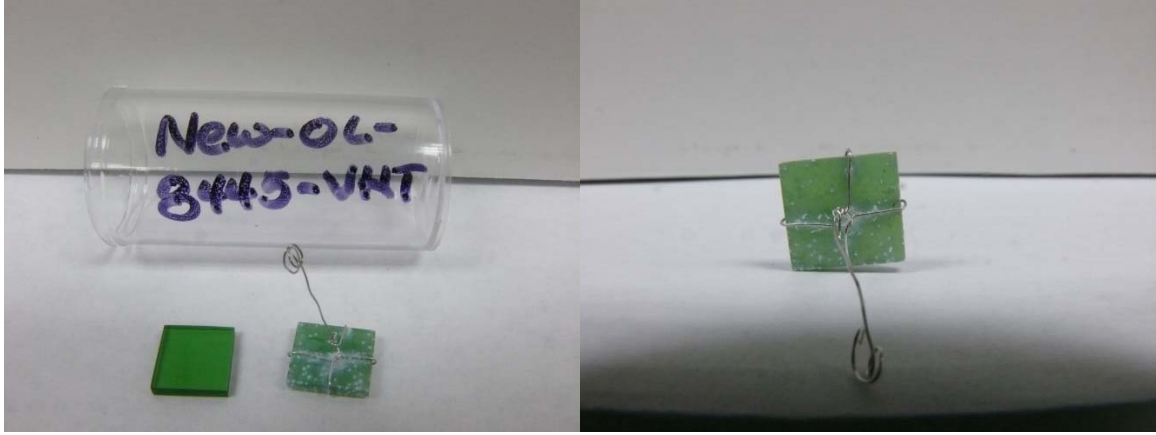
a) Micrograph of glass square after VHT

b) Micrograph of glass surface after VHT



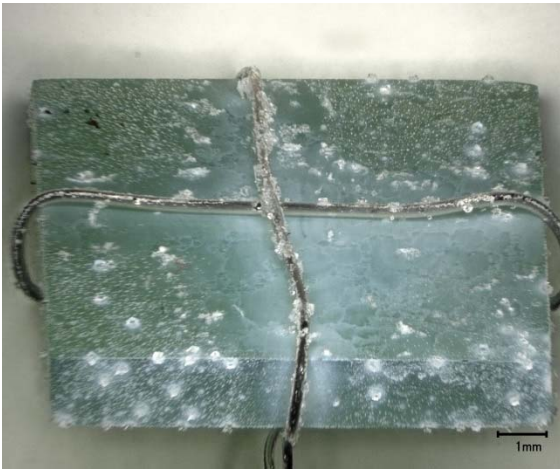
c) Micrograph of glass cross section after VHT

Figure F.22. Glass New-IL-166731 after VHT for 7 Days



a) Photo of glass square (1 cm) before (left) and after (right) VHT

b) Photo of glass square (1 cm) after VHT



c) Micrograph of glass square after VHT

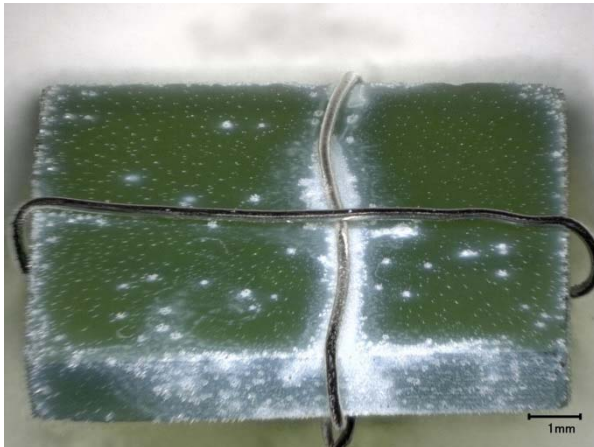


d) Micrograph of glass cross section after VHT

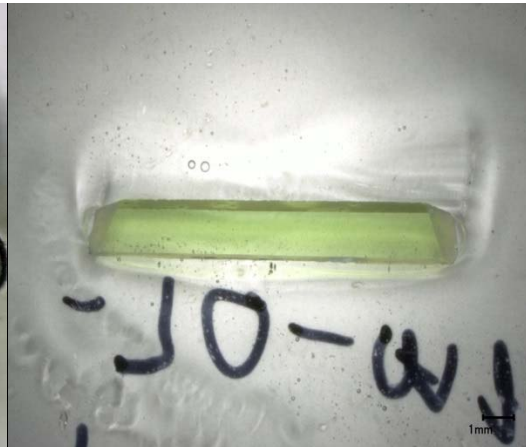
Figure F.23. Glass New-OL-8445 after VHT for 24 Days



a) Photo of glass square after (left) and before (right) VHT



c) Micrograph of glass square after VHT

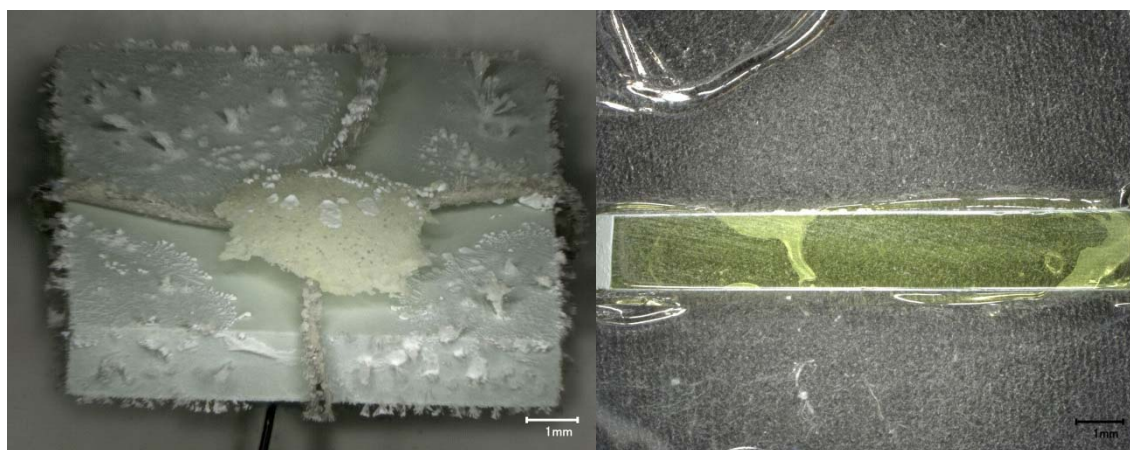


d) Micrograph of glass cross section after VHT

Figure F.24. Glass New-OL-8788(Mod) after VHT for 24 Days



a) Photo of glass square (1 cm) after (left) and before (right) VHT b) Photo of glass square (1 cm) after VHT



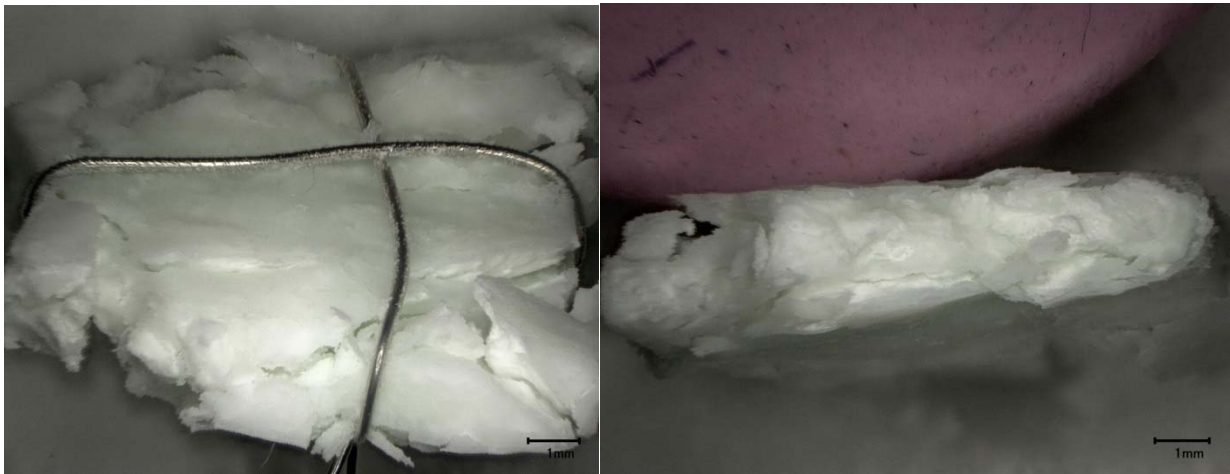
c) Micrograph of glass square after VHT

d) Micrograph of glass cross section after VHT

Figure F.25. Glass New-OL-14844 after VHT for 24 Days

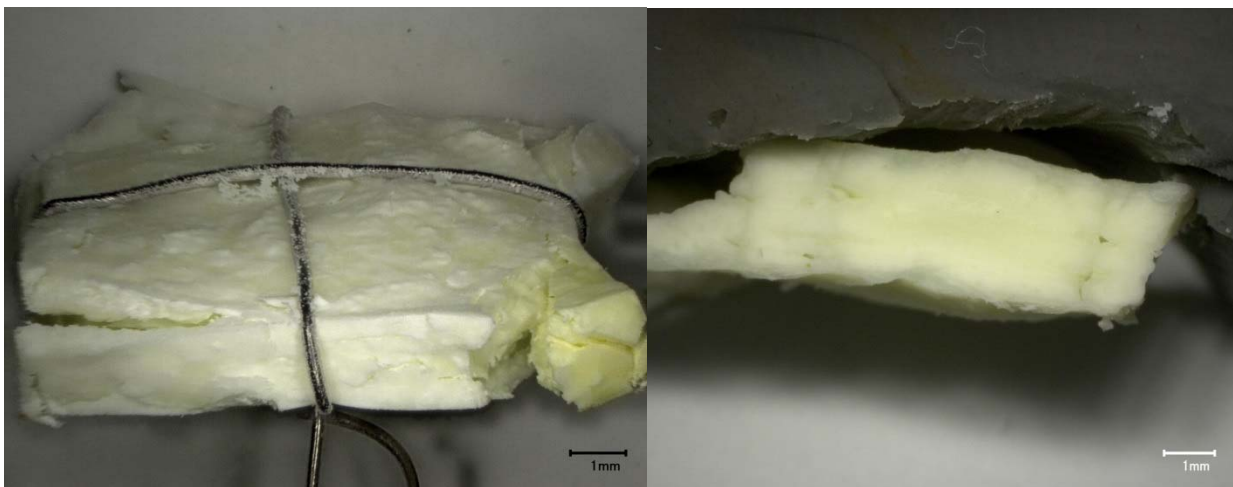


a) Photo of glass square (1 cm) before (left) and after (right) VHT b) Photo of glass square (1 cm) after VHT



c) Micrograph of glass square after VHT d) Micrograph of glass cross section magnified after VHT

Figure F.26. Glass New-OL-15493 after VHT for 24 Days



a) Micrograph of glass square after VHT b) Micrograph of glass cross section after VHT

Figure F.27. Glass New-OL-15493 after VHT for 7 Days



a) Photo of glass square after (left) and before (right) VHT

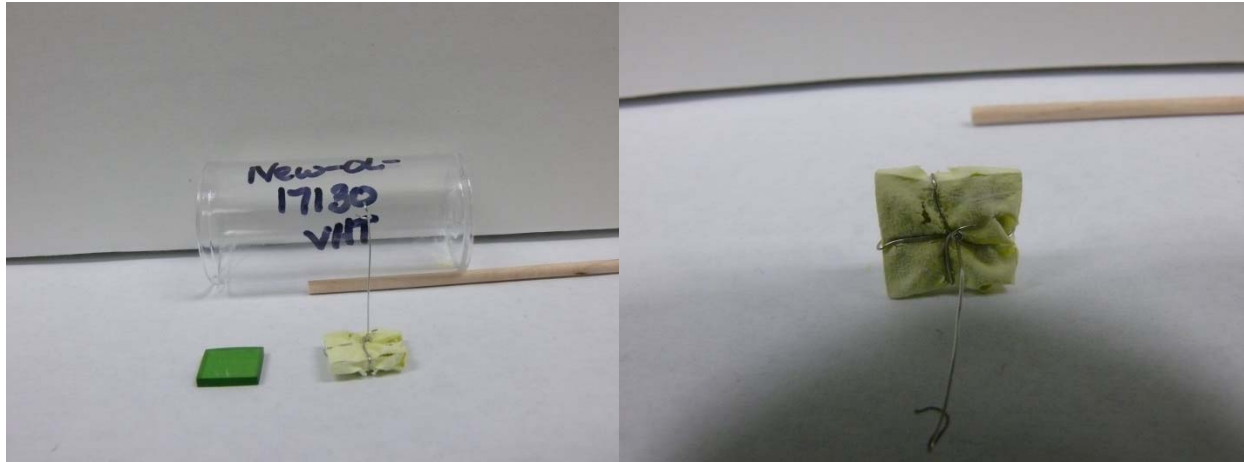


b) Micrograph of glass square after VHT



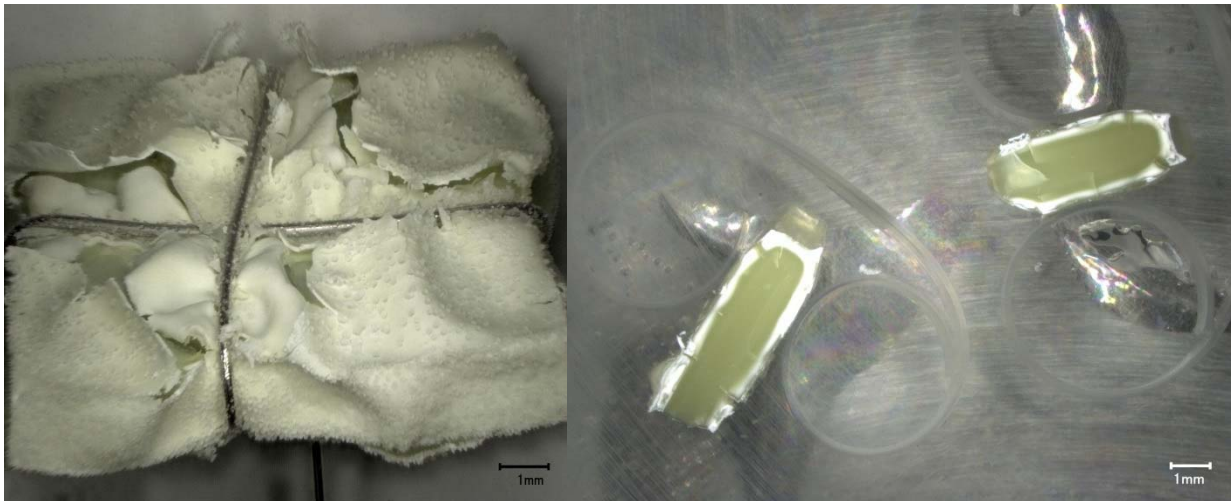
c) Micrograph of glass cross section after VHT

Figure F.28. Glass New-OL-15493 after VHT for 1 Day



a) Photo of glass square (1 cm) before (left) and after (right) VHT

b) Photo of glass square (1 cm) after VHT



c) Micrograph of glass square after VHT

d) Micrograph of glass cross section after VHT

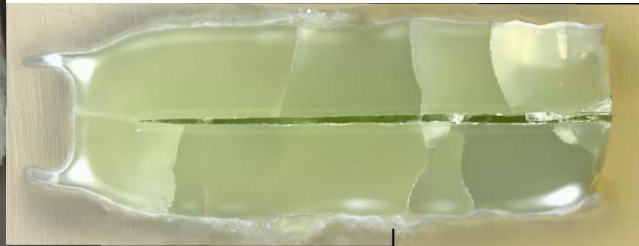
Figure F.29. Glass New-OL-17130 after VHT after 24 Days



a) Photo of glass square after (left) and before (right) VHT



b) Micrograph of glass square after VHT

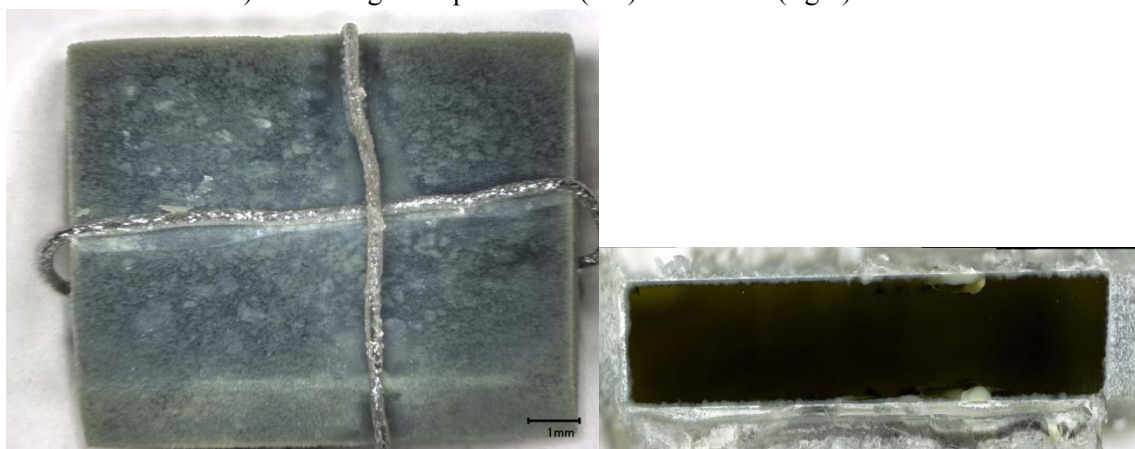


c) Micrograph of glass cross section after VHT

Figure F.30. Glass New-OL-17130 after VHT after 7 Days



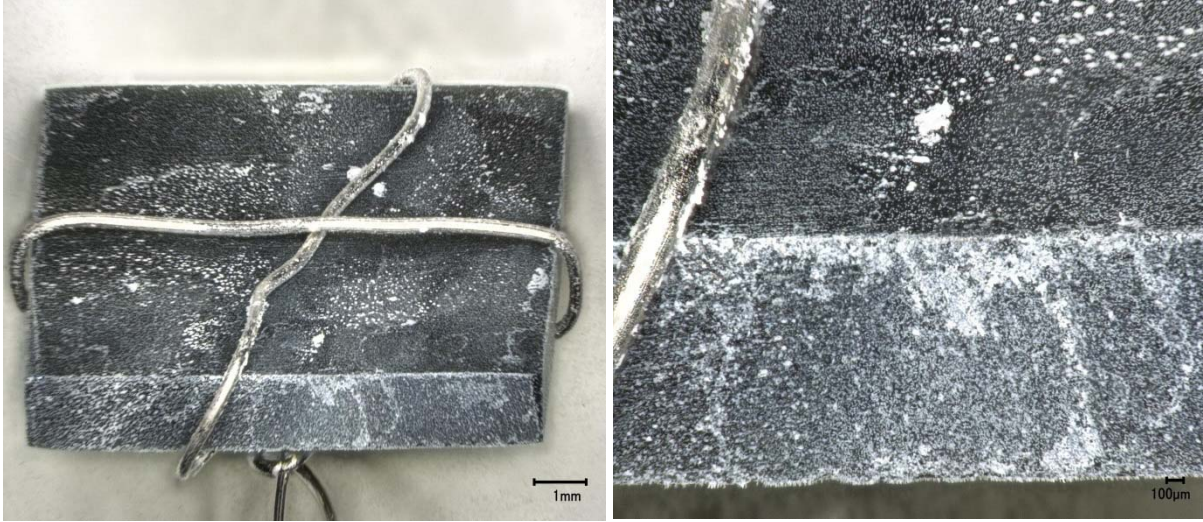
a) Photo of glass square after (left) and before (right) VHT



b) Micrograph of glass square after VHT

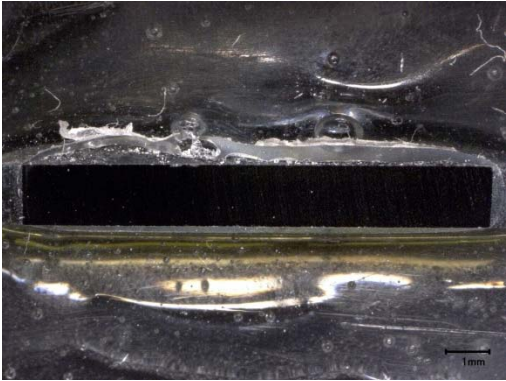
c) Micrograph of glass cross section after VHT

Figure F.31. Glass New-OL-45748 (with Tin Oxalate) after VHT after 24 Days



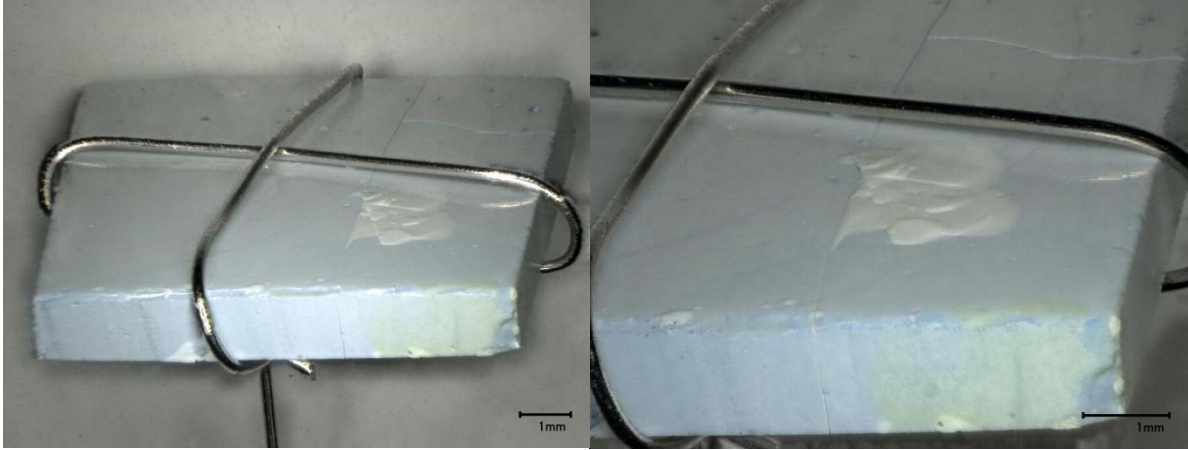
a) Micrograph of glass square after VHT

b) Micrograph of glass surface after VHT



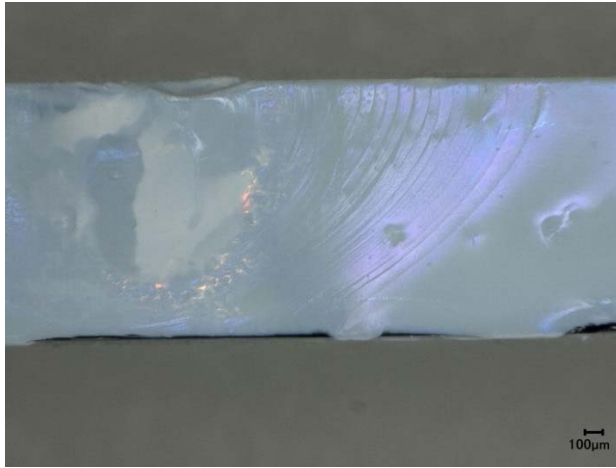
c) Micrograph of glass cross section after VHT

Figure F.32. Glass New-OL-54017 (with Tin Oxalate) after VHT for 24 Days



a) Micrograph of glass square after VHT

b) Micrograph of glass surface after VHT



c) Micrograph of glass cross section after VHT

Figure F.33. Glass New-OL-57284 after VHT for 24 Days



a) Photo of glass square after (left) and before (right) VHT

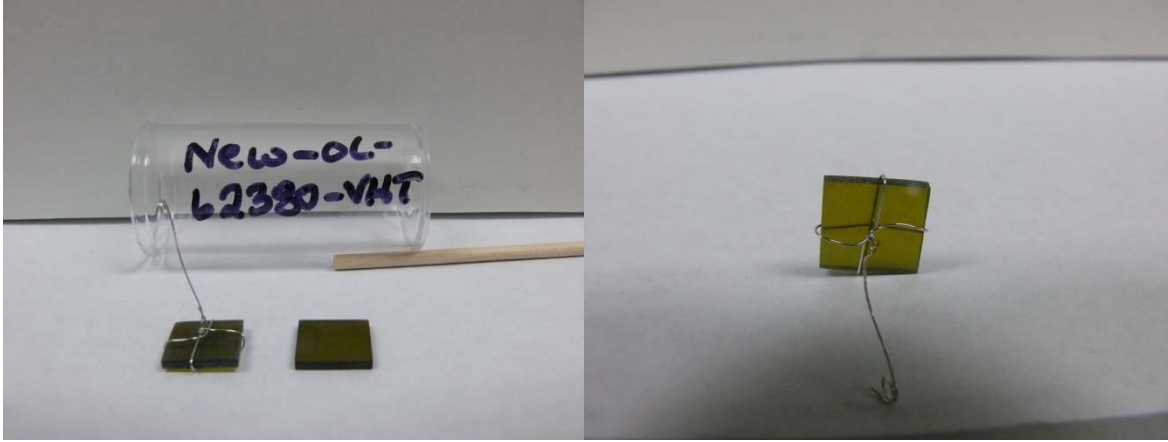


b) Micrograph of glass square after VHT



c) Micrograph of glass cross section after VHT

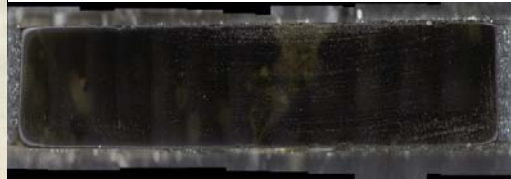
Figure F.34. Glass New-OL-57284 after VHT for 7 Days



a) Photo of glass square (1 cm) after (left) and before (right) VHT b) Photo of glass square (1 cm) after VHT



c) Micrograph of glass square after VHT

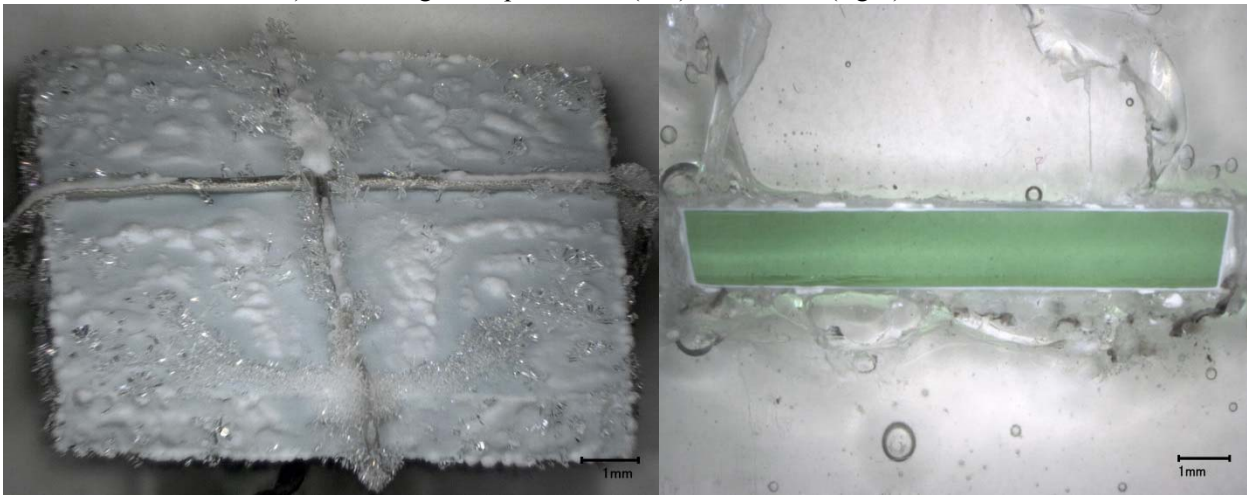


d) Micrograph of glass cross section after VHT

Figure F.35. Glass New-OL-62380 after VHT for 24 Days



a) Photo of glass square after (left) and before (right) VHT



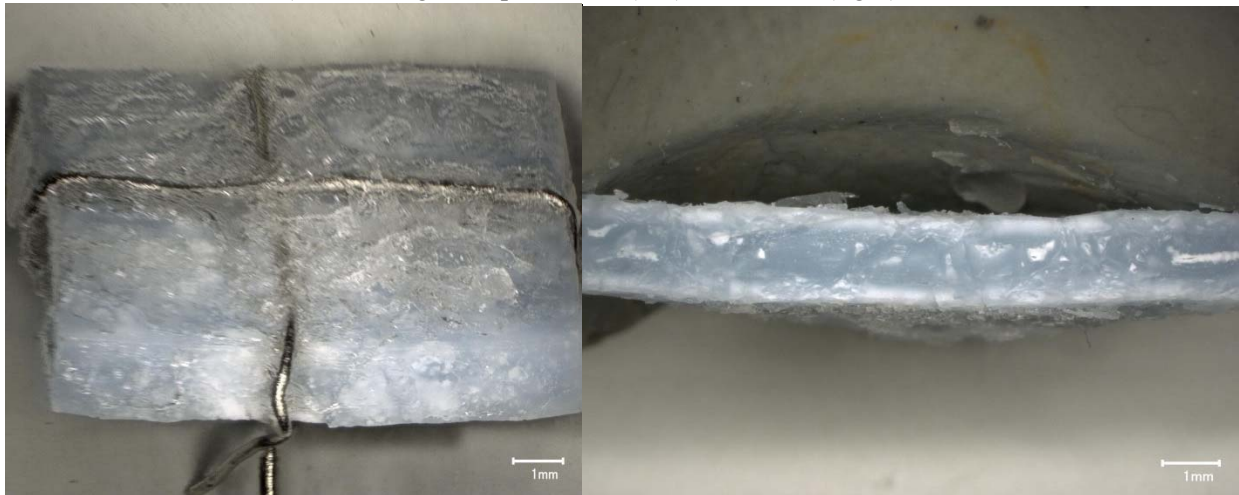
b) Micrograph of glass square after VHT

c) Micrograph of glass cross section after VHT

Figure F.36. Glass New-OL-62909(Mod) after VHT for 24 Days



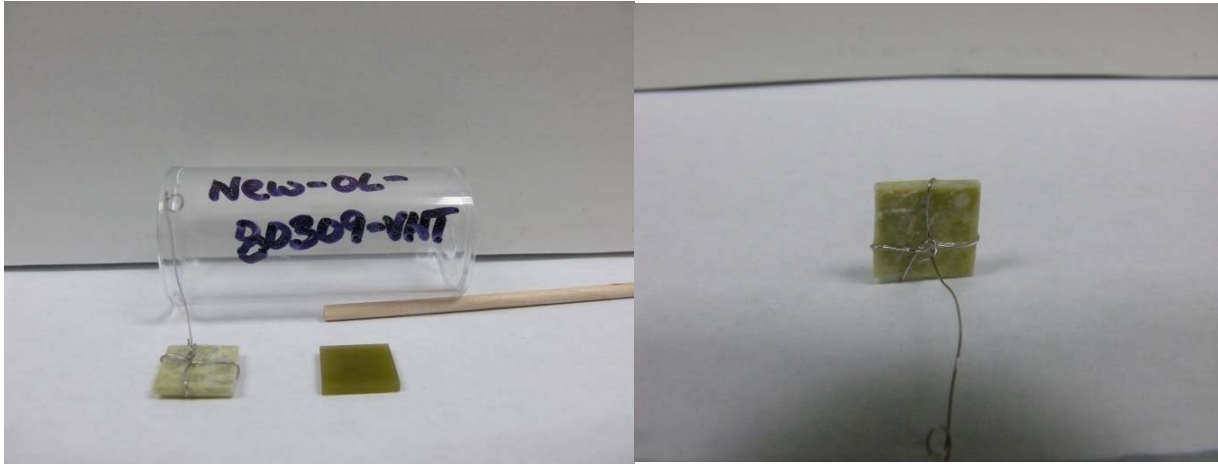
a) Photo of glass square after (left) and before (right) VHT



b) Micrograph of glass square after VHT

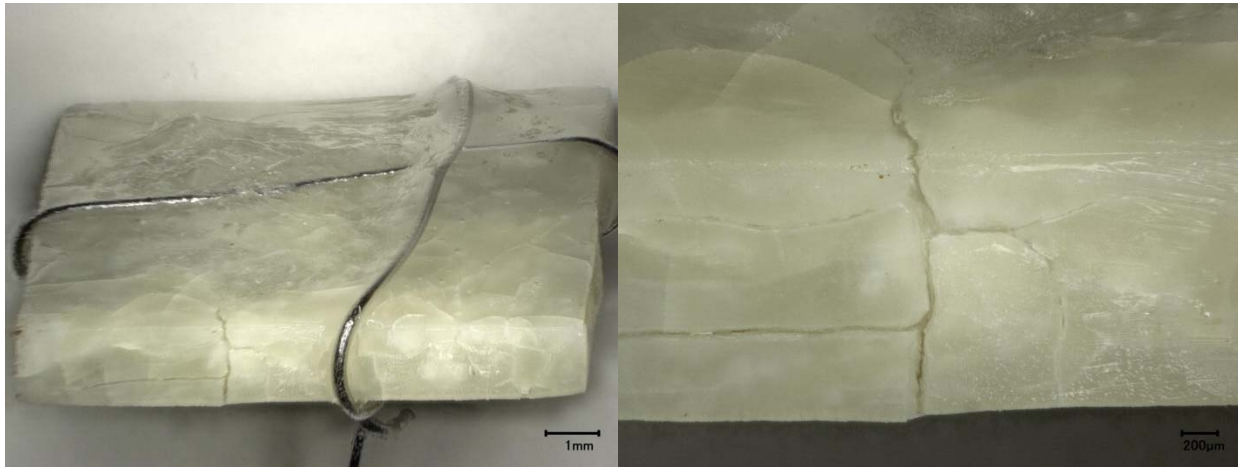
c) Micrograph of glass cross section after VHT

Figure F.37. Glass New-OL-65959(Mod) after VHT for 7 Days



a) Photo of glass square (1 cm) after (left) and before (right) VHT

b) Photo of glass square (1 cm) after VHT



c) Micrograph of glass square after VHT

d) Micrograph of glass surface after VHT

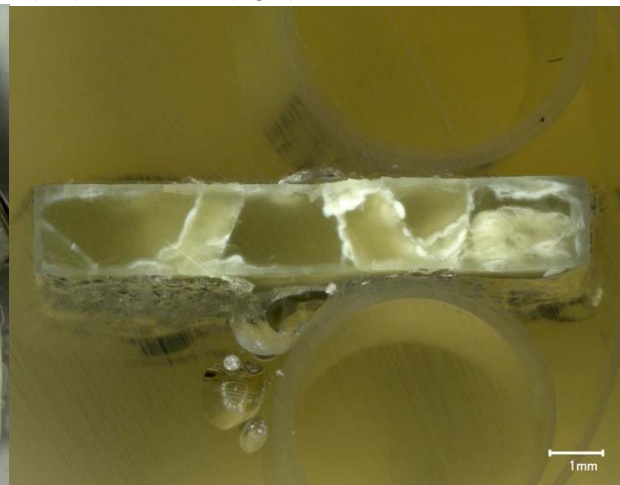
Figure F.38. Glass New-OL-80309 after VHT for 24 Days



a) Photo of glass square after (left) and before (right) VHT



b) Micrograph of glass square after VHT



c) Micrograph of glass cross section after VHT

Figure F.39. Glass New-OL-80309 after VHT for 7 Days



a) Micrograph of glass square after VHT



b) Micrograph of glass surface after VHT



c) Micrograph of glass surface after VHT



d) Micrograph of glass cross section after VHT

Figure F.40. Glass New-OL-90780 after VHT for 24 Days



a) Photo of glass square after (left) and before (right) VHT

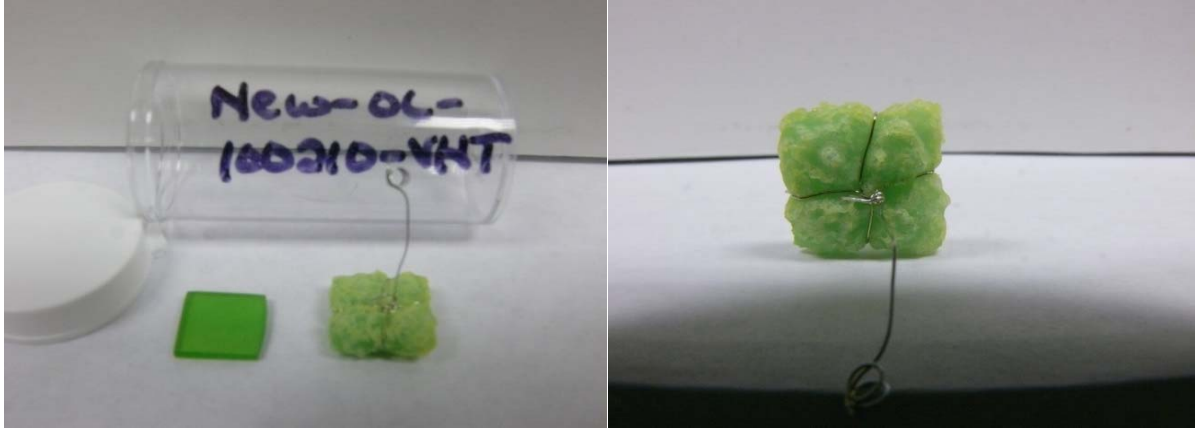


b) Micrograph of glass square after VHT



c) Micrograph of glass cross section after VHT

Figure F.41. Glass New-OL-90780 after VHT for 7 Days



a) Photo of glass square (1 cm) before (left) and after (right) VHT

b) Photo of glass square (1 cm) after VHT

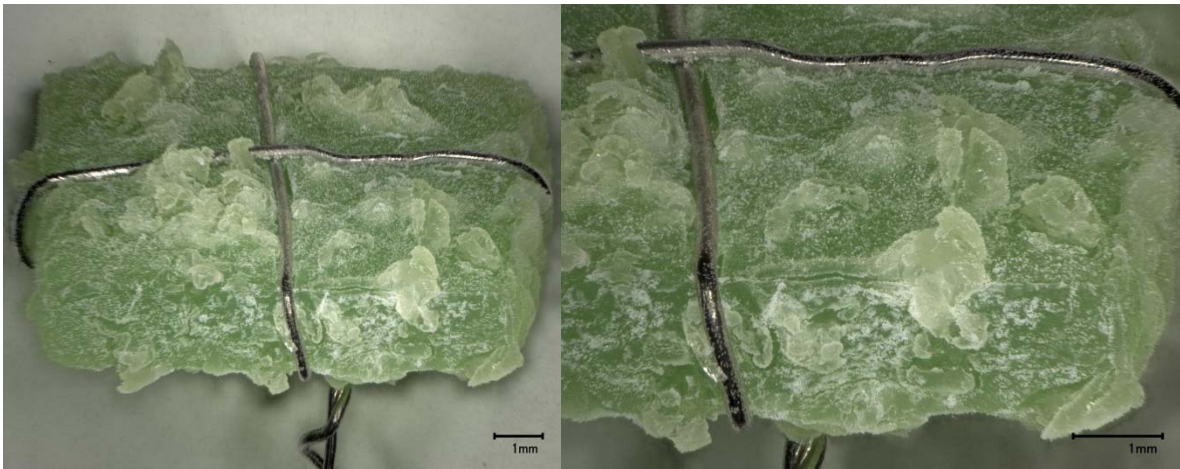


c) Micrograph of glass square after VHT



d) Micrograph of glass surface after VHT

Figure F.42. Glass New-OL-100210 after VHT after 24 Days



a) Micrograph of glass square after VHT

b) Micrograph of glass surface after VHT



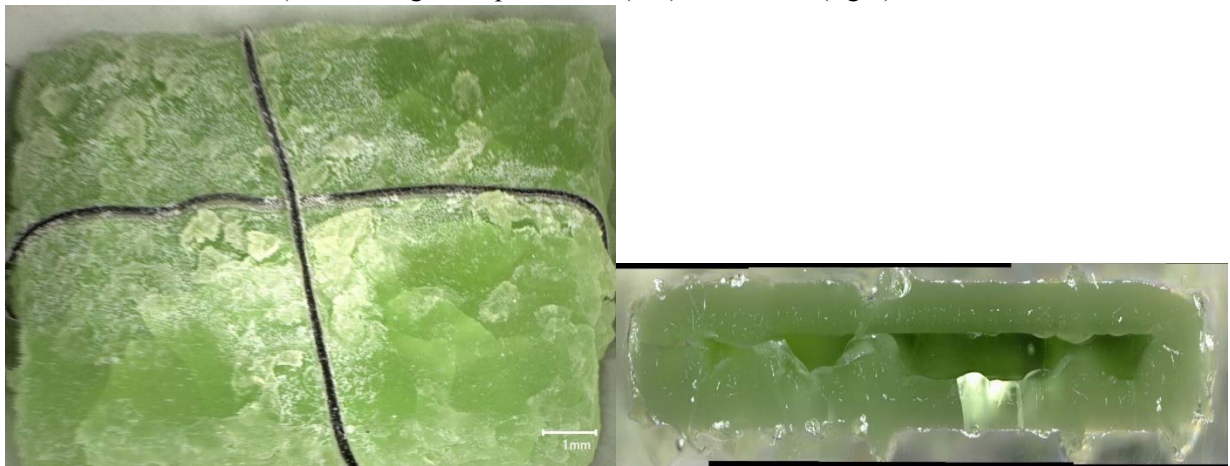
c) Micrograph of glass surface after VHT

d) Micrograph of glass cross section after VHT

Figure F.43. Glass New-OL-100210 after VHT after 7 Days



a) Photo of glass square after (left) and before (right) VHT



b) Micrograph of glass square after VHT

c) Micrograph of glass cross section after VHT

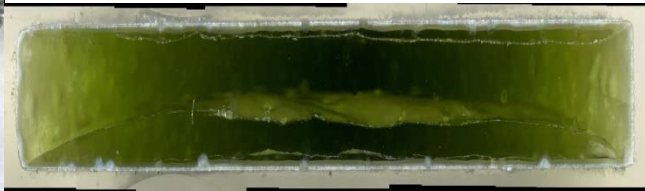
Figure F.44. Glass New-OL-100210 after VHT after 1 Day



a) Photo of glass square after (left) and before (right) VHT



b) Micrograph of glass square after VHT

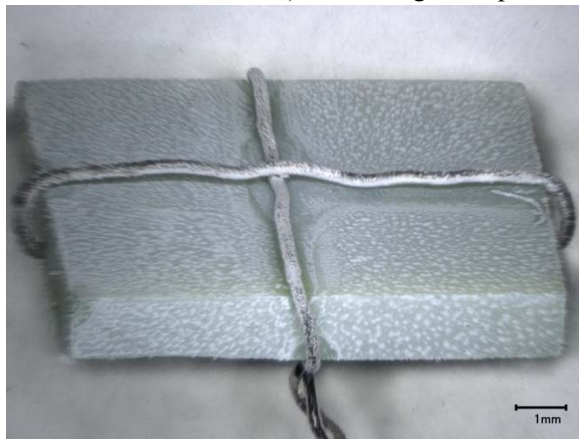


c) Micrograph of glass cross section after VHT

Figure F.45. Glass New-OL-108249 (SO₃ Mod) after VHT for 24 Days



a) Photo of glass square after (left) and before (right) VHT



b) Micrograph of glass square after VHT



c) Micrograph of glass cross section after VHT

Figure F.46. Glass New-OL-116208 (SO₃ Mod) after VHT for 24 Days



a) Photo of glass square after (left) and before (right) VHT

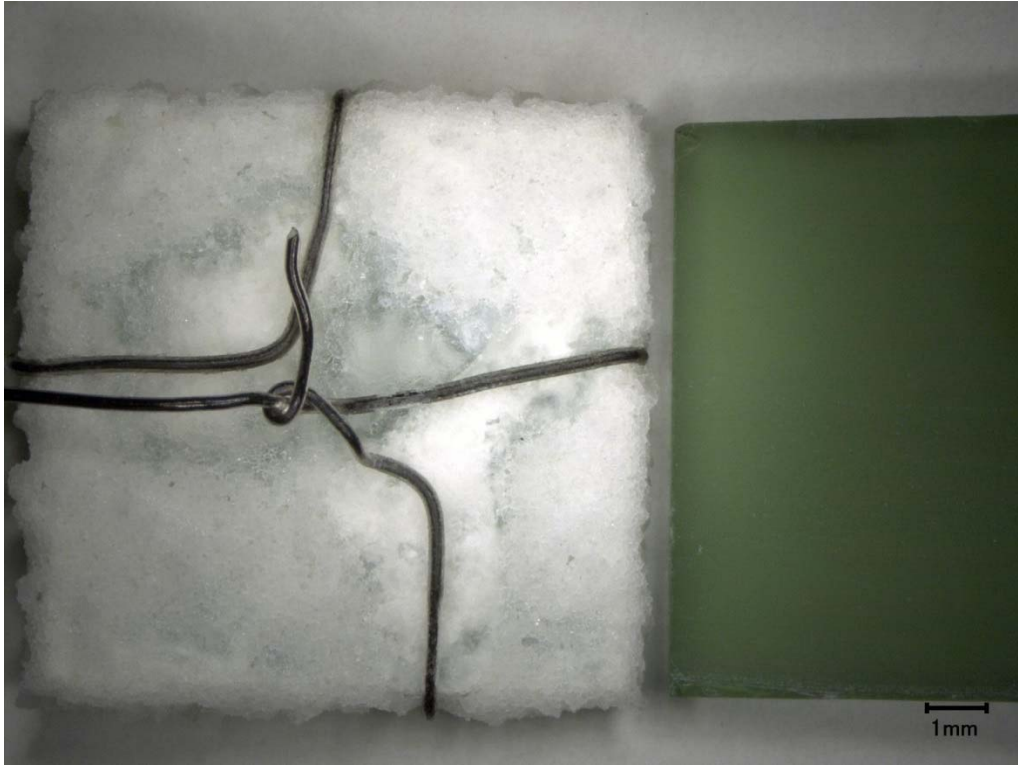


b) Micrograph of glass square after VHT

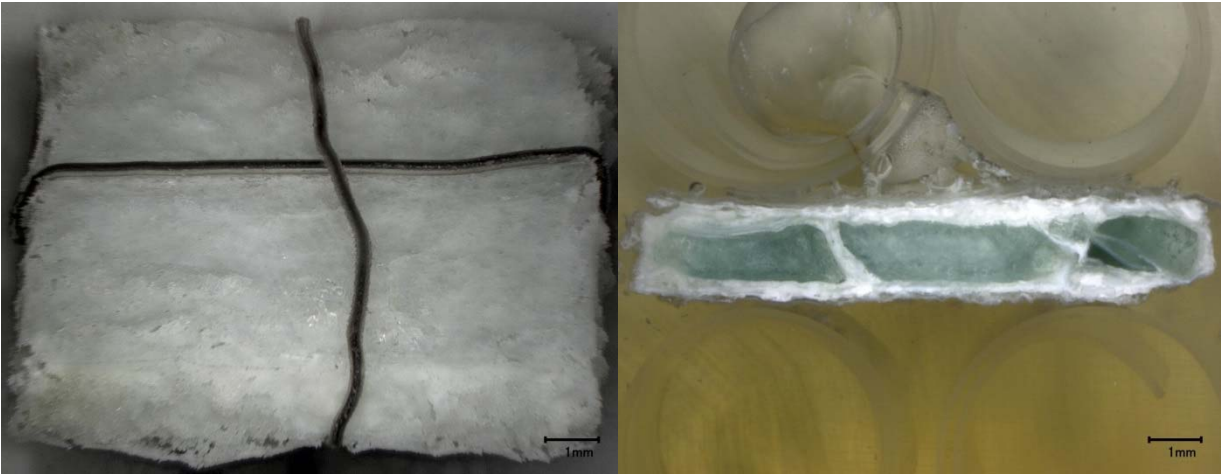


c) Micrograph of glass cross section after VHT

Figure F.47. Glass New-OL-122817 after VHT for 24 Days



a) Photo of glass square after (left) and before (right) VHT



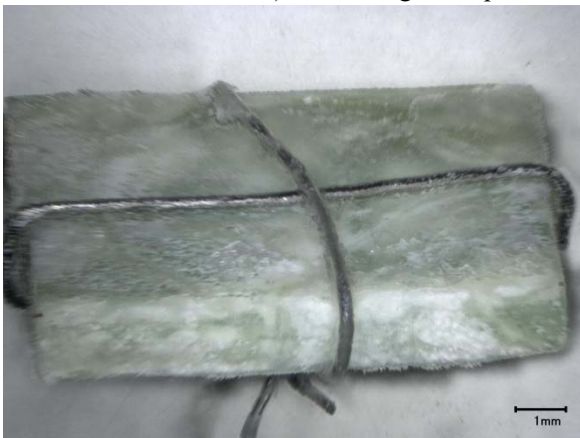
b) Micrograph of glass square after VHT

c) Micrograph of glass cross section after VHT

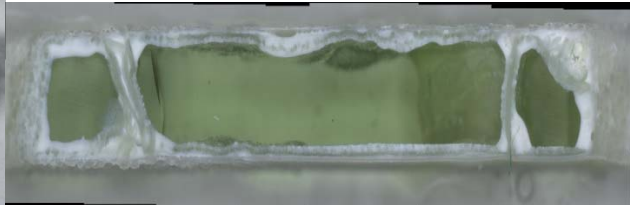
Figure F.48. Glass New-OL-127708(Mod) after VHT for 24 Days



a) Photo of glass square after (left) and before (right) VHT



b) Micrograph of glass square after VHT



c) Micrograph of glass cross section after VHT

Figure F.49. Glass EWG-LAW-Centroid-1 after VHT for 24 Days



a) Photo of glass square after (left) and before (right) VHT



b) Micrograph of glass square after VHT

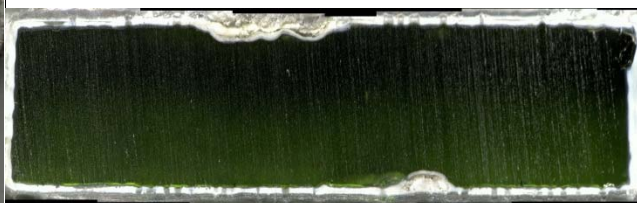


c) Micrograph of glass cross section after VHT

Figure F.50. Glass EWG-LAW-Centroid-2 after VHT for 24 Days

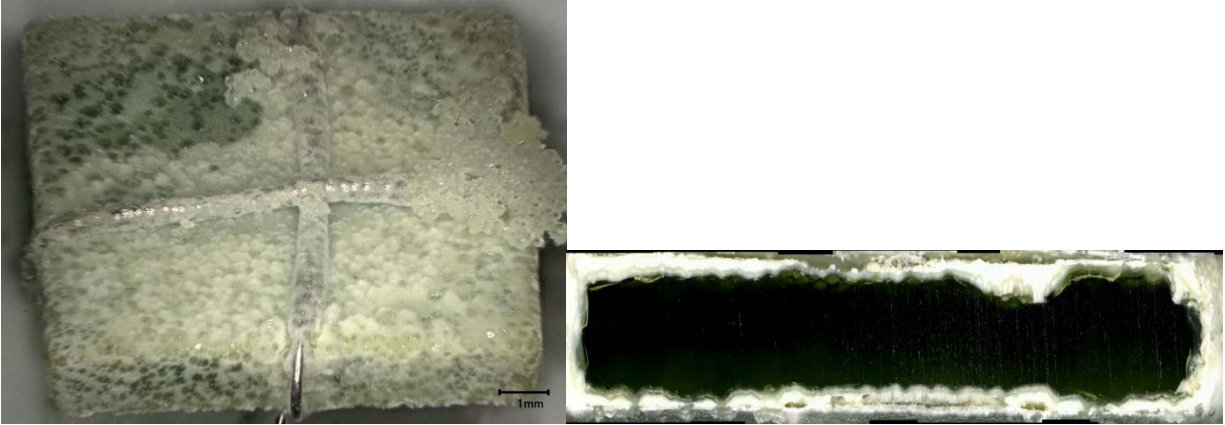


a) Micrograph of glass square after VHT



b) Micrograph of glass cross section after VHT

Figure F.51. Glass LAW-ORP-LD1-1 after VHT for 24 Days



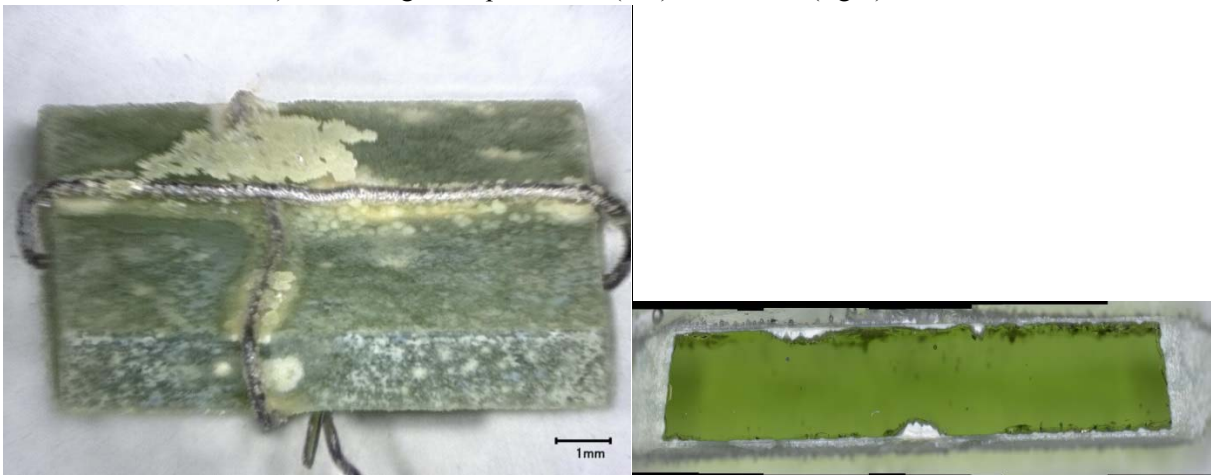
a) Micrograph of glass square after VHT

b) Micrograph of glass cross section after VHT

Figure F.52. Glass LAW-ORP-LD1-2 after VHT for 24 Days



a) Photo of glass square after (left) and before (right) VHT



b) Micrograph of glass square after VHT

c) Micrograph of glass cross section after VHT

Figure F.53. Glass LAW-ORP-LD1-3 after VHT for 24 Days

Appendix G

Analyses for Baseline and Sulfur Saturated Glasses

Appendix G

Analyses for Baseline and Sulfur Saturated Glasses

This appendix presents and compares the normalized compositional analyses of the baseline and sulfur-saturated glasses using ICP-AES and IC. This shows how much sulfur was retained in the glass as well as what was lost from the glass. Glass EWG-LAW_Centroid-1 was not analyzed.

Table G.1. Measured Compositions (normalized) for the Enhanced LAW Glasses (mass fractions: baseline and sulfur-saturated)

Components	Glass ID											
	New-IL-456			New-IL-1721			New-IL-1721 (PNNL)			New-IL-5253		
	Baseline	Sulfur-saturated	% Diff	Baseline	Sulfur-saturated	% Diff	Baseline	Sulfur-saturated	% Diff	Baseline	Sulfur-saturated	% Diff
Al ₂ O ₃	0.0630	0.0618	-1.95	0.0630	0.0627	-0.47	0.0630	0.0635	0.76	0.0634	0.0625	-1.47
B ₂ O ₃	0.0773	0.0793	2.53	0.1164	0.1155	-0.80	0.1164	0.1176	1.01	0.1144	0.1145	0.15
CaO	0.0880	0.0858	-2.43	0.0277	0.0282	1.89	0.0277	0.0272	-1.73	0.0276	0.0280	1.57
Cl	0.0008	0.0000	-100.00	0.0020	0.0009	-57.47	0.0020	0.0009	-53.55	0.0006	0.0000	-100.00
Cr ₂ O ₃	0.0000	0.0007	--	0.0022	0.0018	-15.31	0.0022	0.0018	-16.18	0.0000	0.0007	--
F	0.0013	0.0012	-7.01	0.0036	0.0031	-14.82	0.0036	0.0029	-19.26	0.0014	0.0012	-13.86
Fe ₂ O ₃	0.0128	0.0129	0.76	0.0123	0.0129	4.99	0.0123	0.0121	-1.63	0.0128	0.0129	0.69
K ₂ O	0.0021	0.0019	-7.72	0.0102	0.0096	-6.15	0.0102	0.0088	-13.49	0.0024	0.0019	-18.48
Li ₂ O	0.0340	0.0312	-8.37	0.0338	0.0311	-8.00	0.0338	0.0319	-5.66	0.0339	0.0307	-9.27
MgO	0.0226	0.0220	-2.40	0.0049	0.0048	-1.56	0.0049	0.0045	-7.49	0.0227	0.0232	2.05
Na ₂ O	0.1514	0.1549	2.30	0.1676	0.1689	0.80	0.1676	0.1685	0.53	0.1506	0.1560	3.59
P ₂ O ₅	0.0034	0.0032	-5.89	0.0102	0.0081	-20.91	0.0102	0.0047	-54.11	0.0038	0.0034	-9.64
SiO ₂	0.4402	0.4304	-2.23	0.4388	0.4368	-0.45	0.4388	0.4475	1.97	0.4088	0.4009	-1.92
SO ₃	0.0038	0.0201	421.75	0.0112	0.0171	52.66	0.0112	0.0177	58.30	0.0098	0.0150	53.82
SnO ₂	0.0350	0.0340	-2.98	0.0322	0.0352	9.03	0.0322	0.0349	8.39	0.0353	0.0344	-2.41
V ₂ O ₅	0.0296	0.0281	-5.09	0.0288	0.0289	0.02	0.0288	0.0276	-4.29	0.0298	0.0290	-2.70
ZnO	0.0202	0.0194	-4.24	0.0196	0.0202	3.25	0.0196	0.0190	-2.99	0.0383	0.0404	5.65
ZrO ₂	0.0144	0.0131	-9.19	0.0154	0.0142	-7.53	0.0154	0.0088	-43.02	0.0445	0.0450	1.07

Table G.1. Measured Compositions (normalized) for the Enhanced LAW Glasses (mass fractions: baseline and sulfur-saturated) (cont.)

Components	Glass ID											
	New-IL-5255			New-IL-42295			New-IL-70316			New-IL-87749		
	Baseline	Sulfur-saturated	% Diff	Baseline	Sulfur-saturated	% Diff	Baseline	Sulfur-saturated	% Diff	Baseline	Sulfur-saturated	% Diff
Al ₂ O ₃	0.0630	0.0633	0.46	0.0627	0.0598	-4.63	0.0627	0.0610	-2.78	0.1134	0.1091	-3.79
B ₂ O ₃	0.1152	0.1154	0.13	0.1155	0.1087	-5.83	0.0783	0.0749	-4.44	0.0789	0.0736	-6.68
CaO	0.0276	0.0289	4.70	0.0274	0.0292	6.31	0.0883	0.0945	7.02	0.0889	0.0941	5.88
Cl	0.0007	0.0000	-100.00	0.0008	0.0000	-100.00	0.0006	0.0000	-100.00	0.0007	0.0000	-100.00
Cr ₂ O ₃	0.0000	0.0007	--	0.0000	0.0007	--	0.0000	0.0006	--	0.0000	0.0006	--
F	0.0014	0.0012	-12.24	0.0014	0.0013	-6.63	0.0013	0.0013	-1.30	0.0013	0.0013	-2.05
Fe ₂ O ₃	0.0127	0.0133	4.67	0.0128	0.0115	-10.39	0.0127	0.0115	-9.52	0.0123	0.0111	-9.48
K ₂ O	0.0024	0.0019	-19.61	0.0023	0.0021	-8.95	0.0107	0.0088	-18.00	0.0104	0.0089	-14.31
Li ₂ O	0.0335	0.0316	-5.54	0.0336	0.0291	-13.44	0.0095	0.0067	-29.50	0.0336	0.0292	-13.17
MgO	0.0227	0.0234	3.26	0.0222	0.0234	5.35	0.0225	0.0240	6.32	0.0047	0.0046	-1.87
Na ₂ O	0.1799	0.1812	0.76	0.1785	0.1898	6.32	0.2041	0.2082	2.02	0.1798	0.1907	6.08
P ₂ O ₅	0.0038	0.0028	-27.24	0.0036	0.0032	-11.04	0.0035	0.0032	-8.12	0.0035	0.0033	-5.78
SiO ₂	0.3770	0.3757	-0.33	0.4300	0.4180	-2.78	0.3932	0.3893	-1.01	0.3793	0.3674	-3.15
SO ₃	0.0120	0.0165	37.29	0.0040	0.0174	336.19	0.0126	0.0169	34.27	0.0041	0.0172	315.36
SnO ₂	0.0355	0.0352	-0.82	0.0100	0.0084	-16.78	0.0354	0.0335	-5.23	0.0263	0.0247	-6.10
V ₂ O ₅	0.0298	0.0288	-3.35	0.0292	0.0295	1.05	0.0297	0.0296	-0.37	0.0288	0.0291	0.79
ZnO	0.0382	0.0411	7.62	0.0199	0.0205	2.93	0.0202	0.0210	3.91	0.0198	0.0206	4.00
ZrO ₂	0.0447	0.0389	-12.87	0.0463	0.0477	2.99	0.0147	0.0152	3.88	0.0141	0.0146	3.15

Table G.1. Measured Compositions (normalized) for the Enhanced LAW Glasses (mass fractions: baseline and sulfur-saturated) (cont.)

Components	Glass ID											
	New-IL-93907			New-IL-94020			New-IL-103151			New-IL-151542		
	Baseline	Sulfur-saturated	% Diff	Baseline	Sulfur-saturated	% Diff	Baseline	Sulfur-saturated	% Diff	Baseline	Sulfur-saturated	% Diff
Al ₂ O ₃	0.1134	0.1128	-0.52	0.1139	0.1155	1.47	0.0612	0.0616	0.64	0.0609	0.0604	-0.84
B ₂ O ₃	0.1128	0.1126	-0.17	0.0788	0.0803	1.94	0.0755	0.0748	-0.88	0.0922	0.0918	-0.35
CaO	0.0277	0.0291	5.17	0.0366	0.0347	-5.15	0.0282	0.0304	7.81	0.0887	0.0963	8.60
Cl	0.0007	0.0000	-100.00	0.0005	0.0000	-100.00	0.0008	0.0000	-100.00	0.0017	0.0008	-51.43
Cr ₂ O ₃	0.0000	0.0007	--	0.0000	0.0007	--	0.0000	0.0006	--	0.0022	0.0017	-21.21
F	0.0013	0.0012	-11.56	0.0013	0.0010	-25.36	0.0014	0.0013	-6.65	0.0034	0.0033	-2.87
Fe ₂ O ₃	0.0129	0.0118	-8.40	0.0128	0.0122	-5.07	0.0131	0.0116	-11.32	0.0129	0.0114	-11.64
K ₂ O	0.0111	0.0094	-15.41	0.0023	0.0018	-21.05	0.0112	0.0091	-18.71	0.0023	0.0019	-15.99
Li ₂ O	0.0335	0.0292	-12.63	0.0337	0.0311	-7.74	0.0092	0.0069	-25.71	0.0092	0.0067	-27.66
MgO	0.0050	0.0047	-4.97	0.0223	0.0226	1.29	0.0230	0.0239	3.96	0.0230	0.0241	4.79
Na ₂ O	0.1519	0.1621	6.76	0.1575	0.1522	-3.40	0.2371	0.2270	-4.27	0.1846	0.1878	1.77
P ₂ O ₅	0.0036	0.0032	-10.11	0.0037	0.0029	-21.46	0.0037	0.0032	-15.36	0.0104	0.0070	-32.18
SiO ₂	0.4407	0.4375	-0.73	0.4350	0.4456	2.44	0.4112	0.4226	2.78	0.3972	0.3930	-1.06
SO ₃	0.0095	0.0118	23.45	0.0082	0.0108	32.27	0.0125	0.0154	23.63	0.0108	0.0174	61.09
SnO ₂	0.0356	0.0333	-6.52	0.0352	0.0345	-1.97	0.0265	0.0238	-10.25	0.0343	0.0331	-3.56
V ₂ O ₅	0.0052	0.0048	-6.82	0.0051	0.0044	-13.40	0.0308	0.0294	-4.53	0.0303	0.0305	0.54
ZnO	0.0204	0.0207	1.48	0.0385	0.0375	-2.73	0.0394	0.0430	9.00	0.0204	0.0212	3.60
ZrO ₂	0.0149	0.0151	1.06	0.0146	0.0122	-16.31	0.0152	0.0154	1.28	0.0157	0.0117	-25.71

Table G.1. Measured Compositions (normalized) for the Enhanced LAW Glasses (mass fractions: baseline and sulfur-saturated) (cont.)

Components	Glass ID											
	New-IL-166697			New-IL-166731			New-OL-8445			New-OL-8788(Mod)		
	Baseline	Sulfur-saturated	% Diff	Baseline	Sulfur-saturated	% Diff	Baseline	Sulfur-saturated	% Diff	Baseline	Sulfur-saturated	% Diff
Al ₂ O ₃	0.1090	0.1160	6.49	0.1125	0.1178	4.72	0.1239	0.1256	1.33	0.1228	0.1255	2.22
B ₂ O ₃	0.0990	0.1034	4.45	0.0910	0.0944	3.79	0.1387	0.1388	0.10	0.0611	0.0592	-3.09
CaO	0.0272	0.0277	2.07	0.0279	0.0281	0.97	0.1199	0.1131	-5.70	0.0011	0.0000	-100.00
Cl	0.0018	0.0008	-56.10	0.0015	0.0007	-54.21	0.0030	0.0012	-60.52	0.0032	0.0011	-64.48
Cr ₂ O ₃	0.0021	0.0016	-26.32	0.0022	0.0015	-30.88	0.0033	0.0025	-23.51	0.0029	0.0026	-9.76
F	0.0037	0.0030	-18.48	0.0053	0.0032	-40.52	0.0052	0.0047	-10.38	0.0052	0.0045	-13.32
Fe ₂ O ₃	0.0123	0.0123	0.30	0.0053	0.0044	-17.22	0.0000	0.0000	--	0.0154	0.0144	-6.33
K ₂ O	0.0102	0.0086	-15.73	0.0021	0.0018	-15.39	0.0159	0.0118	-25.84	0.0151	0.0125	-17.29
Li ₂ O	0.0335	0.0324	-3.15	0.0330	0.0322	-2.43	0.0195	0.0170	-12.97	0.0241	0.0210	-12.99
MgO	0.0050	0.0048	-4.00	0.0220	0.0225	2.27	0.0304	0.0293	-3.73	0.0325	0.0305	-6.38
Na ₂ O	0.1806	0.1782	-1.35	0.1874	0.1826	-2.53	0.0983	0.1095	11.37	0.1337	0.1321	-1.20
P ₂ O ₅	0.0104	0.0000	-100.00	0.0106	0.0025	-76.39	0.0145	0.0121	-16.18	0.0095	0.0120	26.85
SiO ₂	0.3796	0.3888	2.42	0.3763	0.3890	3.37	0.3542	0.3534	-0.23	0.4695	0.4797	2.18
SO ₃	0.0111	0.0151	35.88	0.0102	0.0148	44.76	0.0000	0.0139	--	0.0000	0.0057	--
SnO ₂	0.0329	0.0355	8.04	0.0298	0.0323	8.54	0.0000	0.0000	--	0.0000	0.0000	--
V ₂ O ₅	0.0290	0.0277	-4.38	0.0293	0.0275	-6.12	0.0000	0.0000	--	0.0000	0.0000	--
ZnO	0.0373	0.0388	4.03	0.0378	0.0387	2.37	0.0103	0.0090	-12.89	0.0504	0.0480	-4.83
ZrO ₂	0.0155	0.0053	-65.63	0.0157	0.0058	-63.16	0.0629	0.0582	-7.42	0.0535	0.0511	-4.44

Table G.1. Measured Compositions (normalized) for the Enhanced LAW Glasses (mass fractions: baseline and sulfur-saturated) (cont.)

Components	Glass ID											
	New-OL-14844			New-OL-15493			New-OL-17130			New-OL-45748 (Sn Mod)		
	Baseline	Sulfur-saturated	% Diff	Baseline	Sulfur-saturated	% Diff	Baseline	Sulfur-saturated	% Diff	Baseline	Sulfur-saturated	% Diff
Al ₂ O ₃	0.0358	0.0376	4.90	0.0358	0.0362	1.14	0.0358	0.0348	-2.76	0.1363	0.1387	1.82
B ₂ O ₃	0.0587	0.0628	6.98	0.0596	0.0579	-2.90	0.1339	0.1303	-2.72	0.0617	0.0599	-2.87
CaO	0.1257	0.1175	-6.52	0.1205	0.1177	-2.30	0.0163	0.0163	-0.03	0.1263	0.1149	-9.05
Cl	0.0014	0.0007	-49.97	0.0003	0.0000	-100.00	0.0034	0.0020	-40.45	0.0024	0.0009	-61.87
Cr ₂ O ₃	0.0031	0.0014	-54.24	0.0000	0.0003	--	0.0033	0.0028	-14.74	0.0029	0.0020	-28.99
F	0.0043	0.0054	26.45	0.0006	0.0006	3.61	0.0050	0.0043	-13.00	0.0051	0.0045	-11.02
Fe ₂ O ₃	0.0000	0.0000	--	0.0000	0.0000	--	0.0154	0.0141	-8.61	0.0151	0.0144	-4.48
K ₂ O	0.0141	0.0102	-27.74	0.0150	0.0125	-16.91	0.0000	0.0000	--	0.0000	0.0000	--
Li ₂ O	0.0478	0.0479	0.36	0.0000	0.0000	--	0.0484	0.0441	-9.05	0.0493	0.0460	-6.69
MgO	0.0301	0.0308	2.28	0.0299	0.0310	3.78	0.0000	0.0000	--	0.0000	0.0000	--
Na ₂ O	0.1608	0.1539	-4.25	0.2659	0.2417	-9.09	0.1648	0.1754	6.43	0.1175	0.1179	0.32
P ₂ O ₅	0.0138	0.0117	-14.93	0.0000	0.0000	--	0.0154	0.0122	-20.58	0.0096	0.0137	41.92
SiO ₂	0.3584	0.3667	2.32	0.3940	0.4054	2.90	0.4770	0.4653	-2.45	0.3474	0.3534	1.74
SO ₃	0.0000	0.0138	--	0.0000	0.0218	--	0.0000	0.0235	--	0.0000	0.0155	--
SnO ₂	0.0000	0.0000	--	0.0296	0.0302	2.10	0.0307	0.0291	-5.31	0.0465	0.0458	-1.53
V ₂ O ₅	0.0389	0.0355	-8.62	0.0388	0.0351	-9.61	0.0403	0.0363	-9.90	0.0295	0.0261	-11.47
ZnO	0.0461	0.0481	4.45	0.0101	0.0096	-5.77	0.0103	0.0095	-7.49	0.0506	0.0463	-8.49
ZrO ₂	0.0610	0.0557	-8.62	0.0000	0.0000	--	0.0000	0.0000	--	0.0000	0.0000	--

Table G.1. Measured Compositions (normalized) for the Enhanced LAW Glasses (mass fractions: baseline and sulfur-saturated) (cont.)

Components	Glass ID											
	New-OL-54017 (Sn Mod)			New-OL-57284			New-OL-62380			New-OL-62909(Mod)		
	Baseline	Sulfur-saturated	% Diff	Baseline	Sulfur-saturated	% Diff	Baseline	Sulfur-saturated	% Diff	Baseline	Sulfur-saturated	% Diff
Al ₂ O ₃	0.0362	0.0353	-2.35	0.0364	0.0364	0.17	0.0360	0.0357	-0.75	0.1229	0.1239	0.81
B ₂ O ₃	0.0611	0.0588	-3.68	0.1355	0.1393	2.83	0.1300	0.1349	3.76	0.0905	0.0904	-0.12
CaO	0.1140	0.1027	-9.88	0.0294	0.0285	-2.92	0.1233	0.1132	-8.16	0.1258	0.1198	-4.82
Cl	0.0004	0.0000	-100.00	0.0035	0.0015	-57.73	0.0004	0.0000	-100.00	0.0022	0.0009	-60.45
Cr ₂ O ₃	0.0004	0.0005	17.79	0.0032	0.0028	-12.53	0.0000	0.0007	--	0.0030	0.0028	-6.93
F	0.0006	0.0005	-11.66	0.0050	0.0045	-11.19	0.0011	0.0009	-15.47	0.0055	0.0048	-13.55
Fe ₂ O ₃	0.0152	0.0144	-5.64	0.0000	0.0000	--	0.0153	0.0145	-5.49	0.0000	0.0000	--
K ₂ O	0.0000	0.0000	--	0.0164	0.0136	-17.06	0.0152	0.0116	-23.89	0.0000	0.0000	--
Li ₂ O	0.0000	0.0000	--	0.0000	0.0000	--	0.0000	0.0000	--	0.0241	0.0227	-6.00
MgO	0.0319	0.0307	-3.78	0.0000	0.0000	--	0.0000	0.0000	--	0.0340	0.0324	-4.86
Na ₂ O	0.1529	0.1529	0.04	0.1425	0.1427	0.18	0.1422	0.1432	0.66	0.1328	0.1371	3.26
P ₂ O ₅	0.0017	0.0000	-100.00	0.0141	0.0124	-12.34	0.0036	0.0031	-14.31	0.0094	0.0061	-35.10
SiO ₂	0.4751	0.4792	0.86	0.4752	0.4778	0.54	0.3510	0.3504	-0.15	0.3454	0.3483	0.85
SO ₃	0.0000	0.0129	--	0.0000	0.0090	--	0.0000	0.0150	--	0.0000	0.0129	--
SnO ₂	0.0436	0.0479	9.99	0.0000	0.0000	--	0.0455	0.0457	0.34	0.0424	0.0419	-1.09
V ₂ O ₅	0.0178	0.0169	-5.04	0.0405	0.0366	-9.73	0.0264	0.0241	-8.66	0.0000	0.0000	--
ZnO	0.0492	0.0472	-4.02	0.0480	0.0478	-0.28	0.0466	0.0470	0.75	0.0099	0.0095	-4.66
ZrO ₂	0.0000	0.0000	--	0.0503	0.0470	-6.56	0.0635	0.0601	-5.27	0.0520	0.0467	-10.18

Table G.1. Measured Compositions (normalized) for the Enhanced LAW Glasses (mass fractions: baseline and sulfur-saturated) (cont.)

Components	Glass ID											
	New-OL-65959(Mod)			New-OL-80309			New-OL-90780			New-OL-100210		
	Baseline	Sulfur-saturated	% Diff	Baseline	Sulfur-saturated	% Diff	Baseline	Sulfur-saturated	% Diff	Baseline	Sulfur-saturated	% Diff
Al ₂ O ₃	0.1360	0.1341	-1.42	0.0355	0.0369	4.05	0.1385	0.1397	0.88	0.0352	0.0367	4.44
B ₂ O ₃	0.1313	0.1273	-3.09	0.1378	0.1401	1.66	0.1362	0.1372	0.75	0.0574	0.0609	6.12
CaO	0.0000	0.0000	--	0.0000	0.0000	--	0.0000	0.0000	--	0.0187	0.0199	6.68
Cl	0.0003	0.0000	-100.00	0.0004	0.0000	-100.00	0.0025	0.0012	-54.28	0.0035	0.0017	-49.77
Cr ₂ O ₃	0.0004	0.0005	22.89	0.0004	0.0003	-15.81	0.0032	0.0022	-30.46	0.0032	0.0027	-15.83
F	0.0006	0.0005	-14.73	0.0007	0.0006	-17.53	0.0054	0.0051	-4.66	0.0057	0.0055	-4.14
Fe ₂ O ₃	0.0000	0.0000	--	0.0156	0.0148	-4.96	0.0000	0.0000	--	0.0000	0.0000	--
K ₂ O	0.0000	0.0000	--	0.0156	0.0119	-23.46	0.0161	0.0132	-18.22	0.0000	0.0000	--
Li ₂ O	0.0491	0.0451	-8.03	0.0483	0.0462	-4.34	0.0492	0.0441	-10.43	0.0000	0.0000	--
MgO	0.0327	0.0311	-4.82	0.0328	0.0309	-5.80	0.0306	0.0332	8.49	0.0311	0.0332	6.59
Na ₂ O	0.1666	0.1770	6.24	0.1536	0.1507	-1.88	0.1573	0.1611	2.40	0.2741	0.2427	-11.47
P ₂ O ₅	0.0017	0.0000	-100.00	0.0016	0.0000	-100.00	0.0152	0.0128	-16.21	0.0151	0.0129	-14.37
SiO ₂	0.3514	0.3466	-1.37	0.3430	0.3608	5.19	0.3528	0.3567	1.10	0.4655	0.4828	3.72
SO ₃	0.0000	0.0169	--	0.0167	0.0159	-4.53	0.0131	0.0156	19.60	0.0095	0.0157	66.05
SnO ₂	0.0426	0.0406	-4.85	0.0427	0.0436	2.17	0.0300	0.0305	1.42	0.0334	0.0329	-1.39
V ₂ O ₅	0.0362	0.0332	-8.22	0.0400	0.0363	-9.30	0.0395	0.0374	-5.42	0.0000	0.0000	--
ZnO	0.0511	0.0471	-7.76	0.0507	0.0483	-4.75	0.0103	0.0101	-1.91	0.0478	0.0524	9.68
ZrO ₂	0.0000	0.0000	--	0.0647	0.0626	-3.22	0.0000	0.0000	--	0.0000	0.0000	--

Table G.1. Measured Compositions (normalized) for the Enhanced LAW Glasses (mass fractions: baseline and sulfur-saturated) (cont.)

Components	Glass ID											
	New-OL-108249(SO ₃ Mod)			New-OL-108249(SO ₃ Mod) (PNNL)			New-OL-116208(SO ₃ Mod)			New-OL-116208(SO ₃ Mod) (PNNL)		
	Baseline	Sulfur-saturated	% Diff	Baseline	Sulfur-saturated	% Diff	Baseline	Sulfur-saturated	% Diff	Baseline	Sulfur-saturated	% Diff
Al ₂ O ₃	0.1193	0.1207	1.16	0.1193	0.1197	0.35	0.0363	0.0372	2.48	0.0363	0.0366	1.02
B ₂ O ₃	0.0611	0.0618	1.17	0.0611	0.0586	-4.07	0.0612	0.0611	-0.12	0.0612	0.0619	1.20
CaO	0.1037	0.0997	-3.91	0.1037	0.0981	-5.47	0.1227	0.1238	0.90	0.1227	0.1212	-1.24
Cl	0.0029	0.0010	-64.97	0.0029	0.0010	-66.21	0.0029	0.0010	-67.05	0.0029	0.0010	-66.81
Cr ₂ O ₃	0.0029	0.0015	-45.67	0.0029	0.0017	-41.41	0.0028	0.0015	-47.50	0.0028	0.0016	-43.55
F	0.0057	0.0054	-4.92	0.0057	0.0049	-14.81	0.0059	0.0061	3.40	0.0059	0.0051	-13.44
Fe ₂ O ₃	0.0154	0.0159	3.13	0.0154	0.0146	-5.58	0.0154	0.0159	2.96	0.0154	0.0153	-0.78
K ₂ O	0.0147	0.0112	-23.91	0.0147	0.0105	-28.63	0.0000	--	--	0.0000	0.0000	--
Li ₂ O	0.0491	0.0460	-6.19	0.0491	0.0461	-6.12	0.0490	0.0470	-4.08	0.0490	0.0474	-3.31
MgO	0.0000	0.0000	--	0.0000	0.0000	--	0.0352	0.0363	3.30	0.0352	0.0352	0.06
Na ₂ O	0.1601	0.1580	-1.29	0.1601	0.1599	-0.09	0.1638	0.1609	-1.74	0.1638	0.1632	-0.38
P ₂ O ₅	0.0098	0.0131	33.72	0.0098	0.0137	39.68	0.0094	0.0128	35.84	0.0094	0.0118	25.69
SiO ₂	0.3507	0.3538	0.87	0.3507	0.3492	-0.44	0.3573	0.3538	-0.97	0.3573	0.3594	0.58
SO ₃	0.0085	0.0132	56.09	0.0085	0.0130	53.58	0.0092	0.0134	45.07	0.0092	0.0149	61.24
SnO ₂	0.0451	0.0475	5.22	0.0451	0.0608	34.79	0.0450	0.0451	0.21	0.0450	0.0450	0.13
V ₂ O ₅	0.0000	0.0000	--	0.0000	0.0000	--	0.0115	0.0117	1.72	0.0115	0.0113	-2.20
ZnO	0.0510	0.0511	0.12	0.0510	0.0483	-5.30	0.0093	0.0102	8.96	0.0093	0.0095	1.98
ZrO ₂	0.0000	0.0000	--	0.0000	0.0000	--	0.0631	0.0623	-1.28	0.0631	0.0597	-5.38

Table G.1. Measured Compositions (normalized) for the Enhanced LAW Glasses (mass fractions: baseline and sulfur-saturated) (cont.)

Components	Glass ID											
	New-OL-122817			New-OL-127708(Mod)			EWG-LAW_Centroid-2			LAW-ORP-LD1(1)		
	Baseline	Sulfur-saturated	% Diff	Baseline	Sulfur-saturated	% Diff	Baseline	Sulfur-saturated	% Diff	Baseline	Sulfur-saturated	% Diff
Al ₂ O ₃	0.0359	0.0364	1.40	0.1099	0.1078	-1.87	0.0877	0.0874	-0.26	0.1006	0.1014	0.75
B ₂ O ₃	0.0602	0.0608	1.10	0.1401	0.1359	-2.96	0.0965	0.0936	-3.06	0.1181	0.1159	-1.86
CaO	0.1210	0.1200	-0.86	0.0032	0.0031	-4.21	0.0529	0.0580	9.76	0.0778	0.0818	5.24
Cl	0.0027	0.0012	-55.54	0.0003	0.0000	-100.00	0.0014	0.0007	-49.17	0.0018	0.0010	-45.12
Cr ₂ O ₃	0.0032	0.0025	-21.68	0.0004	0.0005	22.62	0.0015	0.0011	-22.21	0.0051	0.0035	-31.08
F	0.0047	0.0049	2.93	0.0005	0.0005	2.18	0.0025	0.0024	-2.94	0.0012	0.0012	-0.67
Fe ₂ O ₃	0.0153	0.0157	2.42	0.0144	0.0153	6.40	0.0105	0.0089	-15.08	0.0101	0.0092	-9.83
K ₂ O	0.0160	0.0127	-21.02	0.0142	0.0132	-7.24	0.0046	0.0037	-19.54	0.0019	0.0015	-22.70
Li ₂ O	0.0000	0.0000	--	0.0247	0.0218	-11.46	0.0188	0.0157	-16.58	0.0000	0.0000	--
MgO	0.0000	0.0000	--	0.0309	0.0317	2.65	0.0140	0.0132	-5.81	0.0094	0.0093	-1.73
Na ₂ O	0.1948	0.1818	-6.64	0.1251	0.1382	10.48	0.1973	0.2002	1.46	0.2118	0.2069	-2.29
P ₂ O ₅	0.0150	0.0140	-6.44	0.0017	0.0000	-100.00	0.0065	0.0055	-14.85	0.0029	0.0025	-12.34
SiO ₂	0.4366	0.4514	3.38	0.4821	0.4700	-2.51	0.3982	0.3951	-0.79	0.3800	0.3830	0.81
SO ₃	0.0130	0.0205	58.05	0.0000	0.0087	--	0.0071	0.0149	111.53	0.0102	0.0133	30.98
SnO ₂	0.0311	0.0306	-1.73	0.0430	0.0433	0.79	0.0207	0.0185	-10.67	0.0000	0.0000	--
V ₂ O ₅	0.0400	0.0377	-5.84	0.0000	0.0000	--	0.0205	0.0197	-3.71	0.0101	0.0093	-7.76
ZnO	0.0105	0.0099	-5.03	0.0095	0.0097	2.72	0.0296	0.0313	5.64	0.0293	0.0305	4.24
ZrO ₂	0.0000	0.0000	--	0.0000	0.0000	--	0.0298	0.0300	0.55	0.0297	0.0296	-0.32

Table G.1. Measured Compositions (normalized) for the Enhanced LAW Glasses (mass fractions: baseline and sulfur-saturated) (cont.)

Components	Glass ID					
	LAW-ORP-LD1(2)			LAW-ORP-LD1(3)		
	Baseline	Sulfur-saturated	% Diff	Baseline	Sulfur-saturated	% Diff
Al ₂ O ₃	0.1015	0.1026	1.11	0.1466	0.1491	1.73
B ₂ O ₃	0.1226	0.1192	-2.78	0.1153	0.1138	-1.33
CaO	0.0813	0.0783	-3.61	0.0782	0.0742	-5.18
Cl	0.0017	0.0006	-62.23	0.0016	0.0006	-64.69
Cr ₂ O ₃	0.0047	0.0033	-30.19	0.0044	0.0027	-37.43
F	0.0012	0.0010	-21.40	0.0012	0.0009	-21.25
Fe ₂ O ₃	0.0106	0.0097	-8.93	0.0093	0.0092	-0.59
K ₂ O	0.0021	0.0016	-26.42	0.0021	0.0014	-32.99
Li ₂ O	0.0000	0.0000	--	0.0000	0.0000	--
MgO	0.0095	0.0093	-2.23	0.0092	0.0095	3.95
Na ₂ O	0.1999	0.2081	4.10	0.1941	0.1957	0.79
P ₂ O ₅	0.0046	0.0026	-44.60	0.0039	0.0025	-36.26
SiO ₂	0.3827	0.3840	0.32	0.3597	0.3668	1.98
SO ₃	0.0087	0.0133	53.30	0.0086	0.0104	21.72
SnO ₂	0.0000	0.0000	--	0.0000	0.0000	--
V ₂ O ₅	0.0097	0.0090	-7.29	0.0090	0.0086	-4.24
ZnO	0.0304	0.0290	-4.57	0.0288	0.0276	-4.10
ZrO ₂	0.0287	0.0285	-0.73	0.0282	0.0270	-4.14

Distribution

**No. of
Copies**

**No. of
Copies**

**2 U.S. Department of Energy
Office of River Protection**
AA Kruger
WF Hamel

1 Savannah River National Laboratory
KM Fox

14 Pacific Northwest National Laboratory
CL Arendt
CB Bonham
SK Cooley
LP Darnell
V Gervasio
T Jin
JB Lang
JM Mayer
BP McCarthy
GF Piepel
RL Russell
MJ Schweiger
JD Vienna
Information Release



Pacific Northwest
NATIONAL LABORATORY

*Proudly Operated by **Battelle** Since 1965*

902 Battelle Boulevard
P.O. Box 999
Richland, WA 99352
1-888-375-PNNL (7665)

U.S. DEPARTMENT OF
ENERGY

www.pnnl.gov